Tsunami Engineering

by

Frederick E. Camfield

SPECIAL REPORT NO. 6
FEBRUARY 1980

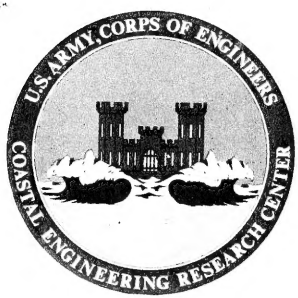

Approved for public release;
distribution unlimited.

U.S. ARMY, CORPS OF ENGINEERS
COASTAL ENGINEERING
RESEARCH CENTER
Kingman Building
Fort Belvoir, Va. 22060

U.S. Army Coastal Engineering Research Center
Kingman Building
Fort Belvoir, Virginia 22060

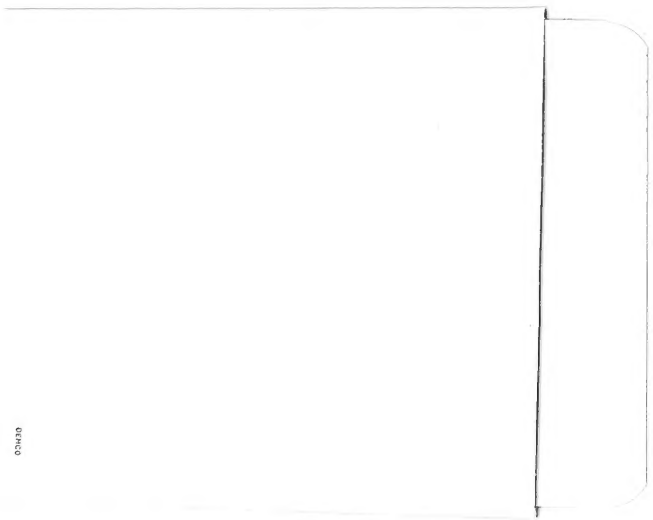

For sale by the Superintendent of Documents, U.S. Government Printing Office, Washington, D.C. 20402

REPORT DOCUMENTATION PAGE

READ INSTRUCTIONS BEFORE COMPLETING FORM

1. REPORT NUMBER: SR-6
2. GOVT ACCESSION NO.:
3. RECIPIENT'S CATALOG NUMBER:
4. TITLE (and Subtitle): TSUNAMI ENGINEERING
5. TYPE OF REPORT & PERIOD COVERED: Special Report
6. PERFORMING ORG. REPORT NUMBER:
7. AUTHOR(s): Frederick E. Camfield
8. CONTRACT OR GRANT NUMBER(s):
9. PERFORMING ORGANIZATION NAME AND ADDRESS:
Department of the Army
Coastal Engineering Research Center (CEREN-CD)
Kingman Building, Fort Belvoir, Virginia 22060
10. PROGRAM ELEMENT, PROJECT, TASK AREA & WORK UNIT NUMBERS: F31234
11. CONTROLLING OFFICE NAME AND ADDRESS:
Department of the Army
Coastal Engineering Research Center
Kingman Building, Fort Belvoir, Virginia 22060
12. REPORT DATE: February 1980
13. NUMBER OF PAGES: 222
14. MONITORING AGENCY NAME & ADDRESS (if different from Controlling Office):
15. SECURITY CLASS. (of this report): UNCLASSIFIED
15a. DECLASSIFICATION/DOWNGRADING SCHEDULE:

16. DISTRIBUTION STATEMENT (of this Report)

Approved for public release; distribution unlimited.

17. DISTRIBUTION STATEMENT (of the abstract entered in Block 20, if different from Report)

18. SUPPLEMENTARY NOTES

19. KEY WORDS (Continue on reverse side if necessary and identify by block number)

Coastal engineering	Mathematical models
Coastal structures	Seismic safety
Edge waves	Tsunamis
Flood frequencies	Water waves

20. ABSTRACT (Continue on reverse side if necessary and identify by block number)

This report provides a source of state-of-the-art information on tsunami engineering. The report summarizes available information, identifies gaps in existing knowledge, and discusses methods of predicting tsunami flooding. The generating mechanisms of tsunamis and the method of determining the probability of occurrence are given.

(continued)

Because of the limited data available on tsunamis, numerical methods are commonly used to predict tsunami flooding of coastal areas. Finite-difference equations are presented for simulating the propagation of tsunamis, but computer programs are omitted because of the continuing work in progress and the availability of up-to-date computer programs from other sources. Known mathematical solutions, for tsunamis approaching the shoreline and tsunami-shoreline interaction, are given to illustrate the effects of tsunamis and provide means of verifying numerical results. The report discusses tsunami-structure interaction and illustrates various types of damage caused by tsunamis.

PREFACE

The high value and high utilization of the coastal zone require the establishment of flood levels that may occur as the result of various natural causes, and the consideration of preventive measures that can be used to minimize losses. This report, prepared as one of a series of reports to be published to form a Coastal Engineering Manual, is concerned with the effects of tsunamis on the coastal zone. Another report in the series, to be published separately, will be concerned with the effect of storm surges. The work was carried out under the coastal engineering research program of the U.S. Army Coastal Engineering Research Center (CERC).

The report was prepared by Dr. Frederick E. Camfield, Hydraulic Engineer, under the general supervision of R.A. Jachowski, Chief, Coastal Design Criteria Branch. The report was reviewed by Dr. F. Raichlen, California Institute of Technology; Drs. H.G. Loomis and L.Q. Spielvogel, Joint Institute of Marine and Atmospheric Research, National Oceanic and Atmospheric Administration; Drs. R.W. Whalin and J.R. Houston, U.S. Army Engineer Waterways Experiment Station; Dr. M. Fliegel, W. Bivins, and L.G. Hulman, Nuclear Regulatory Commission; Dr. R.J. Geller, Stanford University; and Dr. R.E. Meyer, University of Wisconsin. The author expresses his appreciation to the reviewers for their many helpful comments and suggestions.

Some of the background work on tsunami engineering was partially funded by the Nuclear Regulatory Commission.

Comments on this publication are invited.

Approved for publication in accordance with Public Law 166, 79th Congress, approved 31 July 1945, as supplemented by Public Law 172, 88th Congress, approved 7 November 1963.

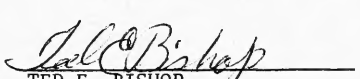

TED E. BISHOP
Colonel, Corps of Engineers
Commander and Director

CONTENTS

CONTENTS--Continued

TABLES

FIGURES

FIGURES--Continued

FIGURES--Continued

FIGURES--Continued

CONVERSION FACTORS, U.S. CUSTOMARY TO METRIC (SI)
UNITS OF MEASUREMENT

U.S. customary units of measurement used in this report can be converted to metric (SI) units as follows:

Multiply	by	To obtain
inches	25.4	millimeters
	2.54	centimeters
square inches	6.452	square centimeters
cubic inches	16.39	cubic centimeters
feet	30.48	centimeters
	0.3048	meters
square feet	0.0929	square meters
cubic feet	0.0283	cubic meters
yards	0.9144	meters
square yards	0.836	square meters
cubic yards	0.7646	cubic meters
miles	1.6093	kilometers
square miles	259.0	hectares
knots	1.852	kilometers per hour
acres	0.4047	hectares
foot-pounds	1.3558	newton meters
millibars	1.0197×10^{-3}	kilograms per square centimeter
ounces	28.35	grams
pounds	453.6	grams
	0.4536	kilograms
ton, long	1.0160	metric tons
ton, short	0.9072	metric tons
degrees (angle)	0.01745	radians
Fahrenheit degrees	5/9	Celsius degrees or Kelvins[1]

[1]To obtain Celsius (C) temperature readings from Fahrenheit (F) readings, use formula: $C = (5/9)(F - 32)$.

To obtain Kelvin (K) readings, use formula: $K = (5/9)(F - 32) + 273.15$.

SYMBOLS AND DEFINITIONS

A a coefficient
- area of uplifting
- projected area of body normal to flow direction

a wave amplitude
- a coefficient
- semimajor axis of ellipse
- interfocal distance of coordinate ellipses
- a distance from the shoreline = $(\sqrt{2} - 1)\, d_s/S$
- length of building in direction of flow

a_n variable used in determining movement of the sea surface

a_1 amplitude of incident tsunami; amplitude in deeper water

a_2 amplitude of tsunami at head of bay or inlet; resonant amplitude

B mean width of a harbor or inlet
- a coefficient

B_j a variable used in determining wave amplitude

B_1 width of outer bay or inlet

B_2 width of inner bay or inlet

b a coefficient
- width of building transverse to direction of flow
- semiminor axis of ellipse
- width of breakwater opening; entrance width of bay, harbor, or inlet

C wave celerity
- a coefficient

C_D drag coefficient

C_e a Mathieu function

C_F force coefficient

C_G group velocity

C_h Chezy roughness coefficient

C_M added mass coefficient

c maximum uplifted elevation
- a constant

c_d	drift speed of the node or antinode of an edge wave
c_R	a coefficient used in determining wave reflection at the shoreline
D	a coefficient
D_f	focal depth of earthquake
D_j	a variable used in determining wave amplitude
d	water depth •projected dimension transverse to direction of flow
d_a	average depth
d_h	average harbor depth
d_o	a length representative of water depth
d_p	depth of water at the point where a wave ray turns parallel to bottom contours
d_s	depth of water at toe of nearshore slope
d_1	depth of deeper water
d_2	depth of shallower water
E	energy
E_i	incident wave energy
E_r	reflected wave energy
E_t	transmitted wave energy
$\overline{E}_{n,ne}$	even Mathieu Transform
F	force
F_B	buoyant force
F_D	drag force
$\overline{F}_{n,ne}$	odd Mathieu Transform
f	friction factor
f_c	coriolis parameter = $2\Omega \cos \theta$

$f_{\beta(Z)}$	probability of an astronomical tide of elevation Z
g	acceleration due to gravity
H	wave height
H_i	incident wave height
$H_o^{(1)}$	zero-order Hankel function
H_r	reflected wave height
H_t	transmitted wave height
$\hat{H}$	wave height when the leading edge is at the shoreline
h	surge height ● uplifting height
$\overline{h}$	average height of uplifting
h_s	surge height at the shoreline
h_w	wall height ● wetted height on a structure
I	relative intensity of secondary undulations
j	an integer used for increments
K	R/h_s
K_n	a constant
K_r	coefficient of reflection = H_r/H_i
K_t	coefficient of transmission = H_t/H_i
k	an integer used for increments ● wave number = $2\pi/L$
k_o	wave number at lowest mode of resonance (Helmholtz mode)
L	distance normal to faultline over which vertical Earth movement occurs ● wavelength
L_b	length of bay, harbor, or inlet
L_c	length of harbor entrance channel

L_e effective length of harbor or inlet

L_f fault length

L_o wavelength at lowest mode of resonance (Helmholtz mode)

L_y longshore wavelength

L_1 wavelength in deeper water

L_2 wavelength in shallower water

ℓ length of slope connecting sea bottom to a shelf

ℓ_s distance across a shelf

M Richter magnitude of earthquakes
- moment

M_o momentum

m tsunami magnitude

N normalized horizontal water particle displacement

n Manning roughness coefficient

n(m) probability of tsunami with magnitude m being generated in any given year

P(Z) probability of runup to elevation Z

p pressure
- a coefficient in wave refraction

Q flow rate under a wave

q a coefficient in wave refraction
- velocity of a water particle under a wave

R a coefficient
- vertical height of runup above the stillwater level at the shoreline

$\overline{R}$ average runup height at a shoreline area

R_e radius of the Earth

R_s radius from the center of curvature to the shoreline

r	radial distance
r_p	radius from the center of curvature to where the wave ray turns parallel to the bottom contours
S	slope of sea bottom in direction of wave motion
S_1	slope of steep transition
S_2	slope of shelf
S_3	nearshore slope
Se_n	even Mathieu Function
So_n	odd Mathieu Function
s	distance along a wave ray
T	wave period
T_B	bottom shear stress
T_h	natural period of harbor inside breakwater
T_n	n^{th} mode of oscillation
T_r	component period of Earth vibration
T_1	period of bay or inlet
T_{1e}	natural period of inlet with effective length, L_e
t	time
t_s	time required for a wave to travel across a shelf
U	normalized wave amplitude ● $(H/d)(L/d)^2$
u	current or particle velocity in direction of wave motion ● velocity in the θ-direction (spherical coordinates)
u_s	current velocity of tsunami surge at the shoreline
u*	a convection term
V	volume of water

v	horizontal velocity in direction transverse to wave motion • velocity in the ϕ-direction (spherical coordinates)
w	velocity in the vertical direction
w^*	a convective term
x	horizontal coordinate in direction of wave motion
x_p	distance between the shoreline and the point where a wave ray turns parallel to bottom contours
y	horizontal coordinate in direction transverse to x-direction
Z	maximum scarp height
Z_o	depth of wave generation
Z_1	a parameter used in wave reflection and transmission
z	vertical coordinate
α	dimensional constant • correction term for harbor entrance channel length
α_1	angle in wave refraction between the incident wave ray and an orthogonal to the contour of the sea bottom
β	angle of the beach slope • wave ray separation distance • angle of nearshore slope given in radians • dimensional constant
γ	specific weight of water • an edge wave parameter
γ_r	dimensionless amplitude
Δ	an incremental distance
δ	a small value
δ_r	dimensional constant
ε	an arbitrary increment • H/d
$\zeta(x,t)$	vertical movement of sea bottom
η	water surface elevation above still water at an arbitrary point

$\eta(x,t)$	vertical movement of sea surface
θ	angle in polar coordinates • angle of inclination of water surface at front of surge • degrees latitude measured from the pole
θ_1	angle of incident wave ray • a constant
θ_2	angle of transmitted wave ray • a constant
ξ	horizontal displacement of a water particle
ρ	density • dimensionless distance from the shoreline = x/a
σ	d/L
σ_γ	$2\pi/T_\gamma$
ϕ	longitude of a point
$\phi(t)$	variable used in determining movement of the sea surface
χ	dimensionless distance measured seaward from the shoreline
ψ	latitude of a point
ψ_1	wave radiation function
ψ_2	wave radiation function
Ω	an arbitrary function • rotational speed of the Earth in radians per second

TSUNAMI ENGINEERING

by
Frederick E. Camfield

I. INTRODUCTION

The term *tsunami* is derived from two Japanese words: "tsu," meaning harbor, and "nami," meaning wave. Tsunamis, or seismic sea waves, have very long periods and are not easily dissipated. The waves may create large surges or oscillations in bays or harbors which are not responsive to the action of normal sea waves. In the original definition, the term tsunami was applied to all large waves, including storm surges. However, recent definitions have limited its application to waves generated by tectonic or volcanic activity. Western literature previously referred to these waves as tidal waves or seismic sea waves, but those terms have generally been replaced by the term tsunami.

Tsunamis are primarily created by disturbances in the crust of the Earth underlying bodies of water, and the resulting uplifting of the water surface over a large area which forms a train of very long-period waves. The waves may have periods exceeding 1 hour, in contrast to normally occurring wind-generated sea waves which have periods less than 1 minute. When tsunamis are generated by volcanic activity or landslides, the wave energy tends to spread along the wave crests and the tsunamis affect mainly the areas near their source. Tsunami waves generated by tectonic uplifting may travel across an ocean basin, causing great destruction at locations far from their source.

Because of the potential destructive effects of tsunamis, it is necessary to understand the mechanisms of their generation and propagation, and to be able to predict the extent of flooding and the effect of wave forces in coastal areas subject to tsunami attack. Proper control must be exercised over the use of such areas, and in designing structures to be placed in these areas. Also, sufficient warning of a tsunami attack must be given to people located in these areas, and procedures must be established for an orderly evacuation when necessary.

This report discusses the prediction of tsunami effects in coastal areas and attempts to provide guidance in determining the flooding and wave forces at any particular location. The present knowledge of tsunamis and the deficiencies in this knowledge are summarized.

1. Nature and Origin of Tsunamis.

Areas of seismic activity which could potentially generate tsunamis are shown in Figure 1. The major part of this activity occurs along the boundaries of the Pacific Ocean, with other regions of strong activity primarily concentrated in the Caribbean and Mediterranean areas. Van Dorn (1965) indicates that the Japan Trench radiates detectable tsunamis at the rate of about one per year. Lesser amounts of activity occur elsewhere.

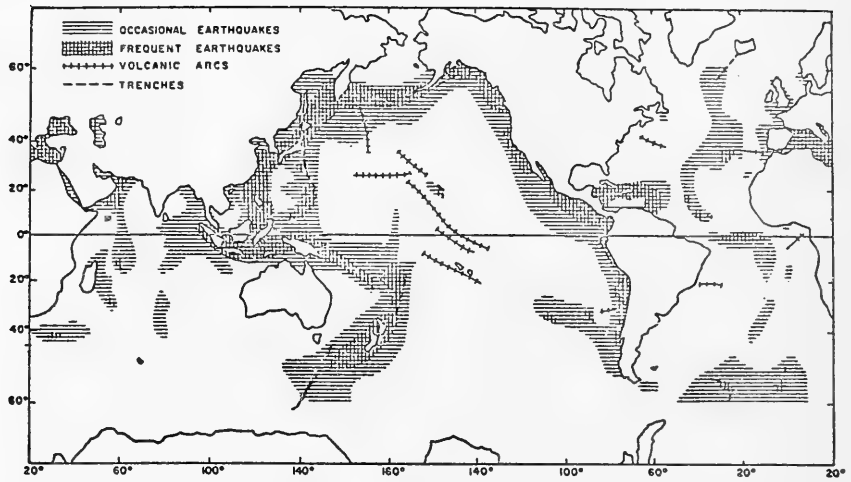

Figure 1. Oceanic zones of recent earthquake activity, showing association with trench systems and island arcs. Pacific preponderance is apparent (from Van Dorn, 1965).

Tsunamis can be generated in any coastal area, including inland seas and large lakes. Spaeth (1964) provides an extensive bibliography on tsunamis. The Appendix summarizes the occurrence of tsunamis from 1891 to 1961, using Spaeth's data and some additional information from Heck (1947), Ambraseys (1965), Pararas-Carayannis (1969), and Cox, Pararas-Carayannis, and Calebaugh (1976). Part of Ambraseys' information has been omitted because of the lack of verification. Tsunamis occurring between 1962 and the present are not listed because a complete summary is not readily available.

Good records are available for more recently occurring tsunamis, particularly in the present century; however, records of tsunamis in past centuries are mostly based on accounts of personal observations. The dates that tsunamis occurred have often been confused with the dates on letters or other accounts rather than the date of the actual event. There have also been many errors in interpreting these older accounts, particularly when translating from one language to another. Soloviev and Ferchev (1961) refer to the reports of an event in 1827 at the Komandorskiye Islands, located between Kamchatka and the Aleutian Islands, Alaska. A Russian expedition, under the command of F.P. Lutke, reported the occurrence of an earthquake and noted that earthquakes were sometimes accompanied by a rise in water level. The original Russian report was translated in French, then into German, then into French, and back into Russian again. The final translation indicated that a tsunami had occurred along with the 1827 earthquake.

A similar instance of errors in interpretation and translation occurred in the reports of an 1840 event at Santa Cruz, California. Heavy rain and high waves caused by a storm resulted in considerable damage. The collapse of buildings caused by flooding from the rain was misinterpreted as an earthquake, and the waves as a tsunami. Holden (1898) reported this as an earthquake and tsunami, when in fact neither occurred.

Consideration must also be given to the fact that records based on visual observations may not include all tsunamis which occurred. The observers probably gave special notice only to those waves which caused substantial flooding or large, rapid variations of the water level in bays and harbors. At a location where the normal tidal range was of the same order as the tsunami height, a tsunami occurring at a low tide stage may have been given only passing notice, if noticed at all, while the same tsunami occurring at a high tide stage would have been recorded as a major tsunami. Likewise, the occurrence of a tsunami in conjunction with high storm waves would have caused more flooding, and therefore, may have been given more significance in the records than a tsunami occurring during a relative calm.

Records of tsunamis in the Mediterranean and Middle East include theories on the eruption of Thira (also known as Santorini) and the tsunami on the coast of Crete that destroyed the Minoan Empire circa 1400 B.C. Factual accounts of tsunamis extend back at least 2,000 years. Accounts of tsunamis in Japan extend back at least 1,300 years. In contrast, records of tsunamis originating in the Chile-Peru coastal areas only cover about 400 years (from 1562 to present), those originating in Alaska about 200 years (from 1788), and those occurring in Hawaii slightly more than 150 years (from 1813). Few records are available of tsunamis occurring on the California-Oregon-Washington coastline. Holden (1898) indicates tsunamis occurred at points on the California coastline in 1812, with various occurrences at later dates, mainly recorded or observed at San Francisco. Townley and Allen (1939) provide similar information.

Knowledge of the action of more recent tsunamis can be helpful in evaluating historical information. Although no record exists of major tsunamis on Puget Sound in Washington State, the *Puget Sound Weekly* (1866) reported that a tide, the highest ever recorded, occurred at Port Townsend, Washington, on 20 December 1866. The report stated, "The main street was filled with drift logs, and the dwellers on lower floors were compelled to elevate to the next story." Camfield's (1975) article on historical accounts gives the date as 27 December 1866. Kelly (Seattle, Washington; personal communication, 1979) also gives the year as 1866. Neither Holden (1898) nor Townley and Allen (1939) report a tsunami occurrence in 1866; both list a 26 December 1856 date, with no additional details, which was probably an incorrect report of the 1866 event. The historical accounts describing a gradual rise in water level indicate this was probably a tsunami, but the origin is unknown.

Although tsunamis occur frequently in the Caribbean, they are much less frequent in the North Atlantic Ocean. The only major recorded tsunami along the east coast of the United States and Canada was the tsunami which devastated the Burin Peninsula along Placentia Bay, Newfoundland, in November 1929. At least 26 lives were lost (Jaggar, 1929). The tsunami was enhanced by an exceptionally high tide and high storm waves; otherwise, it may not have been of major proportions (Hodgson and Doxsee, 1930). This tsunami was reported to have had a height of 0.31 meter (1 foot) at Atlantic City, New Jersey (Murty and Wigen, 1976).

Stein, et al. (in preparation, 1980) report on earthquakes in eastern Canada from Baffin Island to Newfoundland. For the 1929 Grand Banks earthquake, which generated the tsunami, they give a magnitude of 7.2 as reported by Gutenberg and Richter (1965). Stein, et al. suggest that the earthquakes in this area are associated with basement faults which have been reactivated by the removal of Pleistocene glacial loads.

Earthquakes frequently occur in the eastern United States. These include a large earthquake that occurred in New England on 18 November 1755, shortly after the November 1755 earthquake near Lisbon, Portugal (Reid, 1914), and the earthquake near Charleston, South Carolina, on 31 August 1886 (Taber, 1914). All of the earthquakes in the eastern United States have occurred inland from the coastline. The probability of an earthquake having an epicenter in a location that would cause a tsunami, either on the coastline or in an estuary, cannot be determined from available data. Brandsma, Divoky, and Hwang (1979) give probable maximum waves for tsunamis at points near both the Atlantic and Pacific coasts of the United States. Their results are based on mathematical simulation of extreme events.

The only tsunamis of record that traveled across the North Atlantic were those generated near Lisbon, Portugal, in 1755 and 1761. Both of these were recorded on the south coast of England, as well as in the West Indies (Davison, 1936). For comparison, the 1755 tsunami had a maximum rise of 2.4 meters (8 feet) at Penzance (England) and flowed over the wharves and streets at Barbados (West Indies). In 1761, the sea rose about 1.8 meters (6 feet) at Penzance and 1.2 meters (4 feet) at Barbados. Other runup heights in 1755 were estimated at 4.9 meters (16 feet) on the coast of Portugal, 18 meters (60 feet) at Cadiz (Spain), 1.8 meters (5.9 feet) at Gibralter, 15 meters (50 feet) at Tangier (Morocco), 5.6 meters (18 feet) at Madeira, 14.6 meters (48 feet) at Faial (the Azores), 2.5 meters (8.2 feet) at St. Ives (England), 3.7 meters (12 feet) at Antigua (West Indies) 6.4 meters (21 feet) at Saba (West Indies), and the waves overflowed the lowlands on the coasts of Martinique and other French islands.

In general, good data are available for only a limited number of tsunamis. A major gap in the data is tsunami heights in deep water. Because of this gap, only limited verification is available for numerical models for propagating tsunamis across large oceanic distances.

Because of the frequency of tsunamis occurring in the Pacific Ocean, a tsunami warning system has been developed for the inhabitants of Pacific coastal areas. A similar warning system has not been developed for other areas.

2. Probability of Occurrence.

Where sufficient historical data are available on tsunami flood levels, the probability of tsunami flooding at any elevation can be determined by the same methods used for determining the probability of floods on rivers. For a known period of record, the recorded flood levels can be ranked from the largest to the smallest; i.e., the highest flood level is ranked 1, the next highest is ranked 2, and so on. Linsley, Kohler, and Paulhus (1958) show that the probability of each flood level is then given by

$$P(Z) = \frac{m}{n + 1} \tag{1}$$

where

$P(Z)$ = the probability of flooding to the elevation Z in any year

Z = the elevation above a defined datum

m = the rank of the flood level

n = the period of record in years

Houston, Carver, and Markle (1977) have determined the probability of tsunami flood levels for the Hawaiian Islands. For recurrence intervals greater than 10 years, i.e., $P(Z) < 0.1$, they give

$$h_{200} = -B - A \log_{10} P(h_{200}) \tag{2}$$

where h_{200} is the elevation of the maximum tsunami wave crest above mean sea level (MSL) 200 feet (61 meters) shoreward of the coastline, $P(h_{200})$ the probability of a flood level occurring at elevation h_{200} in any given year, and A and B the empirical coefficients which are determined for each point on the coastline. Where sufficient historical data were not available, they generated additional data using a mathematical model. The model data were multiplied by correction factors and compared to historical data. This produced additional data at points along the coastline where historical data were not available, and allowed a determination of the empirical coefficients A and B at all coastal points.

It should be noted that there is a probability of some error in the predicted flood elevations based on available historical data. For example, there is a 37-percent probability that a 100-year flood level

(i.e., a flood level with a recurrence interval of 100 years) will not occur in any period of 100 years. Therefore, a 100-year flood level predicted from a 100-year period of record may be too low. Also, there is a 9.5-percent probability that a 1,000-year flood level will occur at least once in any period of 100 years. Therefore, the predicted 100-year flood level, based on a 100-year period of record, may be too high.

Confidence limits for the predicted flood levels can be obtained using methods similar to those used for river flood levels. However, rivers have a seasonal variation in flow, so a 1-year time increment is significant in that case. In the case of tsunamis, the 1-year time increment is a convenient means of measuring time, but there is no particular relationship between this time increment and the generation of tsunamis. Methods used for obtaining confidence limits for tsunami flood levels should give the same results, regardless of the chosen time increment.

Beard (1962) notes that there is a 5-percent probability that the magnitude of the difference between the real flood level and the predicted flood level will be greater than or equal to twice the standard error. Assuming there is an equal chance of the real flood level being either greater than or less than the predicted value gives +2.5- and -2.5-percent confidence limits.

Where no historical data are available, data may be constructed entirely from a computer model by assigning magnitudes to various tsunamis in the mathematical model, and by determining the probability of generation for each tsunami magnitude. However, the results will not have the same degree of accuracy.

An exact relationship between tsunami magnitude and earthquake magnitude has not been determined. Iida (1961) proposed that tsunamis could be assigned a magnitude based on their energy (the energy of the generated waves), with an increase in magnitude of 0.5 being equal to a doubling of the energy. He also related the tsunami magnitude to the maximum runup height in meters at the shoreline area experiencing the strongest tsunami action (Iida, 1970). The relationship between the runup height R_{max} and the tsunami magnitude m is shown in Figure 2. The dashlines show the range of the expected maximum runup, based on Iida's data, due to differences in the characteristics of the individual tsunamis and coastal areas.

Soloviev (1970) revised the definition of tsunami magnitude by relating it to the average runup height $\overline{R}$ (in meters) at the shoreline area experiencing the strongest tsunami action. This tends to average out any high runup heights related to a particular coastal feature, and should be more representative of the actual tsunami energy. Soloviev does not indicate the length of coastline to be used in the average, but does provide an equation for the magnitude as

$$m = \log_2 (\sqrt{2}\,\overline{R}) \qquad (3)$$

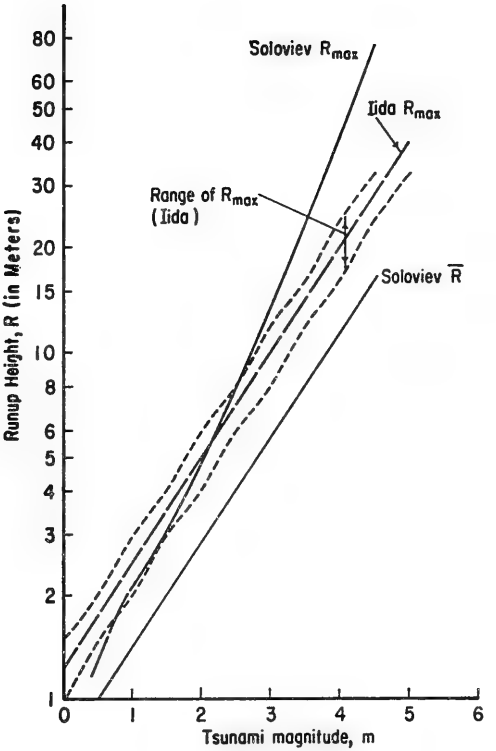

Figure 2. Wave height versus tsunami magnitude.

As shown in Figure 2, Soloviev's scale gives a more rapid increase in maximum wave height than Iida's scale for a given change in tsunami magnitude. This indicates that an increase in magnitude on Soloviev's scale would represent a greater increase in tsunami energy than an equivalent increase in magnitude on Iida's scale.

Abe (1979) suggests that the tsunami magnitude can be represented as a function of the average runup height and a constant which is dependent upon the source region and the station where the tsunami is measured. He shows that the magnitude, obtained by this means, can be related to the seismic moment.

The probability n(m) of a tsunami with magnitude m being generated in any given year in a specified generating area is given by the empirical equation

$$n(m) = ae^{-bm} \tag{4}$$

where the coefficients a and b are determined by a least squares analysis of the available data for the generating area. To calculate probabilities tsunamis may be placed in groups; e.g., a *group of tsunamis* shown with magnitude 3.75 actually includes all tsunamis with magnitudes from 3.5 to 4.0, etc. To analyze the probability of an *individual tsunami* having a magnitude greater than or equal to 3.5, the probabilities would be summed

$$\sum_{j=o}^{2} n(3.75 + 0.5j) = n(3.75) + n(4.25) + n(4.75) \qquad (5)$$

which would include all tsunamis with magnitudes from 3.5 to 5.0. It should be noted that the stress in rock cannot exceed some maximum value; the rock will fracture when the stress reaches that value.

Abe (1975) and Geller (1976) show from empirical results that the fault length of earthquakes is approximately equal to twice the fault width. Using these results and the model of Haskell (1969), Geller gives a maximum earthquake magnitude, M, of 8.22. Because of variations in the assumed fault length-to-width ratio, actual earthquake magnitudes may exceed this value slightly; Geller lists a magnitude of 8.5 for the 1964 Alaska earthquake. However, as noted by Geller, the maximum magnitude occurs because the conventional magnitude scale is saturated and ceases to give a meaningful measure of the earthquake size.

It is assumed that tsunamis do not occur with magnitudes greater than 5.0 where the tsunami magnitude has some relationship to earthquake magnitude as mentioned previously. If tsunami magnitude is related to seismic moment, defined by Kanamori (1972) as a function of rigidity, fault area and average fault slip, Kanamori and Cipar (1974) indicate that the 1960 Chilean earthquake had the largest seismic moment ever reliably determined (2×10^{30} dyne-centimeters).

The method for grouping tsunamis (eq. 5) has been utilized by Houston and Garcia (1974), using statistics for the entire trench along the Chilean coast. Applying revised information for that particular generating area, a major source of tsunamis in the western United States (Houston and Garcia, 1978), a = 0.074 and b = 0.63. Taking the value m = 3.5 for the magnitude of a design tsunami (to be used for determining potential runup in coastal areas), the probability for a tsunami with a magnitude of 3.5 or greater being generated in any given year is

$$n(3.5) = 0.074 \left[e^{-0.63(3.75)} + e^{-0.63(4.00)} + e^{-0.63(4.75)}\right] \qquad (6)$$

which gives a value of 0.0166 or a recurrence interval of 60 years. For a 412-year period for the Chilean coast, the prediction would be seven tsunamis of magnitude 3.5 or greater. This agrees with historical records of tsunamis in this area.

Another major source of tsunamis in the western United States is the Aleutian Trench. Only relatively recent records exist for the area. Analysis of these records by Houston and Garcia (1974), as revised in Houston, et al. (1975b) and Houston and Garcia (1978), gives

$$n(m) = 0.113^{-0.71\ m} \tag{7}$$

which is similar to the previous equation for the Peru-Chile Trench. The probability of tsunami occurrence is assumed to be uniform along the trench. The distribution of recent earthquakes along the Aleutian Trench is shown in Figure 3, and the mean annual number of earthquakes of any given magnitude in Figure 4. The straight lines in Figure 4 are not accurate above an earthquake magnitude, M, of about 8.5 because of the physical limits on allowable stresses in the rock forming the Earth's crust. Also, the straight lines in Figure 4 representing the occurrence of earthquakes in Alaska and the world would intersect at an earthquake magnitude of about 2.5, so the plotted lines should not be extrapolated to values of earthquake magnitude less than those shown.

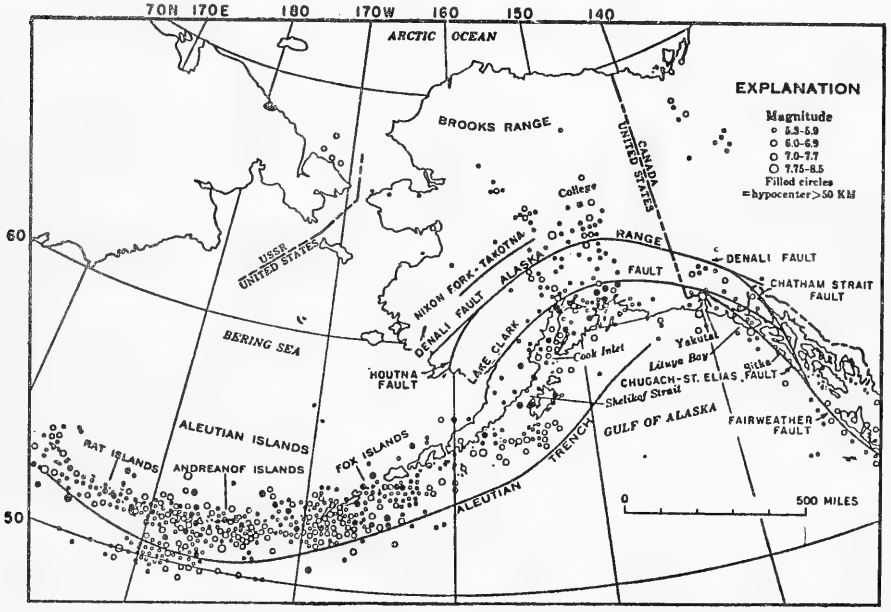

Figure 3. Principal fault systems and distribution of epicenters of major Alaskan earthquakes, 1898-1961 (from Wilson, 1969; adapted from Davis and Echols, 1962).

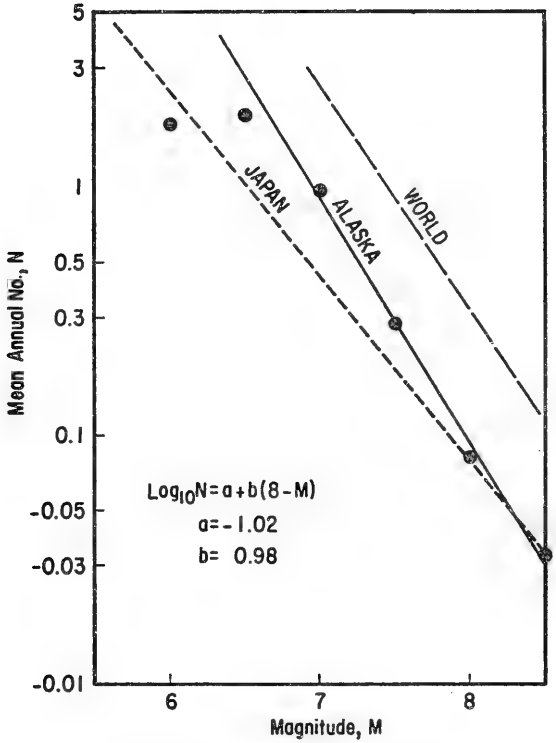

Figure 4. Mean annual occurrence of shallow-focus earthquake shocks for the Aleutian and southeastern Alaska region (from Wilson, 1969; adapted from Berg, 1964). Trends of World and Japanese data are inserted for comparison.

Using equation (7), the probability of a tsunami with a magnitude of 3.5 or greater is

$$n(3.5) = n(3.75) + n(4.25) + n(4.75) \tag{8}$$

which gives a value of 0.0174 for the Aleutian Trench. This value is based on a relatively short period of data for large tsunamis only. Dividing the trench into 12 segments gives the probability of 0.00145 for a tsunami of the given magnitude of 3.5 or greater to be generated at any particular segment of the trench in any given year, assuming an equal probability for each segment. The general equation for a particular segment of the trench becomes

$$n(i) = 0.0094\ e^{-0.71\ i} \tag{9}$$

To determine the probability of runup of a given height at a given location along the coastline, it is necessary to propagate tsunamis across the ocean by numerical means from each segment of the trench for all tsunami magnitudes (i.e., i = 2.0, 2.5, 3.0, 3.5, 4.0, 4.5, and 5.0). The wave train of each tsunami must be superimposed on segments of the tidal cycle of an interval equal to the duration of the wave train. This superposition must be made for each tidal segment of that interval for a 1-year period, and the probability of the resulting runup determined. Tidal variations are discussed by Harris (in preparation, 1980). A cumulative probability can then be established for runup at a particular site.

Determining the probability of tsunami runup at a particular coastal location for tsunamis generated in the Aleutian Trench area, would require the numerical generation of 84 tsunamis (12 segments of trench and 7 intensities of each segment). As shown by Houston and Garcia (1974), each runup value has an associated probability, and the totality of runup values at a given shoreline point defines a probability distribution from which the cumulative probability distribution, $P_S(Z)$, can be obtained for runup greater than or equal to a particular value.

By approximating the probability $f_\beta(Z)$ of the astronomical tide by a Gaussian distribution (Petrauskas and Borgman, 1971; Houston and Garcia, 1974), the probability of runup to a given elevation is given by

$$P(Z) = \int_{-\infty}^{\infty} f_\beta(\lambda)\, P_S(Z - \lambda)\, d\lambda \qquad (10)$$

Probabilities for tsunami runup can then be determined at each coastal point, combining the tsunami with the astronomical tide.

An analysis similar to that used for the Aleutian Trench could be applied to tsunamis generated in other source areas. For the west coast of the United States (excluding Hawaii), only the Aleutian Trench and the Peru-Chile Trench appear to produce significant tsunami runup, although Holden (1898) indicates some occurrence of tsunamis from sources along the California coastline. Using numerical results obtained for tsunamis generated along the Aleutian and Peru-Chile Trenches, Houston and Garcia (1978) have determined probable 100- and 500-year tsunami flood elevations for the west coast of the continental United States.

II. THE GENERATION OF TSUNAMIS

Tsunami-type waves can be generated from a number of sources, including shallow-focus submarine earthquakes, volcanic eruptions, landslides and submarine slumps, and explosions. Each of these sources has its own generating mechanism, and the characteristics of the generated waves are dependent of the generating mechanism. The tsunami waves which travel long, transoceanic distances are normally generated by the tectonic activity associated with shallow-focus earthquakes. However, large waves can be generated locally by the other generating mechanisms.

1. Submarine Earthquakes.

As shown by Iida (1970), tsunamis are generated by shallow-focus earthquakes of a dip-slip fault type; i.e., vertical motion upward on one side of the fault and downward on the other side (Fig. 5). Shepard, MacDonald, and Cox (1950) indicate that tsunamis which travel long distances across the ocean are probably caused by unipolar disturbances. (An example of a unipolar disturbance would be the uplift of a large area of the sea floor where there is a net change in volume.) Waves generated from a unipolar source decay much less rapidly with distance than waves generated by a bipolar disturbance; i.e., a combination uplifting and subsidence, or other apparent transfer of material on the sea floor, without a net change in volume. Hammack and Segur (1974) studied the propagation of waves both experimentally and numerically. They indicate that where there is a positive net change in volume (e.g., a unipolar uplifting of the sea floor), waves of stable form (solitons) evolve, followed by a dispersive train of oscillatory waves. The number and amplitude of the solitons depends on the initial generating mechanism. The wave record for the 1964 tsunami at Wake Island (see Fig. 6) illustrates this type of wave generation. Van Dorn (1965) discusses the generating mechanism of the 1964 tsunami which originated in Alaska. The ground motion was dipolar, having a positive pole (uplifting) under the sea and a negative pole predominantly under the land. As the positive pole was the main tsunami-generating mechanism, this was equivalent to a unipolar source.

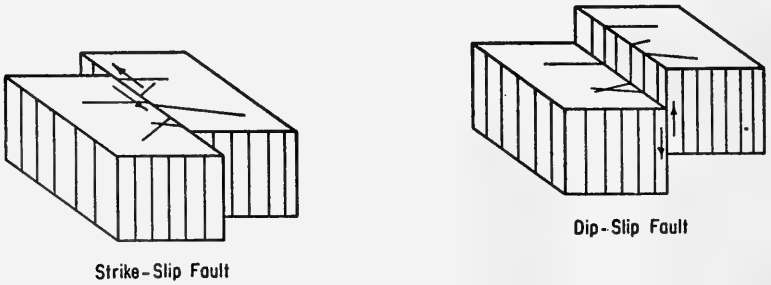

Figure 5. Movement along faultlines.

Heck (1936) indicates that horizontal motion of the sea floor does not appear to generate large tsunamis. However, large "local" tsunamis may be generated by horizontal motion. Iida (1970) shows that major tsunamis (those that cause high water levels at many different coastal locations) do not appear to occur as the result of deep-focus earthquakes or the strike-slip fault type, i.e., horizontal motion along the faultline (Fig. 5). A general expression for the lower limit of the earthquake magnitude, M, of tsunamigenic earthquakes is given by Iida (1970) as

$$M = 6.3 + 0.005\ D_f \qquad (11)$$

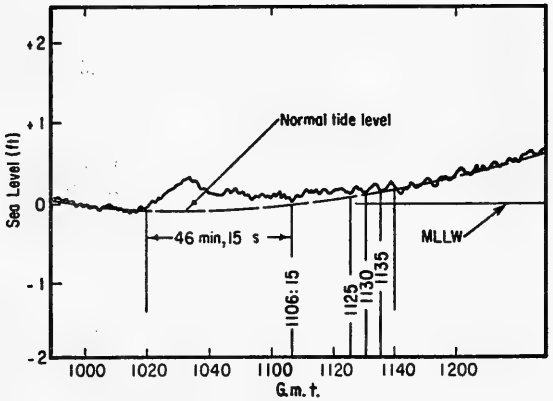

Figure 6. Wave record from Wake Island, showing arrival of tsunami (initial motion is positive and remains above normal tide curve for more than an hour) (from Van Dorn, 1964).

based on tsunamigenic earthquakes in Japan, where D_f is the focal depth in kilometers and M the magnitude on the Richter scale. Tsunamis usually do not occur for earthquake magnitudes less than that given by equation (11), although a small number of tsunamis of lesser magnitude have been associated with lesser magnitude earthquakes. It should be noted that equation (11) does not consider the location of the earthquake with respect to the coastline, the configuration of the coastline, and possible local resonance effects. The Richter scale is given by

$$M = \frac{(\log E - 11.8)}{1.5}$$

where E is the earthquake energy in ergs.

Geller and Kanamori (1977) note that care must be taken when defining earthquake magnitude. Richter (1958) gives higher values for earthquake magnitudes than those listed by Gutenberg and Richter (1954). The difference results from the relationships used to determine earthquake magnitudes from surface wave magnitudes and body wave magnitudes.

Attempts have been made to define lower limits for earthquake magnitudes associated with disastrous tsunamis. However, the definition of "disastrous tsunamis" may be more a function of the location of the origin and the population in the adjacent coastal zone, rather than an analysis of the actual waves generated. Also, the equations developed to define these limits are based on limited data and do not fully consider coastal configurations and resonant effects.

A tsunami generated from a dip-slip fault source will have the characteristics of being generated from a line source; i.e., the length

of the generating area is much greater than the width. When displacement occurs along a substantial length of faultline, the divergence of the wave rays of the generated wave (i.e., the spreading of wave energy along the wave crest) will be much less than for a wave generated from a small source. For a "locally" generated wave, i.e., a wave generated near the coastline under consideration, the main component of the wave energy will travel perpendicular to the faultline and the energy per unit length of wave crest would remain approximately constant for an unrefracted wave.

2. Volcanic Activity.

Although most major tsunamis have been caused by shallow-focus earthquakes, a small percentage have been caused by volcanic activity which includes localized earthquakes, shoreline and submarine slumps, and volcanic explosions. Examples of these are the volcanic activity of April 1868 and November 1975 in Hawaii, with associated earthquakes off the southeast coast of the island of Hawaii, and the August 1883 eruption and explosion of the island of Krakatoa near the Sunda Strait in Indonesia. The explosion of Krakatoa destroyed an estimated 8 cubic kilometers (1.92 cubic miles) of the island. Large shoreline subsidences were associated with the eruptions and earthquakes on Hawaii.

Tsunamis with volcanic origins have the characteristics of waves generated from a small source area. These waves spread geometrically and do not cause large wave runup at locations distant from the source, but may cause very large waves near the source. Also, there may be refraction effects which trap waves along the coastline, or standing edge waves may be generated along the coastline.

Both the 1868 and the 1975 tsunamis in Hawaii caused high waves at points on all sides of the island of Hawaii as well as waves on the other islands (Pararas-Carayannis, 1969; Pararas-Carayannis, International Tsunami Information Center, personal communication, 1975). The 1975 waves persisted for more than 4 hours at all points. Meyer (Department of Mathematics, University of Wisconsin, personal communication, 1975) indicated that trapped waves may exist with many nodes around the island. These trapped waves would gradually decay, leaking energy to the surrounding ocean.

3. Landslides and Submarine Slumps.

Landslides and submarine slumps can occur from various causes, but are often associated with earthquakes. The waves generated by such events will spread geometrically as they propagate from their source in an open ocean, but can be very high near their origin. Waves can be particularly high if they occur in a confined inlet, or if resonant or refraction effects exist.

Examples of landslide-generated waves have been reported by Miller (1960) for Lituya Bay, Alaska, in 1853, 1874, 1936, and 1958. The 1958

wave reached an estimated maximum surge elevation of 530 meters (1,740 feet) on the opposite side of the bay, and generated a 61-meter-high wave seaward in the bay. Waves were also generated by icefalls in Yakutat Bay, Alaska, in 1845 and 1905. Jorstad (1956), as referenced by Wiegel (1964), reported on landslide-generated waves in Tafjord, Norway, in 1718, 1755, 1805, 1868, and 1934.

An example of a wave generated by a shoreline slump is given in Berg, et al. (1970). A survey of the Valdez, Alaska, area after the March 1964 earthquake showed that the water depth at the end of the Valdez Dock had increased from 9 to 37 meters (30 to 120 feet), destroying the dock. Also, at a small-craft harbor breakwater, the water depth increased from 2.7 to 27 meters (9 to 90 feet), destroying the breakwater. The owner of a fishing boat, heading toward the Valdez Narrows from the open sea, reported a wave 10.7 to 15 meters (35 to 50 feet) high, in the narrows, which dispersed after passing the narrows.

The first wave to hit Valdez was generated by the slump of the waterfront, and the second wave by the slump of a shoreline area some distance away. After about 5 to 6 hours, a third wave arrived, followed more than 2 hours later by a fourth wave. These later waves apparently resulted from some reflection or resonant effects within Prince William Sound.

Ambraseys (1960) indicated that the tsunami of 9 July 1956 in the Greek Archipelago was probably produced by a series of landslides on the steep banks of a submarine trench. The wave had an amplitude of 30 meters (100 feet) near its source. Striem and Miloh (1975) report that tsunamis have probably been generated by slumping of the continental slope off the coast of Israel. Van Dorn (1965) indicates that tsunamis generated from this type of source appear to be fairly localized and will not be large at long distances from the source. The generating mechanism is extremely inefficient, and only about 2 percent of the potential energy of a falling or sliding weight is converted into wave energy.

4. Explosions.

An explosion acts as an impulsive-generating mechanism which generates dispersive waves from a point source. Data from nuclear explosion Baker at Bikini Atoll in 1946 show that the wave height is approximately inversely proportional to the radial distance from the point of origin; i.e., Hr = constant where H is the height of the wave, and r is the radial distance from the point source. At a radial distance equal to $35d$, where d is the water depth, the relationship changes slightly, with the wave height decreasing less rapidly. Wilson (1963) discusses data on wave dispersion.

The height of a wave generated by an explosion has been shown to be dependent on the depth of the explosion charge. Van Dorn, Le Mehaute, and Hwang (1968) show that two critical depths exist which will produce the highest waves for any given explosive charge. The critical depths are dependent on the charge yield, given in equivalent pounds of TNT.

Extensive material is available on waves generated by explosions, and will not be considered further here (see Smith, 1967).

III. MECHANICS OF GENERATION

The generation of large, transoceanic tsunamis results from the displacement of water above the area of uplifted sea bottom associated with a dip-slip fault movement. Crustal displacement progresses along a faultline from some initial source. Ben-Menahem (1961) developed a method for determining the direction, speed, and length of rupture propagating from the epicenter of a given earthquake by using recorded seismic surface waves. Various analyses using this method, as reported in Berg, et al. (1970) for the 1964 Alaskan tsunami give speeds from 3.0 to 3.5 kilometers (1.9 to 2.2 miles) per second for rupture propagation and a rupture length of from 600 to 800 kilometers (370 to 500 miles). Because of the high speed of rupturing, it is generally assumed in analyzing wave generation that the total uplifting occurs instantaneously.

1. Area and Height of Uplifting.

Very little data are available on the size of the generating areas and the height of uplifts for various tsunamis which have been recorded at coastal points. After the 1964 tsunami generated in Alaska, extensive surveys were undertaken in the area of origin (Plafker, 1965; Berg, et al., 1970). These surveys included comparisons of tide levels at surviving tide gages, establishment of previous tide levels by visual observation and interviews with area residents, new hydrographic surveys in areas previously surveyed, establishment of new elevations at bench marks, and measurement of the displacement of sessile marine organisms. The uplifted water area on the Continental Shelf was estimated as 1.1×10^{11} square meters (1.184×10^{12} square feet). The potential energy of an incremental area of uplifting is proportional to h^2, where h is the height of uplifting. The average value of h^2 was estimated as 4.1 square meters (44.1 square feet). The uplifted area in Prince William Sound was considered to have a limited effect on the tsunami generation because of the restricted connections between the sound and the shelf area.

An uplifting of the sea bottom will produce a vertical uplifting of the overlying water. As a first approximation, it may be assumed that the uplifting of the water surface equals the uplifting of the sea bottom. The potential energy of the uplifted water is then given as

$$E = \sum_{i=1}^{n} \rho g A_i h_i \frac{h_i}{2} \qquad (13)$$

where

E = the energy in ergs (foot-pounds)

ρ = the density of the seawater and is assumed to equal 1.0252 grams per cubic centimeter (1.989 slugs per cubic foot)

g = gravitational acceleration and is equal to 980.7 centimeters (32.174 feet) per second squared

A_i = an incremental area of uplifting

h_i = the height of uplifting over the incremental area A_i

If the incremental areas are equal, i.e., $A_1 = A_2 = \ldots = A_n$, then equation (13) can be rewritten as

$$E = \rho g A_i \sum_{i=1}^{n} \frac{h_i^2}{2} \tag{14}$$

or, alternatively,

$$E = \rho g n A_i \sum_{i=1}^{n} \frac{h_i^2}{2n} \tag{15}$$

Noting that the total area, A, is given by

$$A = n A_i \tag{16}$$

and that

$$\sum_{i=1}^{n} \frac{h_i^2}{2n} = \frac{h_1^2 + h_2^2 + \ldots + h_n^2}{2n} = \frac{(h^2)_{avg}}{2} \tag{17}$$

equation (15) becomes

$$E = \rho g A \frac{(h^2)_{avg}}{2} \tag{18}$$

where $(h^2)_{avg}$ is the average value of the square of the uplifted heights.

For the 1964 Alaskan earthquake the height of uplifting varied considerably over the area of uplifting, and had a maximum in excess of 15 meters (49 feet) at a point near Montague Island (Malloy, 1964). The tsunami had a calculated potential energy of 2.26×10^{22} ergs (1.67×10^{15} foot-pounds).

When using equation (18) it must be remembered that the average of the height squared, $(h^2)_{avg}$, is not equal to the average height squared, $(h_{avg})^2$. This is easily illustrated by the following example problem.

* * * * * * * * * * * * * EXAMPLE PROBLEM 1 * * * * * * * * * * * * * *

GIVEN: An area of uplifting is divided into five equal-sized areas of 2.3×10^{12} square centimeters (2.48×10^{9} square feet), with upliftings of 30, 60, 90, 120, and 150 centimeters, respectively.

FIND:

(a) The value of $(h_{avg})^2$,

(b) the value of $(h^2)_{avg}$, and

(c) the potential energy of the uplifted seawater.

SOLUTION:

(a) $h_{avg} = \frac{30 + 60 + 90 + 120 + 150}{5} = 90$ centimeters

$(h_{avg})^2 = 8{,}100$ square centimeters (8.72 square feet)

(b) $(h^2)_{avg} = \frac{30^2 + 60^2 + 90^2 + 120^2 + 150^2}{5}$

$(h^2)_{avg} = \frac{49{,}500}{5} = 9{,}900$ square centimeters (10.66 square feet)

(c) From equation (16),

$$E = \rho g A \frac{(h^2)_{avg}}{2}$$

$$E = (1.0252)(980.7)(5)(2.3 \times 10^{12}) \frac{9{,}900}{2}$$

$E = 5.72 \times 10^{19}$ gram-square centimeters per second squared

$= 5.72 \times 10^{19}$ ergs (4.22×10^{12} foot-pounds)

* *

The horizontal motion along a rupture line may contribute very little to tsunami generation. The maximum energy input from the horizontal motion would occur when the rupture line is normal to the continental slope. The motion along the rupture line, in that instance, would be equivalent to a wedge moving a short distance through the water (see Fig. 7). Berg, et al. (1970) show that for a motion equivalent in magnitude to that of the 1964 Alaskan earthquake, and acting normal to the continental slope, the potential energy input to the resulting tsunami would have been 3.12×10^{20} ergs (2.3×10^{13} foot-pounds). This is less than 1.5 percent of the energy input from the vertical uplifting, and seems to confirm Iida's (1970) analysis which showed that major tsunamis are associated with the dip-slip fault type. In fact, the rupture line of the 1964 Alaskan earthquake was almost parallel to the continental slope, and the energy input from the horizontal motion would have been negligible in this case. In other cases, the contribution of horizontal motion may be greater.

2. Initial Wave Formation.

Because of their long periods and corresponding long wavelengths, the train of waves forming a tsunami is taken to be shallow-water waves at their origin, and propagates across the ocean as shallow-water waves. The actual form of the wave train is determined by the initial generating mechanism, i.e., the area of the uplifted sea bottom, the height of and

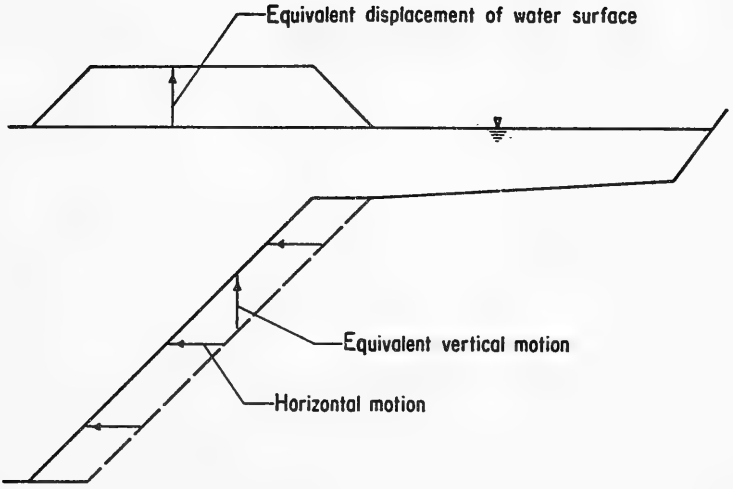

Figure 7. Horizontal motion normal to continental slope (scale exaggerated).

variation of the uplift within the area of uplift, and the depth of water and coastal characteristics in the generating area. While ordinary sea waves are assumed to have a cnoidal shape as they approach a shore (i.e., high crests and shallow troughs), the waves in a tsunami may have various combinations of forms.

Visual observations of tsunamis have led to reports that the initial wave was often a negative wave causing an initial drawdown of the water level at the shoreline. Shepard, MacDonald, and Cox (1950) show that some tide gage records indicate a small positive wave followed by a very deep trough, the amplitude of the trough being about three times the amplitude of the initial wave crest. This may have been misinterpreted by observers who reported initial negative waves. However, Striem and Miloh (1975) indicate that an initial drawdown may occur when the tsunami is generated by slumping of the continental slope. Tsunamis may sometimes produce waves with narrow, deep troughs and low, wide crests at the shoreline, the opposite of the cnoidal waveform.

Wave records from Wake Island for the March 1964 tsunami (Van Dorn, 1964) show a positive surge with a period of 80 minutes (see Fig. 6). There was a series of positive wave crests with the elevations of the intervening troughs above the normal expected tide level. This was followed by a series of crests and troughs with the elevations of the troughs below the normal tide level. Using a shallow-water wave celerity at the source and an average depth of approximately 100 meters (325 feet) for the generating area, the period of the initial positive surge is approximately equivalent to the time required for the trailing edge of the initial uplifted water surface to travel completely across the area

of generation. This indicates that the uplifted water surface at the source formed a series of solitary-type waves. The multiple crest can be accounted for by initial instabilities in the waveform caused by the generating mechanism, and the effect of the varying bathymetry of the ocean basin through which the wave passes. The lower waves following the initial series of wave crests correspond to the expected oscillations from a disturbance in the water surface as the disturbance is damped out.

Wilson, Webb, and Hendrickson (1962) showed that the height of a tsunami at a coastal point *near the source of generation* could be given as a first approximation by the empirical equation

$$\log_{10} H = 0.75\ M - 5.07 \tag{19}$$

where H is the height in meters and M the Richter magnitude. Using the value of M = 8.3 given by Berg, et al. (1970) for the March 1964 tsunami, H = 14.29 meters (46.9 feet). However, this is an empirical relationship which does not completely account for the characteristics of the generating mechanism or the coastline. Although equation (19) might provide a first rule-of-thumb estimate of wave heights, the actual heights could be above or below that estimate. Determination of actual heights would require computation by numerical or empirical means.

Wilson (1969) gives the relationship of Housner (1969) for the fault length L_f in kilometers as

$$\log_{10} L_f = 0.87\ M - 4.44 \tag{20}$$

giving a fault length for the March 1964 tsunami of L_f = 604 kilometers (1.98×10^6 feet). This is within the range of estimates given in Berg, et al. (1970) and approximates the length of the generating area, i.e., the length along the initial wave crest.

Wilson and Tørum (1968) give a relationship for the period T (in minutes) of the primary tsunami (carrying maximum energy) as

$$\log_{10} T = 0.625\ M - 3.31 \tag{21}$$

For the March 1964 tsunami, this equation gives a period of T = 75.4 minutes (using the Richter magnitude M = 8.3). This is very close to the period of the positive surge noted by Van Dorn (1964) at Wake Island, and is equal to that period if the crest of the initial oscillatory wave at the trailing edge of the surge is neglected.

The initial deformation of the water surface, for any tsunami, will collapse into some system of waves which must be defined. The resulting wave system depends on the shape of the seabed deformation and the water depth above the deformation. The simplest means of analysis is to assume

that the water surface has an initial displacement equal to the seabed displacement, that the initial displacement is not time-dependent, and then propagate the initial displacement outward from the generating area using long-wave equations (Brandsma, Divoky, and Hwang, 1975). Other means of establishing the initial waves, of varying degrees of complexity, are described by Wilson, Webb, and Hendrickson (1962) and in other sources.

Many of the mathematical representations of waves generated from bottom uplifting are based on circular source regions; however, Levy and Keller (1961) present one solution in terms of elliptic coordinates for a source region which is more elongated than circular. This solution has the form

$$\eta(r,\ \theta,\ t) = r^{-1}\ A_o(k)\left[\frac{2\pi C_G}{\left(\frac{-dC_G}{dK}\right)}\right]^{1/2} e^{ik(r-ct)+i(\pi/4)}\ I(k,\ \theta) \qquad (22)$$

where

$$A_o(k) = \frac{k^{1/2}\ \cosh[k(Z_o + d)]}{(2\pi)^{3/2}\ \cosh(kd)}\ e^{-i\pi/4} \qquad (23)$$

and

$$I(k,\ \theta) = \left(\frac{\pi}{2}\right)^{1/2} a^2 \sum_{n=o}^{\infty} (-i)^n \left[Se_n\left(\frac{ka}{2}\ ,\ \cos\ \theta\right) \overline{E}_{n,ne}\left(\frac{ka}{2}\right) + So_n\left(\frac{ka}{2}\ ,\ \cos\ \theta\right) \overline{F}_{n,no}\left(\frac{ka}{2}\right)\right] \qquad (24)$$

The terms Se_n and So_n are even and odd Mathieu functions, and $\overline{E}_{n,ne}$ (ka/2) and $\overline{F}_{n,no}$ (ka/2) are even and odd Mathieu transforms. The variables are defined as η the wave height, r and θ the coordinates of a point in polar coordinates, t the time, C the wave celerity, k the wave number, C_G the group velocity, Z_o the depth of generation (negative downward and equal to -d for bottom uplifting), d the water depth, and a the interfocal distance of the coordinate ellipses.

Levy and Keller indicate that the velocity of the bottom uplifting is unimportant if the time of uplifting is small in comparison with the period of the generated waves. This is generally true for tsunamis. They also indicate that only the first few terms of $I(k,\theta)$ may be important in the solution, although a computer solution can sum a relatively large number of terms. The limitations on the solution are that the solution was derived for water of uniform depth, the initial wavelength (or wave period) must be known, and the solution assumes that r is much greater than the dimension (diameter or length) of the source.

Hwang and Divoky (1970, 1972) use a simplified monotonic displacement history to describe ground motion. They propose that, to a first approximation, horizontal displacement of a sloping bottom can be represented as purely vertical displacement.

Houston, et al. (1975b) use an elliptical-shaped generating area, with an instantaneously displaced water surface, as input data for a standard design tsunami in a numerical solution. They define the surface displacement as a modified elliptic paraboloid, having a parabolic cross section parallel to the major axis of the ellipse, and a triangular cross section parallel to the minor axis of the ellipse. The numerical propagation of the wave uses the same procedure as used in Brandsma, Divoky, and Hwang (1975). The potential energy of the uplifted water surface for this type of surface displacement is given by

$$E = 4\left(\frac{\rho g}{6}\right) \frac{b}{a} \frac{c^2}{a^4} \int_0^a (a^2 - x^2)^{5/2} \, dx \qquad (25)$$

where

x = measured along the major axis of the ellipse

a = the length of the semimajor axis

y = measured along the minor axis of the ellipse

b = the length of the semiminor axis

z = the vertical direction upward from the undisturbed water surface

c = the maximum uplifted elevation at coordinates (x = o, y = o, z = c)

ρ = the density of the seawater (taken as 1.026 grams per cubic centimeter)

IV. TSUNAMI PROPAGATION

After determining the initial disturbance of the water surface, as discussed in Section III, the propagation of the tsunami to nearby or distant shorelines must be analyzed. Because tsunamis are long-period waves with long wavelengths in relation to both the water depth and the wave height, long-wave equations can be used.

1. Small-Amplitude Waves.

The simplest means of analyzing the wave motion, where the ratio of the wave height to water depth, H/d, is small, is to use the following small-amplitude solutions to the wave equations:

$$C^2 = \frac{gL}{2\pi} \tanh\left(\frac{2\pi d}{L}\right) \tag{26}$$

$$u = 2\pi \frac{a}{T} \frac{\cosh\left[\frac{2\pi(z + d)}{L}\right]}{\sinh\left[\frac{2\pi d}{L}\right]} \cos\left[2\pi\left(\frac{x}{L} - \frac{t}{T}\right)\right] \tag{27}$$

$$\xi = -a \frac{\cosh\left[\frac{2\pi(z + d)}{L}\right]}{\sinh\left[\frac{2\pi d}{L}\right]} \sin\left[2\pi\left(\frac{x}{L} - \frac{t}{T}\right)\right] \tag{28}$$

where

C = the wave celerity

L = the wavelength

d = the depth of the undisturbed water

u = the horizontal velocity of a water particle in the direction of the wave motion

a = the amplitude of the wave above the undisturbed water level

T = the wave period

z = the vertical distance of the particle from the undisturbed water surface

x = distance measured in the direction of wave motion

t = time

ξ = the horizontal displacement of the water particle from its undisturbed position

Tsunamis are shallow-water waves; i.e., the ratio of wavelength to water depth, L/d, is very large. Therefore, equations (26), (27), and (28) can be reduced to more basic small-amplitude, shallow-water equations. Letting $d/L \to 0$,

$$\tanh\left(\frac{2\pi d}{L}\right) \to \frac{2\pi d}{L} \tag{29}$$

substituting equation (29) into equation (26) gives

$$C^2 = \frac{gL}{2\pi}\left(\frac{2\pi d}{L}\right) \tag{30}$$

which gives small-amplitude, shallow-water wave celerity as

$$C = \sqrt{gd} \tag{31}$$

Because $z < d$, it will always be true that $z/L \to 0$ whenever $d/L \to 0$. Therefore,

$$\sinh \frac{2\pi z}{L} \to \frac{2\pi z}{L} \tag{32}$$

$$\sinh \frac{2\pi d}{L} \to \frac{2\pi d}{L} \tag{33}$$

$$\cosh \frac{2\pi z}{L} \to 1 \tag{34}$$

$$\cosh \frac{2\pi d}{L} \to 1 \tag{35}$$

Considering that

$$\cosh \frac{2\pi(z + d)}{L} = \cosh \frac{2\pi z}{L} \cosh \frac{2\pi d}{L} + \sinh \frac{2\pi z}{L} \sinh \frac{2\pi d}{L} \tag{36}$$

and substituting equations (32) to (35) into equation (36),

$$\cosh \frac{2\pi(z + d)}{L} = 1 + \left(\frac{2\pi z}{L}\right)\left(\frac{2\pi d}{L}\right) \tag{37}$$

The disturbed water surface elevation, η, at any point in relation to its undisturbed location is given by

$$\eta = a \cos\left[2\pi\left(\frac{x}{L} - \frac{t}{T}\right)\right] \tag{38}$$

Substituting equations (33), (37), and (38) into equation (27),

$$u = 2\pi \frac{\eta}{T} \frac{1 + \left(\frac{2\pi z}{L}\right)\left(\frac{2\pi d}{L}\right)}{\left(\frac{2\pi d}{L}\right)} \tag{39}$$

Noting that $z/L \to 0$,

$$u = \frac{\eta}{d}\frac{L}{T} \tag{40}$$

but, from the basic wave equation for all waves,

$$C = \frac{L}{T} \tag{41}$$

so that

$$u = \frac{\eta}{d}\sqrt{gd} = \frac{\eta\, g^{1/2}}{d^{1/2}} \tag{42}$$

The water surface elevation can also be defined as

$$\eta = a \sin\left[2\pi\left(\frac{x}{L} - \frac{t}{T}\right)\right] \tag{43}$$

so that by substituting equations (33), (37), and (43) into equation (28),

$$\xi = -\eta \frac{1 + \left(\frac{2\pi z}{L}\right)\left(\frac{2\pi d}{L}\right)}{\left(\frac{2\pi d}{L}\right)} \tag{44}$$

and noting again that $z/L \to 0$,

$$\xi = -\frac{\eta L}{2\pi d} \tag{45}$$

The wave energy, E, for a small-amplitude wave is given by

$$E = \frac{\rho g\, H^2 L}{8} \tag{46}$$

where ρ is the density of the seawater. If energy is conserved between two points for an unrefracted wave,

$$\left(\frac{\rho g\, H^2 L}{8}\right)_1 = \left(\frac{\rho g\, H^2 L}{8}\right)_2 \tag{47}$$

$$\frac{H_2}{H_1} = \left(\frac{L_1}{L_2}\right)^{1/2} \tag{48}$$

but as $L = CT$, and T is assumed to be constant, and as $C = \sqrt{gd}$ for a shallow-water wave, then

$$\frac{H_2}{H_1} = \left(\frac{d_1}{d_2}\right)^{1/4} \tag{49}$$

which is the well-known Green's Law. Noting that $\eta_{max} = a$, the amplitude, equations (42) and (45) can be written as

$$\left|u_{max}\right| = \frac{ag^{1/2}}{d^{1/2}} \tag{50}$$

$$\left|\xi_{max}\right| = \frac{aL}{2\pi d} \tag{51}$$

For the unrefracted wave, noting that

$$\frac{a_2}{a_1} = \frac{H_2}{H_1} \tag{52}$$

$$\frac{\left|u_{max}\right|_2}{\left|u_{max}\right|_1} = \left(\frac{a_2}{a_1}\right) \frac{\left(\frac{g}{d_2}\right)^{1/2}}{\left(\frac{g}{d_1}\right)^{1/2}} = \left(\frac{d_1}{d_2}\right)^{1/4} \left(\frac{d_1}{d_2}\right)^{1/2} \tag{53}$$

$$\frac{\left|u_{max}\right|_2}{\left|u_{max}\right|_1} = \left(\frac{d_1}{d_2}\right)^{3/4} \tag{54}$$

Also,

$$\frac{\left|\xi_{max}\right|_2}{\left|\xi_{max}\right|_1} = \left(\frac{a_2}{a_1}\right)\left(\frac{L_2}{L_1}\right)\frac{\left(\frac{1}{2\pi d}\right)_2}{\left(\frac{1}{2\pi d}\right)_1} = \left(\frac{d_1}{d_2}\right)^{1/4} \left(\frac{d_2}{d_1}\right)^{1/2} \left(\frac{d_1}{d_2}\right) \tag{55}$$

$$\frac{\left|\xi_{max}\right|_2}{\left|\xi_{max}\right|_1} = \left(\frac{d_1}{d_2}\right)^{3/4} \tag{56}$$

Equations (49), (54), and (56) provide a simple, first-order solution for the shoaling of an unrefracted, small-amplitude, shallow-water wave.

* * * * * * * * * * * * * EXAMPLE PROBLEM 2 * * * * * * * * * * * * * *

GIVEN: A long wave with a period of 20 minutes and a height, H, of 0.4 meter (1.31 feet) passes from a 1,000-meter (3,280 feet) water depth into a 500-meter (1,640 feet) water depth. The wave is assumed to be nondispersive.

FIND:

(a) The unrefracted wave height in the 500-meter depth,

(b) the water particle velocity $|u_{max}|$ in each water depth, and

(c) the horizontal water particle motion $|\xi_{max}|$ in each water depth.

SOLUTION:

(a) $H_1 = 0.4$ meter, $d_1 = 1{,}000$ meters, $d_2 = 500$ meters

From equation (49),

$$\frac{H_2}{H_1} = \left(\frac{d_1}{d_2}\right)^{1/4}$$

$$\frac{H_{500}}{0.4} = \left(\frac{1{,}000}{500}\right)^{1/4} = 1.189$$

$$H_{500} = 0.4(1.189) = 0.48 \text{ meter (1.56 feet)}$$

(b) From equation (50),

$$\left|u_{max}\right| = \frac{ag^{1/2}}{d^{1/2}}$$

Assuming $a = H_1/2 = 0.2$ meter, at $d_1 = 1{,}000$ meters,

$$\left|u_{max}\right|_{1,000} = \frac{0.2(9.807)^{1/2}}{(1{,}000)^{1/2}} = 0.02 \text{ meter (0.065 foot) per second}$$

From equation (54) where $d_2 = 500$ meters,

$$\frac{\left(u_{max}\right)_2}{\left(u_{max}\right)_1} = \left(\frac{d_1}{d_2}\right)^{3/4}$$

$$\frac{\left|u_{max}\right|_{500}}{\left|u_{max}\right|_{1,000}} = \left(\frac{1{,}000}{500}\right)^{3/4}$$

$$\left|u_{max}\right|_{500} = 0.02\left(\frac{1{,}000}{500}\right)^{3/4} = 0.034 \text{ meter (0.11 foot) per second}$$

(c) First solving for L where d_1 = 1,000 meters and T = 20 minutes,

$$L = CT = \sqrt{gd}\, T = \sqrt{9.807 \times 1{,}000}\ (20 \times 60)$$

$$L = 118{,}800 \text{ meters } (73.8 \text{ miles})$$

From equation (51),

$$\left|\xi_{max}\right|_{1,000} = \frac{aL}{2\pi d}$$

$$\left|\xi_{max}\right|_{1,000} = \frac{0.2(118{,}800)}{2\pi(1{,}000)} = 3.78 \text{ meters } (12.4 \text{ feet})$$

From equation (56) where d_2 = 500 meters,

$$\frac{\left(\xi_{max}\right)_2}{\left(\xi_{max}\right)_1} = \left(\frac{d_1}{d_2}\right)^{3/4}$$

$$\frac{\left|\xi_{max}\right|_{500}}{\left|\xi_{max}\right|_{1,000}} = \left(\frac{1{,}000}{500}\right)^{3/4}$$

$$\left|\xi_{max}\right|_{500} = 3.78 \left(\frac{1{,}000}{500}\right)^{3/4} = 6.36 \text{ meters } (20.9 \text{ feet})$$

* *

Soloviev, et al. (1976) compared solutions for tsunami amplitude using equation (49) and a numerical integration method. Equation (49) does not account for wave reflection from bottom slopes and results in calculated wave amplitudes that are too high. Also, equations (49), (54), and (56) do not account for wave refraction, diffraction, or dispersion; they cannot be used with any degree of accuracy when the ratio of H/d becomes large. When waves travel long distances, it is necessary to consider the curvature of the Earth, discussed later in this section.

2. Long-Wave Equations.

To increase the accuracy of computations, the long-wave equations can be expressed in various forms of partial differential equations which can be solved numerically. As given by Peregrine (1970) for two-dimensional waves propagating in water of constant depth, the equations may be written as follows in rectangular coordinates:

Linear equations:

$$\frac{\partial u}{\partial t} + g \frac{\partial \eta}{\partial x} = 0 \tag{57}$$

$$\frac{\partial \eta}{\partial t} + d \frac{\partial u}{\partial x} = 0 \tag{58}$$

Finite-amplitude equations:

$$\frac{\partial u}{\partial t} + u \frac{\partial u}{\partial x} + g \frac{\partial \eta}{\partial x} = 0 \tag{59}$$

$$\frac{\partial \eta}{\partial t} + \frac{\partial [(d + \eta)\, u]}{\partial x} = 0 \tag{60}$$

Boussinesq equations:

$$\frac{\partial u}{\partial t} + u \frac{\partial u}{\partial x} + g \frac{\partial \eta}{\partial x} = \frac{1}{3} d^2 \frac{\partial^2 u}{\partial x^2} t \tag{61}$$

$$\frac{\partial \eta}{\partial t} + \frac{\partial [(d + \eta)\, u]}{\partial x} = 0 \tag{62}$$

In addition, for waves traveling in only one direction, the Boussinesq equations may be reduced to the Korteweg-deVries equations which are then written as

$$2 \frac{\partial u}{\partial t} + 2(gd)^{1/2} \frac{\partial u}{\partial x} + 3u \frac{\partial u}{\partial x} + \frac{1}{3} d^2 (gd)^{1/2} \frac{\partial^3 u}{\partial x^3} = 0 \tag{63}$$

$$\eta = \left(\frac{d}{g}\right)^{1/2} u + \frac{u^2}{4g} - \frac{d^3 \frac{\partial^2 u}{\partial x^2}}{6(gd)^{1/2}} \tag{64}$$

When considering the means of describing the propagation of long-period waves, the parameter, U, should be evaluated where U is defined as

$$U = \frac{H}{d} \left(\frac{L}{d}\right)^2 \tag{65}$$

and sometimes referred to as the Stokes or Ursell parameter. The importance of this parameter was first noted by Stokes (1847) when he stated that the parameter must be small if his equations were to remain valid for long waves.

Murty (1977) indicates that the value of $(L/d)^2$ is a measure of frequency dispersion; the value of H/d is a measure of amplitude dispersion. Murty points out that the linear long-wave equations are valid when $U << 1$. In this case H/d is small and amplitude dispersion can be ignored.

When U is of the order one [$U = 0(1)$], both amplitude and frequency dispersion are important. In this case Boussinesq or Korteweg-deVries equations should be used. Where $U >> 1$ amplitude dispersion dominates the solution, and the finite-amplitude, nonlinear long-wave equations should be used. It should be emphasized that when $U = 0(1)$ it is not necessary that $U \simeq 1$. Zabusky and Galvin (1971) show that the Korteweg-deVries equation accurately describes wave propagation for $U < 800$ in some cases.

For tsunamis with very long periods (and therefore long wavelengths), the condition that $U << 1$ is usually never satisfied. However, the error which results from the use of the linear equations is quite small as long as the value of H/d is small. The acceptable limit of the value for H/d (i.e., the point where the error in the calculations becomes significant) depends in part on the rate of shoaling of the wave, i.e., the shoreward slope of the bottom topography.

* * * * * * * * * * * * * * EXAMPLE PROBLEM 3 * * * * * * * * * * * * * *

GIVEN: A tsunami has a period of 20 minutes and a wave height of 0.05 meter (0.16 foot) in a 1,000-meter (3,280 feet) water depth.

FIND: The parameter U.

SOLUTION: From equation (31),

$$C = \sqrt{gd} = \sqrt{9.807 \times 1{,}000} = 99 \text{ meters (325 feet) per second}$$

$$L = CT = 99 \times 20 \times 60 = 118{,}800 \text{ meters}$$

From equation (65),

$$U = \frac{H}{d}\left(\frac{L}{d}\right)^2 = \frac{0.05}{1{,}000}\left(\frac{118{,}800}{1{,}000}\right)^2$$

$$U = 0.706$$

* *

In more recent investigations, the parameter U given by equation (65) has been redefined as U^* where

$$U^* = \left(\frac{H}{d}\right) \frac{1}{(\eta_x)^2_{max}} \tag{66}$$

and

$$\eta_x = \frac{\partial \eta}{\partial x} \tag{67}$$

This is discussed by Peregrine (1970). He points out that nonlinear terms which were neglected in the linear equations (57) and (58) cause a cumulative error that may become appreciable in a numerical solution after a time given by

$$t = \frac{d^{3/2}}{H\, g^{1/2}} \tag{68}$$

Where rapid shoaling occurs, i.e., where a wave passes over a large change in water depth in a relatively short period of time, the accumulated error will be much smaller than for slow shoaling, where the wave passes over the same change in water depth in a relatively long period of time.

The finite-amplitude equations (59) and (60) are valid as long as

$$U^* > 1$$

but generally become invalid after a finite time as the front face of the wave steepens. The Boussinesq equations are also applicable where $U^* > 1$; i.e., where $(\eta_x)^2_{max} < (H/d)$. Peregrine (1970) points out that the Boussinesq approximation works well for values of H/d up to about 0.5. The Boussinesq or the Korteweg-deVries equations are used for waves approaching a shoreline where values of H/d become large.

Hammack (1973) gives the value of U^* as

$$U^* = \left(\frac{\eta_{max}}{d}\right)^3 \frac{1}{(\eta_x)^2_{max}} \tag{69}$$

to describe a particular region of a complex waveform. However, the value of U^* would be expected to vary from region to region of the waveform in this case. This variation would indicate that using a single set of equations to describe a *complex* waveform may lead to incorrect results.

3. Distantly Generated Tsunamis.

When a tsunami travels a long distance across the ocean, the sphericity of the Earth must be considered to determine the effects of the

tsunami on a distant shoreline. Waves which diverge near their source will converge again at a point on the opposite side of the ocean. An example of this was the 1960 tsunami whose source was on the Chilean coastline, 39.5° S., 74.5° W. (Pararas-Carayannis, 1969). The coast of Japan lies between 30° and 45° N. and about 135° to 140° E., a difference of 145° to 150° longitude from the source area. As a result of the convergence of *unrefracted* wave rays, the coast of Japan suffered substantial damage and many deaths occurred (U.S. Army Engineer District, Honolulu, 1960; Hirono, 1961). Figure 8 illustrates the convergence of the wave rays due to the Earth's sphericity.

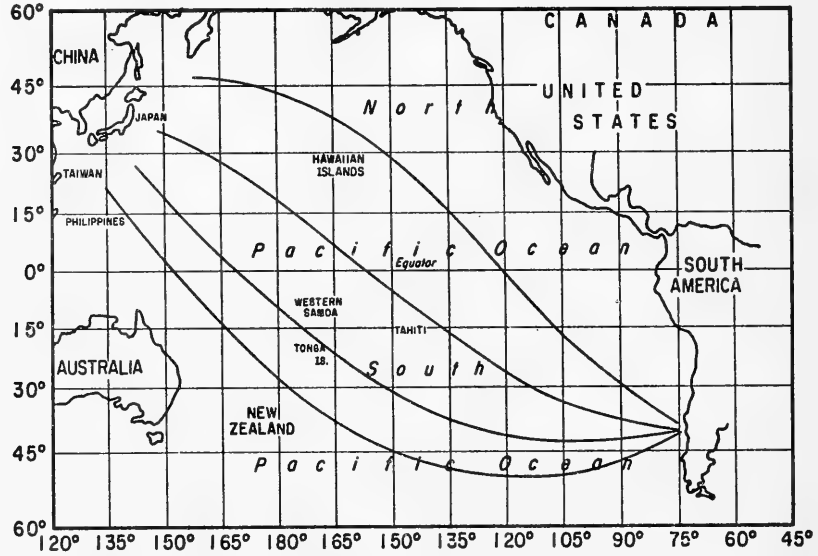

Figure 8. Convergence of wave rays.

Chao (1970) gives the equation for *wave refraction* in spherical coordinates as

$$\frac{dx}{ds} = -\frac{1}{C}\left(\frac{dC}{dw}\right) - \frac{\cos\alpha \tan\psi}{R_e} \tag{70}$$

where ray separation is defined by the equation

$$\frac{d^2\beta}{ds^2} + p\frac{d\beta}{ds} + q\beta = 0 \tag{71}$$

and the coefficients p and q are defined as

$$p = -\frac{1}{C}\left(\frac{dC}{ds}\right) - \frac{1}{R_e}\sin\alpha \tan\psi \tag{72}$$

$$q = \left(\frac{\sin \alpha}{R_e \cos \psi}\right)^2 \left(\frac{1}{C} \frac{\partial^2 C}{\partial \phi^2}\right) - \left(\frac{\sin 2\alpha}{R_e^2 \cos \psi}\right)\left(\frac{1}{C} \frac{\partial^2 C}{\partial \psi \partial \phi}\right)$$

$$+ \left(\frac{\cos \alpha}{R_e}\right)^2 \left(\frac{1}{C} \frac{\partial^2 C}{\partial \psi^2}\right) + \left(\frac{2 \cos \alpha \tan \psi}{R_e}\right)\left(\frac{1}{C} \frac{dC}{dw}\right)$$

$$+ \left(\frac{\cos \alpha \tan \psi}{R_e}\right)^2 + \left(\frac{\tan \psi \sec \psi}{R_e^2}\right)\left(\frac{\partial \alpha}{\partial \phi}\right) \qquad (73)$$

$$\frac{1}{C} \frac{dC}{ds} = \frac{1}{R_e}\left[\left(\frac{\cos \alpha}{\cos \psi}\right)\left(\frac{1}{C} \frac{\partial C}{\partial \phi}\right) + (\sin \alpha)\left(\frac{1}{C} \frac{\partial C}{\partial \psi}\right)\right] \qquad (74)$$

$$\frac{1}{C} \frac{dC}{dw} = \frac{1}{R_e}\left[-\left(\frac{\sin \alpha}{\cos \psi}\right)\left(\frac{1}{C} \frac{\partial C}{\partial \phi}\right) + (\cos \alpha)\left(\frac{1}{C} \frac{\partial C}{\partial \psi}\right)\right] \qquad (75)$$

where

R_e = the radius of the Earth

ϕ = longitude of the point on the surface the wave ray is passing through

ψ = latitude of the point

C = celerity of the wave

s = a measure of distance in the direction the wave is traveling

α = the angle between the wave ray and a line of equal latitude

β = a ray separation term

Using the spherical coordinate system shown in Figure 9, Hwang and Divoky (1975) give the linear long-wave equations as

$$\frac{\partial u}{\partial t} = -\frac{g}{R_e} \frac{\partial n}{\partial \theta} + f_c\, v \qquad (76)$$

and

$$\frac{\partial v}{\partial t} = -\frac{g}{R_e \sin \theta} \frac{\partial n}{\partial \phi} - f_c\, u \qquad (77)$$

where

R_e = the radius of the Earth

θ = degrees latitude (measured from the pole)

ϕ = degrees longitude (measured eastward)

u = the velocity in the θ-direction

v = the velocity in the ϕ-direction

t = time

f_c = the coriolis parameter = $2\ \Omega \cos \theta$

Ω = the rotational speed of the Earth in radians per second

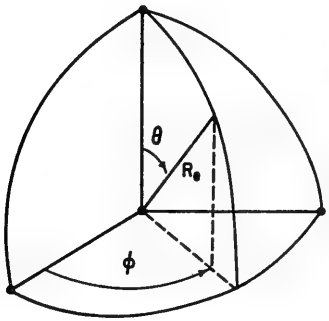

Figure 9. Spherical coordinate system.

For linear long-wave equations, the acceleration component in the radial direction is considered to be negligible. The continuity equation is

$$\frac{\partial \eta}{\partial t} = -\frac{1}{R_e \sin \theta}\left\{\frac{\partial}{\partial \theta}\left[(d + \eta)\, u \sin \theta\right] + \frac{\partial}{\partial \phi}\left[(d + \eta)\, v\right]\right\} + \frac{\partial \zeta}{\partial t} \qquad (78)$$

where ζ is a time-dependent vertical bottom displacement in the generating area and equal to zero elsewhere.

For instantaneous bottom displacement, the initial wave is assumed to be a water surface displacement equivalent to the bottom displacement, and $\partial\zeta/\partial t = 0$. If a wave is generated near a coastline, i.e., in relatively shallow water, the parameter U may initially be quite large. For a wave propagating *away from* the coastline, it is assumed that the

linear long-wave equations can be applied to the initial propagation, and that the resulting errors are of a size that can be accepted in the calculations.

4. Nearshore Propagation.

The linear long-wave equations may be used for the propagation of waves from a shoreline, across an ocean basin, and up to an area near another shoreline. It is also necessary to consider the propagation of a tsunami toward a shoreline from a nearby generating area, or into the nearshore area at a distant shoreline where the linearized long-wave equations will not provide solutions with sufficient accuracy. Peregrine (1967) derived equations for three-dimensional long waves in water of varying depth (i.e., shoaling waves) which correspond to the Boussinesq equations for solitary waves in water of constant depth. An expansion is used similar to that used by Keller (1948).

The dimensional variables are defined with an *, and the dimensionless variables by the following equations:

$$x = \frac{x^*}{d_o} \ , \ y = \frac{y^*}{d_o} \ , \ z = \frac{z^*}{d_o}$$

$$t = t^* \left(\frac{g}{d_o}\right)^{1/2} \ , \ p = \frac{p^*}{\rho g\, d_o}$$

$$u = \frac{u^*}{(gd_o)^{1/2}} \ , \ v = \frac{v^*}{(gd_o)^{1/2}} \ , \ w = \frac{w^*}{(gd_o)^{1/2}}$$

where d_o is a length representative of water depth; p the pressure; the velocity u in the x-direction, v in the y-direction, w in the z-direction; and the other variables are defined as before. Defining

$$q = (u^2 + v^2)^{1/2} \text{ and } Q = \int_{-d}^{\eta} q\,dz \tag{79}$$

where q is velocity and Q the flow rate, the continuity equation is

$$\frac{\partial Q_x}{\partial x} + \frac{\partial Q_y}{\partial y} + \frac{\partial \eta}{\partial t} = 0 \tag{80}$$

where Q_x is the component of Q in the x-direction, and Q_y the component of Q in the y-direction.

Euler's equations of motion are

$$\frac{\partial q}{\partial t} + u\frac{\partial q}{\partial x} + v\frac{\partial q}{\partial y} + w\frac{\partial q}{\partial z} + \frac{\partial p}{\partial x} + \frac{\partial p}{\partial y} = 0 \tag{81}$$

and

$$\frac{\partial w}{\partial t} + u\frac{\partial w}{\partial x} + v\frac{\partial w}{\partial y} + w\frac{\partial w}{\partial z} + \frac{\partial p}{\partial z} + 1 = 0 \tag{82}$$

At the boundary $z = -d$,

$$u \frac{\partial d}{\partial x} + v \frac{\partial d}{\partial y} + w = 0 \tag{83}$$

The variables η, p, q, and Q are expanded in the form

$$\eta = \eta_o + \varepsilon \eta_1 + \varepsilon^2 \eta_2 + \ldots \tag{84}$$

$$Q = Q_o + \varepsilon Q_1 + \varepsilon^2 Q_2 + \ldots \tag{85}$$

where ε is the ratio of wave amplitude to depth H/d. The variable w is expanded as

$$w = \sigma(w_o + \varepsilon w_1 + \varepsilon^2 w_2 + \ldots) \tag{86}$$

where σ is the ratio of water depth to wavelength d/L. The zero-order solution gives

$$p_o = -z$$

The first-order solution gives

$$\frac{\partial q_1}{\partial t_1} + \frac{\partial \eta_1}{\partial x_1} + \frac{\partial \eta_1}{\partial y_1} = 0 \tag{87}$$

$$\frac{\partial \eta_1}{\partial t_1} + \frac{\partial (du_1)}{\partial x_1} + \frac{\partial (dv_1)}{\partial y_1} = 0 \tag{88}$$

$$w_1 = - \frac{\partial (du_1)}{\partial x_1} - \frac{\partial (dv_1)}{\partial y_1} - z \left(\frac{\partial u_1}{\partial x_1} + \frac{\partial v_1}{\partial y_1} \right) \tag{89}$$

The second-order solution gives

$$\begin{aligned} q_2 = {} & \Omega_2(x_1, t_1) - z \frac{\partial}{\partial x_1} \left[\frac{\partial (du_1)}{\partial x_1} + \frac{\partial (dv_1)}{\partial y_1} \right] \\ & - z \frac{\partial}{\partial y_1} \left[\frac{\partial (du_1)}{\partial x_1} + \frac{\partial (dv_1)}{\partial y_1} \right] - \frac{1}{2} z^2 \frac{\partial}{\partial x_1} \left[\frac{\partial u_1}{\partial x_1} + \frac{\partial v_1}{\partial y_1} \right] \\ & - \frac{1}{2} z^2 \frac{\partial}{\partial y_1} \left[\frac{\partial u_1}{\partial x_1} + \frac{\partial v_1}{\partial y_1} \right] \end{aligned} \tag{90}$$

where $\Omega_2(x_1, t_1)$ is an arbitrary function arising from integration. The momentum equation is

$$\frac{\partial \Omega_2}{\partial t} + u_1 \frac{\partial q_1}{\partial x_1} + v_1 \frac{\partial q_1}{\partial y_1} + \frac{\partial \eta_2}{\partial x_1} + \frac{\partial \eta_2}{\partial y_1} = 0 \tag{91}$$

and the continuity equation is

$$\frac{\partial \eta_2}{\partial t_1} + \frac{\partial (Q_2)\ x}{\partial x_1} + \frac{\partial (Q_2)\ y}{\partial y_1} = 0 \tag{92}$$

Peregrine (1967) points out that second-order terms will have first-order effects where t_1 is not of small value. He accounts for these effects by incorporating second-order terms into the first-order variables.

Mei and Le Mehaute (1966) derived a solution for waves propagating in one direction which gives the equations as

$$\frac{\partial \eta}{\partial t} + u \frac{\partial \eta}{\partial x} + (d + \eta) \frac{\partial u}{\partial x} - \frac{d^3}{6} \frac{\partial^3 u}{\partial x^3} = Au + B \frac{\partial u}{\partial x} + \left(\frac{3}{2}\right) d^2 \frac{\partial d}{\partial x} \frac{\partial^2 u}{\partial x^2} \tag{93}$$

and

$$\frac{\partial u}{\partial t} + u \frac{\partial u}{\partial x} + \frac{\partial \eta}{\partial x}\left(\frac{L}{d}\right) - \frac{d^2}{2} \frac{\partial^3 u}{\partial^2 x \partial t} = \frac{\partial}{\partial x}\left(d \frac{\partial d}{\partial x}\right) \frac{\partial u}{\partial t}$$

$$+ 2 \left(d \frac{\partial d}{\partial x}\right) \frac{\partial^2 u}{\partial x \partial t} - \frac{\partial p}{\partial x} \tag{94}$$

where

$$A = - \frac{\partial d}{\partial x} + \left(\frac{\partial d}{\partial x}\right)^3 + 3d \frac{\partial d}{\partial x} \frac{\partial^2 d}{\partial x^2} + \frac{d^2}{2} \frac{\partial^3 d}{\partial x^3} \tag{95}$$

and

$$B = \frac{3}{2} \frac{\partial}{\partial x}\left(d^2 \frac{\partial d}{\partial x}\right) \tag{96}$$

It can be seen that equation (94) has mixed derivatives, with respect to x and t, where equation (63) has a third-order derivative with respect to x only. Benjamin, Bona, and Mahony (1972) show that the Korteweg-deVries equations with mixed derivatives, such as equation (94), are the preferred form for describing the behavior of long waves.

Street, Chan, and Fromm (1970) expanded on the work of Peregrine, and for waves propagating in one direction give

$$\frac{\partial u}{\partial t} + u \frac{\partial u}{\partial x} + \frac{\partial \eta}{\partial x} + \frac{1}{3} d^2 \frac{\partial^3 u}{\partial t \partial x^2} + d \frac{\partial d}{\partial x} \frac{\partial^2 u}{\partial t \partial x} + \frac{1}{2} \frac{\partial^2 d}{\partial x^2} \frac{\partial u}{\partial t} \tag{97}$$

and

$$\frac{\partial \eta}{\partial t} + \frac{\partial}{\partial x}[(d + \eta)\ u] = 0 \tag{98}$$

The numerical solution of these equations gives results comparable to experiments for varying bottom topography where $H/d \leq 0.4$.

Using the work of Mei and Le Mehaute (1966), Madsen and Mei (1969) developed characteristic equations which could be solved numerically. Defining

$$\frac{d\eta}{dt} = w \text{ and } \frac{dw}{dt} = a$$

along the coinciding characteristics x = constant, along the two distinct characteristics

$$\frac{dx}{dt} = \pm C_o(x) = \pm \sqrt{\frac{3d\left[1 - \left(\frac{\partial d}{\partial x}\right)^2 - d\,\frac{\partial^2 d}{\partial x^2}\right]}{\sigma\left(1 - \frac{1}{2}\,d\,\frac{\partial^2 d}{\partial x^2}\right)}} \tag{99}$$

and

$$\left(\frac{Cd}{6} + \frac{ud}{2}\right)\frac{d\eta}{d\beta} + \frac{5}{12}\,d^2\,\frac{\partial d}{\partial x}\,\frac{dw}{d\beta} + \left(1 - \frac{1}{2}\,d\,\frac{\partial^2 d}{\partial x^2}\right)\frac{\sigma dC^2}{6}\,\frac{du}{d\beta}$$

$$+ \frac{\sigma Cd^2}{12}\,\frac{da}{d\beta} = \left(\frac{Cd}{2}\,D + \frac{\sigma\,\frac{\partial d}{\partial x}\,C^2}{6}\,u\right)u$$

$$+ \frac{d\,\frac{\partial d}{\partial x}}{6}\left(\frac{5}{2}\,d - \sigma C^2\right)a + \left[\frac{\eta C}{2} - \frac{dC}{3} + \left(\frac{d}{2} + \frac{\sigma C^2}{6}\right)u\right]w \tag{100}$$

where

$$D = \frac{1}{d}\,\frac{\partial d}{\partial x}\,\eta - \frac{\partial d}{\partial x} + \left(\frac{\partial d}{\partial x}\right)^3 + \frac{1}{3}\,d^2\,\frac{\partial^3 d}{\partial x^3} + 2d\,\frac{\partial d}{\partial x}\,\frac{\partial^2 d}{\partial x^2} \tag{101}$$

and

$$C = \pm C_o(x) \text{ along } \beta = \left(\frac{\beta_1}{\beta_2}\right) = \frac{1}{2}\left(t \mp \int \frac{dx}{C_o(x)}\right) = \text{constant} \tag{102}$$

The Korteweg-deVries equations provide a solution for wave propagation in one direction only, i.e., for an unrefracted wave. The solutions generated could be used to provide shoaling coefficients to obtain refracted wave heights.

Alternative methods of obtaining solutions for refracted waves in two dimensions are to use the linear long-wave equations with additional terms added to account for nonlinear effects, or to use solutions based on the Boussinesq equations. Butler and Durham (1976) suggest a solution using equations similar to those in a tidal hydraulic model. The momentum equations for the tidal model are

$$\frac{\partial u}{\partial t} + u\frac{\partial u}{\partial t} + v\frac{\partial u}{\partial t} + \frac{\partial \eta}{\partial x} - f_c v + \frac{T_{Bx}}{d + \eta} = 0 \tag{103}$$

$$\frac{\partial v}{\partial t} + u\frac{\partial v}{\partial x} + v\frac{\partial v}{\partial y} + g\frac{\partial \eta}{\partial y} + f_c u + \frac{T_{By}}{d + \eta} = 0 \tag{104}$$

and the continuity equation is

$$\frac{\partial \eta}{\partial t} + \frac{\partial}{\partial x}(du + \eta u) + \frac{\partial}{\partial y}(dv + \eta v) = 0 \tag{105}$$

where the bottom stress is given by

$$T_{Bx} = \frac{gu}{C^2}\sqrt{u^2 + v^2} \tag{106}$$

and

$$T_{By} = \frac{gv}{C^2}\sqrt{u^2 + v^2} \tag{107}$$

Chen, Divoky, and Hwang (1975) give numerical equations for the two-dimensional case based on the Boussinesq equations (see Sec. IV, 5).

5. Computer Models.

Solutions of the equations for long water waves are obtained by numerical means. Leendertse (1967) gives the following method for solving the linearized long-wave equations by using a space staggered scheme as shown in Figure 10. Taking the subscript n to indicate the value at time t, the subscript $n + 1/2$ to indicate the value at time $t + \Delta t/2$, and the subscript $n + 1$ to indicate the value at time $t + \Delta t$, the computations use alternate sets of equations at alternate time steps Δt as shown below. First u and η are calculated implicitly and v explicitly at time $t + \Delta t/2$, then v and η implicitly and u explicitly at time $t + \Delta t$, then u and η implicitly and v explicitly at time $t + 3\Delta t/2$, etc. Calculating u at point $(j + 1/2, k)$, η at (j,k), and v at $(j,k + 1/2)$, as defined in Figure 10, the calculations are, at times $t + \Delta t/2$, $t + 3\Delta t/2$, $t + 5\Delta t/2$, . . .

$$u_{n+1/2} = u_n + \frac{1}{2}\Delta t\, f_c \bar{\bar{v}}_n - \frac{1}{2}\frac{\Delta t}{\Delta s} g \left(\frac{\partial \eta}{\partial x}\right)_{n+1/2} \tag{108}$$

$$\eta_{n+1/2} = \eta_n - \frac{1}{2}\frac{\Delta t}{\Delta s}\left\{\frac{\partial}{\partial x}\left[(\bar{d}^{y} + \bar{\eta}^{x})^{*}\, u\right]_{n+1/2} + \frac{\partial}{\partial y}\left[(\bar{d}^{x} + \bar{\eta}^{y})\, v\right]_n\right\} \tag{109}$$

$$v_{n+1/2} = v_n - \frac{1}{2}\Delta t\, f_c \bar{\bar{u}}_{n+1/2} - \frac{1}{2}\frac{\Delta t}{\Delta s} g \left(\frac{\partial \eta}{\partial y}\right)_n \tag{110}$$

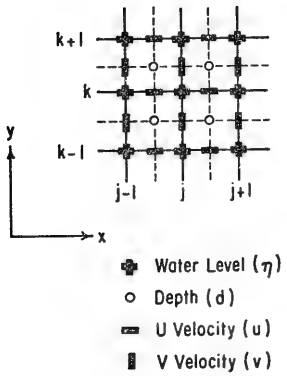

Figure 10. Coordinate system, rectangular coordinates.

and at times $t + \Delta t$, $t + 2\Delta t$, $t + 3\Delta t$, . . .

$$v_{n+1} = v_{n+1/2} - \frac{1}{2}\Delta t\, f_c\, \bar{\bar{u}}_{n+1/2} - \frac{1}{2}\frac{\Delta t}{\Delta s}\, g \left(\frac{\partial \eta}{\partial y}\right)_{n+1} \tag{111}$$

$$\eta_{n+1} = \eta_{n+1/2} - \frac{1}{2}\frac{\Delta t}{\Delta s}\left\{\frac{\partial}{\partial x}\left[(\bar{d}^{y} + \bar{\eta}^{x})\, u\right]_{n+1/2} + \frac{\partial}{\partial y}\left[(\bar{d}^{x} + \bar{\eta}^{y})^{*}\, v\right]_{n+1}\right\} \tag{112}$$

$$u_{n+1} = u_{n+1/2} + \frac{1}{2}\Delta t\, f_c\, \bar{\bar{v}}_{n+1} - \frac{1}{2}\frac{\Delta t}{\Delta s}\, g \left(\frac{\partial \eta}{\partial x}\right)_{n+1/2} \tag{113}$$

These equations omit convective inertia terms, bottom effects, and any forcing functions. The various terms used are defined as follows:

$$\bar{\eta}^{x} = \frac{1}{2}\left(\eta_{j-1/2,\ k} + \eta_{j+1/2,\ k}\right) \tag{114}$$

$$\bar{\eta}^{y} = \frac{1}{2}\left(\eta_{j,\ k-1/2} + \eta_{j,\ k+1/2}\right) \tag{115}$$

$$\frac{\partial \eta}{\partial x} = \left(\eta_{j+1/2,k} - \eta_{j-1/2,k}\right) \tag{116}$$

$$\frac{\partial \eta}{\partial y} = \left(\eta_{j,k+1/2} - \eta_{j,k-1/2}\right) \tag{117}$$

$$\bar{\bar{u}} = \frac{1}{4}\left(u_{j-1/2,k} + u_{j+1/2,k} + u_{j-1/2,k+1} + u_{j+1/2,k+1}\right) \tag{118}$$

$$\bar{\bar{v}} = \frac{1}{4}\left(v_{j,k-1/2} + v_{j+1,k-1/2} + v_{j,k+1/2} + v_{j+1,k+1/2}\right) \tag{119}$$

The additional terms

$$\frac{\partial}{\partial x}\left[(\bar{h}^{y} + \bar{\eta}^{x})u\right],\ \frac{\partial}{\partial y}\left[(\bar{h}^{x} + \bar{\eta}^{y})v\right],\ \frac{\partial}{\partial x}\left[(\bar{h}^{y} + \bar{\eta}^{x})*u\right],$$

and

$$\frac{\partial}{\partial y}\left[(\bar{h}^{x} + \bar{\eta}^{y})*v\right]$$

require special computational procedures for η. These are described by Leendertse (1967).

Hwang and Divoky (1975) show the same equations in spherical coordinates with u the velocity in the θ-direction, and v the velocity in the ϕ-direction as defined in Figure 9. They use a different approach for the computation of the terms noted above which allows more direct computation. Similar equations are shown by Houston, et al. (1975b). For the coordinate system in Figure 11, the equations given by Hwang and Divoky (with coriolis terms added) are, at times $t + \Delta t/2$, $t + 3\Delta t/2$, $t + 5\Delta t/2$, . . .

$$u_{n+1/2} = u_n - \frac{g}{2R_e}\frac{\Delta t}{\Delta\theta}\left(\frac{\partial \eta}{\partial \theta}\right)_{n+1/2} + \frac{1}{2}\Delta t\, f_c\, \bar{\bar{v}}_n \tag{120}$$

$$\eta_{n+1/2} = \eta_n - \frac{\Delta t}{2\, R_e \sin\theta}\left\{\frac{1}{\Delta\theta}\frac{\partial}{\partial\theta}\left[\left(\overline{d+\eta}\right)^{\phi} u \sin\theta\right]_{n+1/2} + \frac{1}{\Delta\phi}\frac{\partial}{\partial\phi}\left[\left(\overline{d+\eta}\right)^{\theta} v\right]_{n}\right\} \tag{121}$$

$$v_{n+1/2} = v_n - \frac{g}{2\, R_e \sin\theta}\frac{\Delta t}{\Delta\phi}\left(\frac{\partial \eta}{\partial \phi}\right)_{n} - \frac{1}{2}\Delta t\, f_c\, \bar{\bar{u}}_{n+1/2}$$

with terms such as $\partial\eta/\partial\theta$, $\partial\eta/\partial\phi$, $\bar{\bar{u}}$, and $\bar{\bar{v}}$ computed as before. At times $t + \Delta t$, $t + 2\Delta t$, $t + 3\Delta t$, . . .

$$v_{n+1} = v_{n+1/2} - \frac{g}{2\, R_e \sin\theta}\frac{\Delta t}{\Delta\phi}\left(\frac{\partial \eta}{\partial \phi}\right)_{n+1} - \frac{1}{2}\Delta t\, f_c\, \bar{\bar{u}}_{n+1/2} \tag{122}$$

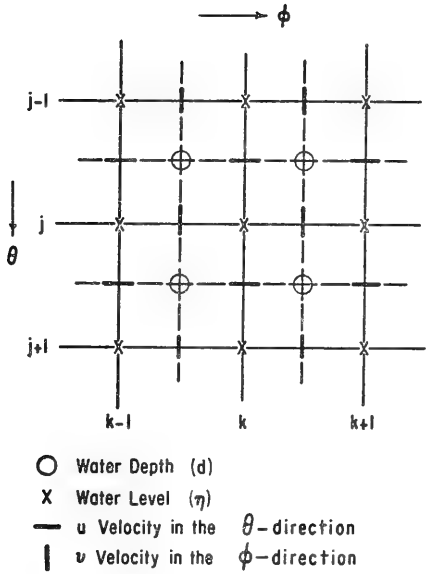

Figure 11. Coordinate system, spherical coordinates.

$$\eta_{n+1} = \eta_{n+1/2} - \frac{\Delta t}{2 R_e \sin\theta}\left\{\frac{1}{\Delta\theta}\frac{\partial}{\partial\theta}\left[\overline{(d+\eta)}^{\phi} u \sin\theta\right]_{n+1/2} + \frac{1}{\Delta\phi}\frac{\partial}{\partial\phi}\left[\overline{(d+\eta)}^{\theta} v\right]_{n+1}\right\} \quad (123)$$

$$u_{n+1} = u_{n+1/2} - \frac{g}{2 R_e}\frac{\Delta t}{\Delta\theta}\left(\frac{\partial\eta}{\partial\theta}\right)_{n+1/2} + \frac{1}{2}\Delta t\, f_c \bar{\bar{v}}_{n+1} \quad (124)$$

Again, the bottom-friction, forcing functions, and convective inertia terms are ignored. Terms like $\overline{(d+\eta)}^{\theta}$ are computed by averaging in the θ-direction, and $\overline{(d+\eta)}^{\phi}$ by averaging in the ϕ-direction.

In addition to specifying equations of motion, boundary conditions for the computational area must be established. Hwang and Divoky (1975) use solid boundaries at coastlines and fictitious open boundaries at edges of the computational area where it is necessary to truncate the region of computation. At solid boundaries, complete reflection is assumed. At open boundaries, the wave is assumed to travel without change in form across the final space step, so that

$$\frac{\eta_B - \eta_2}{\eta_1 - \eta_2} = \frac{\Delta t\sqrt{gd}}{\Delta s} \quad (125)$$

with the terms defined in Figure 12.

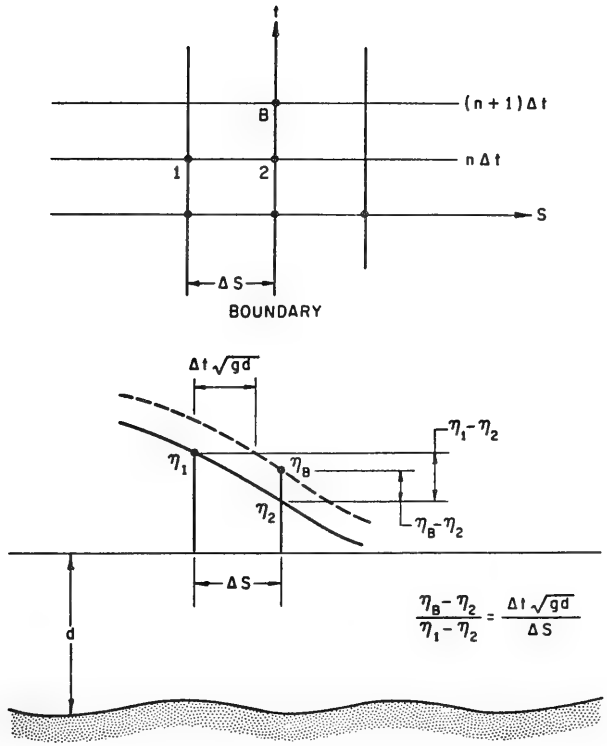

Figure 12. Graphical representation of the total transmission open boundary condition (from Hwang and Divoky, 1975).

Houston and Garcia (1974) and Hwang and Divoky (1975) used numerical techniques to obtain predicted wave heights for the 1964 tsunami originating in Prince William Sound, Alaska. The uplifting and subsidence determined from field surveys (Plafker, 1965; Berg, et al., 1970) was used as the initial deformation of the water surface. Predicted wave heights 13,000 seconds (3.61 hours) after the time of generation are shown in Figure 13.

The assumptions that complete reflection occurs at a solid boundary (i.e., at a shoreline) and that equation (125) will describe an open boundary introduce errors into the computations which limit the length of real-time records which can be simulated numerically. At a shoreline, some amount of wave energy may be trapped so that complete reflection does not occur. Wave trapping is discussed later in this report.

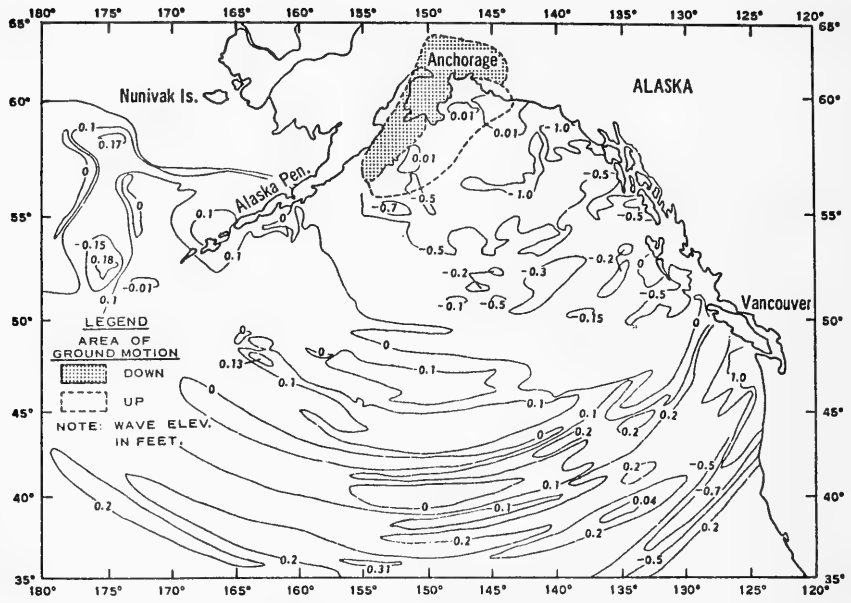

Figure 13. Surface elevation contours 13,000 seconds after the 1964 Alaska earthquake (from Hwang and Divoky, 1975).

The use of equation (125) at the open boundaries results in an error in the computed wave heights at those boundaries. As computations are carried out for the entire computational grid at each time step, the error propagates through the grid at successive time steps. This error will have the appearance of a wave reflected from the open boundary. Shaw (1974, 1975; Shaw, Department of Engineering Science, State University of New York, Buffalo, personal communication, 1977) suggests that an outer boundary integral equation method can be used to eliminate the error at the open boundaries. The outer boundary integral equation would be used to determine the wave height, η, and its normal derivatives at the boundary; those values would be used in the finite-difference solutions for the interior region.

6. Nearshore Computer Models.

For waves in the nearshore region, Peregrine (1967) developed finite-difference equations for the two-dimensional case of a wave shoaling on a beach. Defining

$$u_{r,s} = u(r\Delta x,\ s\Delta t) \quad (r = 1,\ldots,n \quad s = 1,\ldots,n)$$

$$\eta_{r,s} = \eta(r\Delta x,\ s\Delta t)$$

he calculated the values of u and η with a time-stepping procedure, first using an approximation to the continuity equation which gives $\eta^*_{r,s+1}$, a provisional value of $\eta_{r,s+1}$, by the equation

$$\frac{\eta^*_{r,s+1} - \eta_{r,s}}{\Delta t} + (ax + \eta_{r,s}) \frac{u_{r+1,s} - u_{r-1,s}}{2\Delta x} + u_{r,s} \left[\frac{\eta_{r+1,s} - \eta_{r-1,s}}{2\Delta x} + \alpha \right] = 0 \qquad (126)$$

Then, $u_{r,s+1}$ is calculated from an approximation to the momentum equation

$$\frac{u_{r,s+1} - u_{r,s}}{\Delta t} + u_{r,s} \frac{u_{r+1,s+1} - u_{r-1,s+1} + u_{r+1,s} - u_{r-1,s}}{4\Delta x} + \frac{\eta^*_{r+1,s+1} - \eta^*_{r-1,s+1} + \eta_{r+1,s} - \eta_{r-1,s}}{4\Delta x}$$

$$= \frac{1}{3} (\alpha x)^2 \frac{u_{r+1,s+1} - 2u_{r,s+1} + u_{r-1,s+1} - u_{r+1,s} + 2u_{r,s} - u_{r-1,s}}{\Delta x^2 \Delta t} + \alpha^2 x \frac{u_{r+1,s+1} - u_{r-1,s+1} - u_{r+1,s} + u_{r-1,s}}{\Delta x \Delta t} \qquad (127)$$

Finally, the continuity equation is used again to give an improved value for $\eta_{r,s+1}$

$$\frac{\eta_{r,s+1} - \eta_{r,s}}{\Delta t} + (\alpha x + \eta_{r,s}) \frac{u_{r+1,s+1} - u_{r-1,s+1} + u_{r+1,s} - u_{r-1,s}}{\Delta x} + \frac{u_{r,s+1} + u_{r,s}}{2} \left[\frac{\eta_{r+1,s} - \eta_{r-1,s}}{2\Delta x} + \alpha \right] = 0 \qquad (128)$$

Street, Chan, and Fromm (1970) and Chan, Street, and Fromm (1970) extended Peregrine's work, using a Marker-and-Cell numerical technique to obtain solutions for waves propagating in one direction. Where values are known at time t, they compute the values of u and w at time $t + \Delta t$ using the equations

$$u_{j+1/2,k} = u^*_{j+1/2,k} + g_x \Delta t + \frac{\Delta t}{\Delta x} (p_{j,k} - p_{j+1,k}) \qquad (129)$$

$$w_{j,k+1/2} = w^*_{j,k+1/2} + g_z \Delta t + \frac{\Delta t}{\Delta z} (p_{j,k} - p_{j,k+1}) \qquad (130)$$

where the coordinate system is shown in Figure 14, p is pressure, g_x

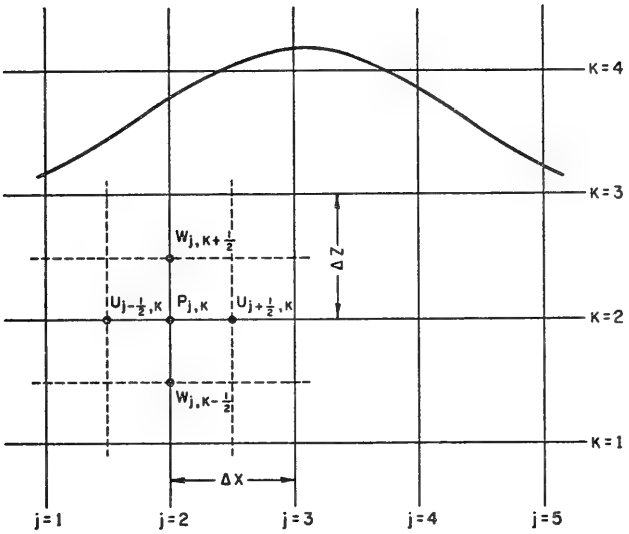

Figure 14. Position of variables.

and g_z the components of gravitational acceleration, and u* and w* convective terms. The terms on the right side of equations (129) and (130) are taken at time t. Then, the pressures are recomputed from the equation

$$p_{j,k} = \frac{1}{B}\left(\frac{p_{j+1,k} + p_{j-1,k}}{\Delta x^2} + \frac{p_{j,k+1} + p_{j,k-1}}{\Delta z^2} + R_{j,k}\right) \tag{131}$$

where

$$B = 2\left(\frac{1}{\Delta x^2} + \frac{1}{\Delta z^2}\right) \tag{132}$$

and

$$R_{j,k} = -\frac{1}{\Delta t}\left(\frac{u^*_{j+1/2,k} - u^*_{j-1/2,k}}{\Delta x} + \frac{w^*_{j,k+1/2} - w^*_{j,k-1/2}}{\Delta z}\right) \tag{133}$$

The convective terms are defined as shown by Fromm (1968). The equation for $u^*_{j+1/2,k}$ is

$$u^*_{j+1/2,k} = \tilde{u}_{j+1/2,k-1} + \frac{\beta - 1}{2}\left(u_{j+1/2,k-2} - \tilde{u}_{j+1/2,k}\right) + \frac{(\beta - 1)^2}{2}\left(\tilde{u}_{j+1/2,k-2} - 2\tilde{u}_{j+1/2,k-1} + \tilde{u}_{j+1/2,k}\right) \tag{134}$$

where

$$\tilde{u}_{j+1/2,k} = u_{j-1/2,k} + \frac{\alpha - 1}{2}(u_{j-3/2,k} - u_{j+1/2,k}) + \frac{(\alpha - 1)^2}{2}(u_{j-3/2,k} - 2u_{j-1/2,k} + u_{j+1/2,k}) \quad (135)$$

$$\alpha = u_{j+1/2,k}\frac{\Delta t}{\Delta x} \quad (136)$$

$$\beta = w_{j+1/2,k}\frac{\Delta t}{\Delta z} \quad (137)$$

Similar expressions can be developed for other convective terms.

For points near the free surface (Fig. 15), Chan and Street (1970a) give the equation for $P_{j,k}$ as

$$p_{j,k} = \frac{\delta_1\delta_2\delta_3\delta_4}{2(\delta_2\delta_4 + \delta_1\delta_3)}\left[\frac{\delta_3 p_1 + \delta_1 p_3}{\delta_1\delta_3\left(\frac{\delta_1 + \delta_3}{2}\right)} + \frac{\delta_4 p_2 + \delta_2 p_4}{\delta_2\delta_4\left(\frac{\delta_2 + \delta_4}{2}\right)} + R_{j,k}\right] \quad (138)$$

The free-surface position, as given by Chan, Street, and Fromm (1970) at time t + Δt is

$$\frac{\eta_j}{\Delta t} = w_j - u_j\left(\frac{\eta_{j+1} - \eta_{j-1}}{2\Delta x}\right) + \frac{\eta_j(t)}{\Delta t} \quad (139)$$

where $\eta_j(t)$ is the elevation at time t, and u_j and w_j the horizontal and vertical velocities, respectively, at the free surface at time t + Δt.

For refracting waves propagating in two dimensions in the plane of the water surface, Chen, Divoky, and Hwang (1975) give the equations below using dimensionless expansions similar to those proposed by Peregrine (1967). A time-staggered scheme is used, with the velocities and wave amplitudes calculated explicitly at alternate time steps of Δt/2. The amplitudes at t_o + Δt/2 will be calculated using amplitude at t_o - Δt/2 and velocities at t_o; then, the velocities at t_o + Δt will be calculated using velocities at t_o and amplitudes at t_o + Δt/2. At time t_o + Δt/2, the amplitude is

$$\eta_{j,k} = \eta_{j,k} - \frac{\Delta t}{2\Delta x}\left[\left\{(d + \eta)\,\bar{u}\right\}_{j+1,k} - \left\{(d + \eta)\,\bar{u}\right\}_{j-1,k}\right] - \frac{\Delta t}{2\Delta y}\left[\left\{(d + \eta)\,\bar{v}\right\}_{j,k+1} - \left\{(d + \eta)\,\bar{v}\right\}_{j,k-1}\right] \quad (140)$$

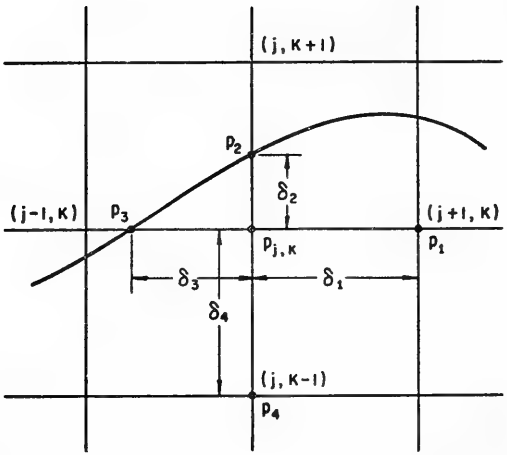

Figure 15. Computation of pressure near the free surface.

where the j,k subscripts refer to positions in the plane of the still-water surface as shown in Figure 10, and $\bar{u}$ and $\bar{v}$ the velocities satisfying the linear long-wave equations. Where the initial velocity field is known, $\bar{u}$ and $\bar{v}$ can be computed at time $t_o + \Delta t$ using values of $\bar{u}$ and $\bar{v}$ at time t_o and amplitudes at time $t_o + \Delta t/2$. This gives the equations

$$\bar{u}_{j,k} = \bar{u}_{j,k} - \frac{\Delta t}{2\Delta x} (\eta_{j+1,k} - \eta_{j-1,k}) \tag{141}$$

$$\bar{v}_{j,k} = \bar{v}_{j,k} - \frac{\Delta t}{2\Delta y} (\eta_{j,k+1} - \eta_{j,k-1}) \tag{142}$$

At time $t_o + \Delta t$, the velocities $\bar{u}$ and $\bar{v}$ are given by

$$u_{j,k} = u_{j,k} - \frac{\Delta t}{2\Delta x} \bar{u}_{j,k} (\bar{u}_{j+1,k} - \bar{u}_{j-1,k}) - \frac{\Delta t}{2\Delta y} \bar{v}_{j,k} (\bar{u}_{j,k+1} - \bar{u}_{j,k-1}) - \frac{\Delta t}{2\Delta x} (\eta_{j+1,k} - \eta_{j-1,k}) \tag{143}$$

$$v_{j,k} = v_{j,k} - \frac{\Delta t}{2\Delta x} \bar{u}_{j,k} (\bar{v}_{j+1,k} - \bar{v}_{j-1,k}) - \frac{\Delta t}{2\Delta y} \bar{v}_{j,k} (\bar{v}_{j,k+1} - \bar{v}_{j,k-1}) - \frac{\Delta t}{2\Delta y} (\eta_{j,k+1} - \eta_{j,k-1}) \tag{144}$$

where the values on the right side of the equations are at previous time steps as indicated.

Chen, Divoky, and Hwang (1975), using a stability criterion obtained by Benjamin, Bona, and Mahony (1972), use a higher order solution for the amplitude when

$$d < \frac{\Delta x}{(20\ \Delta t)^{1/3}}$$

where the variables are expressed in dimensionless form. The solution then becomes

$$\eta_{j,k} = \eta_{j,k} - \frac{\Delta t}{2\Delta x}\left[\left\{(d + \eta)\ \bar{u}\right\}_{j+1,k} - \left\{(d + \eta)\ \bar{u}\right\}_{j-1,k}\right]$$

$$- \frac{\Delta t}{2\Delta y}\left[\left\{(d + \eta)\ \bar{v}\right\}_{j,k+1} - \left\{(d + \eta)\ \bar{v}\right\}_{j,k-1}\right]$$

$$- \Delta t\ (\text{higher order derivative terms}) \qquad (145)$$

The higher order derivatives are approximated by central difference equations as follows

$$\frac{\partial^3 \bar{u}}{\partial x^3} = \frac{1}{2(\Delta x)^3}\left[\bar{u}_{j+2,k} - 2\bar{u}_{j+1,k} + 2\bar{u}_{j-1,k} - \bar{u}_{j-2,k}\right] \qquad (146)$$

$$\frac{\partial^3 \bar{v}}{\partial y^3} = \frac{1}{2(\Delta y)}\left[\bar{v}_{j,k+2} - 2\bar{v}_{j,k+1} + 2\bar{v}_{j,k-1} - \bar{v}_{j,k-2}\right] \qquad (147)$$

$$\frac{\partial^2 d}{\partial x \partial y} = \frac{1}{4\Delta x \Delta y}\left[d_{j+1,k+1} - d_{j-1,k+1} - d_{j+1,k-1} + d_{j-1,k-1}\right] \qquad (148)$$

etc. Computed surface elevations were smoothed when one of the following conditions was satisfied:

(a) A crest or trough has wave amplitude less than 25 percent of the maximum wave amplitude at that instant;

(b) the local velocity component (u) or (v) has a different sign from the average value of the surrounding four points;

(c) at a matching point where equations change from linear to higher order equations.

Smoothing is accomplished by the average

$$\eta_{j,k} = 0.5[\eta_{j,k} + \bar{\eta}_{j,k}] \qquad (149)$$

where the values on the right side are before smoothing, and

$$\bar{\eta}_{j,k} = \frac{\tilde{\eta}_{j,k}}{12k + 4} \tag{150}$$

where

$$\tilde{\eta}_{j,k} = (1 + 4k)(\eta_{j-1,k} + \eta_{j+1,k} + \eta_{j,k-1} + \eta_{j,k+1}) - k(\eta_{j-2,k} + \eta_{j+2,k} + \eta_{j,k-2} + \eta_{j,k+2}) \tag{151}$$

and k represents a weighting spline coefficient that varies from 0 to ∞. The influence from the surrounding points is controlled by the values of (k). For the case k = 0, the equation reduces to Laplacian interpolation.

To avoid numerical instability, Chen, Divcky, and Hwang (1975) imposed the condition at matching points that

$$\eta_{matching} = 0.5(\eta_{linear} + \eta_{higher\ order})$$

Also, the partial derivative with respect to time was approximated by

$$\frac{\partial \eta}{\partial t} = \frac{\eta_{j,k} - \bar{\eta}_{j,k}}{\Delta t} \tag{152}$$

where η is taken at time $t_o + \Delta t/2$ and $\bar{\eta}$ at $t_o - \Delta t/2$, and

$$\bar{\eta}_{j,k} = 0.5\ \eta_{j,k} + 0.125(\eta_{j-1,k} + \eta_{j+1,k} + \eta_{j,k-1} + \eta_{j,k+1}) \tag{153}$$

For the open boundary condition previously mentioned (Fig. 12), the finite-difference equation becomes

$$\eta_{B,k} = \eta_{B,k} - \frac{\bar{C}\Delta t}{\Delta x}(\eta_{B,k} - \eta_{B-1,k}) - \frac{\Delta t}{2\Delta y}\left[\left\{(d + \eta)\ v\right\}_{j,k+1} - \left\{(d + \eta)\ v\right\}_{j,k-1}\right] \tag{154}$$

where

$$\bar{C} = [g(d + \eta)]^{1/2}\left(1 + 0.5\ \frac{\eta}{d + \eta}\right) \tag{155}$$

Listings of typical computer programs for solutions of long-wave equations can be found in Brandsma, Divoky, and Hwang (1975) for linear long-wave equations, and in Chen, Divoky, and Hwang (1975) for Boussinesq-type equations.

V. TSUNAMIS APPROACHING THE SHORELINE

As a tsunami approaches a coastline, the waves are modified by the various offshore and coastal features. Submerged ridges and reefs, continental shelves, headlands, various shaped bays, and the steepness of the beach slope may modify the wave period and wave height, cause wave resonance, reflect wave energy, and cause the waves to form bores which surge onto the shoreline.

Ocean ridges provide very little protection to a coastline. While some amount of the energy in a tsunami might reflect from the ridge, the major part of the energy will be transmitted across the ridge and into the coastline. The 1960 tsunami which originated along the coast of Chile is an example of this. That tsunami had high wave heights along the coast of Japan, including Shikoku and Kyushu which lie behind the South Honshu Ridge (Hirono, 1961).

1. Abrupt Depth Transitions.

An ocean shelf along a coastline may cause greater modification to a tsunami than an ocean ridge. Waves may become higher and shorter, and dispersion may occur. Lamb (1932) gave the equations for a single wave passing over an abrupt change in water depth as shown in Figure 16. He considered only the case of a wave at a zero angle of incidence, i.e., $\theta_1 = \theta_2 = 0$. The equations he derived are

$$\frac{H_r}{H_i} = \frac{d_1^{1/2} - d_2^{1/2}}{d_1^{1/2} + d_2^{1/2}} \tag{156}$$

$$\frac{H_t}{H_i} = \frac{2d_1^{1/2}}{d_1^{1/2} + d_2^{1/2}} \tag{157}$$

and

$$\frac{H_t}{H_i} = 1 + \frac{H_r}{H_i} \tag{158}$$

or

$$H_t = H_i + H_r$$

where

H_i = the incident wave height

H_r = the reflected wave height

H_t = the transmitted wave height

d_1 = the initial water depth

d_2 = the water depth under the transmitted wave

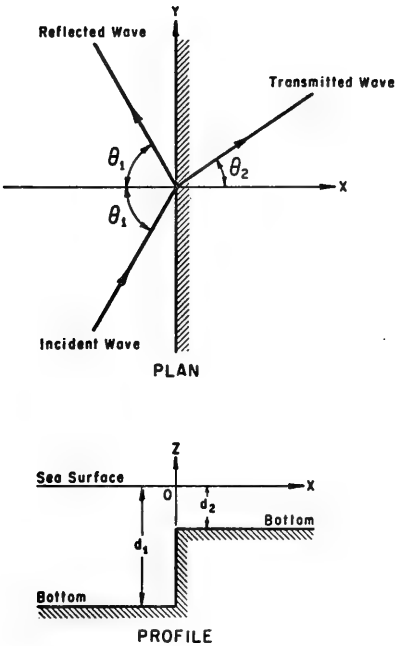

Figure 16. Wave passing onto shelf.

The equations predict that substantial reflection will occur when a wave passes from deep water to shallow water, and also when a wave passes from shallow water to deep water. It is assumed that no energy loss occurs, and that a single incident wave splits into a single reflected wave and a single transmitted wave. Taking E_i as the wave energy of the incident wave, E_r as the wave energy of the reflected wave, and E_t as the wave energy of the transmitted wave,

$$\frac{E_r}{E_i} = \frac{H_r^2 L_r}{H_i^2 L_i} = \frac{H_r^2 C_r}{H_i^2 C_i} = \left(\frac{d_1^{1/2} - d_2^{1/2}}{d_1^{1/2} + d_2^{1/2}}\right)^2 \frac{d_1^{1/2}}{d_1^{1/2}} = \left(\frac{d_1^{1/2} - d_2^{1/2}}{d_1^{1/2} + d_2^{1/2}}\right)^2 \tag{159}$$

$$\frac{E_t}{E_i} = \frac{H_t^2 L_t}{H_i^2 L_i} = \frac{H_t^2 C_t}{H_i^2 C_i} = \left(\frac{2d_1^{1/2}}{d_1^{1/2} + d_2^{1/2}}\right)^2 \frac{d_2^{1/2}}{d_1^{1/2}} \tag{160}$$

and from equations (159) and (160)

$$\frac{E_r}{E_i} + \frac{E_t}{E_i} = \left(\frac{d_1^{1/2} - d_2^{1/2}}{d_1^{1/2} + d_2^{1/2}}\right)^2 + \left(\frac{2d_1^{1/2}}{d_1^{1/2} + d_2^{1/2}}\right)^2 \frac{d_2^{1/2}}{d_1^{1/2}} \tag{161}$$

which reduces to

$$\frac{E_r + E_t}{E_i} = 1 \tag{162}$$

Cochrane and Arthur (1948) extended Lamb's work to consider waves approaching a shelf at varying angles of incidence. They give the ratio of reflected wave height to incident wave height as

$$\frac{H_r}{H_i} = \frac{\sqrt{d_1}\cos\theta_1 - \sqrt{d_2}\cos\theta_2}{\sqrt{d_1}\cos\theta_1 + \sqrt{d_2}\cos\theta_2} \tag{163}$$

for an abrupt change in water depth. The water depths d_1 and d_2, and the angles θ_1 and θ_2, are defined in Figure 16. This equation also applies to a single wave with a reflected component and a transmitted component.

For a given incident wave angle θ_1, the value of θ_2 can be determined using Snell's Law so that

$$\sin\theta_2 = (\sin\theta_1)\left(\frac{d_2}{d_1}\right)^{1/2} \tag{164}$$

Equation (163), as written, applies to shallow-water waves; wave dispersion on the shelf is not considered. The solutions to equations (163) and (164) are presented graphically in Figures 17 and 18, respectively.

The ratio of transmitted wave height H_t to the incident wave height is given by

$$\frac{H_t}{H_i} = \frac{2\sqrt{d_1}\cos\theta_1}{\sqrt{d_1}\cos\theta_1 + \sqrt{d_2}\cos\theta_2} \tag{165}$$

or, alternatively,

$$\frac{H_t}{H_i} = 1 + \frac{H_r}{H_i}$$

as before.

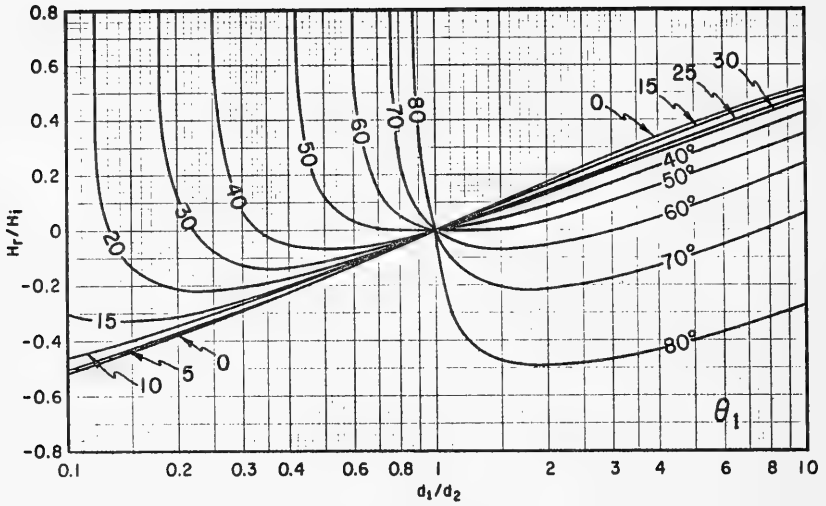

Figure 17. Wave reflection from a shelf (after Cochrane and Arthur, 1948).

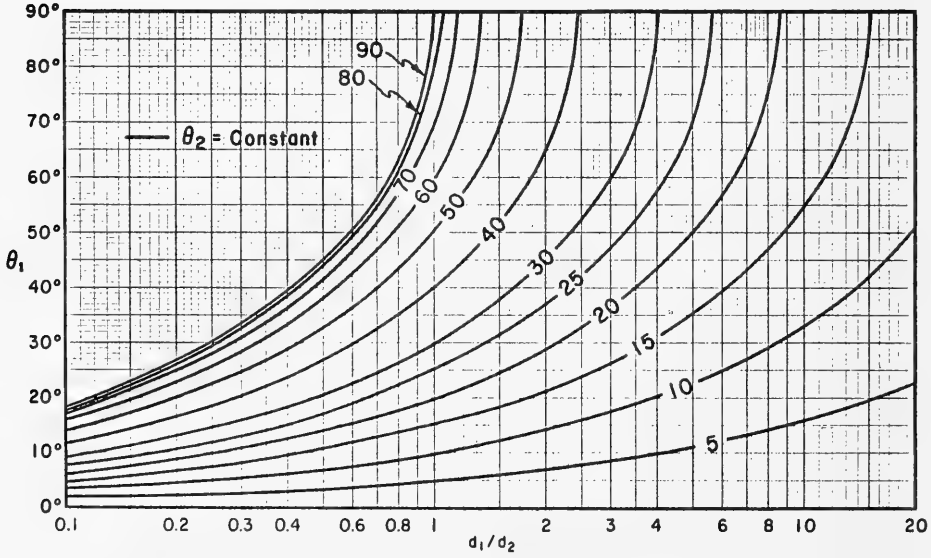

Figure 18. Transmitted wave angle θ_2 versus incident wave angle θ_1.

* * * * * * * * * * * * * * EXAMPLE PROBLEM 4 * * * * * * * * * * * * * *

GIVEN: An incident wave with a height of 1 meter (3.28 feet) and a period of 30 minutes approaches a coastline through water 2,500 meters (8,200 feet) deep, and passes onto a shelf where the water depth is 100 meters, at an angle of incidence $\theta_1 = 30°$

FIND:

(a) The angle at which the transmitted wave propagates onto the shelf,

(b) the height of the reflected wave, and

(c) the height of the transmitted wave.

SOLUTION:

(a) From equation (164)

$$\sin \theta_2 = \left(\frac{d_2}{d_1}\right)^{1/2} \sin \theta_1$$

$$\theta_2 = \sin^{-1}\left[\left(\frac{100}{2,500}\right)^{1/2} \sin 30°\right] = \sin^{-1}(0.1)$$

$$\theta_2 = 5.74°$$

(b) From equation (163)

$$H_r = \frac{\sqrt{d_1} \cos \theta_1 - \sqrt{d_2} \cos \theta_2}{\sqrt{d_1} \cos \theta_1 + \sqrt{d_2} \cos \theta_2} (H_i)$$

$$H_r = \frac{\sqrt{2,500} \cos 30° - \sqrt{100} \cos 5.74°}{\sqrt{2,500} \cos 30° + \sqrt{100} \cos 5.74°} (1) = 0.626 \text{ meter (2.05 feet)}$$

(c) From equation (158)

$$H_t = H_i + H_r$$

$$H_t = 1 + 0.626 = 1.626 \text{ meters (5.33 feet)}$$

* *

When the initial angle of incidence $\theta_1 > 0$, the distance between adjacent wave rays is different for the incident and transmitted waves. As the energy equations are written for a unit length of wave crest, from conservation of energy,

$$E_i = E_t \frac{b_t}{b_i} + E_r \tag{166}$$

or, alternatively,

$$E_i = E_t \frac{\cos \theta_2}{\cos \theta_1} + E_r \tag{167}$$

where b_t is the distance between adjacent wave rays for the transmitted wave, and b_i the distance between adjacent wave rays for the incident wave. Rewriting equation (167),

$$\frac{E_t}{E_i} \frac{\cos \theta_2}{\cos \theta_1} + \frac{E_r}{E_i} = 1 \tag{168}$$

which gives

$$\frac{H_t^2 L_t}{H_i^2 L_i} \frac{\cos \theta_2}{\cos \theta_1} + \frac{H_r^2 L_r}{H_i^2 L_i} = 1 \tag{169}$$

Noting that $L_t/L_i = C_t/C_i = \sqrt{d_2/d_1}$ and that $L_r/L_i = C_r/C_i = \sqrt{d_1/d_1} = 1$, and substituting equations (163) and (165) into equation (169),

$$\left(\frac{2\sqrt{d_1} \cos \theta_1}{\sqrt{d_1} \cos \theta_1 + \sqrt{d_2} \cos \theta_2}\right)^2 \left(\frac{d_2}{d_1}\right)^{1/2} \frac{\cos \theta_2}{\cos \theta_1}$$

$$+ \left(\frac{\sqrt{d_1} \cos \theta_1 - \sqrt{d_2} \cos \theta_2}{\sqrt{d_1} \cos \theta_1 + \sqrt{d_2} \cos \theta_2}\right)^2 = 1 \tag{170}$$

which reduces to

$$\left(\frac{\sqrt{d_1} \cos \theta_1 + \sqrt{d_2} \cos \theta_2}{\sqrt{d_1} \cos \theta_1 + \sqrt{d_2} \cos \theta_2}\right)^2 = 1 \tag{171}$$

proving that the equations of Cochrane and Arthur conserve the energy of the incident wave.

Cochrane and Arthur (1948) compared a calculated value for a wave from the 1946 tsunami, which reflected from the continental slope off southern Oregon, with an actual recorded wave height at Hanasaki, Japan. Using a rough approximation for the wave height at the top of the continental slope, it was determined that the reflected wave arriving at Hanasaki would have a height of 17 centimeters (0.56 foot). The observed

wave height, for an arrival time equal to the calculated time for the reflected wave, was in good agreement with the calculated wave height.

Figure 17 shows that for waves arriving with a higher angle of incidence there will be some value of d_1/d_2 for which equation (163) predicts no reflected wave. For these same values of d_1/d_2, the predicted transmitted wave height would equal the incident wave height. Cochrane and Arthur note that reflected waves are normally of secondary, but not negligible, magnitude according to theory. At given stations, convergence may cause reflected waves to be of primary magnitude, but this occurs only in relatively few cases. Shepard, MacDonald, and Cox (1950) note that the highest and most damaging waves at Napoopoo and Hokeena, on the island of Hawaii, from the 1 April 1946 tsunami originating in the Aleutian Islands, Alaska, were reflected waves from the continental slopes of Japan and the Bonin Islands.

2. Linear Depth Transitions.

Cochrane and Arthur (1948) indicate that the length of a continental slope, as well as the difference in water depth, should be considered in the calculations. Dean (1964) considered the case of a wave normally incident on a linear change in water depth shown in Figure 19. Defining a parameter, Z_1, as

$$Z_1 = \frac{4\pi d_1}{L_1 S} \tag{172}$$

the transmission coefficient

$$K_t = \frac{H_t}{H_i} \tag{173}$$

and the reflection coefficient

$$K_r = \frac{H_r}{H_i} \tag{174}$$

Dean found the results shown in Figure 20. As before, for the zero angle of incidence assumed by Dean, when $d_1/d_2 < 1.0$ the value of the reflection coefficient K_r is negative. When $d_1/d_2 > 1.0$ the value of K_r is positive.

* * * * * * * * * * * * * * EXAMPLE PROBLEM 5 * * * * * * * * * * * * * *

GIVEN: An incident wave, which is 0.5 meter (1.64 feet) high and has a period of 40 minutes, recedes from the coastline through water 100 meters deep and passes from the shallow water over a shelf into water 3,025 meters (9,925 feet) deep. The transition between the two water

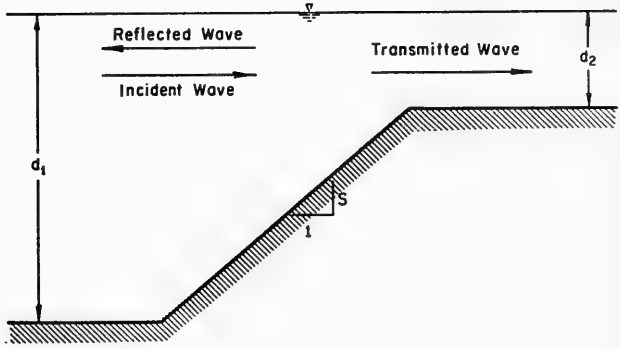

Figure 19. Linear slope and shelf.

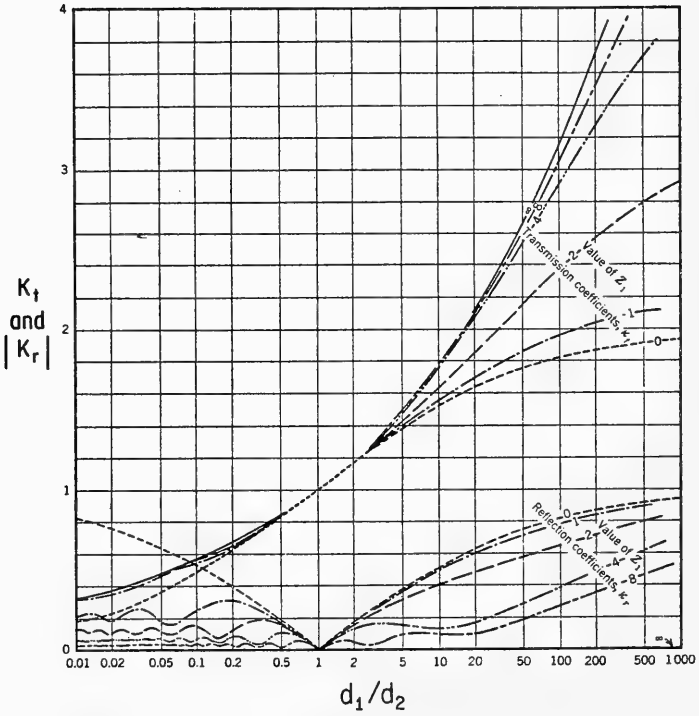

Figure 20. Reflection and transmission coefficients (from Dean, 1964).

depths is a linear slope S = 0.1 and the wave is at a zero angle of incidence with the slope transition, i.e., $\theta_1 = 0$.

FIND:

(a) The height of the reflected wave,

(b) the height of the transmitted wave, and

(c) show that energy is conserved, i.e., that the total energy in the reflected and transmitted waves equals the incident wave energy.

SOLUTION:

(a) $L_1 = C_1 T = \sqrt{gd_1}\, T$

$$L_1 = \sqrt{9.8 \times 100}\ (40 \times 60) = 75{,}100 \text{ meters}$$

From equation (172),

$$Z_1 = \frac{4\pi d_1}{L_1 S}$$

$$Z_1 = \frac{4\pi \times 100}{75{,}100 \times 0.1} = 0.167$$

From Figure 20, where

$$\frac{d_1}{d_2} = \frac{100}{3{,}025} = 0.033 \text{ and } Z_1 = 0.167$$

it is found that

$K_r \simeq -0.62$ (the negative sign indicates that the reflected wave is π radians out of phase with incident wave)

$H_r = 0.62\ H_i = 0.62(0.5) = 0.31$ meter (1.02 feet)

(b) From Figure 20,

$K_t \simeq 0.32$

$H_t = 0.32\ H_i = 0.32(0.5) = 0.16$ meter (0.52 foot)

(c) $\gamma = \rho g$ = (1,026 kilograms per cubic meter) (9.8 meters per second squared)

$\gamma = 10.055$ kilograms per square meter - second squared

The energy per meter length of wave crest is

$$E_i = \frac{\gamma H_i^2 L_i}{8} = \frac{10{,}055(0.5)^2\ 75{,}100}{8}$$

$$= 2.36 \times 10^7 \text{ kilogram-meters per second squared}$$

$$= 2.36 \times 10^7 \text{ joules}$$

$$E_r = \frac{\gamma H_r^2 L_r}{8} = \frac{10{,}055(0.31)^2\ 75{,}100}{8} = 9.07 \times 10^6 \text{ joules}$$

$$L_t = C_2 T = \sqrt{gd_2}\ T = \sqrt{9.8 \times 3{,}025}\ (40 \times 60) = 413{,}000 \text{ meters}$$

$$E_t = \frac{\gamma H_t^2 L_t}{8} = \frac{10{,}055(0.16)^2\ 413{,}000}{8} = 1.33 \times 10^7 \text{ joules}$$

As K_r is negative, i.e., the reflected wave is out of phase, then for energy to be conserved

$$E_i - E_r = E_t$$

$$E_i - E_r = 2.36 \times 10^7 - 9.07 \times 10^6 = 1.45 \times 10^7 \text{ joules}$$

compared to the computed value of $E_t = 1.33 \times 10^7$ joules. The difference results from the minor errors which occur using Figure 20.

* *

3. Nonlinear Depth Transitions.

Kajiura (1963) investigated waves passing from deep water to shallow water over the nonlinear slope profile shown in Figure 21. The profile is defined by the equation

$$\frac{1}{d(x)} = \frac{1}{2}\left(\frac{1}{d_1} + \frac{1}{d_2}\right) - \frac{1}{2}\left(\frac{1}{d_2} - \frac{1}{d_1}\right)\tanh\left(\frac{nx}{2}\right) \tag{175}$$

where the effective slope length ℓ is given by

$$\ell = \frac{2\pi}{n} \tag{176}$$

L_1 is the wavelength at depth d_1, L_2 is the wavelength at depth d_2, and n is an arbitrary small number in equation (175) which fits the equation to the actual slope and determines the length of the slope in equation (176).

The reflection coefficient obtained by Kajiura is given by the equation

$$\frac{H_r}{H_i} = \left| \frac{\sinh\left[\pi\left(\frac{\ell}{L_2} - \frac{\ell}{L_1}\right)\right]}{\sinh\left[\pi\left(\frac{\ell}{L_2} + \frac{\ell}{L_1}\right)\right]} \right| \tag{177}$$

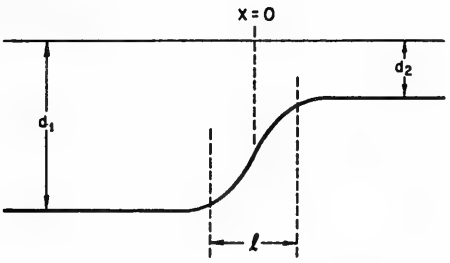

Figure 21. Slope and shelf.

The solution of equation (177) is plotted in Figure 22. As shown in the figure, the reflection coefficient approaches zero as the slope length ℓ approaches the length of the incident wave L_1.

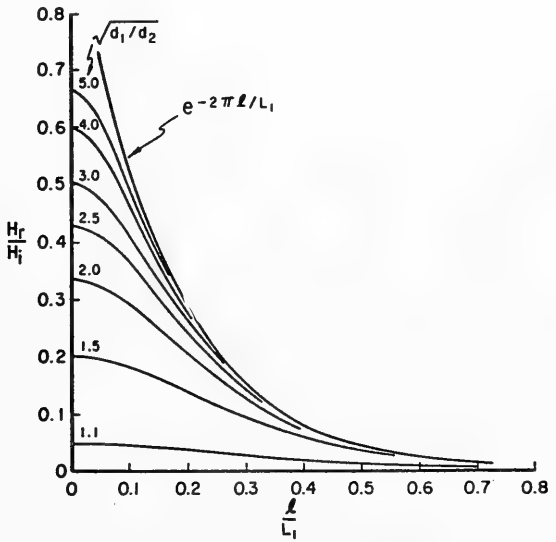

Figure 22. Reflection coefficients (from Kajiura, 1963).

* * * * * * * * * * * * * EXAMPLE PROBLEM 6 * * * * * * * * * * * * * *

GIVEN: An incident wave which is 0.6 meter (1.97 feet) high and has a period of 20 minutes, approaches the coastline through water 2,500 meters deep and passes onto a shelf where the water depth is 100 meters, at a zero angle of incidence ($\theta_1 = 0$). The effective length of the slope between the two water depths is ℓ = 24,000 meters (14.9 miles). It is assumed that the slope is defined by equation (175) and that energy is conserved; i.e., the total of the reflected and transmitted wave energy equals the incident wave energy.

FIND:

(a) The height of the reflected wave,

(b) the height of the transmitted wave, and

(c) the height of the reflected wave for a linear slope of the same length.

SOLUTION:

(a) $L_1 = C_1 T = \sqrt{gd_1}\, T = \sqrt{9.8(2,500)}\ (20 \times 60)$

$L_1 = 187,800$ meters (116.7 miles)

$$\frac{\ell}{L_1} = \frac{24,000}{187,800} = 0.128$$

$$\sqrt{\frac{d_1}{d_2}} = \sqrt{\frac{2,500}{100}} = 5$$

From Figure 22

$$\frac{H_r}{H_i} = 0.46$$

$H_r = 0.46\ H_i = 0.46(0.6) = 0.28$ meter (0.91 foot)

(b) From conservation of energy,

$$E_i = \frac{\gamma H_i^2 L_1}{8} = \frac{10,055(0.6)^2\ 187,800}{8} = 8.50 \times 10^7 \text{ joules}$$

$$E_r = \frac{\gamma H_r^2 L_1}{8} = \frac{10,055(0.28)^2\ 187,800}{8} = 1.85 \times 10^7 \text{ joules}$$

$E_t = E_i - E_r = 6.65 \times 10^7$ joules

$L_t = L_2 = C_2 T = \sqrt{gd_2}\, T = \sqrt{9.8(100)}\ (20 \times 60)$

$L_t = 37,600$ meters (23.3 miles)

$$E_t = \frac{\gamma H_t^2 L_t}{8} = 6.65 \times 10^7 \text{ joules}$$

$$H_t = \left(\frac{8 \times 6.65 \times 10^7}{10,055 \times 37,600}\right)^{1/2}$$

$$H_t = 1.19 \text{ meters } (3.89 \text{ feet})$$

(c) The slope is defined by

$$S = \frac{(d_1 - d_2)}{\ell} = \frac{(2,500 - 100)}{24,000} = 0.1$$

From equation (172),

$$Z_1 = \frac{4\pi d_1}{L_1 S} = \frac{4\pi(2,500)}{187,800(0.1)} = 1.67$$

From Figure 20, where $d_1/d_2 = 25$

$$\frac{H_r}{H_i} = 0.55$$

$$H_r = 0.55\ H_i = 0.55(0.6) = 0.33 \text{ meter } (1.08 \text{ feet})$$

which indicates that a linear slope gives a higher reflected wave and lower transmitted wave than a slope defined by equation (176).

* *

4. Experimental Measurements.

Bourodimos and Ippen (1968) obtained experimental results for waves passing from deep water to shallow water over a slope where S = 0.125. Their experimental curves for K_t and K_r as functions of d_1/d_2 are given in Figure 23. Gagnon and Bocco (1962) obtained measurements for waves passing from shallow water to deep water at an abrupt transition in depth. However, their results indicated a fairly constant value of $|K_r| \approx 0.2$, including the case where $d_1 = d_2$ (i.e., where no transition occurs).

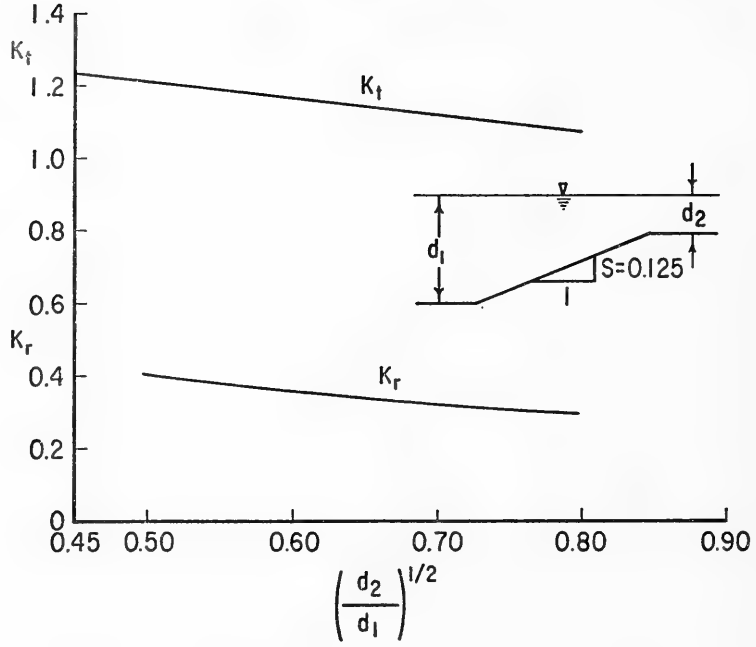

Figure 23. Reflection and transmission coefficients (modified from Bourodimos and Ippen, 1968).

5. Solitons and Shoaling-Induced Dispersion.

For certain conditions, a wave will decompose into a train of waves. Examples of this are shown in Figures 24 to 28. This train of waves will consist of an initial wave having the highest amplitude, followed by a finite number of waves of decreasing amplitude. Wave decomposition has been investigated by Mason and Keulegan (1944), Horikawa and Wiegel (1959), Benjamin and Feir (1967), Street, Burgess, and Whitford (1968), Madsen and Mei (1969), Byrne (1969), Street, Chan, and Fromm (1970), Galvin (1970), Zabusky and Galvin (1971), and Hammack and Segur (1974).

Benjamin and Feir (1967) discuss the stability of waves, and indicate that the waves will only be unstable if $kd > 1.363$, where k is the wave number $2\pi/L$. Whitham (1967) showed that equations governing extremely gradual variations in wave properties are elliptic if $kd > 1.363$, and hyperbolic if $kd < 1.363$. For tsunamis, where $d/L \ll 1$, the equations will be hyperbolic and the waves will be stable, at least in a constant water depth.

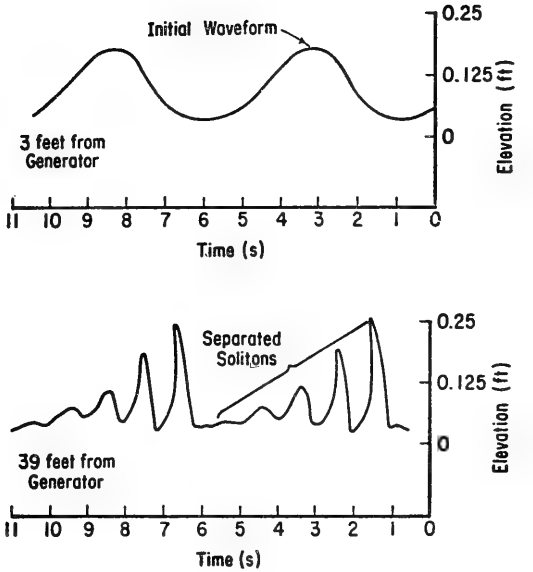

Figure 24. Separation of solitons (from Galvin, 1970).

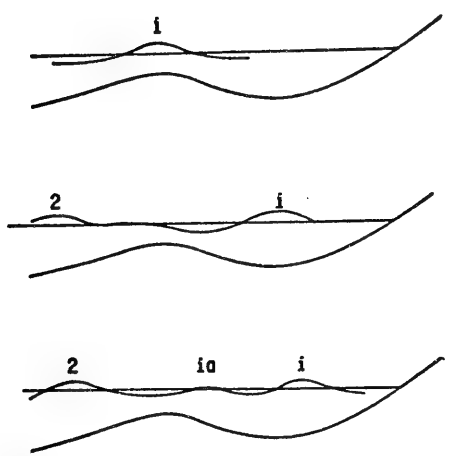

Figure 25. Induced wave generation over a submerged bar (from Byrne, 1969).

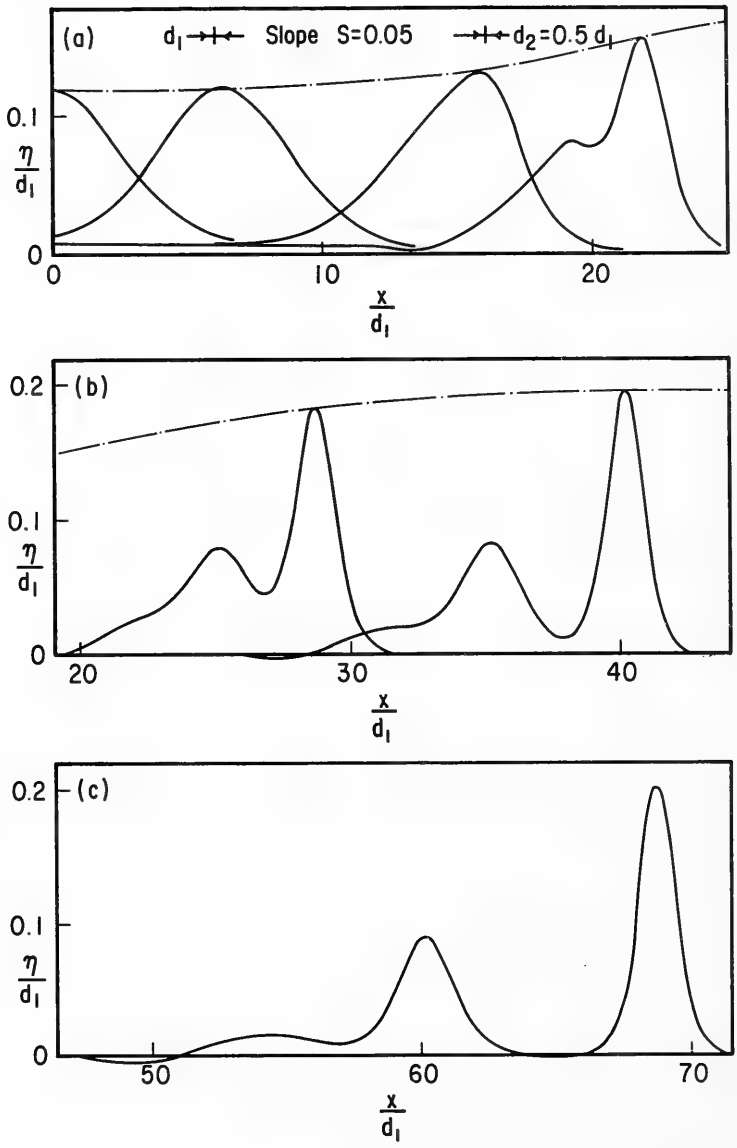

Figure 26. Solitary wave propagating over a slope onto a shelf (from Madsen and Mei, 1969).

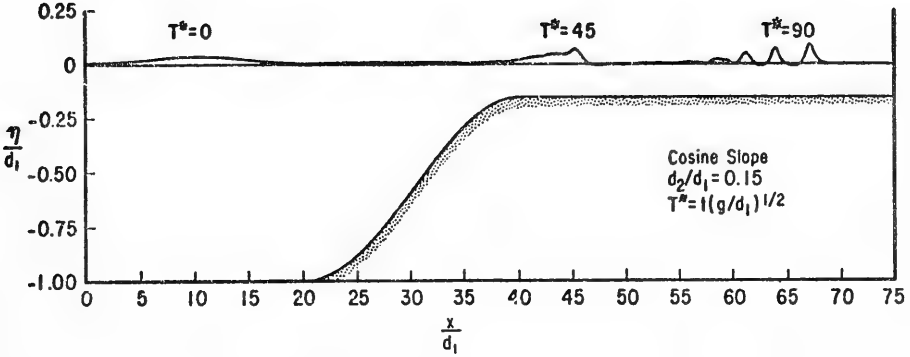

Figure 27. Solitary wave propagating onto a shelf (from Street, Chan, and Fromm, 1970).

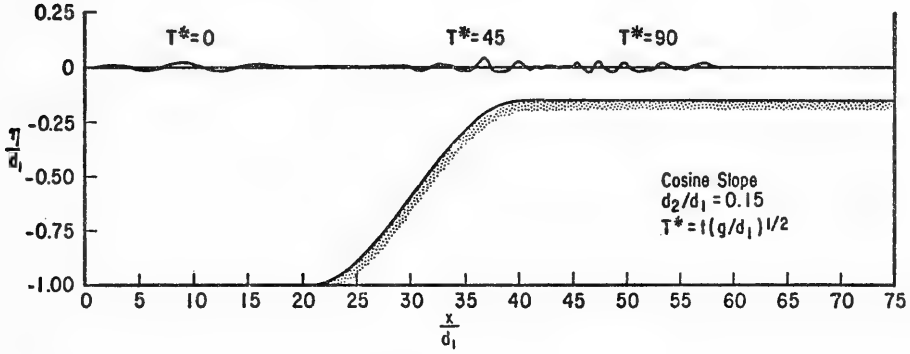

Figure 28. Wave train propagating onto a shelf (from Street, Chan, and Fromm, 1970).

* * * * * * * * * * * * * * * EXAMPLE PROBLEM 7 * * * * * * * * * * * * * * *

GIVEN: A tsunami with a wave period of 15 minutes travels through water 3,000 meters (9,840 feet) deep.

FIND: If the wave is stable.

SOLUTION: The wave celerity is given by

$$C = \sqrt{gd} = \sqrt{9.807 \times 3{,}000} = 171.5 \text{ meters (563 feet) per second}$$

The wavelength is

$$L = CT = 171.5 \times 15 \times 60 = 154{,}350 \text{ meters (95.9 miles)}$$

From this

$$\frac{d}{L} = \frac{3{,}000}{154{,}350} = 0.0194$$

and

$$kd = 0.0194(2\pi) = 0.122$$

Therefore, kd < 1.363 and the wave is stable.

* *

Galvin (1970) investigated waves propagating through water of uniform depth in a laboratory wave tank. He found that the initial generated waves broke down into several waves which are called solitons. Figure 24 illustrates an example where, for a water depth of 0.15 meter (0.5 foot) and a generator period of 5.2 seconds, each of the initial waves broke down into five solitons. Taking these waves as shallow-water waves, the wavelength is approximately 6.4 meters, and kd $\simeq$ 0.15 which would indicate that the waves are stable. However, it may be assumed that the generated waves were not actually single waves, but rather a combination of several solitons. Galvin noted that if a group of such waves traveled over a sufficiently long distance, the solitons would recombine into single waves, separate again into solitons, etc. There are commonly two or three solitons, but as many as seven could exist in some instances. If a generated tsunami had the characteristics of a group of solitons, it could appear differently at various coastal points, depending on the distance from the generating area.

Zabusky and Galvin (1971) compared numerical and experimental results for solitons, using the Korteweg-deVries equations, for cases where $22 \leq U \leq 777$, where U is defined as $(H/d)(L/d)^2$. They found good comparisons for slightly dissipative waves. Hammack and Segur (1974) also studied numerical and experimental results. They found that soliton generation is dependent on the net volume change in the body of water. When the net volume of the initial wave system was positive (e.g., from uplifting of the sea bottom), solitons evolved followed by a dispersive train of oscillatory waves. If the initial generating mechanism was negative everywhere (sea bottom subsidence), no solitons evolved.

Byrne (1969) made field observations of waves passing over a near-shore bar. He noted that a wave passing over a bar would sometimes produce a second, trailing wave as shown schematically in Figure 25. As these additional waves developed near the shoreline, he was unable to determine if such waves would recombine with the waves in the initial wave train.

Mason and Keulegan (1944) investigated waves passing into a shallower water depth, with an abrupt change in depth. The condition for instability obtained from their experiments was

$$(a_1 L_1)^{1/2} > 2d_2 \tag{178}$$

where a_1 is the wave amplitude in the deeper water, L_1 the wavelength in the deeper water, and d_2 the depth in the shallower water. Their results were confirmed by Horikawa and Wiegel (1959), although in the latter report there is an apparent discrepancy in the presentation of the results; the right side of equation (178) has been multiplied by $\sqrt{2}$.

* * * * * * * * * * * * * * EXAMPLE PROBLEM 8 * * * * * * * * * * * * * *

GIVEN: A tsunami with a period of 15 minutes passes from water 3,000 meters deep onto a shelf where the water depth is 200 meters (656 feet).

FIND: The maximum wave amplitude for a stable wave which will not decompose into a train of waves.

SOLUTION: The wave celerity in deep water is

$$C_1 = \sqrt{gd_1} = \sqrt{9.807 \times 3{,}000} = 171.5 \text{ meters per second}$$

and the wavelength is

$$L_1 = C_1 T = 171.5 \times 15 \times 60 = 154{,}350 \text{ meters (95.9 miles)}$$

The condition for wave instability is given by equation (178) as

$$(a_1 L_1)^{1/2} > 2d_2$$

$$(a_1 \times 154{,}350)^{1/2} > 2 \times 200$$

$$a_1 > 1.04 \text{ meters (3.40 feet)}$$

Thus, waves with a deepwater amplitude less than 1.04 meters would not decompose.

* * * * * * * * * * * * * * EXAMPLE PROBLEM 9 * * * * * * * * * * * * * *

GIVEN: A tsunami travels from a 3,000-meter water depth into a 200-meter water depth. The wave period is 60 minutes.

FIND: The maximum wave amplitude for a stable wave which will not decompose into a train of waves.

SOLUTION: The deepwater wave celerity is given as

$$C_1 = (gd_1)^{1/2} = (9.807 \times 3{,}000)^{1/2} = 171.5 \text{ meters per second}$$

and the wavelength is

$$L_1 = C_1 T = 171.5 \times 60 \times 60 = 617{,}400 \text{ meters (384 miles)}$$

From equation (178), wave instability is given by

$$(a_1 L_1)^{1/2} > 2d_2$$

$$(a_1 \times 617{,}400)^{1/2} > 2 \times 200$$

$$a_1 > 0.26 \text{ meter (0.85 foot)}$$

Waves with a deepwater amplitude less than 0.26 meter will not decompose.

* *

Using the results of Mason and Keulegan (1944), the above examples illustrate that the longer period tsunamis are much more likely to decompose where the waves have the same height in the deep ocean.

Street, Burgess, and Whitford (1968) investigated solitary waves passing from an initial water depth, over a steep slope, and into a shallower water depth. They obtained results similar to those of other investigators, showing that each wave changed from a single wave into a train of several waves. In some instances, there was also a significant increase in wave height. Defining the initial water depth as d_1, the shallower depth as d_2, the initial wave height as H_i, and the wave height in the shallower water depth as H_t, as the ratio d_1/d_2 increased, relative wave height H_t/H_i reached a maximum value for any initial wave height H_i and then decreased. As H_i/d_1 decreased, the maximum value of H_t/H_i became greater and occurred at a higher value of d_1/d_2. The locus of the maximum values of wave enhancement, H_t/H_i, are shown in Figure 29 with the results for the solitary wave experiments.

Madsen and Mei's (1969) numerical results for the propagation of long waves give the results shown in Figure 26 for a solitary wave passing over a slope and onto a shelf. The numerical results of Street, Chan, and Fromm (1970) give the results shown in Figure 27 for a solitary wave, and the results shown in Figure 28 for a train of waves. Goring (1978) has also recently carried out experiments on solitary waves propagating onto a shelf. His results are similar to those of Street, Chan, and Fromm (1970) and Madsen and Mei (1969).

In all cases where a single wave produced a series of wave crests, the first wave crest of the series was the highest. It may be presumed that a number of initial wave crests will produce the same number of groups of wave crests, each having a high initial wave followed by smaller waves. The numerical work of Street, Chan, and Fromm (1970) for wave trains is inconclusive in this regard as Figure 28 shows the additional wave crests, but does not separate the waves into groups associated with the initial crests.

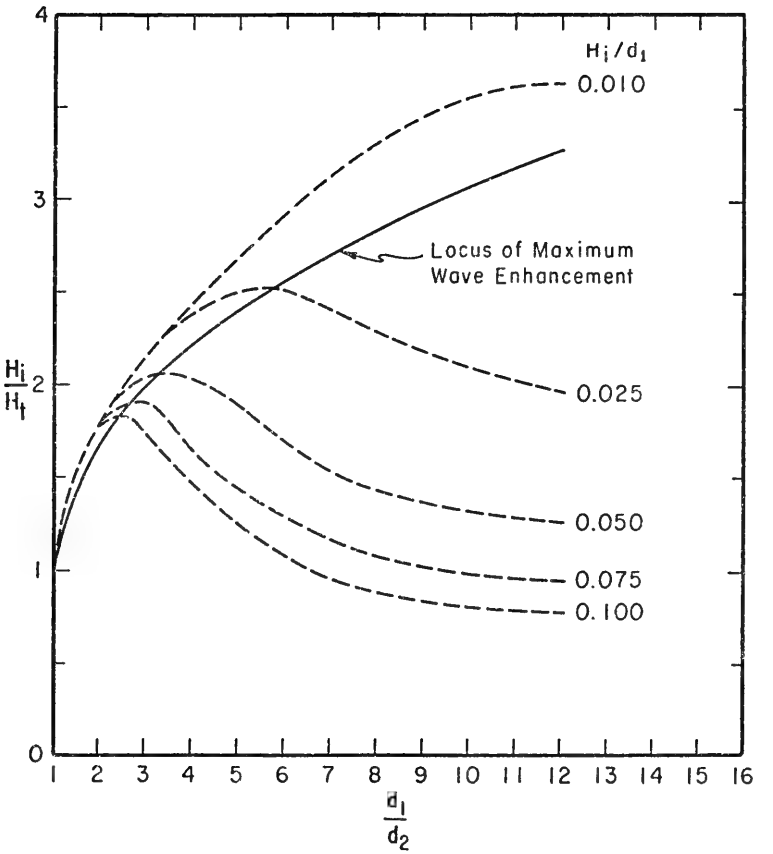

Figure 29. Wave enhancement (from Street, Burgess, and Whitford, 1968).

VI. TSUNAMI-SHORELINE INTERACTION

In addition to the shoaling of waves on the nearshore slope, a tsunami may interact with a shoreline in a number of different ways, including standing wave resonance at the shoreline, the generation of edge waves by the impulse of the incident waves, the trapping of reflected incident waves by refraction, and, as the reflected wave from the shoreline propagates seaward, the reflection of wave energy from an abrupt change in water depth at the seaward edge of a shelf. Also, a wave arriving at an oblique angle to the shoreline may produce a Mach-stem along the shoreline. All of the above interactions depend on wave reflection at the shoreline. Tsunamis entering inlets and harbors may also produce resonant conditions within the inlets and harbors. LeBlond and Mysak (1977) provide a general discussion of edge waves and wave trapping.

1. Wave Reflection.

The reflection of an incident wave ray from a shoreline is illustrated in Figure 30. The angle, α_1, between the wave ray and a line normal to a tangent to the shoreline will have the same value for the incident and the reflected wave rays. For a steep nearshore slope, the reflected wave will be in phase with the incident wave.

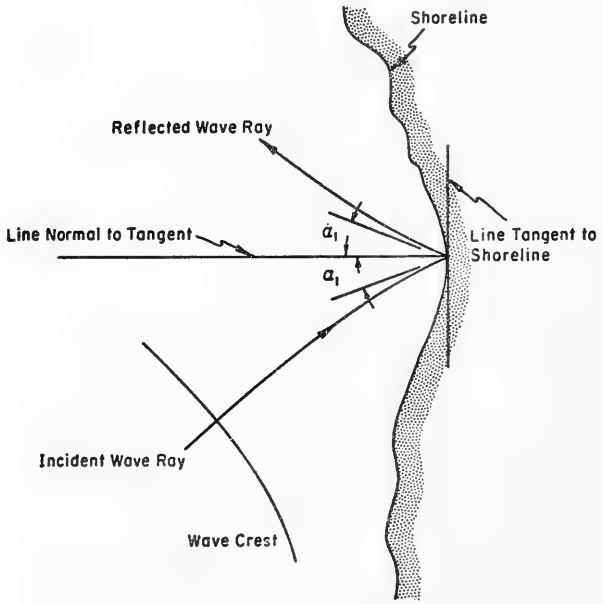

Figure 30. Wave reflection from a shoreline.

Miche (1944) defined the wave reflection at a shoreline in terms of a critical wave steepness, $(H/L)_c$, which is given by

$$\left(\frac{H}{L}\right)_c = \left(\frac{2\beta}{\pi}\right)^{1/2} \frac{\sin^2\beta}{\pi} \tag{179}$$

where β is the angle of the beach slope in radians. Complete reflection will occur if the wave steepness, H/L, in deeper water is given by

$$\frac{H}{L} \leq \left(\frac{H}{L}\right)_c \tag{180}$$

* * * * * * * * * * * * * * EXAMPLE PROBLEM 10 * * * * * * * * * * * * * *

GIVEN: A tsunami has a height of 0.5 meter and a period of 20 minutes in a 1,000-meter water depth. The nearshore slope $S_3 = 0.1$ ($\beta = 0.0997$ radians).

FIND: If the wave is completely reflected at the shoreline.

SOLUTION: In the deeper water, the wave celerity, C, is

$$C = \sqrt{gd} = \sqrt{9.807 \times 1{,}000} = 99 \text{ meters per second}$$

$$L = CT = 99 \times 20 \times 60 = 118{,}800 \text{ meters}$$

$$\frac{H}{L} = \frac{0.5}{118{,}800} = 4.21 \times 10^{-6}$$

From equation (179)

$$\left(\frac{H}{L}\right)_c = \left(\frac{2\beta}{\pi}\right)^{1/2} \frac{\sin^2\beta}{\pi} = \left(\frac{2 \times 0.997}{\pi}\right)^{1/2} \frac{\sin^2(0.0997)}{\pi}$$

$$\left(\frac{H}{L}\right)_c = 7.94 \times 10^{-4}$$

$$\frac{H}{L} < \left(\frac{H}{L}\right)_c$$

thus, the wave is completely reflected at the shoreline.

* *

Wiegel (1964) indicates that where

$$\frac{H}{L} > \left(\frac{H}{L}\right)_c \tag{181}$$

that the reflection will be defined by

$$\frac{H_r}{H_i} = c_R \frac{\left(\frac{H}{L}\right)_c}{\left(\frac{H}{L}\right)} \tag{182}$$

where c_R is a coefficient of roughness and permeability which has a value of $c_R = 0.8$ for a smooth impervious beach. Various values of c_R were defined for rough slopes for short-period waves. However, the effect of the slope roughness on longer period waves has not been adequately determined.

* * * * * * * * * * * * * EXAMPLE PROBLEM 11 * * * * * * * * * * * * * *

GIVEN: A tsunami has a height of 0.5 meter and a period of 4 minutes in a 1,000-meter water depth. The nearshore slope $S_3 = 0.01$ ($\beta = 0.01$ radians), and the slope is smooth and impervious.

FIND: The coefficient of reflection H_r/H_i at the shoreline.

SOLUTION: In the deeper water, the wave celerity, C, is

$$C = \sqrt{gd} = \sqrt{9.807 \times 1{,}000} = 99 \text{ meters per second}$$

$$L = CT = 99 \times 4 \times 60 = 23{,}800 \text{ meters (14.8 miles)}$$

$$\frac{H}{L} = \frac{0.5}{23{,}800} = 2.10 \times 10^{-5}$$

From equation (179), where β is given in radians,

$$\left(\frac{H}{L}\right)_c = \left(\frac{2\beta}{\pi}\right)^{1/2} \frac{\sin^2\beta}{\pi} = \left(\frac{2 \times 0.01}{\pi}\right)^{1/2} \frac{\sin^2(0.01)}{\pi}$$

$$\left(\frac{H}{L}\right)_c = 2.54 \times 10^{-6}$$

$$\frac{H}{L} > \left(\frac{H}{L}\right)_c$$

$$\frac{H_r}{H_i} = c_r \frac{\left(\frac{H}{L}\right)_c}{\left(\frac{H}{L}\right)} = 0.8 \frac{2.54 \times 10^{-6}}{2.10 \times 10^{-5}} = 0.097$$

which indicates a low-reflected wave height where the shoreline has a very gradual slope.

* *

2. Shelf Resonance.

Hidaka (1935a, 1935b) carried out a theoretical investigation of a vertical wall at the shoreline, where the water depth at the wall was d_s, and the sea bottom sloped seaward. The depth d at any arbitrary distance x from the shoreline is given by

$$d = d_s \left(1 + \frac{x^2}{a^2}\right)^{1/2} \tag{183}$$

where the horizontal distance, x, is positive measured seaward from the shoreline, $x = 0$ at the shoreline, and a is the distance from the shoreline to the depth $d = \sqrt{2}\, d_s$. The depth variation defined by equation (183) can be compared to a linear (constant) bottom slope, S_2, between the toe of the nearshore slope (taken to be a vertical wall) and a point at the distance $x = a$ from the shoreline. For the linear bottom slope, S_2,

$$S_2 = \frac{d - d_s}{x} \tag{184}$$

or at a distance, a, from the shoreline

$$S_2 = \frac{\sqrt{2}\, d_s - d_s}{a} \tag{185}$$

from which

$$a = \frac{(\sqrt{2} - 1)\, d_s}{S_2} \tag{186}$$

The variables are shown in Figure 31.

Defining the wave by the equation

$$\frac{\partial^2 \eta}{\partial t^2} = g \frac{\partial}{\partial x}\left[d \frac{\partial \eta}{\partial x}\right] \tag{187}$$

Hidaka defined the surface elevation η above the undisturbed water as

$$\eta = U \cos\left(\frac{2\pi t}{T}\right) \tag{188}$$

and U a dimensionless amplitude obtained by dividing the amplitude at any point by the amplitude at the shoreline ($U = 1$ at the shoreline), T the wave period, and t time. Hidaka obtained a theoretical solution for wave resonance on the sloping shelf defined by equation (183) using Mathieu functions (see Blanch, 1964). The primary mode of oscillation

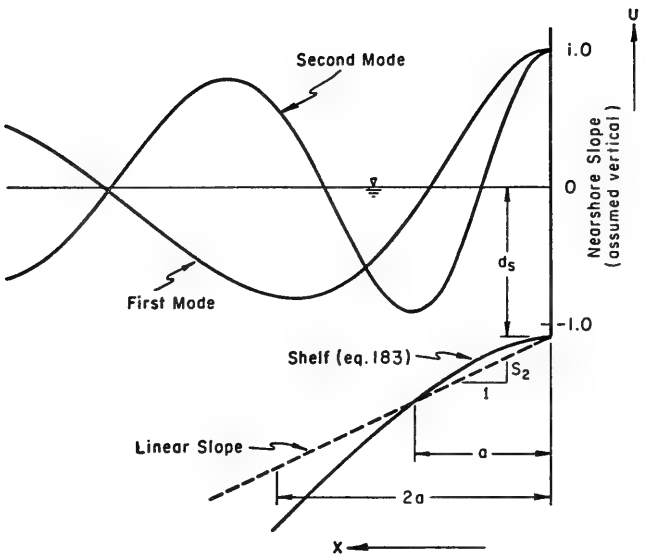

Figure 31. Shelf resonance.

for the shelf is defined by the Mathieu function $Ce_1(\xi, \theta_1)$ where $\theta_1 = 7.51361$. The period is given by

$$T_1 = \frac{2a}{\sqrt{\frac{\theta_1 \, gd_s}{2}}} = 3.2417 \frac{a}{\sqrt{gd_s}} \tag{189}$$

The second mode of oscillation is proportional to the Mathieu function $Ce_2(\xi, \theta_2)$ where $\theta_2 = 21.29863$, and the period T_2 is

$$T_2 = 1.9254 \frac{a}{\sqrt{gd_s}} \tag{190}$$

The first and second modes are shown in Figure 31. The values obtained by Hidaka for resonant periods are for a shelf extending a long distance offshore; i.e., the shelf width $\ell_s >> L$, where L is the wavelength of the incident wave. These results have not been verified by other investigators, but Hidaka's results of the variation of wave amplitude agree very well with those obtained by Wilson (1972) for a constant (linear) shelf slope, as shown in example problem 14.

To determine the variation of wave amplitude with respect to distance from the shoreline, the equation for U is put in the form

$$\frac{d^2U}{d\rho^2} + \left[\frac{\frac{\theta}{2}}{(1+\rho^2)^{1/2}} + \frac{\frac{1}{4}}{(1+\rho^2)} + \frac{\frac{3}{4}}{(1+\rho^2)^2} \right] U = 0 \qquad (191)$$

where $\rho = x/a$. This equation was solved by Hidaka using Stormer's method (see Milne, 1953). The wave profile is defined in Table 1.

Table 1. Distribution of amplitude U (from Hidaka, 1935b).

First mode				Second mode			
x/α	U	x/α	U	x/α	U	x/α	U
0.0	1.0000	2.0	-0.7985	0.0	1.0000	2.0	0.5600
0.1	0.9813	2.1	-0.7766	0.1	0.9474	2.1	0.6665
0.2	0.9265	2.2	-0.7432	0.2	0.7964	2.2	0.7392
0.3	0.8391	2.3	-0.6998	0.3	0.5668	2.3	0.7773
0.4	0.7244	2.4	-0.6476	0.4	0.2868	2.4	0.7818
0.5	0.5889	2.5	-0.5880	0.5	-0.0115	2.5	0.7548
0.6	0.4392	2.6	-0.5224	0.6	-0.2972	2.6	0.6995
0.7	0.2822	2.7	-0.4520	0.7	-0.5445	2.7	0.6197
0.8	0.1239	2.8	-0.3781	0.8	-0.7346	2.8	0.5200
0.9	-0.0305	2.9	-0.3018	0.9	-0.8566	2.9	0.4052
1.0	-0.1766	3.0	-0.2241	1.0	-0.9070	3.0	0.2800
1.1	-0.3110	3.1	-0.1462	1.1	-0.8887	3.1	0.1493
1.2	-0.4313	3.2	-0.0688	1.2	-0.8096	3.2	0.0176
1.3	-0.5357	3.3	0.0072	1.3	-0.6807	3.3	-0.1110
1.4	-0.6233	3.4	0.0810	1.4	-0.5149	3.4	-0.2327
1.5	-0.6936	3.5	0.1521	1.5	-0.3256	3.5	-0.3443
1.6	-0.7466	3.6	0.2197	1.6	-0.1261	3.6	-0.4430
1.7	-0.7827	3.7	0.2834	1.7	0.0716	3.7	-0.5267
1.8	-0.8028	3.8	0.3428	1.8	0.2572	3.8	-0.5940
1.9	-0.8076	3.9	0.3975	1.9	0.4221	3.9	-0.6436
		4.0	0.4473			4.0	-0.6754

* * * * * * * * * * * * * EXAMPLE PROBLEM 12 * * * * * * * * * * * * * *

GIVEN: Water depth, d_s, at the toe of a nearshore slope is 30 meters; the distance a = 12,430 meters (7.72 miles). Complete reflection occurs at the nearshore slope, and it can be assumed to behave as a vertical slope.

FIND:

(a) The primary and secondary periods of oscillation, and

(b) the relative wave height of the wave at a distance one wavelength from the shoreline in relation to the wave height at the shoreline, for the second mode.

SOLUTION:

(a) d_s = 30 meters and a = 12,430 meters

From equation (189)

$$T_1 = 3.2417 \frac{a}{\sqrt{gd_s}}$$

$$T_1 = 3.2417 \frac{12,430}{\sqrt{9.807(30)}} = 2,350 \text{ seconds (39.2 minutes)}$$

From equation (190)

$$T_2 = 1.9254 \frac{a}{\sqrt{gd_s}}$$

$$T_2 = 1.9254 \frac{12,430}{\sqrt{9.807(30)}} = 1,395 \text{ seconds (23.3 minutes)}$$

(b) Both the first and second modes of oscillation are in the range of tsunami periods which are likely to occur. Taking h_s as the wave height at the shoreline, Table 1 gives, for the second mode, a height equal to 0.7818 h_s where x/a = 2.4 or where x = 2.4 (12,430) = 29,800 meters (18.5 miles). The values in Table 1 and Figure 32 show that this is approximately the distance between second-mode wave crests (one wavelength).

* *

* * * * * * * * * * * * * EXAMPLE PROBLEM 13 * * * * * * * * * * * * * *

GIVEN: The water depth, d_s, at the toe of a nearshore slope is 15 meters; the distance a = 621 meters (2,039 feet). Complete reflection occurs at the nearshore slope.

FIND: The primary and secondary periods of oscillation.

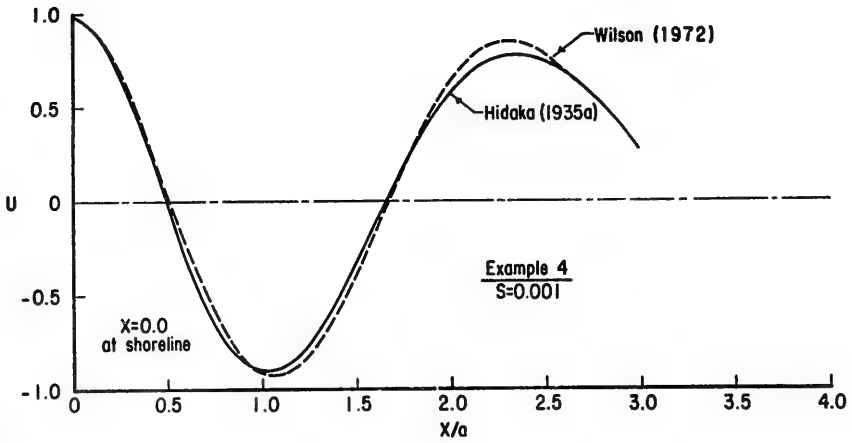

Figure 32. Resonant amplification on a shelf.

SOLUTION: d_s = 15 meters and a = 621 meters.

From equation (189)

$$T_1 = 3.2417 \frac{a}{\sqrt{gd_s}}$$

$$T_1 = 3.2417 \frac{621}{\sqrt{9.807(15)}} = 166 \text{ seconds (2.77 minutes)}$$

From equation (190)

$$T_2 = 1.9254 \frac{a}{\sqrt{gd_s}}$$

$$T_2 = 1.9254 \frac{621}{\sqrt{9.807(15)}} = 98.6 \text{ seconds (1.64 minutes)}$$

* *

A different means of calculating the amplitude U, which will also account for refraction effects (i.e., the effect of a nonuniform offshore bathymetry), is suggested by Wilson (1972). These equations are

$$N_{j+1} = \frac{(B_j D_j - C) N_j - U_j}{C + B_j D_{j+1}} \qquad (192)$$

$$U_{j+1} = U_j + 2C(N_{j+1} + N_j) \tag{193}$$

$$B_j = \frac{2}{[\Delta(b_{j+1} + b_j)]} \tag{194}$$

$$C = \frac{\Delta\omega^2}{(4g)} \tag{195}$$

$$D_j = b_j d_j \tag{196}$$

$$j = 1, 2, 3, \ldots$$

where b_j and b_{j+1} represent the distance between refracted wave rays at stations j and $j + 1$, respectively, N the horizontal displacement of a water particle, and Δ the horizontal distance between stations j and $j + 1$. For an unrefracted wave,

$$B_j D_j = \frac{d_j}{\Delta} \tag{197}$$

$U_o = 1$ at the shoreline (as in the case of Hidaka) and $N_o = 0$ at the shoreline.

Looking at unrefracted waves on a constant shelf slope S_2 for the same wave periods previously defined by equations (189) and (190),

$$T_n = K_n \frac{a}{\sqrt{gd_s}} \tag{198}$$

where $K_1 = 3.2417$ and $K_2 = 1.9254$ as previously defined in equations (189) and (190). From this

$$\omega_n = \frac{2\pi\sqrt{gd_s}}{K_n a} \tag{199}$$

and for the constant slope, from equation (186),

$$\frac{d_s}{a} = \frac{d_s S_2}{(\sqrt{2} - 1)\, d_s} = \frac{S_2}{\sqrt{2} - 1} \tag{200}$$

Defining $\Delta = \varepsilon a$ where ε is an arbitrary increment,

$$B_j D_j = \frac{d_j}{\Delta} = \frac{d_j}{\varepsilon a} = \frac{d_s + jS\ \varepsilon a}{\varepsilon a} \tag{201}$$

$$B_j D_j = S\left[\frac{1}{\varepsilon(\sqrt{2} - 1)} + j\right] \tag{202}$$

at the j^{th} increment.

The equations of Wilson (1972) can then be expressed as

$$N_{j+1} = \frac{\left[S\left(\frac{1}{\varepsilon(\sqrt{2} - 1)} + j - \frac{\pi^2 \varepsilon}{K_n^2(\sqrt{2} - 1)}\right) N_j - U_j\right]}{S\left(\frac{\pi^2 \varepsilon}{K_n^2(\sqrt{2} - 1)} + \frac{1}{\varepsilon(\sqrt{2} - 1)} + j + 1\right)} \tag{203}$$

$$U_{j+1} = U_j + S\left(\frac{2(\pi)^2\ \varepsilon}{K_n^2(\sqrt{2} - 1)}\right)\left(N_{j+1} + N_j\right) \tag{204}$$

* * * * * * * * * * * * * EXAMPLE PROBLEM 14 * * * * * * * * * * * * * * *

GIVEN: The water depth, d_s, at the toe of a nearshore slope is 30 meters; the slope of the shelf is $S_2 = 0.001$. Complete reflection occurs at the nearshore slope.

FIND: The wave profiles using the methods of Hidaka (1935b) and Wilson (1972).

SOLUTION: From example problem 12,

$$a = \frac{(\sqrt{2} - 1)\ d_s}{S} = \frac{(\sqrt{2} - 1)\ 30}{0.001} = 12{,}430 \text{ meters}$$

$$T_1 = 3.2417\ \frac{a}{\sqrt{g d_s}} = 2{,}350 \text{ seconds}$$

$$T_2 = 1.9254\ \frac{a}{\sqrt{g d_s}} = 1{,}395 \text{ seconds}$$

Exploring the second mode of oscillation as before, and using values of

$$\Delta = 0.1\ a = 1{,}243 \text{ meters } (4{,}078 \text{ feet})$$

the values of U obtained by Hidaka (1935b) are given in Table 1. The values obtained by Wilson (1972) are given in Table 2. The wave profiles are plotted in Figure 32.

Table 2. Values of horizontal water particle displacement, N, and wave amplitude, U.

T_2 = 1,395 s	ω_2 = 0.0045	d_s = 30 m	S = 0.001		
x/α	N	U	x/α	N	U
0.0	0	1.0000	1.4	69.50	-0.5928
0.1	-38.79	0.9501	1.5	80.41	-0.4001
0.2	-70.95	0.8090	1.6	85.71	-0.1865
0.3	-94.23	0.5967	1.7	85.49	0.0336
0.4	-107.48	0.3374	1.8	80.14	0.2465
0.5	-110.56	0.0571	1.9	70.33	0.4399
0.6	-104.20	-0.2190	2.0	56.92	0.6035
0.7	-89.82	-0.4684	2.1	40.90	0.7292
0.8	-67.27	-0.6729	2.2	23.31	0.8117
0.9	-44.66	-0.8194	2.3	5.20	0.8484
1.0	-18.17	-0.9002	2.4	-12.43	0.8391
1.1	8.15	-0.9131	2.5	-28.71	0.7862
1.2	32.47	-0.8609	2.6	-42.90	0.6941
1.3	53.29	-0.7507			

For the given conditions, Figure 32 shows that Wilson's method produces almost the same results as those obtained by Hidaka; however, Wilson's results would predict slightly less amplification over the same distance.

* *

In comparing the work of Hidaka (1935a, 1935b) with that of Wilson (1972), the numerical method proposed by Wilson for determining the wave profile is much more readily used for a particular shelf slope. Table 1 (Hidaka, 1935b) has the advantage of being a general solution. The value of shelf slope, S_2 = 0.001, used in example problem 14 is typical of slopes found on many continental shelves. Figure 32 shows that the two methods produce comparable results. Wilson's method has the added feature of considering wave refraction.

3. Reflection from Seaward Edge of Shelf.

Section V discussed the reflection of waves from an abrupt transition in water depth. It was shown that when a wave propagates seaward from

the shoreline some of the wave energy is reflected shoreward from the transition in water depth at the seaward limit of the shelf. This is further illustrated in Figure 33 where d_s is the water depth at the toe of the nearshore slope, d_2 the water depth at the seaward limit of the shelf, d_1 the water depth at the seaward limit of the steep transition in water depth, S_1 the slope of the steep transition, S_2 the slope of the shelf, and S_3 the nearshore slope.

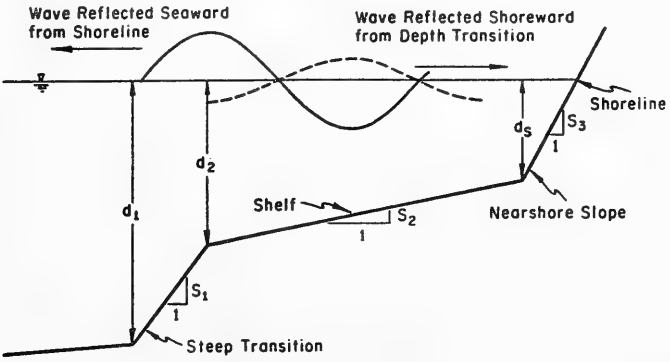

Figure 33. Reflected waves on a shelf.

The wave reflected shoreward from the steep transition may be π radians out of phase with the wave transmitted seaward across the transition. However, the actual phase difference will depend on the geometry of the shelf and transition, and the water depth. This was illustrated in example problem 5. For perfect reflection, the wave reflected from the shoreline will be in phase with the initial wave incident on the shoreline. The time, t_s, for the wave to travel the distance, ℓ_s, from the steep transition to the nearshore slope will be the same as the time required for the reflected wave from the nearshore slope to travel back to the steep transition in depth. Therefore, where the wave reflected from the transition is π radians out of phase with the incident wave, resonance will occur if

$$2t_s = \frac{nT}{2} \tag{205}$$

where T is the incident wave period, and $n = 1, 2, 3, \ldots$

Noting that $C = \sqrt{gd}$ where $d_s \leq d \leq d_2$, for a wave with a normal angle of incidence,

$$t_s = \int_0^{\ell_s} \frac{dx}{C} \tag{206}$$

where x is measured seaward from the toe of the nearshore slope. By definition

$$\frac{dd}{dx} = S_2 \tag{207}$$

or defining dx,

$$dx = \frac{dd}{S_2} \tag{208}$$

This gives

$$\frac{dx}{C} = \frac{dd}{S_2\sqrt{gd}} \tag{209}$$

and, for a constant shelf slope,

$$t_s = \int_{d_s}^{d_2} \frac{dd}{S_2\sqrt{gd}} = \frac{2(d_2^{1/2} - d_s^{1/2})}{S_2\ g^{1/2}} \tag{210}$$

Substituting equation (210) into equation (205) gives

$$T = \frac{8}{n} \frac{(d_2^{1/2} - d_s^{1/2})}{S_2\ g^{1/2}} \tag{211}$$

where T is a resonant wave period where the reflected wave and incident wave are π radians out of phase, and n = 1, 2, 3, . . . Equation (211) provides a first approximation for the resonant wave periods.

* * * * * * * * * * * * * * EXAMPLE PROBLEM 15 * * * * * * * * * * * * * *

GIVEN: The water depth, d_s, at the toe of a nearshore slope is 30 meters. The width of the shelf, ℓ_s, is 30,000 meters (18.6 miles) and the water depth, d_s, at the the seaward edge of the shelf is 60 meters (196.9 feet).

FIND: The resonant wave periods for the shelf.

SOLUTION: The slope of the shelf, S_2, for a constant slope is given by

$$S_2 = \frac{d_2 - d_s}{\ell_s} = \frac{60 - 30}{30{,}000} = 0.001$$

From equation (211),

$$T = \frac{8}{n} \frac{(d_2^{1/2} - d_s^{1/2})}{S_2 \, g^{1/2}} \, , \; n = 1, 2, 3, \ldots$$

$$T = \frac{8}{n} \frac{(60^{1/2} - 30^{1/2})}{0.001 \; (9.807)^{1/2}} = \frac{5,800}{n} \, , \; n = 1, 2, 3, \ldots$$

T_1 = 5,800 seconds (96.7 minutes), n = 1

T_2 = 2,900 seconds (48.3 minutes), n = 2

T_3 = 1,933 seconds (32.2 minutes), n = 3

T_4 = 1,450 seconds (24.2 minutes), n = 4

etc.

* *

Nagaoka (1901) considered the possibility of currents parallel to the coast acting as boundaries which would reflect waves. He speculated that the currents would act as quasi-elastic boundaries. In this case waves generated near a shoreline could be trapped between the shoreline and an offshore current, creating a resonant condition between two boundaries.

4. Edge Waves.

The impulse of incident waves reflecting from the shoreline may generate edge waves in the longshore direction. These edge waves, the trapped mode of longshore wave motion, have wave periods which will be longer than the incident wave periods; standing edge waves will have peaks and nodes at points along the shoreline, although edge waves may be either standing or progressive waves. Guza and Bowen (1975) indicate that experimental results confirm the work of Galvin (1965) and Bowen and Inman (1971) which show that incident waves that are not strongly reflected will not excite edge waves visible at the shoreline.

Guza and Inman (1975) have defined the water surface profile of edge waves in the seaward direction using the dimensionless wave amplitude, U, and a dimensionless distance, χ, in the seaward direction given as

$$\chi = \frac{\omega^2 \, x}{g \tan \beta} \tag{212}$$

where ω is the radian frequency ($2\pi/T$) of the edge wave, x the distance measured from the shoreline in the seaward direction, and β the angle of the nearshore slope ($\tan \beta = S$). The water surface profile is given in Figure 34 which shows that higher modes of standing edge waves

will have peaks and nodes in the seaward direction in addition to the peaks and nodes in the longshore direction.

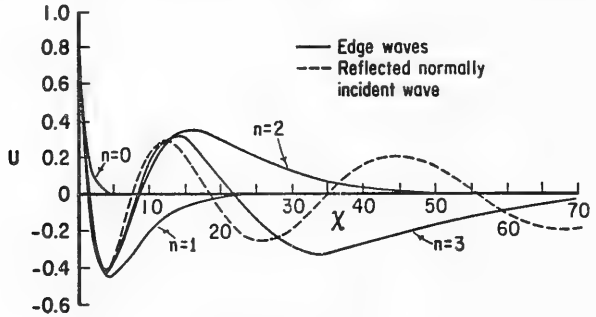

Figure 34. Offshore profiles of edge waves (from Guza and Inman, 1975).

Guza and Davis (1974) carried out a theoretical investigation of the mechanism of edge wave generation by normally incident, shallow-water waves on a constant beach slope. They define the longshore wavelength of the edge wave by the longshore wave number, k_y, given by

$$k_y = \frac{2\pi}{L_y} = \left(\frac{2\pi}{T_y}\right)^2 \frac{1}{g(2n + 1) \tan \beta} \tag{213}$$

where

$$(2n + 1)\ \beta << 1 \tag{214}$$

L_y is the wavelength of the edge wave, T_y the period of the edge wave, and β the angle of the nearshore slope in radians. Guza and Davis attribute the generating mechanism to a nonlinear interaction between the incident wave and a pair of progressive edge waves with frequencies defined by ω_1 and ω_2 where $\omega = 2\pi/T$ and

$$\omega = \omega_1 + \omega_2 \tag{215}$$

i.e., the incident wave frequency is equal to the sum of the two edge wave frequencies. The two edge waves have the same wavelength, but propagate in opposite directions along the shoreline. Therefore, the edge wave pair forms a standing wave. This standing wave will always have a frequency equal to one-half the incident wave frequency (a period twice the incident wave period) even though the frequencies of the edge wave pairs may vary, as shown in Table 3. Where the frequencies of the two progressive edge waves forming the pair are different, the nodes and antinodes of the standing wave will move in the direction of the edge wave with the higher frequency (shorter period). Defining the edge wave with the lower frequency by

Table 3. Resonant edge wave parameters.

N_1	N_2	ω_1	ω_2	k_y	c	K
0	0	0.5	0.5	0.25	1.68×10^{-2}	13
0	1	0.366	0.634	0.134	4.40×10^{-3}	51
0	2	0.309	0.691	0.095	2.28×10^{-3}	100
0	3	0.274	0.726	0.075	1.44×10^{-3}	160
1	1	0.5	0.5	0.083	1.56×10^{-3}	180
1	2	0.427	0.563	0.063	0.88×10^{-3}	330
1	3	0.396	0.604	0.052	0.56×10^{-3}	520
2	2	0.5	0.5	0.05	0.52×10^{-3}	610
2	3	0.458	0.542	0.041	0.36×10^{-3}	810
3	3	0.5	0.5	0.035	0.28×10^{-3}	1,200

$$\omega_1 = (0.5 - p)\ \omega \tag{216}$$

where p is a variable given as $0 < p < 0.5$, and the edge wave with the higher frequency by

$$\omega_2 = (0.5 + p)\ \omega \tag{217}$$

the drift speed, c_d, of the nodes and antinodes of the standing wave is given by

$$c_d = p\ \frac{\omega}{k_y} \tag{218}$$

where ω is the radian frequency of the incident wave and k_y the wave number, $2\pi/L_y$, of the edge wave.

Munk, Snodgrass, and Gilbert (1964) note that because of coriolis splitting, in general, the frequency of edge waves moving left (looking seaward) exceeds the frequency of waves moving to the right in the Northern Hemisphere. In the Southern Hemisphere the opposite would be true. Therefore, for a uniform straight coastline, the higher frequency edge waves would display a preference for moving in a particular direction. Guza and Davis (1974) obtained values for resonant edge wave parameters. Corrected values were presented by Guza and Bowen (1975), and values of the parameters are given in Table 3 for various modes of resonance. The parameters shown in Table 3 are in dimensionless form. The parameter K defines a critical value of incident wave amplitude by

$$K = \frac{a_c^2\ \omega}{\nu} = \frac{k_y^2 (\omega_1 \omega_2)^{1/2}}{8c^2} \tag{219}$$

where c is a coupling coefficient reevaluated by Guza and Bowen and given in Table 3 in dimensionless form, a_c the dimensional critical incident wave amplitude, ν the dimensional kinematic viscosity, and the values N_1 and N_2 define n for ω_1 and ω_2, respectively. The dimensionless value of k_y used in Table 3 and equation (219) is given by

$$k_y = k_y^* \frac{g\beta}{(\omega^*)^2} \tag{220}$$

where k_y^* is the dimensional wave number of the edge wave defined by equation (213) and ω^* the dimensional radian frequency, $2\pi/T$, of the incident wave. The dimensionless values of ω_1 and ω_2 used in Table 3 and equation (219) are given by

$$\omega_1 = \frac{\omega_1^*}{\omega^*}, \quad \omega_2 = \frac{\omega_2^*}{\omega^*}$$

where ω_1^* and ω_2^* are the dimensional values. Table 3 shows that the number of edge wave pairs would increase as the incident wave amplitude increases, i.e., the primary pair ($N_1 = N_2 = 0$) would be excited while the wave is still some distance from the shoreline and the other pairs would be excited closer to the shoreline as the wave amplitude increases. Therefore, the primary pair of edge waves would experience the greatest growth.

* * * * * * * * * * * * * * EXAMPLE PROBLEM 16 * * * * * * * * * * * * * *

GIVEN: A tsunami with a period of 20 minutes approaches the shoreline on a constant shelf slope $S_2 = 0.001$ ($\beta = 0.001$). It is assumed that the nearshore slope is steep enough for the wave to reflect strongly from the shoreline.

FIND:

(a) The wave periods and wavelengths of the first three edge wave pairs ($N_1 = 0_1$, $N_2 = 0$), ($N_1 = 0$, $N_2 = 1$), and ($N_1 = 0$, $N_2 = 2$), and

(b) the wave amplitudes necessary to excite the first three edge wave pairs.

SOLUTION:

(a) From Table 3

$$(N_1 = 0,\ N_2 = 0)\ \omega_1 = 0.5\ \omega$$

$$\frac{2\pi}{T_1} = 0.5\ \frac{2\pi}{T} = 0.5\ \frac{2\pi}{20 \times 60}$$

$$T_1 = \frac{(20 \times 60)}{0.5} = 2{,}400 \text{ seconds (40 minutes)}$$

$$\omega_2 = 0.5\ \omega$$

$$T_2 = T_1 = 2{,}400 \text{ seconds}$$

$(N_1 = 0, N_2 = 1)$ $\omega_1 = 0.366\ \omega = 0.366\ \frac{2\pi}{T}$

$$T_1 = \frac{T}{0.366} = \frac{20 \times 60}{0.366}$$

$$T_1 = 3{,}280 \text{ seconds (54.6 minutes)}$$

$$T_2 = \frac{T}{0.634} = \frac{20 \times 60}{0.634}$$

$$T_2 = 1{,}893 \text{ seconds (31.5 minutes)}$$

$(N_1 = 0, N_2 = 2)$ $\omega_1 = 0.309\ \omega$

$$T_1 = \frac{T}{0.309} = \frac{20 \times 60}{0.309}$$

$$T_1 = 3{,}880 \text{ seconds (64.7 minutes)}$$

$$T_2 = \frac{T}{0.691} = \frac{20 \times 60}{0.691}$$

$$T_2 = 1{,}737 \text{ seconds (28.9 minutes)}$$

The wavelength of the first edge wave pair is given by equation (213) where $n = 0 (N_1 = 0, N_2 = 0)$,

$$k_y = \frac{2\pi}{L_y} = \left(\frac{2\pi}{T}\right)^2 \frac{1}{g(2n + 1) \tan \beta}$$

$$k_y = \left(\frac{2\pi}{2{,}400}\right)^2 \frac{1}{9.807(1)\ 0.001} = 6.99 \times 10^{-4}$$

and $L_y = 8{,}990$ meters (5.6 miles) for both edge waves.

For the second edge wave pair, $N_1 = 0$ for ω_1 and $N_2 = 1$ for ω_2

$$k_y = \left(\frac{2\pi}{3{,}280}\right)^2 \frac{1}{9.807(1)\ 0.001} = 3.74 \times 10^{-4}$$

and L_y = 16,780 meters (10.4 miles) for the first edge wave

$$k_y = \left(\frac{2\pi}{1,893}\right)^2 \frac{1}{9.807(3)\ 0.001} = 3.74 \times 10^{-4}$$

and L_y = 16,780 meters for the second edge wave. Note that the two edge waves of a pair have the same length as indicated by the single value for the dimensionless wave number, k_y, in Table 3.

For the third edge wave pair, $N_1 = 0$ for ω_1 and $N_2 = 2$ for ω_2

$$k_y = \left(\frac{2\pi}{3,880}\right)^2 \frac{1}{9.807(1)\ 0.001} = 2.66 \times 10^{-4}$$

and L_y = 23,500 meters (14.6 miles) for the first edge wave

$$k_y = \left(\frac{2\pi}{1,737}\right)^2 \frac{1}{9.807(5)\ 0.001} = 2.66 \times 10^{-4}$$

and L_y = 23,500 meters for the second edge wave.

(b) The incident wave amplitude needed to generate the first edge wave pair is given by equation (219) as

$$a_c = \left(\frac{K\nu}{\omega}\right)^{1/2}$$

where K is given in Table 3 and $\nu = 1.5 \times 10^{-2}$ stokes (square centimeters per second) (1.6×10^{-5} square feet per second) = 1.5×10^{-6} square meters per second, and $\omega = 2\pi/1,200$

$$a_c = \left(\frac{13 \times 1.5 \times 10^{-6}}{\frac{2\pi}{1,200}}\right)^{1/2} = 0.061 \text{ meter (0.20 foot)}$$

For the second edge wave pair

$$a_c = \left(\frac{51 \times 1.5 \times 10^{-6}}{\frac{2\pi}{1,200}}\right)^{1/2} = 0.12 \text{ meter (0.39 foot)}$$

For the third edge wave pair

$$a_c = \left(\frac{100 \times 1.5 \times 10^{-6}}{\frac{2\pi}{1,200}}\right)^{1/2} = 0.17 \text{ meter (0.56 foot)}$$

* *

Guza and Bowen (1975) investigated edge waves generated by incident waves at some arbitrary angle of incidence, α_1, with the shoreline (see Fig. 30). Defining a parameter

$$\gamma = \sin \alpha_1 \tan \beta \tag{221}$$

the longshore wave numbers, k_1 and k_2, of the primary edge wave pair ($N_1 = 0$, $N_2 = 0$) are given as

$$k_1 = \frac{\omega^2}{4g \tan \beta} (1 + 2\gamma) \tag{222}$$

and

$$k_2 = \frac{\omega^2}{4g \tan \beta} (1 - 2\gamma) \tag{223}$$

when the angle of incidence, α_1, is small, and where ω is the radian frequency of the incident wave. Where $\alpha_1 = 0$, equations (222) and (223) reduce to equation (214). The standing edge wave where $\alpha_1 > 0$ will progress along the shoreline, and the drift speed, c_d, of a node or antinode of the *primary* edge wave pair is now given as

$$c_d = \frac{\gamma \omega}{2k_y} \tag{224}$$

Gallagher (1971) shows that an increase in the angle of incidence, α_1, will produce greater edge wave energy at higher frequencies (shorter periods).

Guza and Bowen (1976) discuss the height of the edge waves occurring along a coastline. They show that the maximum edge wave amplitude at the shoreline is theoretically three times the amplitude of the incident wave for a straight coastline. Gallagher (1971) indicates that energy would be lost because of bottom friction and the disperison caused by irregularities in the coastline. Guza and Bowen (1976) indicate that edge wave growth is limited by radiation of energy to deep water and by finite-amplitude demodulation; i.e., as the edge waves increase in height their natural frequency increases and no longer matches the forcing frequency. From equation (213) and the work of Munk, Snodgrass, and Gilbert (1964) relating trapped modes to leaky modes, it can be seen that leaky modes (i.e., edge waves radiating energy to deep water) will only occur on steep nearshore slopes. These nearshore slopes are very short in comparison to the tsunami wavelength, and are not of concern here. The edge waves associated with the tsunami are assumed to occur over the wider and flatter shelf slope shown in Figure 33.

A progressive edge wave moving along a coastline may be reflected from an obstacle such as a large headland. Guza and Bowen (1975) demonstrate that this could produce a standing edge wave with higher amplitudes near the obstacle. Reflection could also occur from a depth discontinuity such as a submarine canyon in the manner described in Section VI, 3.

5. Refracted Waves and Caustics.

When very long waves such as tsunamis arrive at a shoreline, a substantial amount of wave energy will be reflected seaward from the shoreline. These reflected waves will interact with the bottom topography, and will refract as they travel seaward. Refraction diagrams of these waves show a tendency for the waves to turn parallel to the shoreline as they move into deeper water. When a shelf slopes away from the shoreline, and extends a sufficient distance seaward, the waves may be turned back shoreward (see Fig. 35). The line tangent to the wave rays where they turn shoreward is a caustic. The wave rays will not cross the caustic, and the wave energy tends to be trapped, although some wave energy will leak across the caustic (Chao, 1970; Chao and Pierson, 1970; Pierson, 1972).

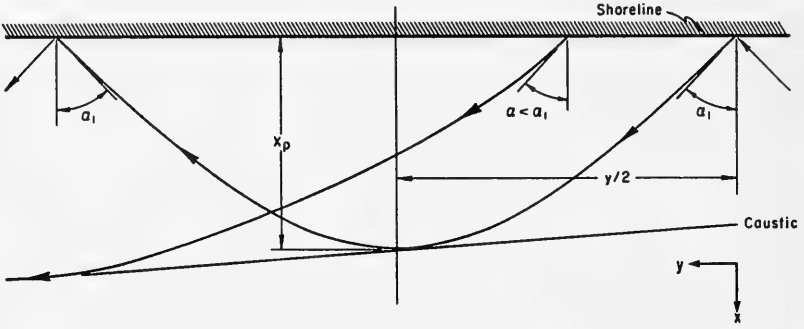

Figure 35. Schematic of caustic (uniform bottom slope).

Chao (1970) and Chao and Pierson (1970) investigated higher frequency waves trapped by a caustic. They demonstrate that lower frequency (longer period) waves will form caustics closer to the coastline, and that waves with frequencies above some maximum value will propagate seaward into deep water. For tsunamis, only the lower frequency waves are significant.

As the wave rays are not normal to the shoreline, different parts of the wave crest would arrive at the shoreline at different times. Where a coastline is irregular, parts of a wave crest reflected from one section of coastline may be refracted and trapped so that they coincide with an incident wave on another section of coastline. Palmer, Mulvihill, and Funasaki (1965) illustrated the effects of wave trapping at Hilo, Hawaii, where the reflected wave rays were turned by refraction so that they arrived simultaneously at a point inside Hilo Harbor (see Fig. 36).

The case of wave energy being trapped by refraction can be most easily illustrated for a long, shallow-water wave on a straight section of shoreline, with some water depth, d_s, at the toe of the shoreline slope, and with a constant shelf slope extending seaward. It is assumed that the wave reflects from the shoreline slope and refracts on the shelf.

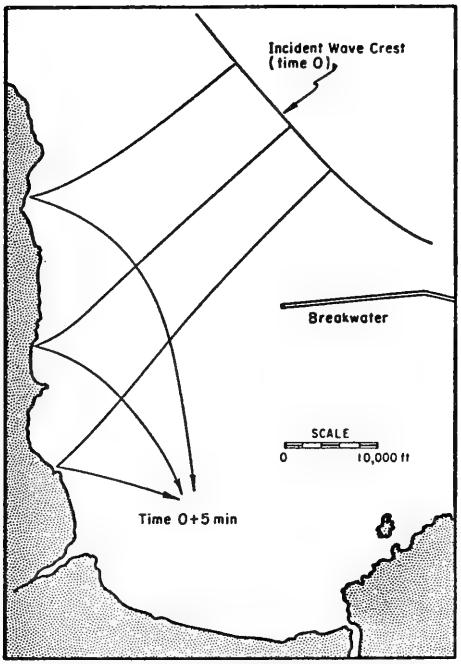

Figure 36. 1960 tsunami refraction, Hilo, Hawaii (after Palmer, Mulvihill, and Funasaki, 1965).

Applying Snell's Law where the wave moves through some incremental distance, with an incremental change in water depth d, and assuming that there is a shallow-water wave so that the celerity C is given by

$$C = (gd)^{1/2} \tag{225}$$

then the incremental refraction of a wave ray is defined by

$$\frac{\sin(\alpha + d\alpha)}{\sin \alpha} = \left(\frac{d + dd}{d}\right)^{1/2} \tag{226}$$

or, squaring both sides of equation (226),

$$\frac{\sin^2(\alpha + d\alpha)}{\sin^2 \alpha} = \frac{(d + dd)}{d} \tag{227}$$

Now, if the numerator of the left side of equation (227) is expanded, the term can be written

$$\sin^2(\alpha + d\alpha) = \frac{1}{2}[1 - \cos 2(\alpha + d\alpha)]$$

$$= \frac{1}{2}[1 - \cos(2\alpha)\cos(2d\alpha) + \sin(2\alpha)\sin(2d\alpha)]$$

$$= \frac{1}{2}[1 - (\cos^2\alpha - \sin^2\alpha)(\cos^2 d\alpha - \sin^2 d\alpha)$$

$$+ 2 \sin\alpha \cos\alpha(2 \sin d\alpha \cos d\alpha)] \quad (228)$$

But, where $d\alpha \to 0$,

$$\cos d\alpha \to 1$$

$$\sin d\alpha \to d\alpha$$

$$\sin^2 d\alpha \to (d\alpha)^2 \simeq 0$$

Then equation (228) can be written as

$$\sin^2(\alpha + d\alpha) = \frac{1}{2}[1 - (\cos^2\alpha - \sin^2\alpha)(1) + 4 \sin\alpha \cos\alpha\, d\alpha]$$

$$= \frac{1}{2}[2 \sin^2\alpha + 4 \sin\alpha \cos\alpha\, d\alpha] \quad (229)$$

and equation (227) becomes

$$\frac{2 \sin^2\alpha + 4 \sin\alpha \cos\alpha\, d\alpha}{2 \sin^2\alpha} = \frac{(d + dd)}{d} \quad (230)$$

which reduces to

$$1 + 2 \cot\alpha\, d\alpha = 1 + \frac{dd}{d} \quad (231)$$

$$2 \cot\alpha\, d\alpha = \frac{dd}{d} \quad (232)$$

Now, integrating along the wave ray from the shoreline to the point where it turns parallel to the shoreline, taking d_p as the water depth where the ray is parallel to the shoreline and x_p as the distance from the shoreline at that point, α_1 as the initial direction of the wave ray at the shoreline (Fig. 35), and noting that $\alpha = \pi/2$ radians for a straight, uniform coastline at the point where the wave ray turns parallel to the bottom contour,

$$\int_{d_s}^{d_p} \frac{dd}{d} = \int_{\alpha_1}^{\pi/2} 2 \cot \alpha \, d\alpha \tag{233}$$

which when integrated gives

$$\ell n \, d \Big|_{d_s}^{d_p} = 2 \, \ell n(\sin \alpha) \Big|_{\alpha_1}^{\pi/2} \tag{234}$$

which reduces to

$$\ell n \, d_p - \ell n \, d_s = -2 \, \ell n \sin \alpha_1 \tag{235}$$

Taking the antilogs

$$d_p = \frac{d_s}{\sin^2 \alpha_1} \tag{236}$$

But $d_p = d_s + Sx_p$ where S is the bottom slope, so

$$x_p = \frac{d_s}{S \sin^2 \alpha_1} - \frac{d_s}{S} \tag{237}$$

To compute the coordinate parallel to the shoreline of a point on the wave ray, note that

$$\tan \alpha = \frac{dy}{dx} \tag{238}$$

The x coordinate is given by

$$x = \frac{d_s \sin^2 \alpha}{S \sin^2 \alpha_1} - \frac{d_s}{S} \tag{239}$$

or, differentiating equation (240) with respect to α,

$$dx = \frac{2 \, d_s \sin \alpha \cos \alpha \, d\alpha}{S \sin^2 \alpha_1} \tag{240}$$

substituting equation (240) into equation (238), equation (238) becomes

$$dy = \frac{2 \, d_s}{S \sin^2 \alpha_1} \sin \alpha \cos \alpha \tan \alpha \, d\alpha \tag{241}$$

Collecting terms and integrating

$$\int_0^{y/2} dy = \frac{2\, d_s}{S \sin^2 \alpha_1} \int_{\alpha_1}^{\pi/2} \sin^2 \alpha \, d\alpha \tag{242}$$

This gives

$$\frac{y}{2} = \frac{2\, d_s}{S \sin^2 \alpha_1} \left[\frac{\pi}{4} - \frac{\alpha_1}{2} + \frac{\sin 2\alpha_1}{4} \right] \tag{243}$$

These equations are limited to the particular case of a long, straight coastline, but may provide a first approximation for solutions on some sections of continental shelves. Refraction diagrams would be required to obtain exact solutions for irregular coastlines. If the waves travel for long distances over a shelf, it may be desirable to use wave refraction equations in spherical coordinates such as the equations given by Chao (1970) (see Sec. IV, 3).

* * * * * * * * * * * * * * * EXAMPLE PROBLEM 17 * * * * * * * * * * * * * * *

GIVEN: A wave ray reflects from a straight shoreline at an initial angle $\alpha_1 = \pi/4$ radians. The water depth at the toe of the shoreline slope $d_s = 30$ meters and the shelf at the toe of the shoreline slope has a uniform seaward slope $S_2 = 0.003$.

FIND: The distance the wave ray will travel away from the shoreline, and the distance along the shoreline to the point where the reflected wave ray will impinge upon the shoreline.

SOLUTION:

From equation (237)

$$x_p = \frac{d_s}{S \sin^2 \alpha_1} - \frac{d_s}{S}$$

$$x_p = \frac{30}{0.003 \sin^2 \frac{\pi}{4}} - \frac{30}{0.003}$$

$$x_p = 10{,}000 \text{ meters } (6.214 \text{ miles})$$

From equation (243)

$$\frac{y}{2} = \frac{2\, d_s}{S \sin^2 \alpha_1} \left[\frac{\pi}{4} - \frac{\alpha_1}{2} + \frac{\sin 2\alpha_1}{4} \right]$$

$$\frac{y}{2} = \frac{2(30)}{0.003(0.707)^2} \left[\frac{\pi}{4} - \frac{\pi}{8} + \frac{\sin \frac{\pi}{2}}{4} \right]$$

$$\frac{y}{2} = 25{,}700 \text{ meters } (15.97 \text{ miles})$$

For this example, the shelf needs to extend 10,000 meters from the toe of the shoreline slope to have the wave ray turn parallel to the bottom contours. The wave ray which was reflected from the shoreline will impinge upon the shoreline again at a point 51,400 meters (31.94 miles) along the coast, provided the wave is trapped.

* *

For the particular case of a shallow-water wave on a straight section of coastline and uniform shelf slope, given by equations (237) and (243) and illustrated in Figure 35, as the angle α_1 decreases the distance of the caustic from the shoreline increases and the distance y between the point of reflection and the point where the wave ray impinges again on the coastline also increases.

When the tsunami energy becomes trapped between a caustic and a coastline, the energy will tend to propagate along the coastline. This will excite longshore edge waves along the coastline, and may substantially increase observed wave heights. When the coastline is irregular, the trapped waves may concentrate their energy at particular coastal points. An investigation of the wave rays using the usual wave refraction techniques will define the caustic locations, and the locations of any coastal points where energy concentrates.

Tsunamis generated in coastal areas may have part of their energy trapped along the coastline, as waves radiating away from a source area may become trapped within a caustic in the same manner as reflected waves. For a wave ray originating within the coastal area, d_s is the water depth at the point of origin, x_p the distance seaward from the point of origin, and α_1 the angle between the wave ray and the orthogonal to the bottom contours as before. This is illustrated in the following example problem and in Figure 37.

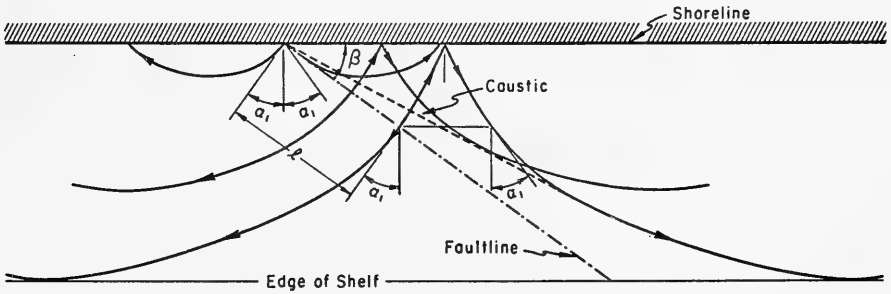

Figure 37. Trapping of generated tsunami.

* * * * * * * * * * * * * * EXAMPLE PROBLEM 18 * * * * * * * * * * * * * *

GIVEN: A tsunami is generated by uplifting along a faultline located on a coastal shelf (Fig. 37). The faultline is oriented so that the angle between the coastline and the faultline is $\beta = 40°$. The faultline extends to the outer edge of the shelf which is 100 kilometers (62.14 miles) from the toe of the shoreline slope. The shelf has a uniform slope seaward of S = 0.003 and a 30-meter water depth at the toe of the shoreline slope. The uplifting is uniform along the faultline so that it acts as a line source.

FIND: The percentage of the wave energy trapped on the shelf.

SOLUTION: The depth of water at the outer edge of the shelf is

$$d = d_s + Sx = 30 + 0.003(100{,}000)$$

$$= 330 \text{ meters } (1{,}083 \text{ feet}) .$$

Looking first at wave rays traveling seaward from the faultline, at the inner end of the faultline, using equation (237),

$$x_p = \frac{d_s}{S \sin^2 \alpha_1} - \frac{d_s}{S}$$

$$= \frac{30}{0.003 \sin^2 40°} - \frac{30}{0.003}$$

$$x_p = 14{,}200 \text{ meters } (8.83 \text{ miles})$$

At the outer end of the faultline, taking d_s as the depth of water at the faultline, i.e., where the wave ray originates

$$x_p = \frac{330}{0.003 \sin^2 40°} - \frac{330}{0.003}$$

$$x_p = 156.23 \text{ kilometers } (97.08 \text{ miles})$$

which is beyond the limits of the shelf. Noting that x_p varies linearly with d_s, from proportionality the length ℓ of the part of the faultline (of length L_f) contributing trapped energy is

$$\ell = \frac{L_f(100 - 14.2)}{(100 + 156.23 - 14.2)}$$

$$\ell = 0.355 \, L_f$$

or 35.5 percent of the energy generated seaward in the example is trapped.

Consider now the wave rays generated shoreward. If the wave ray generated from the point at distance ℓ along the faultline is considered for the straight, uniform section of shoreline (Fig. 37), the wave ray will reflect from the shoreline and be directed at the angle α_1 at the position shown in the figure. This wave ray will turn parallel to the shoreline (i.e., parallel to the bottom contours) at the edge of the shelf. Therefore, 35.5 percent of the energy generated shoreward in the example will also be trapped. Note that the energy generated shoreward would have a tendency to form a Mach-stem along the shoreline if β is greater than 45°.

A caustic, by definition, is a line tangent to a family of wave rays. For the waves generated seaward, a caustic will be formed by those wave rays refracted back to the shoreline (i.e., the trapped wave rays), after they have reflected from the shoreline. For the wave rays generated landward from the faultline, a caustic is formed after reflection as shown by the dashline in Figure 37.

* *

As illustrated in Figure 37, wave rays trapped on a shelf may diverge apart. These wave rays may reconverge at various points along the coastline, producing high waves at the points of convergence.

Chao (1970), Chao and Pierson (1970), and Pierson (1972) discuss the case of short-period waves reflected from a shoreline, where several wave crests exist between the point of reflection and the caustic. The wave rays follow similar paths to those discussed above, but the wave crests propagating shoreward from the caustic will interact with the wave crests propagating seaward from the coastline, producing many peaks and nodes between the coastline and the caustic.

For the straight coastline shown in Figure 35, the traveltime, t, along the wave ray between the shoreline and the caustic can be easily determined. Where the distance s is measured along the wave ray,

$$c = \frac{ds}{dt} \tag{244}$$

but

$$d_s = \frac{dx}{\cos \alpha} \tag{245}$$

so that

$$\int_0^t dt = \int_0^{x_p} \frac{dx}{c \cos \alpha} \tag{246}$$

Also, from shallow-water assumptions,

$$c = \sqrt{gd} = \sqrt{g(d_s + Sx)} \tag{247}$$

and from equation (240),

$$\frac{dx}{\cos \alpha} = \frac{2\, d_s \sin \alpha \, d\alpha}{S \sin^2 \alpha_1} \tag{248}$$

Using equation (239) to define x and substituting equations (247) and (248) into equation (246), it becomes

$$t = \int_{\alpha_1}^{\pi/2} \frac{2\, d_s}{S \sin^2 \alpha_1 \sqrt{g}} \frac{\sin \alpha \, dx}{\sqrt{d_s + S\left(\frac{d_s \sin^2 \alpha}{S \sin^2 \alpha_1} - \frac{d_s}{S}\right)}} \tag{249}$$

Collecting terms,

$$t = \frac{2\sqrt{d_s}}{S \sin \alpha_1 \sqrt{g}} \int_{\alpha_1}^{\pi/2} d\alpha \tag{250}$$

which gives

$$t = \frac{2\sqrt{d_s}}{S \sin \alpha_1 \sqrt{g}} \left[\frac{\pi}{2} - \alpha_1\right] \tag{251}$$

Shen and Meyer (1967) and Shen (1972) give a solution for curved coastlines. For a circular arc, wave trapping can be defined using the equations

$$\tan \alpha = \frac{r d\theta}{dr} = \pm(n^2 r^2 - c^2)^{-1/2} \tag{252}$$

and

$$n \tanh\left[n\left(\frac{n_2}{c}\right) d\right] = 1 \tag{253}$$

where

r = the radius of curvature of a contour line (taking circular bottom contours to define the shelf around the coastline)

θ = the coordinate angle in polar coordinates of a point along the wave ray at radius r

c = a constant

n = a variable along the wave ray

d = the water depth at radius r

n_2 = 1, 2, 3. . . defines an integer number of wave crests around a circular island

Taking the radius at the shoreline as R_s, and the radius where the wave ray turns parallel to the bottom contours as r_p, at the shoreline

$$\tan \alpha_1 = \pm(n^2 R_s^2 - c^2)^{-1/2} \tag{254}$$

$$n = \left(\frac{1 + c^2 \tan^2 \alpha_1}{R_s^2 \tan^2 \alpha_1} \right)^{1/2} \tag{255}$$

$$\left(\frac{1 + c^2 \tan^2 \alpha_1}{R_s^2 \tan^2 \alpha_1} \right)^{1/2} \tanh \left[\left(\frac{1 + c^2 \tan^2 \alpha_1}{R_s^2 \tan^2 \alpha_1} \right)^{1/2} \frac{n_2}{c} d_s \right] = 1 \tag{256}$$

Where the wave ray turns parallel to the bottom contours

$$(n^2 r_p^2 - c^2) = 0 \tag{257}$$

$$n = \frac{c}{r_p} \tag{258}$$

Substituting into equation (253),

$$\frac{c}{r_p} \tanh \left[\frac{n_2}{r_p} d \right] = 1 \tag{259}$$

where d is the water depth at radius r_p. Equation (256) can be solved to determine c for any integer value n_2 satisfying the equation, and equation (259) can then be solved to obtain a value for r_p corresponding to each value of c which will provide a solution. Shen and Meyer (1967) indicate that a number of caustics may exist. For a circular island, resonance will occur between the shoreline and the caustics for wave periods defined by integer values of n_2 for which solutions exist.

Equations (252) and (253) were derived for dimensionless variables where the dimensional values of length had been divided by some horizontal length scale. Camfield (1979) gives the following development to express the solution in terms of several dimensionless parameters. Shen and Meyer (1967) infer that the radius r_p of the caustic (i.e., where the wave ray turns parallel to the bottom contours) is an appropriate length scale. Using an asterisk (*) to define dimensional values, the radius of curvature r_p is normalized so that its dimensionless value is

$$r_p = 1 \tag{260}$$

The derivation of the equations also assumes that

$$\frac{\text{vertical length scale}}{\text{horizontal length scale}} = \varepsilon \tag{261}$$

so the vertical dimensions in equations (252) to (259) are assumed to represent dimensional values divided by $r_p^* \varepsilon$, where the term $r_p^* \varepsilon$ is the vertical length scale. Shen (1972) takes $\varepsilon M = 1$. It is assumed $\varepsilon \to \delta$, where $0 < \delta << 1$, so that M must be large. Shen defines M as

$$M = \frac{(\omega^*)^2 (\text{horizontal length scale})}{g}$$

which gives

$$M = \left(\frac{2\pi}{T}\right)^2 \left(\frac{r_p^*}{g}\right) \tag{262}$$

For long-period waves (e.g., tsunamis) where the period T is large, the caustic radius r_p^* must be large in order for M to be large. In general, the solution is for cases where the shoreline radius R_s^* (and therefore the caustic radius r_p^*) is much greater than the wavelength. Using Shen's work, equation (256) now reduces to

$$\left(\frac{1 + c^2 \tan^2 \alpha_1}{\left(\frac{(R_s^*)^2 \tan^2 \alpha_1}{(r_p^*)^2}\right)}\right)^{1/2} \tanh\left[\left(\frac{1 + c^2 \tan^2 \alpha_1}{\left(\frac{(R_s^*)^2 \tan^2 \alpha_1}{(r_p^*)^2}\right)}\right)^{1/2} \frac{n_2}{c} \frac{d_s^*}{r_p^* \varepsilon}\right] = 1 \tag{263}$$

Shen has defined $M = n_2/c$ so that $\varepsilon = 1/M = c/n_2$. Equation (263) further reduces to

$$\left(\frac{1 + c^2 \tan^2 \alpha_1}{\tan^2 \alpha_1}\right)^{1/2} \tanh\left[\left(\frac{1 + c^2 \tan^2 \alpha_1}{\tan^2 \alpha_1}\right)^{1/2} \frac{n_2^2 \, d_s^*}{c^2 \, R_s^*}\right] = \frac{R_s^*}{r_p^*} \tag{264}$$

in its dimensional form, where d_s^* is the dimensional depth at the toe of the shoreline slope, R_s^* the dimensional radius of curvature of the shoreline, and r_p^* the dimensional radius to the point where the wave ray turns parallel to the bottom contours. Also the dimensional form of equation (259) becomes

$$c \tanh\left[\frac{n_2^2 \, d^*}{r_p^* \, c}\right] = 1 \tag{265}$$

where d^* is the water depth at radius r_p^*.

Consider first a concave coastline, such as a large bay, where the radii r_p^* and R_s^* are measured from the center of curvature offshore, and $r_p^* < R_s^*$. In the limiting case, a concave coastline would form a closed circular basin with radius R_s^*. Therefore, all wave rays could obviously be trapped by this type of coastline.

Where $\alpha_1 \to 90°$ the wave rays become trapped very close to the shoreline so that $r_p^* \to R_s^*$. As α_1 becomes smaller, r_p^* becomes smaller so that the caustics are farther from the shoreline. As $\alpha_1 \to 0$, $r_p^* \to 0$, meaning that a wave ray reflected along an orthogonal to the shoreline will pass through the center of curvature.

Equations (264) and 265) are used to investigate wave rays at any angle α_1. From equation (265), $c \geq 1$ as $\tanh [n_2^2 \, d^*/(r_p^* \, c)] \leq 1$. To determine the limiting values of n_2 which will provide solutions, it may be noted that, in equation (264),

$$\frac{R_s^*}{r_p^*} > 1 \tag{266}$$

From equation (265), as $c \to 1$, $n_2 \to \infty$. From the definition that $1/M \propto T^2$ (eq. 262), and that $1/M = c/n_2$, it can be seen that waves would be trapped where $T \to 0$, which is a restatement of the fact that all waves would be trapped where the coastline is concave; e.g., a large, circular bay. Finding the caustic location, i.e., the radius, r_p, when $n \to \infty$ and $T \to 0$ is of interest. From equation (264), when $n \to \infty$, and $\alpha_1 > 0$,

$$\tanh \left[\left(\frac{1 + c^2 \tan^2 \alpha_1}{\tan^2 \alpha_1} \right)^{1/2} \frac{n_2^2 \, d_s^*}{c^2 \, R_s^*} \right] \to 1 \tag{267}$$

which then gives

$$\left(\frac{1 + c^2 \tan^2 \alpha_1}{\tan^2 \alpha_1} \right)^{1/2} \to \frac{R_s^*}{r_p^*} \tag{268}$$

and as $c \to 1$,

$$\left(\frac{1 + \tan^2 \alpha_1}{\tan^2 \alpha_1} \right)^{1/2} \to \frac{R_s^*}{r_p^*} \tag{269}$$

which reduces to

$$(r_p^*)_{min} = R_s^* \sin \alpha_1 \tag{270}$$

Where the angle α_1 is known, defining the angle between the reflected wave ray at the shoreline and the normal to the shoreline (see Fig. 35), the wave energy will always be trapped between the radius, r_p^*, defining the caustic and the radius, R_s^*, defining the shoreline if the concave shoreline extends a sufficient distance. Where the wave period becomes longer, it will be trapped closer to the shoreline.

It is of interest to note that equation (270) provides a solution independent of water depth or shelf slope. Equation (270) defines the distance from the center of curvature to a chord across a circular arc, where α_1 is the angle between the chord and a radius drawn to the end

of the chord. This defines the path of an unrefracted wave ray (the expected result when $T \to 0$), and therefore verifies equations (264) and (265) for a concave coastline such as a large bay.

For a convex coastline (e.g., a circular island), the wave rays which would probably be trapped are those where α_1 is large, i.e., the wave rays most nearly parallel to the shoreline. Letting $\alpha_1 \to \pi/2$, $\tan \alpha_1 \to \infty$ so that the term

$$\left(\frac{1 + c^2 \tan^2 \alpha_1}{\tan^2 \alpha_1} \right)^{1/2} \to c \tag{271}$$

From equation (264)

$$c \tanh \left(\frac{n_2^2}{c} \frac{d_s^*}{R_s^*} \right) = \frac{R_s^*}{r_p^*} \tag{272}$$

Substituting equation (265) in equation (272) above,

$$\tanh \left(\frac{n_2^2}{c} \frac{d_s^*}{R_s^*} \right) = \frac{R_s^*}{r_p^*} \tanh \left(\frac{n_2^2}{c} \frac{d^*}{r_p^*} \right) \tag{273}$$

as $r_p^* > R_s^*$ for a convex coastline, then $R_s^*/r_p^* < 1$. Therefore,

$$\frac{d^*}{r_p^*} > \frac{d_s^*}{R_s^*} \tag{274}$$

as a condition of wave trapping on a convex coastline. This means that the slope of the shelf must be greater than some minimum value defined by d_s^*/R_s^* in order to have a caustic, i.e., to have waves trapped on the shelf. This is necessary in order to have the rate of curvature of the wave ray exceed the rate of curvature of the bottom contours, a necessary condition of wave trapping. Where a circular island has a small radius, R_s^*, in relation to the water depth at the shoreline, d_s^*, there is a greater probability of the wave rays spiraling off into deep water than there would be for an island with a large radius.

The minimum and maximum values of n_2 which will produce solutions can be found as follows:

From equation (264), where $|c| \to \infty$

$$c \tanh \left(\frac{n_2^2}{c} \frac{d_s^*}{R_s^*} \right) = \frac{R_s^*}{r_p^*}, \quad \tan \alpha_1 > 0 + \delta \tag{275}$$

where δ is some small value. But as $c \to \infty$,

$$\tanh\left(\frac{n_2^2\ d_s^*}{c\ R_s^*}\right) \to \frac{n_2^2\ d_s^*}{c\ R_s^*} \tag{276}$$

and from equation (275)

$$\frac{n_2^2\ d_s^*}{R_s^*} = \frac{P_s^*}{r_p^*} \tag{277}$$

$$n_2^2 = \frac{(R_s^*)^2}{d_s^*\ r_p^*} \tag{278}$$

From equation (265), noting, that for $c \to \infty$,

$$\tanh\left[\frac{n_2^2\ d^*}{r_p^*\ c}\right] \to \frac{n_2^2\ d^*}{r_p^*\ c} \tag{279}$$

it is found that

$$\frac{n_2^2\ d^*}{r_p^*} = 1 \tag{280}$$

Substituting the value of r_p^* from equation (278), and noting that for a uniform slope

$$d^* = d_s^* + (r_p^* - R_s^*)\ S_2 \tag{281}$$

equation (280) is then

$$n_2^4\ [d_s^*\ R_s^*\ S_2 - (d_s^*)^2] - n_2^2\ (R_s^*)^2\ S_2 + (R_s^*)^2 = 0 \tag{282}$$

Equation (282) is a quadratic equation for n_2^2 which provides minimum and maximum values given by

$$(n_2)^2_{min} = \frac{R_s^*}{R_s^*\ S_2 - d_s^*} \tag{283}$$

$$(n_2)^2_{max} = \frac{\dfrac{(R_s^*)^2\ S_2}{d_s^*} - R_s^*}{R_s^*\ S_2 - d_s^*} \tag{284}$$

At the minimum value of n_2,

$$n_2^2 \frac{d_s^*}{R_s^*} = \frac{\frac{d_s^*}{R_s^* S_2}}{1 - \frac{d_s^*}{R_s^* S_2}} \tag{285}$$

and at the maximum value of n_2,

$$n_2^2 \frac{d_s^*}{R_s^*} = 1 \tag{286}$$

For a solution to exist for given values of d_s^* and R_s^*, the maximum value of $n_2^2 \, d_s^*/R_s^*$ defined by equation (285) must be less than or equal to 1, so the minimum value of S_2 for wave trapping to occur is given by

$$\frac{\frac{d_s^*}{R_s^* S_2}}{1 - \frac{d_s^*}{R_s^* S_2}} = 1 \tag{287}$$

which reduces to

$$\frac{d_s^*}{S_2 R_s^*} < 0.5 \tag{288}$$

The parameter $d_s^*/(S_2 R_s^*)$ is a shelf parameter which determines wave trapping. A continuous band of solutions exists for equations (264) and (265), for values of n_2 between the minimum and maximum values defined by equations (283) and (284). Solutions are not limited to integer values of n_2, which define resonant periods for a circular island.

Solutions for equations (264) and (265) are plotted in Figure 38. Equation (264) is plotted on lines of constant $n_2^2 \, d_s^*/R_s^*$; equation (265) is plotted on lines of constant $d_s^*/(R_s^* S_2)$. Solutions for trapped waves are obtained where the two families of curves intersect. From equation (288) it is seen that solutions will only exist where $d_s^*/(R_s^* S_2) \leq 0.5$. From equation (262) note that

$$\frac{2\pi}{gT^2} = \frac{M}{2\pi r_p^*} \tag{289}$$

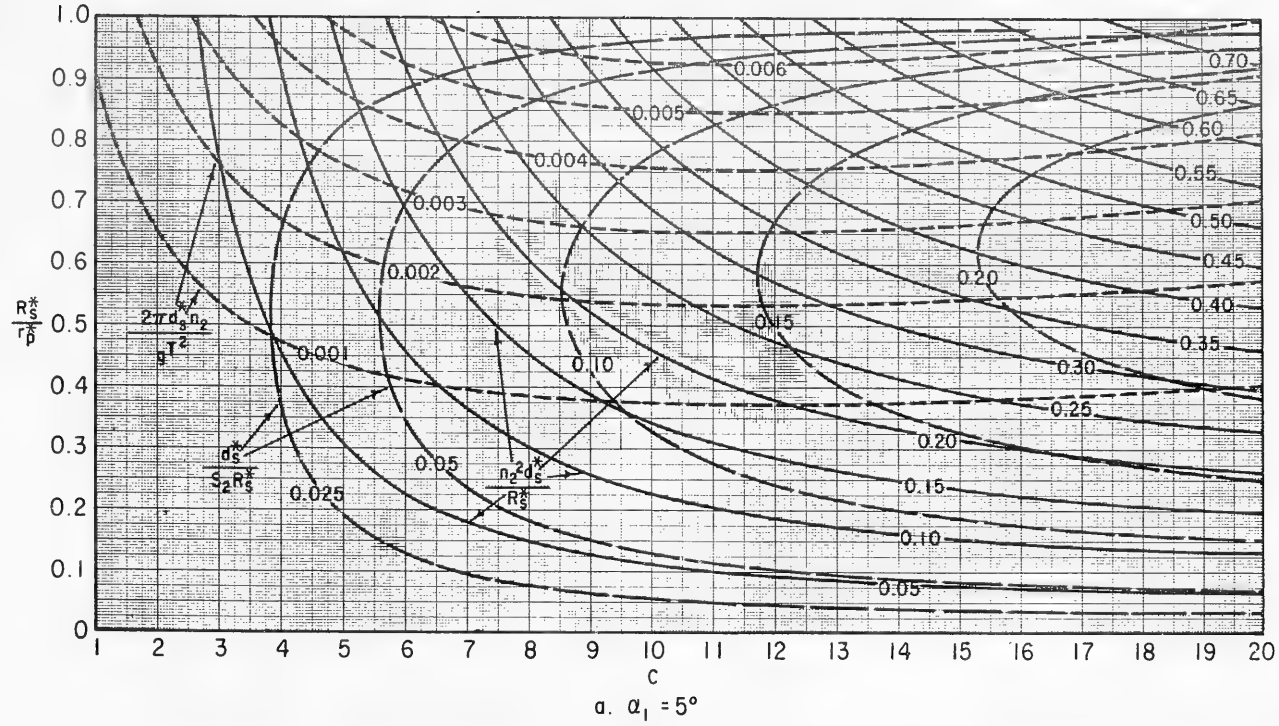

Figure 38. Solution to equations (264) and (265).

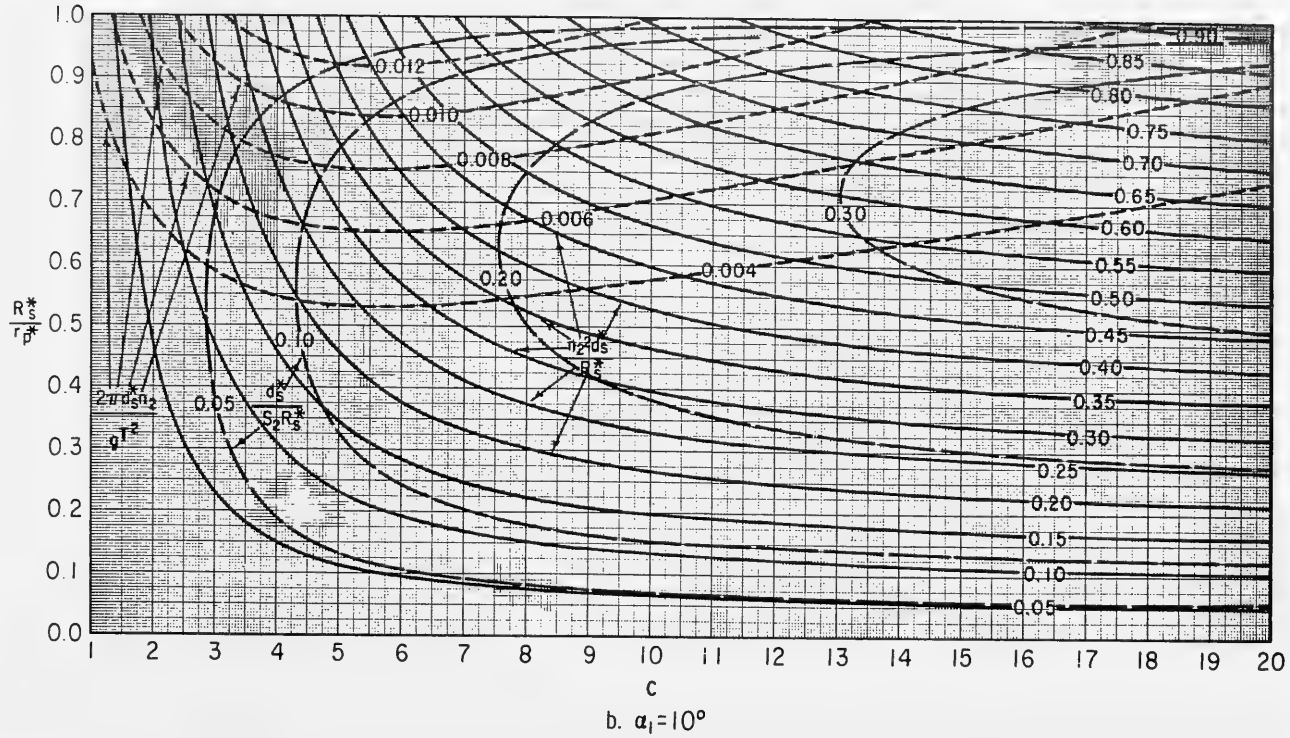

b. $\alpha_1 = 10°$

Figure 38. Solution to equations (264) and (265).--Continued

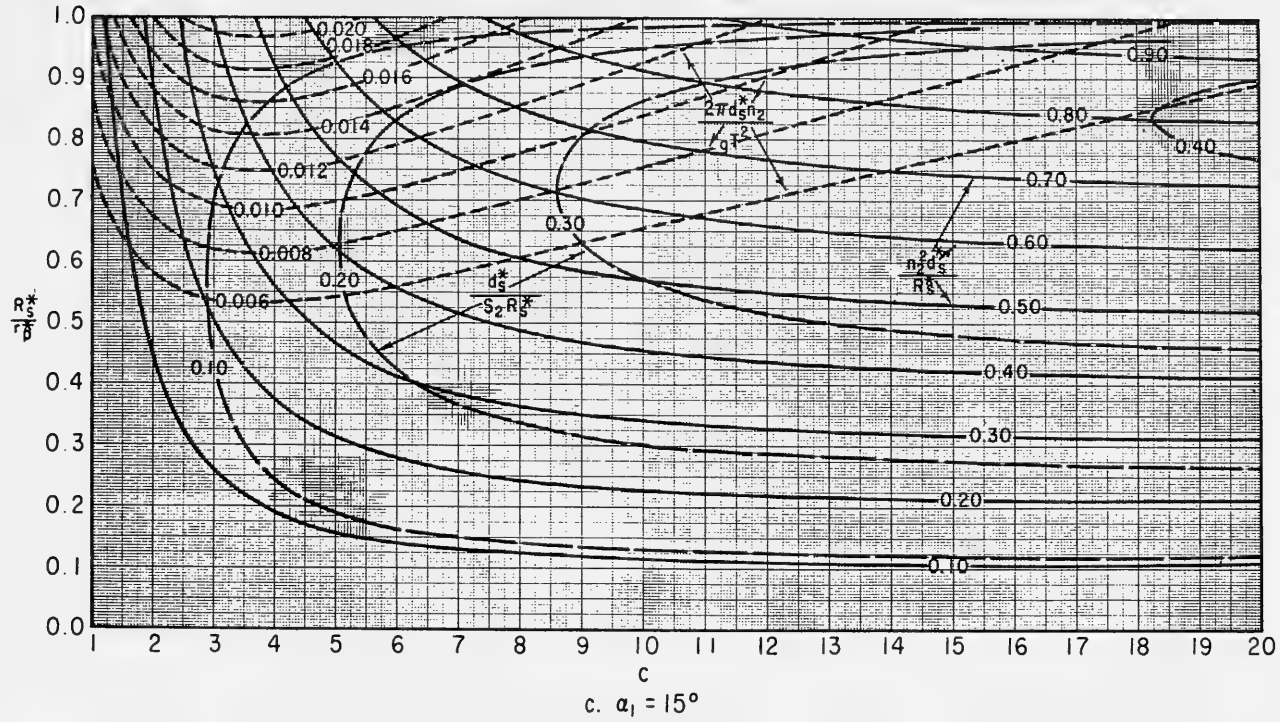

c. $\alpha_1 = 15°$

Figure 38. Solution to equations (264) and (265).--Continued

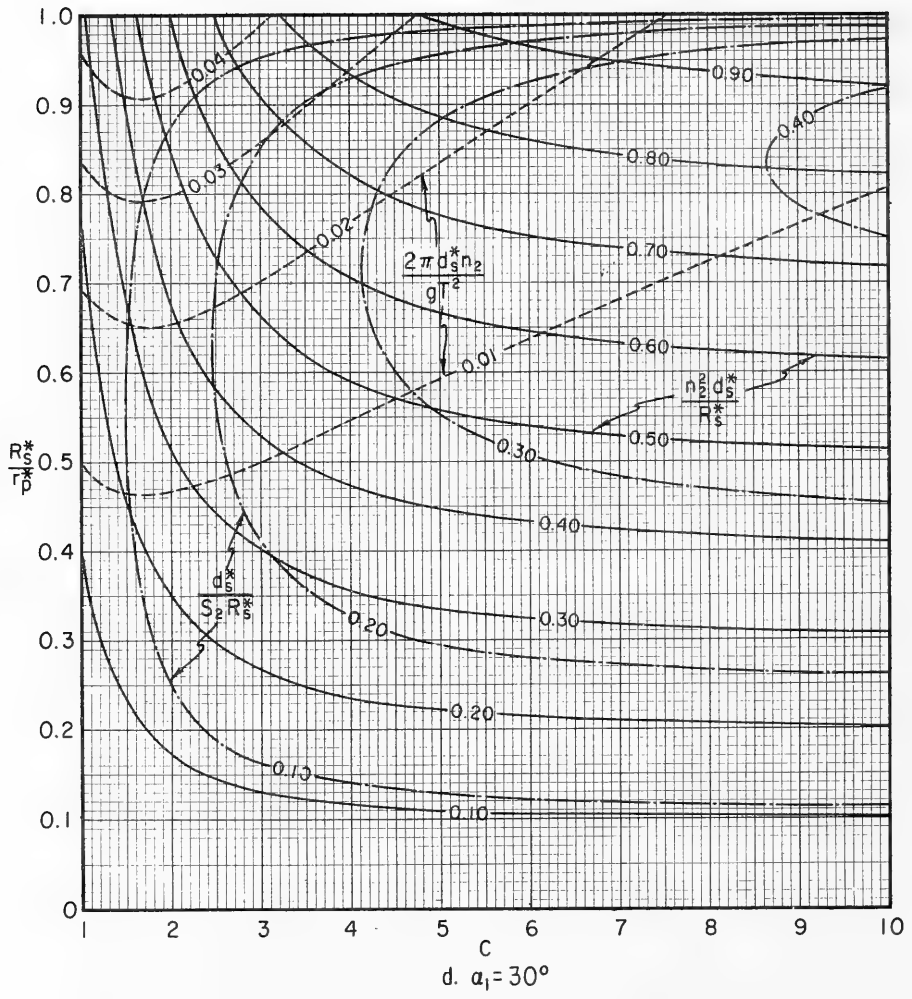

Figure 38. Solution to equations (264) and (265).--Continued

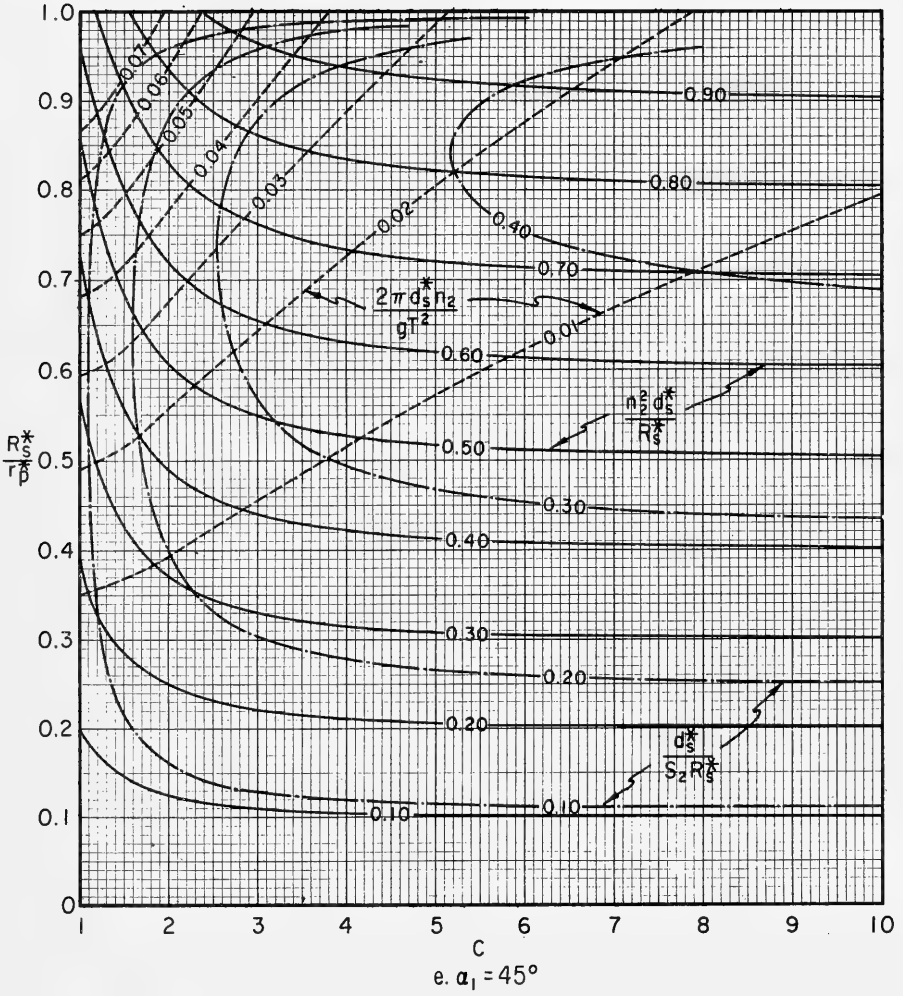

Figure 38. Solution to equations (264) and (265).--Continued

and as $M = n_2/c$, as previously defined, this can be rewritten as

$$\frac{2\pi}{gT^2} = \frac{n_2}{2\pi\ r_p^*\ c}\left(\frac{R_s^*}{R_s^*}\right)\left(\frac{d_s^*}{d_s^*}\right)\left(\frac{n_2}{n_2}\right) \tag{290}$$

which reduces to

$$\frac{2\pi\ d_s^*\ n_2}{gT^2} = \frac{1}{2\pi c}\left(\frac{R_s^*}{r_p^*}\right)\left(\frac{n_2^2\ d_s^*}{R_s^*}\right) \tag{291}$$

Lines of constant $2\pi\ d_s^*\ n_2/(gT^2)$ are also plotted in Figure 38. The minimum period of the trapped waves is defined where a line of constant $2\pi\ d_s^*\ n_2/(gT^2)$ is tangent to the line where $d_s^*/(S_2\ R_s^*)$ is constant for the given values of d_s^*, S_2, and R_s^*. Solutions for equations (264) and (265) at greater values of R_s^*/r_p^* (at longer wave periods) define trapped waves. Solutions for equations (264) and (265) for smaller values of R_s^*/r_p^* (at longer wave periods) define the damping zone discussed by Lozano and Meyer (1976).

Solutions of equations (264) and (265) for values of n_2, defined by equation (286), define caustics at the inner limit of the trapped wave zone near the shoreline (i.e., where $r_p^* \rightarrow R_s^*$). These solutions will give the maximum trapped wave periods, T_{max}, but the solutions tend to break down at this point as the parameter, U, defined by equation (66) as $U = (H/d)(L/d)^2$, becomes very large ($U >> 1$). However, the minimum trapped wave period and the outer limit of the trapped wave zone can be approximated using equations (264) and (265).

Figure 38 shows that, for varying values of α_1, the minimum trapped wave period will increase as α_1 decreases. This is expected since shorter period waves, at lower values of α_1, tend to pass into deep water and are not trapped.

The theoretical solutions given by equations (264) and (265) are for the case of a coastline approximated by a circular arc. In the limiting case, this will approach a straight coastline. Solutions for irregular coastlines must be obtained by numerical methods. The theoretical solutions presented here can be used to verify numerical methods used for more complex solutions for irregular coastlines. An example of a numerical solution is given by Houston, Carver, and Markle (1977) using a finite-element numerical model developed by Chen and Mei (1974).

* * * * * * * * * * * * * * EXAMPLE PROBLEM 19 * * * * * * * * * * * * * *

GIVEN: A curved section of coastline is convex, with a radius of curvature R_s^* = 100,000 meters (62.14 miles), and the depth at the toe of the shoreline slope d_s^* = 30 meters. A tsunami reflects from the shoreline slope and refracts over a shelf where the bottom slope of the shelf

is $S_2 = 0.003$. The angle between the reflected wave ray and the orthogonal to the shoreline $\alpha_1 = 45°$.

FIND:

(a) The minimum shelf slope required for trapped waves to exist,

(b) the radius, r_p, defining the outer limit of the trapped wave zone where $\alpha_1 = 45°$, and

(c) the minimum period of waves trapped by refraction, where $\alpha_1 = 45°$.

SOLUTION:

(a) From equation (288), for wave trapping to exist

$$\frac{d_s^*}{S_2 \; R_s^*} < 0.5$$

$$S_2 > 2 \frac{d_s^*}{R_s^*} = \frac{2(30)}{100{,}000} = 0.0006$$

(b) The shelf parameter is

$$\frac{d_s^*}{S_2 \; R_s^*} = \frac{30}{0.003(100{,}000)} = \frac{30}{300} = 0.1$$

From Figure 38, for $\alpha_1 = 45°$, the minimum wave period is at

$$\frac{2\pi \; d_s^* \; n_2}{gT^2} = 0.068$$

where

$$\frac{n_2^2 \; d_s^*}{R_s^*} = 0.71$$

$$n_2^2 = 0.71 \frac{R_s^*}{d_s^*} = 0.71 \frac{100{,}000}{30} = 2{,}367$$

$$n_2 = 48.65$$

and

$$\frac{R_s^*}{r_p^*} = 0.93$$

which gives

$$r_p^* = \frac{R_s^*}{0.93} = \frac{100{,}000}{0.93} = 107{,}530 \text{ meters (66.8 miles)}$$

The width of the trapped wave zone from the shoreline to the outer limit is given by

$$r_p^* - R_s^* = 107{,}530 - 100{,}000 = 7{,}530 \text{ meters (4.68 miles)}$$

(c) $$\frac{2\pi\, d_s^*\, n_2}{gT^2} = 0.068 \text{ or } T^2 = \frac{2\pi\, d_s^*\, n_2}{0.068\, g}$$

$$T^2 = \frac{2\pi(30)(48.65)}{9.81(0.068)} = 13{,}747$$

$$T = 117.2 \text{ seconds (1.95 minutes)}$$

for the minimum trapped wave period.

* *

6. Mach-Stem Formation.

Figure 38 illustrates solutions for trapped waves for angles $\alpha_1 \leq 45°$. Perroud (1957) showed that $\alpha_1 = 45°$ defines a critical angle for wave reflection. When $\alpha_1 < 45°$ regular reflection occurs, i.e., the wave reflects in a manner described in Section VI, 1 and 5. When $\alpha_1 = 45°$ the end of the wave crest at the shoreline turns perpendicular to the shoreline (see Fig. 39). Regular reflection no longer occurs when $\alpha_1 > 45°$.

Perroud showed that, for $\alpha_1 > 45°$, the incident wave produces two components. The first is a reflected wave, lower than the incident wave, and with the angle, α_2, between the reflected wave ray and the normal to the shoreline defined by $\alpha_2 < \alpha_1$. The second component is a Mach stem which moves along the shoreline in the direction of the longshore component of the incident wave, growing in size as it progresses along the shoreline. Figure 39 shows the initial growth of a Mach stem along a vertical wall for the critical angle $\alpha_1 = 45°$.

Experimental measurements by Perroud (1957) show that the Mach stem has a profile at the shoreline similar to the profile of the incident wave, giving the Mach stem the appearance of a large wave moving along the shoreline. The Mach stem remains attached to the shoreline end of the incident wave crest, so its speed of propagation, C_ℓ, along the shoreline is given as

$$C_\ell = \frac{C}{\sin \alpha_1} \tag{292}$$

where C is the celerity of the incident wave near the shoreline.

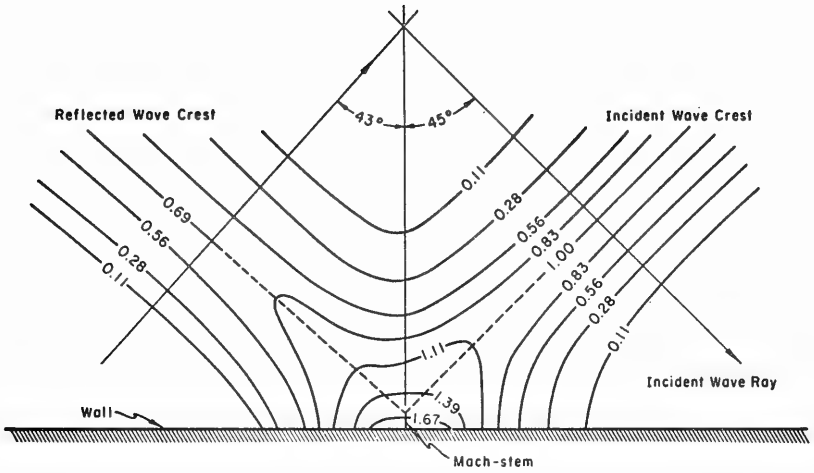

Figure 39. Mach-stem formation, solitary wave. Lines of equal surface elevation above still water normalized to unit incident wave amplitude (after Perroud, 1957).

Chen (1961) studied Mach-stem development using a range of values for the nearshore slope. He showed that where the angle of the nearshore slope $\beta < 60°$, and $\alpha_1 > 55°$, the Mach stem formed a breaking wave along the shoreline. The relationship between the wavelength and the slope length was not considered in this case, and was not varied during the experiments.

It was generally found by Perroud (1957) and Chen (1961) that the incident waves neither reflected from the shoreline nor formed Mach stems when $\alpha_1 > 70°$. This would be the case for an incident wave traveling nearly parallel to the section of shoreline; e.g., a wave entering an inlet with a gradually varying cross section.

7. Bay and Harbor Resonance.

When a bay or harbor is very long in relation to the tsunami wavelength, the tsunami may cause resonance if a natural mode of oscillation of a bay or harbor corresponds to the period of the tsunami. Murty, Wigen, and Chawla (1975) have tabulated the approximate periods of inlets on the Pacific coast of North and South America based on the formula

$$T_1 = \frac{4L_b}{\sqrt{gd_a}} \tag{293}$$

where T_1 is the primary period, L_b the length of the inlet, and d_a the average depth of the inlet. Values of length, depth, width, period, and relative intensity of secondary oscillations of the water level, as given by Murty, Wigen, and Chawla, for inlets on the coast of Alaska and British Columbia, and for Puget Sound, are given in Table 4. These values are only approximate because variations in inlet cross section, restricted entrances, and the effects of branched inlets are not considered.

Referring to the work of Nakano (1932) which showed secondary undulations to be proportional to the length of an inlet, L_b, and inversely proportional to the width, B, and to $d_a^{3/2}$, Murty, Wigen, and Chawla (1975) proposed that the relative intensity, I, of the secondary undulations could be given as

$$I = \frac{L_b}{B d_a^{3/2}} \tag{294}$$

Values of I for inlets of Alaska, British Columbia, and for Puget Sound are shown in Table 4. Inlets with higher relative intensities, I, would be expected to excite larger amplitudes of oscillation. As indicated by Murty, Wigen, and Chawla, some bays which have small ratios of L_b/B have large secondary oscillations. They point out that equations (293) and (294) are based on a one-dimensional theory which is not valid for low ratios of L_b/B, and that transverse motion is important in these cases.

Fukuuchi and Ito (1966) consider a tsunami passing from a larger bay or inlet into a smaller inlet. Where the larger inlet has a width B_1, and the width narrows to a width B_2 in the smaller inlet (see Fig. 40), they give the amplitude a_2 at the head of the smaller inlet as

$$a_2 = \frac{2\sqrt{2}\, a_1 \dfrac{B_1}{B_2}}{\left[\left(\dfrac{B_1}{B_2}\right)^2 + 1 + \left\{\left(\dfrac{B_1}{B_2}\right)^2 - 1\right\} \cos\left(\pi \dfrac{T_1}{T}\right)\right]^{1/2}} \tag{295}$$

where a_1 is the incident tsunami amplitude in the larger inlet, T the period of the tsunami, and T_1 the period of the smaller inlet as given by equation (293). The maximum amplitude a_2 will occur when T_1/T = 1, 3, 5. . . while the minimum amplitude would be at T_1/T = 2, 4, 6. . . etc. Equation (295) would predict very high values of a_2/a_1 where B_1/B_2 is large. This is not consistent with the work of other investigators.

Ippen, Raichlen, and Sullivan (1962) carried out a hydraulic model investigation of an inlet connected to an "infinite ocean." The ocean was simulated in a wave basin, using wave absorbers to minimize reflected

Table 4. Dimensions, periods of fundamental mode, and intensity of secondary undulations of inlets of Alaska and British Columbia, and of Puget Sound (from Murty, Wigen, and Chawla, 1975).

Inlet	L_b, length (km)	d_a, mean depth (km)	Period, T_1 (min)	B, mean width (km)	L_b/B	$\frac{L_b/B}{d_a^{3/2}}$
Alaska						
Tarr Inlet-Glacier Bay	111	0.220	159	5.6	19.8	192
Muir Inlet	35	0.215	51	3.5	10.0	100
Lynn Canal	146	0.360	164	6.6	22.1	102
Gastineau Canal	18	0.040	61	1.3	13.8	1,725
Taku Inlet-Stephens Passage	133	0.295	165	13.0	10.2	64
Tracy Arm	43	0.270	56	1.8	23.9	170
Endicott Arm	44	0.260	58	3.3	13.3	100
Frederick Sound	80	0.165	133	22.2	3.6	54
Thomas Bay	20	0.150	35	2.8	7.1	122
Tenakee Inlet	64	0.140	115	3.2	20.0	382
Peril Strait	71	0.210	104	4.0	17.8	185
Bradfield Canal-Ernest Sound	80	0.310	97	5.7	14.0	81
Behm Canal West-Bell Arm	72	0.425	74	5.2	13.8	50
Burroughs Bay-Behm Canal East	113	0.420	174	3.5	32.3	119
Rudyerd Bay	22	0.170	36	0.9	24.4	348
Boca de Quadra	56	0.245	76	1.3	43.1	355
Carroll Inlet	44	0.130	82	1.6	27.5	587
George Inlet	22	0.225	31	1.4	15.7	147
British Columbia						
Portland Canal	115	0.255	153	2.2	52.3	406
Observatory Inlet-Hastings Arm	76	0.385	82	2.2	34.5	144
Alice Arm	19	0.240	26	1.3	14.6	124
Khutzeymateen Inlet	25	0.120	49	1.0	25.0	601
Work Channel	54	0.240	74	2.0	27.0	230
Prince Rupert Inlet	19	0.045	60	1.2	15.6	1,634
Douglas Channel	83	0.330	97	3.5	23.7	125
Kildala Arm	19	0.175	31	1.5	12.7	173
Gardner Canal	91	0.275	117	1.9	47.9	332
Surf Inlet	22	0.220	32	0.9	24.4	236
Laredo Inlet	39	0.295	48	1.5	26.0	162
Sheep Passage-Mussel Inlet	33	0.275	42	1.5	22.0	153
Spiller Channel	46	0.255	61	1.9	24.2	188
Roscoe Inlet	43	0.135	79	1.1	39.1	788
Cousins Inlet	12	0.070	31	0.8	15.0	810
Cascade Inlet	26	0.250	35	1.1	23.6	189
Dean Channel	111	0.420	115	2.4	46.3	170
Kwatna Inlet	24	0.345	28	2.0	12.0	59
South Bentinck Arm	37	0.240	51	2.2	16.8	143
Rivers Inlet	46	0.295	57	3.0	15.3	95
Moses Inlet	26	0.200	39	0.9	28.9	323

Table 4. Dimensions, periods of fundamental mode, and intensity of secondary undulations of inlets of Alaska and British Columbia, and of Puget Sound (from Murty, Wigen, and Chawla, 1975).--Continued

Inlet	L_b, length (km)	d_a, mean depth (km)	Period, T_1 (min)	B, mean width (km)	L_b/B	$\frac{L_b/B}{d_a^{3/2}}$
Smith Inlet	33	0.270	43	1.3	25.4	181
Mereworth Sound	19	0.090	43	0.4	47.5	1,759
Belize Inlet	52	0.255	69	1.1	47.3	367
Nugent Sound	24	0.075	59	0.7	34.3	1,669
Seymour Inlet	67	0.420	70	1.7	39.4	145
Drury Inlet	22	0.040	74	1.3	16.9	2,112
Knight Inlet	130	0.295	161	3.0	43.3	270
Call Inlet	28	0.135	51	1.5	18.7	377
Loughborough Inlet	35	0.190	54	1.7	20.6	249
Bute Inlet	76	0.510	72	3.7	20.5	56
Toba Inlet	37	0.390	40	2.6	14.2	58
Jervis Inlet	89	0.495	85	3.2	27.8	80
Howe Sound	43	0.225	61	7.0	6.1	57
Vancouver Island British Columbia						
Holberg-Rupert Inlet	44	0.165	73	1.4	31.4	469
Quatsino Sound-Neroutsos Inlet	59	0.150	103	2.2	26.8	461
Forward Inlet	11	0.030	43	1.1	10.0	1,925
Klaskino Inlet	11	0.035	40	0.7	15.7	2,398
Ououkinsh Inlet	14	0.085	32	1.2	11.7	472
Port Eliza	11	0.050	33	0.7	15.7	1,404
Espinosa Inlet	14	0.215	20	1.3	10.8	108
Nuchalitz Inlet	15	0.025	64	1.3	11.5	2,909
Tahsis Inlet	29	0.120	56	0.9	32.2	775
Cook Channel-Tlupana Inlet	31	0.150	54	1.9	16.3	281
Zuciarte Channel-Mechalat Inlet	48	0.220	69	1.5	32.0	310
Sydney Inlet	20	0.080	48	1.3	15.4	681
Shelter Inlet	19	0.115	38	1.3	14.6	374
Herbert Inlet	23	0.100	49	2.0	11.5	364
Pipestem Inlet	9	0.045	29	0.7	12.9	1,351
Effingham Inlet	17	0.095	37	1.2	14.2	485
Alberni Inlet	69	0.145	122	1.3	53.1	962
Saanich Inlet	23	0.180	37	2.5	9.2	120
Puget Sound						
Puget Sound	111	0.165	184	6.0	18.5	276
Hood Canal	102	0.110	207	2.5	40.8	1,118
Possession Sound-Saratoga Passage	70	0.090	157	3.7	18.9	700

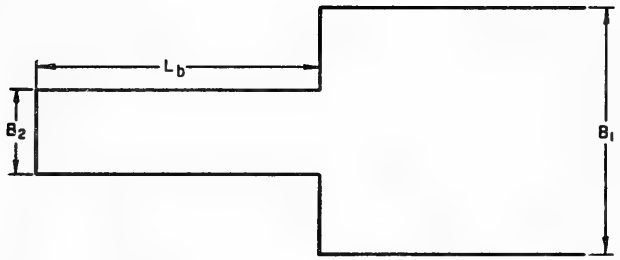

Figure 40. Plan view of inlet.

waves. It is assumed in this case that $B_1 \to \infty$. The experimental results of Ippen, Raichlen, and Sullivan are shown in Figure 41, where k is the wave number $2\pi/L$. The results are for a fixed inlet width and varying wavelength, the variation in the curves illustrating the dependence of the results on the ratio of wavelength to inlet width, particularly for short, wide inlets.

Each curve in Figure 41 was obtained by varying the inlet length for a fixed wavelength. The results were dependent upon the efficiency of the wave filters and wave absorbers used in the experiments. Using equation (293) to define T_1,

$$kL_b = \frac{\pi}{2}\frac{T_1}{T} \tag{296}$$

Therefore, Figure 41 shows that the maximum amplification occurs where $T_1/T < 1$. Ippen, Raichlen, and Sullivan did not explore the amplification for shorter period waves; i.e., $T_1/T \simeq 3, 5, 7. \ . \ .$ etc. The maximum amplification occurring where $T_1/T < 1$ is equivalent to resonance for a longer inlet. It can be assumed, therefore, that the inlet has an effective length L_e extending into the open sea; i.e., since a node does not exist at the entrance, $L_e > L_b$ and the effective primary period, T_{1e}, is

$$T_{1e} = \frac{4L_e}{\sqrt{gd_a}} \tag{297}$$

The length L_e, is defined by equation (297) if it is assumed that $T_{1e}/T = 1$ where maximum amplification occurs.

Nishimura, Horikawa, and Shuto (1971) carried out similar experiments for an inlet with the entrance partially closed by a breakwater. They also found that the inlet had an effective length greater than the actual length. Ippen, Raichlen, and Sullivan (1962) and Nishimura, Horikawa, and

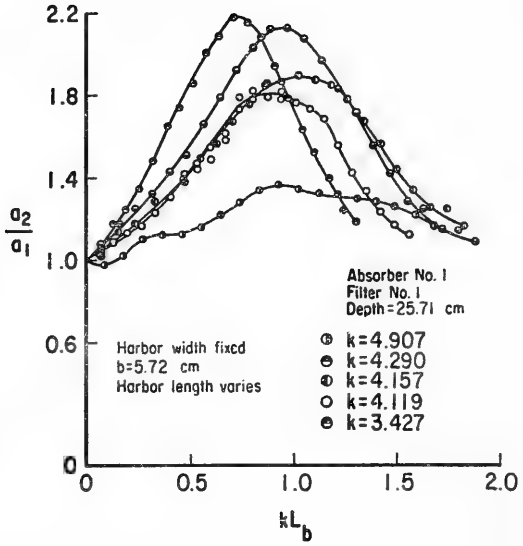

Figure 41. Amplification factor versus relative harbor length (from Ippen, Raichlen, and Sullivan, 1962).

Shuto all indicate that the effective length may be determined by the ratio of inlet width to inlet length.

Nishimura, Horikawa, and Shuto reported that variations in opening width at the mouth of an inlet did not affect the effective length. However, they investigated a half-harbor width and assumed symmetry would produce the same resonant motion in the half harbor as it would in a full harbor. Ippen and Goda (1963) indicated this would not be true because the half harbor has a asymmetric entrance one-half the width of the centered entrance of the full harbor. Ippen and Goda showed that the harbor entrance width determined the value of wave radiation functions which are used to determine water surface elevations.

For a fully open inlet or harbor (see Fig. 40), Ippen and Goda defined resonant amplification (the ratio of an amplitude in the harbor to the amplitude at the closed harbor entrance) as

$$\frac{a_2}{a_1} = \frac{1}{[(\cos kL_b - \psi_2 \sin kL_b)^2 + \psi_1^2 \sin^2 kL_b]^{1/2}} \qquad (298)$$

where ψ_1 and ψ_2 are wave radiation functions given in Figure 42. The resonant amplification would occur where $T_{Le}/T = 1$ as before. The functions shown in Figure 42 apply to all harbor openings, where b is the width of the opening.

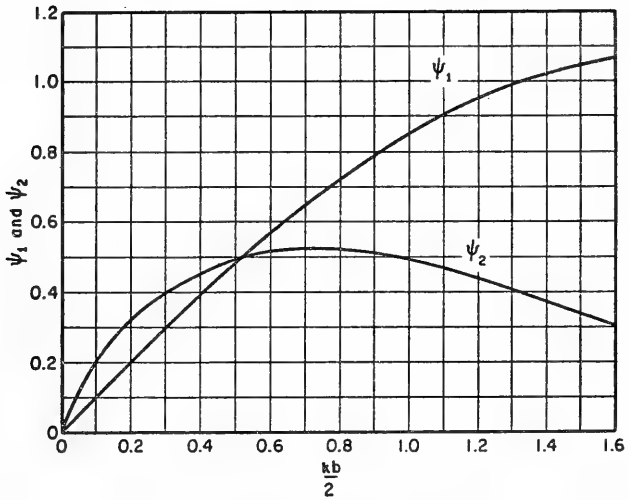

Figure 42. Wave radiation functions (from Ippen and Goda, 1963).

* * * * * * * * * * * * * * * EXAMPLE PROBLEM 20 * * * * * * * * * * * * * * *

GIVEN: A fully open inlet has a width, B, given by B = 0.194 L_b, where L_b is the length of the inlet. The incident wavelength L = 25B.

FIND: The resonant amplification in the inlet.

SOLUTION:

$$\frac{kB}{2} = \frac{2\pi(0.04L)}{2L} = 0.1257$$

From Figure 42, where b = B for a fully open inlet

$$\psi_1 = 0.12$$

and

$$\psi_2 = 0.24$$

From equation (298),

$$\frac{a_2}{a_1} = \frac{1}{[(\cos kL_b - \psi_2 \sin kL_b)^2 + \psi_1 \sin^2 kL_b]^{1/2}}$$

$$\frac{a_2}{a_1} = \frac{1}{\left[\left(\cos\left\{2\pi \frac{0.04}{0.194}\right\} - 0.24 \sin\left\{2\pi \frac{0.04}{0.194}\right\}\right)^2 + (0.12)^2 \sin^2\left(2\pi \frac{0.04}{0.194}\right)\right]^{1/2}}$$

$$\frac{a_2}{a_1} = 8.16$$

* *

Ippen and Goda (1963) compared theoretical and experimental results of a fully open harbor (Fig. 43). They also obtained theoretical results for partially closed harbors with both symmetric and asymmetric entrances (Fig. 44). Their experimental results for partially closed harbors generally showed that amplification factors were less than those predicted theoretically. However, comparisons between experiments and theory were only obtained for higher modes of oscillation.

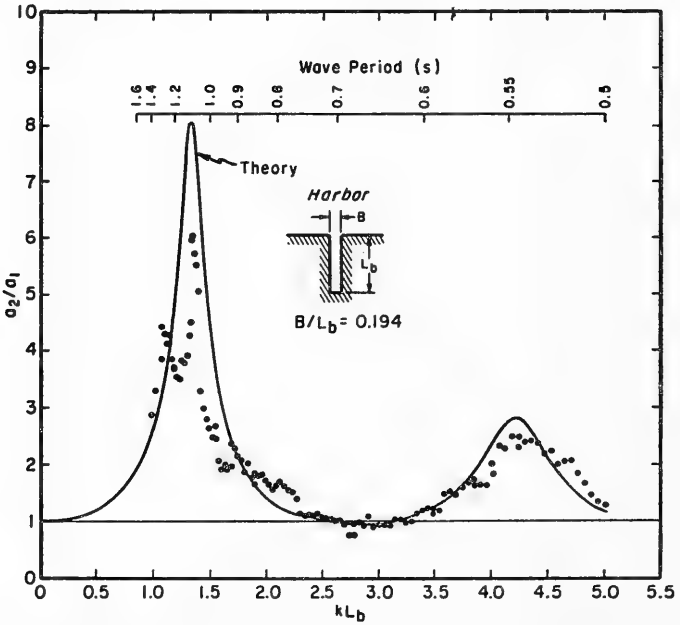

Figure 43. Frequency response of a fully open harbor (from Ippen and Goda, 1963).

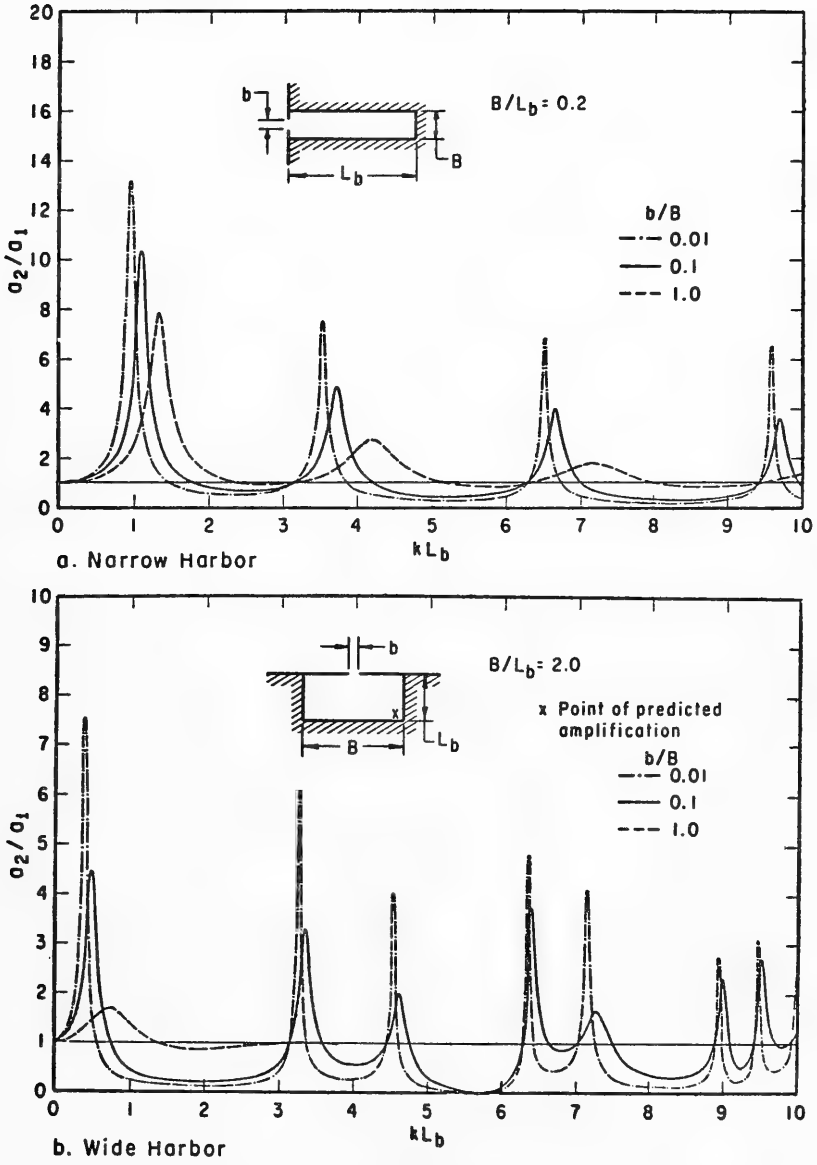

Figure 44. Theoretical frequency response curves of harbors (from Ippen and Goda, 1963).

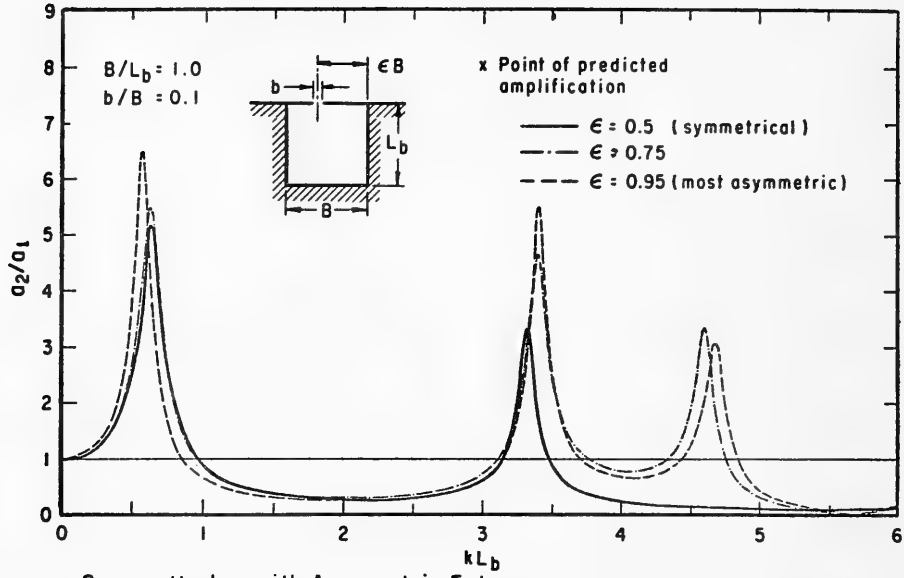

c. Square Harbor with Asymmetric Entrance

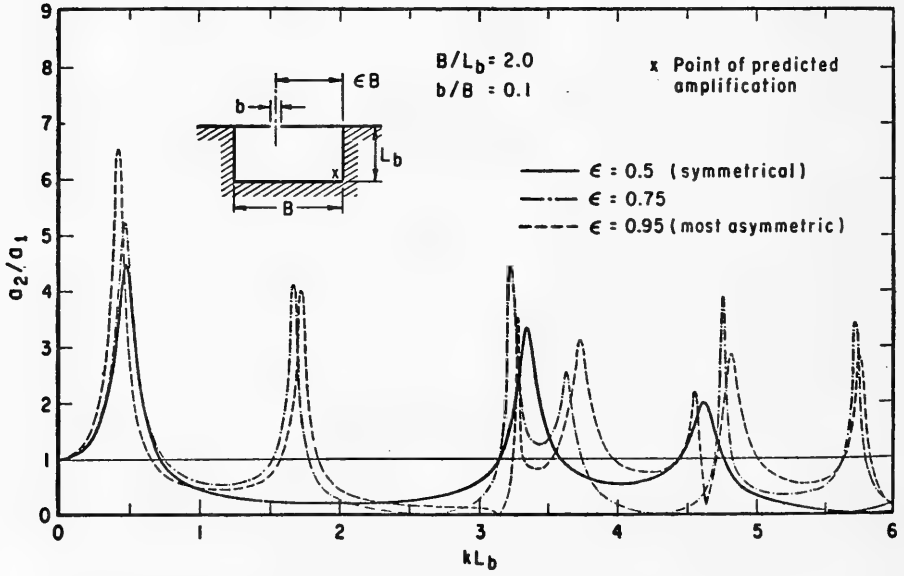

d. Wide Harbor with Asymmetric Entrance

Figure 44. Theoretical frequency response curves of harbors (from Ippen and Goda, 1963).--Continued

Miles (1972) indicates that for waves passing from a Continental Shelf into a harbor, where the dimensions of the harbor and the entry channel are small compared to the local wavelength of the tsunami, the response of the harbor is essentially restricted to the Helmholtz mode; i.e., the lowest mode of resonance. The harbor undergoes a pumping motion where the water level in the harbor is assumed to rise and fall uniformly across the total area of the harbor (Carrier, Shaw, and Miyata, 1971). The water passing through the entry channel is assumed to have a high velocity, represented as kinetic energy; the water in the harbor has a much lower velocity, and the rise and fall of the water level in the harbor is represented as potential energy.

Carrier, Shaw, and Miyata (1971) show that the wave number, k_o, for Helmholtz resonance is represented

$$k_o = \left(\frac{b}{L_c - \frac{b}{\pi} \ell n \left(k_o \frac{b}{2} \right)} \right)^{1/2} \left(\frac{1}{L_b B} \right)^{1/2} \qquad (299)$$

where L_c is the length of the entrance channel (Fig. 45). The term $(b/\pi)\ \ell n\ (k_o\ b/2)$ in the denominator represents the effect of energy radiation from the seaward end of the entrance channel (Rayleigh, 1945; Miles, 1948). Equation (299) is restricted to very limited cases, and Figure 46 shows a comparison of equation (299) and the results of Miles (1971) for a harbor with a zero-length entrance channel ($L_c = 0$). Figure 46 shows that equation (299) will generally predict resonant wavelengths that are too short (and therefore predicted resonant periods with values lower than the actual resonant periods).

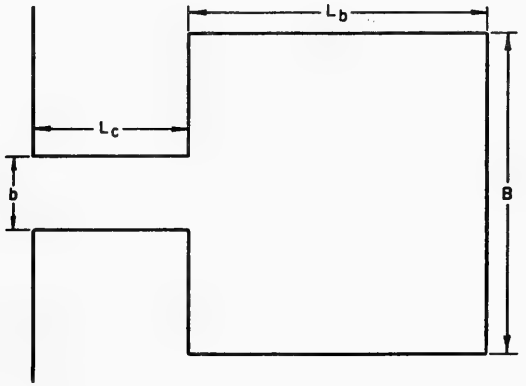

Figure 45. Harbor with an entrance channel.

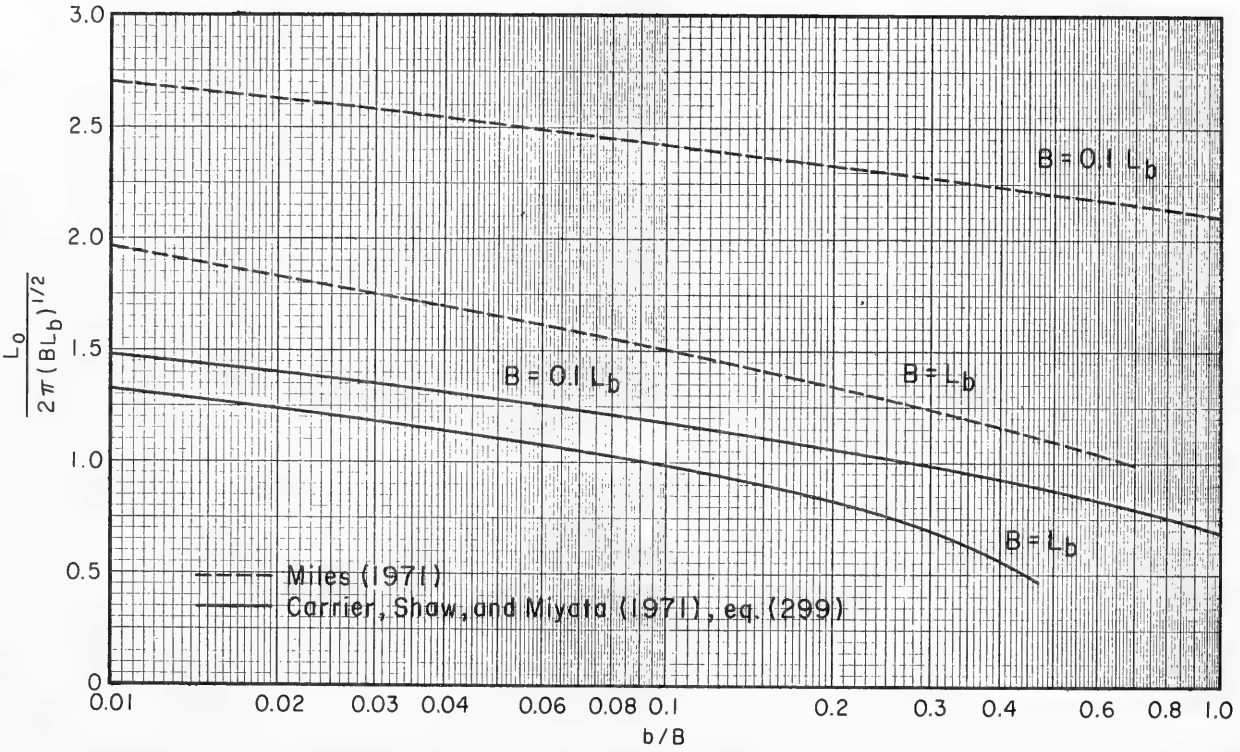

Figure 46. Wavelength for Helmholtz resonance (centered harbor entrance, entrance length L_e = 0).

Carrier, Shaw, and Miyata (1971) suggest an approximate method for determining resonant wavelengths, for harbors with entrance channels, which will be more generally applicable than equation (299). Their method assumes that the resonant wavelength, $L_o(L_c = 0)$, for an equivalent harbor of the same dimensions but having no entrance channel ($L_c = 0$), can be obtained. Correcting an error which appears in Carrier, Shaw, and Miyata, the resonant wavelength for the harbor with an entrance channel is then given by the equation

$$\frac{L_o}{2\pi} = \left[\frac{L_c\ L_b\ B}{b} + \frac{L_o^2(L_c = 0)}{(2\pi)^2}\right]^{1/2} \tag{300}$$

The resonant wavelength where $L_c = 0$ can be obtained using Miles' (1971) results (see Fig. 46).

For a harbor with an entrance channel (Fig. 45), Miles (1971) indicates that narrowing the entrance width or increasing the length of the entrance channel will significantly increase the response of the harbor to the Helmholtz mode, which may dominate tsunami response. This narrowing or lengthening also has the effect of decreasing the resonant frequency (Carrier, Shaw, and Miyata, 1971). Carrier, Shaw, and Miyata point out that lengthening the entrance channel to a harbor also increases the frictional resistance so amplification factors for a very long entrance channel may be significantly reduced (although the resonant frequencies would still be less than for a harbor without an entrance channel; i.e., where $L_c = 0$).

Seelig, Harris, and Herchenroder (1977) present a numerical means for analyzing harbors responding to the Helmholtz mode of resonance. The method uses a Runge-Kutta-Gill technique where

$$\frac{dh_b}{dt} = \frac{Q}{A_b} \tag{301}$$

h_b is the surface elevation of the water in the harbor above some arbitrary fixed datum, Q the flow rate through the entrance channel, and A_b the area of the harbor ($A_b = L_b\ B$). The governing differential equation is

$$\frac{dQ}{dt} = \frac{I_g}{2}\left(\frac{1}{A_{bc}^2} - \frac{1}{A_{sc}^2}\right)Q^2 - g\ I_g(h_b - h_s) - I_g\ F \tag{302}$$

where

$$I_g = \frac{1}{\int_{X_s}^{X_b} \frac{dx}{A_c}} \tag{303}$$

A_c is the cross-sectional area of flow through the entrance channel at any point X between the seaward end at X_s and the harbor end X_b (A_c, therefore, being a function of X), A_{bc} the cross-sectional area at the bay end, A_{sc} the cross-sectional area at the sea end, h_s the height of the sea level above the arbitrary fixed datum, and F defined as the total bottom friction in the entrance channel. A sample computation for a tsunami entering a bay is given in Seelig, Harris, and Herchenroder (1977) (Fig. 47). It can be seen that the peak water levels in the bay occur slightly after the peak water levels just seaward from the entrance channel. Also, the peak water levels were slightly lower in this case.

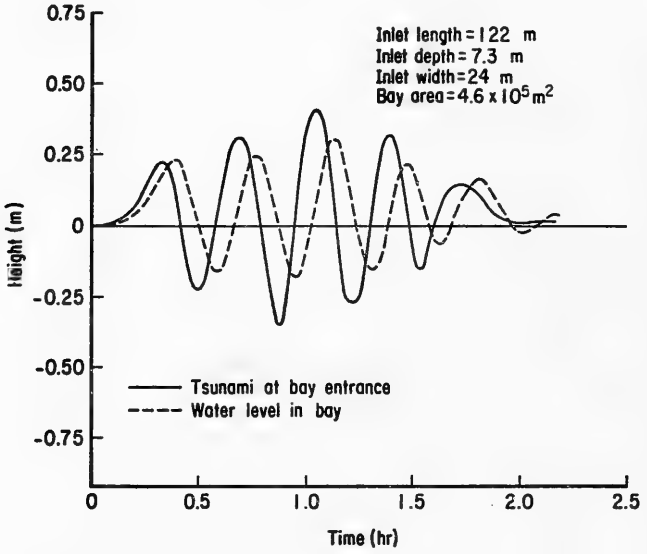

Figure 47. Tsunami water levels in a bay (tide excluded) (after Seelig, Harris, and Herchenroder, 1977).

Miles (1971) found that he could transform his equations for wave-induced oscillations in a harbor to an integral equation equivalent to the equation formulated by Lee (1969, 1971). Lee expresses the governing equations for wave oscillations in an arbitrary-shaped harbor as

$$\frac{d^2Z}{dZ^2} = K^2 Z \tag{304}$$

and

$$\frac{\partial^2 f(x,y)}{\partial x^2} + \frac{\partial^2 f(x,y)}{\partial y^2} + k^2 f(x,y) = 0 \tag{305}$$

where

$$Z = - \frac{ag \cosh [k(z + d)]}{\cosh(kd)} \tag{306}$$

and $f(x,y)$ is a wave function to be determined. Equation (305) is the Helmholtz equation. The following boundary conditions are assumed:

(a) $f(x,y)/\partial n = 0$ along all fixed boundaries where n is in the normal direction to the boundary.

(b) The harbor does not affect the wave system where $(x^2 + y^2)^{1/2} \to \infty$; i.e., at large distances from the harbor entrance.

Lee determines the value of the unknown wave function $f(x,y)$ by determining the function $f_1(x,y)$ in the open sea and the function $f_2(x,y)$ in the harbor, then matching the functions at the harbor entrance; i.e., the wave amplitude and the slope of the water surface must be the same for $f_1(x,y)$ and $f_2(x,y)$ at the entrance.

The function $f_2(x,y)$ at some position (x,y) within the harbor is defined by a line integral $\int_s$ taken around the harbor boundary in a counterclockwise direction giving

$$f_2(x,y) = - \frac{i}{4} \int_s \left\{ f_2(x_o,y_o) \frac{\partial}{\partial n} [H_o^{(1)}(kr)] - H_o^{(1)}(kr) \frac{\partial}{\partial n} [f_2(x_o,y_o)] \right\} d_s \tag{307}$$

where $H_o^{(1)}$ is a zero-order Hankel function of the first kind, $f_2(x_o,y_o)$ the function at a boundary point (x_o,y_o), and r the distance between the boundary point (x_o,y_o) and the interior point (x,y).

The wave function in the open sea is represented by the sum of three functions

$$f_1(x,y) = f_i(x,y) + f_r(x,y) + f_{ra}(x,y) \tag{308}$$

where $f_i(x,y)$ is the known incident wave function, $f_r(x,y)$ the reflected wave function, and $f_{ra}(x,y)$ the wave function for the wave radiating seaward from the harbor entrance. The reflected wave function is determined from the incident wave function for total reflection. The radiated wave function is determined as

$$f_{ra}(o,y) = - \frac{i}{2} \int_s H_o^{(1)}(kr) \frac{\partial}{\partial n} [f_2(o,y_o)] \, d_s \tag{309}$$

where the line integral $\int_S$ is taken across the harbor entrance, y is measured along the coastline (across the harbor entrance), and x is measured normal to the coastline.

Lee (1969) expressed equations (307) and (309) in matrix form and solved them numerically. Figure 48 is an example of his experimental results for a small laboratory model of an arbitrary-shaped harbor.

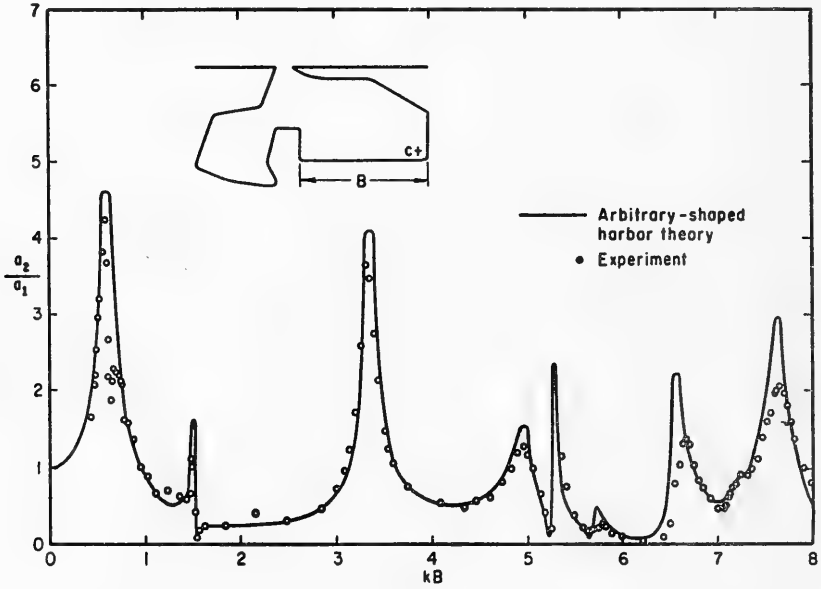

Figure 48. Response curve at point C of the Long Beach harbor model (from Lee, 1969).

Chen and Mei (1974) have developed a finite-element numerical model which can be used to study water level oscillations in a harbor. Houston (1976, 1977) applied Chen and Mei's model to studies of Los Angeles and Long Beach harbors.

VII. TSUNAMI RUNUP AND INTERACTION WITH STRUCTURES

The arrival of a tsunami at a shoreline may cause an increase in water level as much as 30 meters or greater in an extreme case. Increases of 10 meters (32.8 feet) are not uncommon. The large increase in water level, combined with the surge of the tsunami, can impose powerful forces on shore protection structures and on structures located near the shoreline. Structures may be seriously damaged or destroyed by the tsunami. Damage may be caused by strong currents produced by waves overtopping the structures, by the direct force of the surge produced by a wave, by the

hydrostatic pressure created by flooding behind a structure combined with the loss of equalizing forces at the front of a structure due to extreme drawdown of the water level when the waves recede, and by erosion at the base of the structure. Major damage may also be caused by debris carried forward by the tsunami in the nearshore area.

To determine the potential damage to structures located along a shoreline, the probable increase in water level caused by the tsunami, i.e., the runup height, must be estimated. Estimates of tsunami runup are also needed for flood zone planning along the shoreline, and for operation of the tsunami warning system to evacuate people from endangered areas.

1. Tsunami Runup on a Shoreline.

The height of a tsunami will vary from point to point along a coastline. The numerical models for prediction of tsunami height at the shoreline, i.e., the elevation of water at the shoreline due to the tsunami, must be applied to a sufficient number of points along the shoreline to determine this variation. When the variation is large between adjacent points, calculations for tsunami heights should be carried out at additional shoreline points between those points. After the height of the tsunami at a point along the shoreline has been determined, the vertical runup height at that point can be estimated.

When the tsunami height along a section of coastline is relatively constant, and the variations in onshore topography are relatively minor, the runup height may be assumed to be constant along that section of coastline as a first approximation. Variations in tsunami height and shoreline topography will actually cause some variation in runup characteristics along any section of coastline. An example of how extreme this variation can be is given by Shepard, MacDonald, and Cox (1950) for Haena, on the Island of Kauai, Hawaii, where there was a gentle rise of water level on the western side of the bay, but less than 1 mile to the east, waves rushed onshore, flattening groves of trees and destroying houses. An example of the variation in runup height is given by Wilson and Tørum (1968) for Kodiak City, Alaska (Fig. 49). The mean runup height at Kodiak City was a little more than 6 meters (20 feet) above mean lower low water (MLLW), with variations from about 5 to 8 meters (17 to 27 feet). Because these variations are difficult to predict, the predicted runup heights may contain substantial errors. Where tsunamis of a known height have produced variations in runup at a particular section of coastline, the higher heights should normally be used for conservative design.

It should be noted that the characteristics of the waves may vary from one wave to another at the same coastal point. Shepard, MacDonald, and Cox (1950) cite a case in Hawaii where the first waves came in so gently that a man was able to wade through chest-high water ahead of the rising water. Later waves were so violent that they destroyed houses and left a line of debris against trees 150 meters (500 feet) inland.

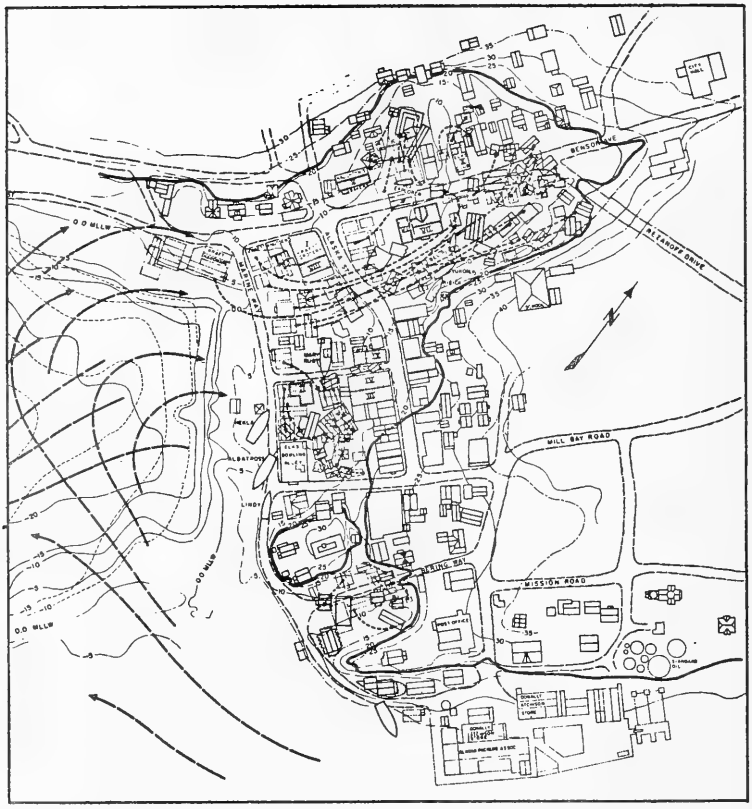

Figure 49. 1964 tsunami runup, Kodiak City, Alaska (contours in feet); heavy line is maximum flood level (from Wilson and Tørum, 1968).

An added complication, which is an important consideration in computing runup heights, is the possibility of storm waves occurring simultaneously with the tsunami. The prediction of maximum runup heights would require the consideration of joint probabilities of tsunamis and storm waves, as well as the probability of a high tidal stage. The probability of a high tide, tsunami, and storm waves occurring simultaneously may appear to be small; however, such an event did occur in Newfoundland in 1929 (Hodgson and Doxsee, 1930).

Because a tsunami has a very long period relative to storm waves, it causes an apparent variation in water depth over a long distance. Storm waves riding on top the tsunami will have a wave celerity corresponding to the depth (including tsunami height) at any particular point. If two storm waves are otherwise equivalent (e.g., the same period and wave

height), and one is at the crest of the tsunami while the other is at the leading edge, the storm wave at the tsunami crest will have a higher celerity (U.S. Army Engineer District, Honolulu, 1960). Therefore, the tsunami can cause one storm wave to overtake and superimpose itself on another storm wave, producing higher waves at the shoreline.

Storm waves alone may be more severe than a tsunami at some exposed coastal points. Shepard, MacDonald, and Cox (1950) refer to the Kalaupapa Peninsula, on the Island of Molokai, Hawaii, where the 1946 tsunami left driftwood at elevations slightly more than 2 meters (7 or 8 feet) above normal sea level, but winter storms had left driftwood 6 meters above the same datum plane. A combination of a winter storm and a large tsunami could be very destructive.

Houston and Garcia (1974) assume that tsunami runup on a shoreline will have a runup height (vertical rise) equal to the wave height at the shoreline. This assumption is based on the idea that a tsunami will act like a rapidly rising tide. The assumption was compared with a few cases where both height and runup data were available. For those cases, which included the 1960 tsunami at Hilo, Hawaii, that produced a bore-fronted wave, the predicted value of runup equal to wave height at the shoreline compared well with the maximum runup measured in the area. Nasu's (1934) data for a tsunami occurring in Japan also indicate that the total runup was about equal to the wave height at the shoreline at many locations. Wiegel (1965) reports that maximum runup elevations above MLLW at Crescent City, California, were equal to or greater than the maximum wave height (crest-to-trough) at the Crescent City tide gage for the 1952, 1960, and 1964 tsunamis. Magoon (1965) indicates that the 1964 tsunami at Crescent City had an elevation of about 6 meters above MLLW along a substantial length of shoreline, and that the line of maximum tsunami inundation generally followed a contour at that elevation. While the assumption that maximum runup heights will equal the tsunami height at the shoreline provides an initial estimate, this assumption cannot always be used with accuracy. The effects of ground slope, wave period, and the possible convergence or divergence of the runup must be considered.

The results of Nasu (1934) indicate that the tsunami height at the shoreline and the runup height are dependent on the configuration of the coastline. At Kamaisi, Japan (Fig. 50), on the north side of a bay, the runup height was actually somewhat less than the wave height at the shoreline, equal to slightly more than 3 meters. At Hongo (Fig. 51), at the head of a bay, the tsunami flowed directly up a canyon along a streambed, and the maximum runup height was about 11 meters (36 feet). At Ryoisi (Fig. 52), the tsunami intruded into a small inlet opening onto the main bay, flowed up a canyon along a streambed and highway, and reached a maximum runup height equal to about 10.5 meters (34 feet). The wave at Kamaisi was probably traveling parallel to the shoreline as it flooded into the bay. The wave at Hongo and Ryoisi was probably traveling in a direction oriented directly along the axis of the canyons as the surge came onshore.

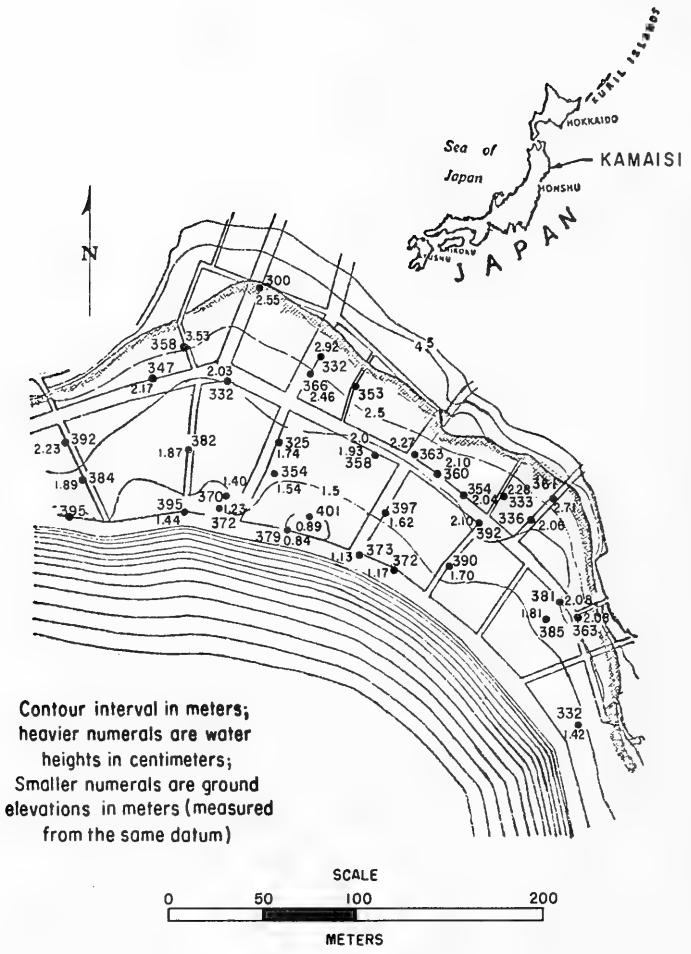

Figure 50. Tsunami runup at Kamaisi, Japan (after Nasu, 1934).

Iwasaki and Horikawa (1960) show that the period of the waves will be a major factor in determining maximum inundation levels. The waves from the tsunami which struck the coast of Japan on 24 May 1960 had periods of about 60 minutes, while the 1933 tsunami reported on by Nasu (1934) had wave periods of about 12 minutes. The 1960 tsunami did not form a bore or a spilling front, and the water level gradually gained height over the entire surface of the bays where it was observed. For the longer period waves of the 1960 tsunami, the orientation of the bays appeared to have no influence on the runup heights; the height of the

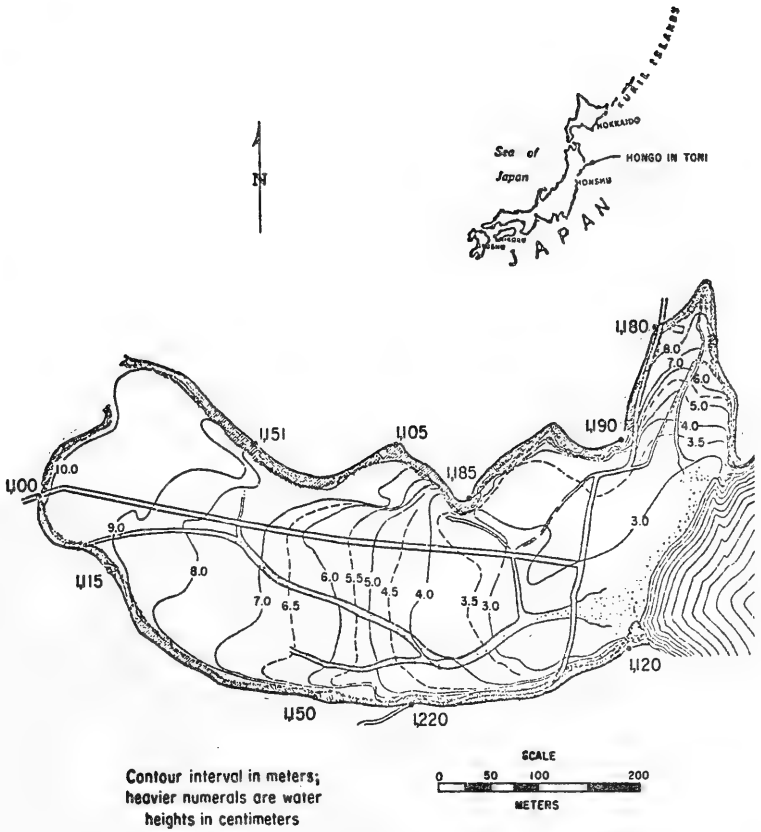

Figure 51. Tsunami runup at Hongo in Toni, Japan (after Nasu, 1934).

runup was equal to (or sometimes less than) the height of the wave at the shoreline.

Tsunamis at a shoreline could be categorized into three types of waves: nonbreaking waves (i.e., a tsunami which acts as a rapidly rising tide); waves which break far from the shoreline and become fully developed bores before reaching the shoreline; and waves which break near the shoreline and act as partially developed bores which are not uniform in height. In addition, there are some cases where reflected waves become bores after reflecting from a shoreline.

For the nonbreaking wave, the assumption that the runup height equals the wave height at the shoreline may be reasonable and possibly even conservative. Field observations (e.g., Nasu, 1934) indicate that the runup

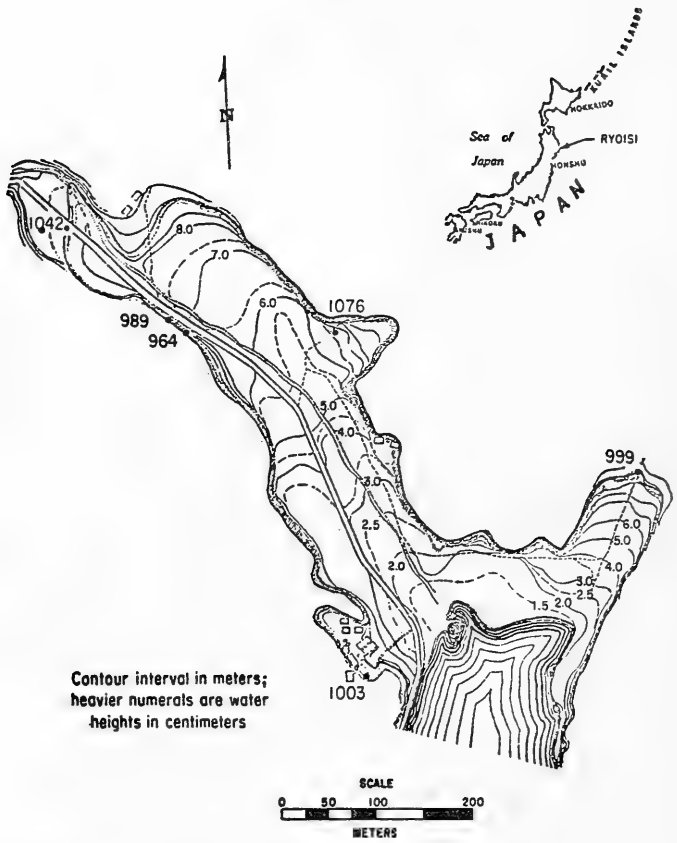

Figure 52. Tsunami runup at Ryoisi, Japan (after Nasu, 1934).

height is sometimes less than that value. To analyze the runup of breaking waves and fully developed bores, where maximum runup heights have been observed to be much higher than the wave or bore height at the shoreline, it is necessary to consider the actual form of the runup.

Using solitary waves, Camfield and Street's (1967) experimental results for an 8° nearshore slope fronted by a slope $S_2 = 0.01$ indicated that the runup takes the initial form of a horizontal water surface at an elevation equal to the wave height at the shoreline (Fig. 53), and that the higher runup on the slope washes up the slope at a shallow depth. Results for plunging breakers on 4° and 8° slopes fronted by a slope $S_2 = 0.01$, and on 4°, 8°, and 12° slopes fronted by a slope $S_2 = 0.03$, indicated similar runup characteristics. The higher, shallow runup may cause some flooding, but would not be expected to otherwise cause damage

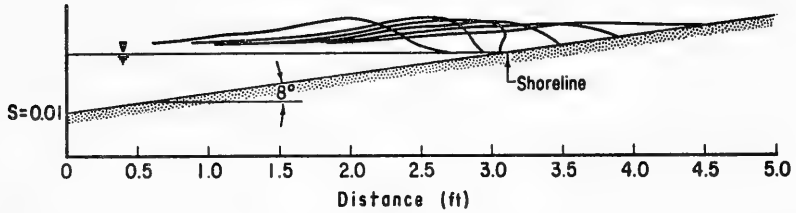

Figure 53. Solitary wave runup (from Camfield and Street, 1967).

because of the shallow depth. Also, this higher, shallow runup may not be representative of prototype runup. O'Brien (1977) points out that a fraction of the uprush percolates into a natural, permeable beach. This percolation tends to partially dissipate the shallow part of the runup observed on the impermeable model beach.

Kononkova and Reihrudel (1976) studied the runup of solitary waves on uniform slopes which were apparently fronted by a horizontal tank bottom. For nearshore slopes less than 8°, their results were comparable to those of Camfield and Street (1967). For nearshore slopes greater than 8°, they found runup values higher than the wave height at the shoreline.

Miller (1968) gives results for borelike waves which act as surge runup on a shoreline. He shows that the runup in this case also takes the initial form of a horizontal water surface at an elevation equal to the wave height at the shoreline, and that the higher runup flows up the slope as a thin sheet. Miller comments that, "In the later stages of runup, the form of the wave was of a thin, fast-moving greatly elongated wedge."

The experimental work of Camfield and Street (1967), Miller (1968), and Kononkova and Reihrudel (1976) was for flat, uniform slopes with no convergence of the wave crest. In general, the experiments show that for flatter slopes (less than 8°) the runup height appears equal to or less than the wave height at the shoreline. For steeper slopes, the runup height increases as the slope increases, and the ratio of runup height to wave height at the shoreline appears to reach a maximum value for vertical walls. However, the higher runup on the steeper slopes appears to have a relatively shallow depth.

Some attempts have been made to develop theoretical solutions. Freeman and Le Mehaute (1964) give a formula for surge runup as

$$R = \frac{u_s^2(1 + A)(1 + 2A)}{2g\left(1 + \frac{f}{A^2 S}\right)} \tag{310}$$

where

R = the vertical height of runup above the stillwater level

u_s = the current velocity of the surge at the shoreline

f = the friction factor

S = the ground slope

g = gravitational acceleration

A = a coefficient

Adapting the work of Keulegan (1950), they obtain a maximum value of A = 0.5. Using a value for u_s given by

$$u_s = \frac{1}{A} (gh_s)^{1/2} \tag{311}$$

where h_s is the surge height at the shoreline, taking the friction factor, f, as

$$f = \frac{8g}{C_h^2} \tag{312}$$

where C_h is the Chezy coefficient, and using the maximum value for A, equation (310) reduces to

$$\frac{R}{h_s} = \frac{6}{1 + \frac{32g}{C_h^2 S}} \tag{313}$$

As C_h varies with depth, this equation would predict that the relative runup R/h_s varies between a prototype and model unless proper roughness scaling is used. Because C_h decreases with increasing roughness, the relative runup would decrease as the roughness increases. Also, as slope increases, the relative runup increases. As the slope approaches infinity (a vertical wall), the relative runup $R/h_s = 6$. This value is somewhat higher than experimentally obtained values. Camfield and Street (1967, 1968) obtained values of relative runup between 4.5 and 5.0 from solitary wave experiments for breaking waves running up on a vertical wall. Equation (313) does not consider the effects of wave period.

Freeman and Le Mehaute (1964) noted that coefficient A in equation (310) should be somewhat less than 0.5. Kishi and Saeki (1966) indicate that the value of A decreases as the slope decreases, which is consistent with Freeman and Le Mehaute that the value of A depends on the form of the wave at the shoreline.

It is also necessary to account for the dependence of C_h on the varying height, h, of the surge traveling up the onshore slope. Noting that, for uniform flow, C_h can be related to the Manning roughness coefficient n by

$$C_h^2 = \frac{h^{1/3}}{n^2} \tag{314}$$

in metric units (the right side of eq. 314 is multiplied by 2.22 for the foot-pound-second system of units), and that a plot of $h^{1/3}$ versus h for $0 \leq h \leq h_s$ will give an average value of $h = 0.75\, h_s$. It is proposed equation (314) can then be written

$$C_h^2 = \frac{0.91\, h_s^{1/3}}{n^2} \tag{315}$$

in metric units. This allows equation (310) to be rewritten as

$$\frac{R}{h_s} = \frac{1}{2A^2} \frac{(1 + A)(1 + 2A)}{1 + \dfrac{8gn^2}{0.91\, A^2 S\, h_s^{1/3}}} \tag{316}$$

in metric units (the coefficient 0.91 on the right side is equal to 2.02 in the foot-pound-second system of units). Kishi and Saeki give a log-log plot for A versus S, with A = 0.25 when S = 0.03, and A = 0.04 when S = 0.07. Values of A were only obtained for that range of slopes. Also, the effect of wave period on the results was apparently not investigated.

Camfield and Street's (1967) laboratory results for borelike solitary waves running up a 4° slope (S = 0.0699), fronted by a slope S = 0.01, give a total relative runup R/H_s of 3.3 for a value of $h_s = 0.061$ meter (0.2 foot) on a smooth aluminum slope. Using a value of n = 0.01 in equation (316), and using a value of A = 0.4 suggested by Kishi and Saeki (1966), R/h_s would have a calculated value of 2.67, which is close to the measured value. Kishi and Saeki obtain similar results for rough slopes. As previously mentioned, the runup values of Camfield and Street (1967) include a shallow flooding which may not be an accurate prediction of prototype conditions. If only the greater water depths were considered, such as shown in Figure 53, then the measured value of $R/h_s \simeq 1.0$.

It should be noted that the above equations assume a uniform slope. For runup on a shoreline where the slope varies, it would be necessary to use a numerical solution to determine the limits of the runup. Freeman and Le Mehaute have carried out numerical calculations for slopes $S \geq 0.1$, but present no results for very flat slopes. Very little data exist to verify such equations or to determine their full range of application.

The solution of equation (316) is very dependent on a correct choice of the roughness coefficient. Only very limited data are presently available for estimating values of the roughness coefficient n. For prototype conditions, the "roughness" may consist of groves of trees or subdivisions of houses. Also, the roughness elements, e.g., trees and houses, may be moved by the waves.

Bretschneider and Wybro (1976) investigated the effect of bottom friction on tsunami inundation by using the Manning n to describe the roughness of the onshore slope. Although this is not entirely correct (the Manning relationship was developed for uniform flow), it provides a simple means of investigating the effects of roughness on the limits of inundation. It was shown that decreasing the Manning roughness coefficient, n, from n = 0.025 (long grass with brush) to n = 0.015 (short, cut grass and pavement) could increase the distance required for dissipation of the surge by 160 percent (from 670 to 1,770 meters or 2,200 to 5,800 feet in the example used, where h_s = 10 meters or 33 feet). Bretschneider and Wybro also demonstrated that a bore would be dissipated faster than a tsunami acting as a rapidly rising tide.

Chan, Street, and Strelkoff (1969) and Chan and Street (1970a, 1970b) use a modified Marker and Cell (SUMMAC) numerical finite-difference technique for calculating the wave runup of solitary waves on a 45° slope and on a vertical wall. Their results compared well with the experimental results of Street and Camfield (1966), but their numerical method was not applied to wave runup on the shoreline for flatter slopes. Heitner (1969) developed a numerical method based on finite elements. However, he provides only limited results for simulating waves in laboratory channels, and the results depend on the choice of a bottom-friction factor and an artificial viscosity.

Spielvogel (1975) developed a theoretical solution for tsunami runup based on the wave or surge height at the shoreline, h_s, and the wave height, $\hat{H}$, at the point where the leading edge of the wave is at the shoreline. This relates the runup to the rate of shoaling just before the wave reaches the shoreline, and effectively includes the influence of the bottom slope and the wave period. Replotting Spielvogel's results into a more usable form gives the equation

$$\frac{R}{h_s} = \frac{2.94}{\frac{h_s}{\hat{H}} - 0.8} \qquad (317)$$

Equation (317) indicates that the higher values of relative runup, R/h_s, occur when the values of $h_s/\hat{H}$ are the lowest. Spielvogel indicates that equation (317) is correct for $3.74 > h_s/\hat{H} > 2.12$, has limited application where $2.12 > h_s/\hat{H} > 1.76$, and is invalid where $h_s/\hat{H} < 1.76$. This latter, invalid case would be a nearshore bore or breaking wave.

In addition to considering wave runup, it is necessary to consider the drawdown of the water when the wave trough arrives at the shoreline.

Not as much attention has been given to wave rundown; however, the drawdown of the water level may result in the seaward collapse of seawalls, result in damage to ships in a harbor, or expose seawater-intake pipelines. It should also be noted that a gradual increase in water level, with very low velocity currents, may be followed by a sudden withdrawal of water producing very strong currents.

During the 1946 tsunami in Hawaii, waves at Hanamaulu Bay rose 2.7 meters at a breakwater and wharf, but the water receded to a level 5.6 meters below normal sea level between waves (Shepard, MacDonald, and Cox, 1950). Most of the damage was caused by the violent withdrawal of the water.

The rundown elevations will depend on the wave train generated at the tsunami source. For the 1946 tsunami, the tide gage record at Honolulu, Hawaii, indicated some very narrow, deep wave troughs with the initial troughs having greater amplitudes than the initial crests.

Consideration must also be given to the current velocities of the runup. Ishimoto and Hagiwara (1934) investigated the large 1933 tsunami at Kamaisi, Japan, and estimated current velocities with a maximum value of 1 meter per second. Houston and Garcia (1974) estimated that small tsunamis in southern California acting as rapidly rising tides would have maximum current velocities of about 0.5 meter per second. The current velocity for the 1933 tsunami, which was about double the velocity estimated by Houston and Garcia for small tsunamis, destroyed some buildings when the water depth reached a height of 2 meters (6.15 feet).

Water overflowing a coastal barrier will have a current velocity determined by the difference in height between the top of the barrier and the ground level behind the barrier, as well as the quantity of water overtopping the barrier, rather than acting like a rapidly rising tide. The barrier will also limit the height of the runup; however, large drain openings must be provided to prevent water levels from building up behind the barrier if it is overtopped by successive waves. Magoon (1965) cites one example south of Crescent City, California, during the 1964 tsunami where water flowed over narrow coastal dunes. The quantity of water overflowing the dunes was insufficient in some instances to fill the low areas to landward, reducing the resulting runup height.

Where the slope is very long compared to the wavelength, and friction effects must be considered, it can be seen that for low velocities the retarding effect of the slope roughness (deceleration) may prevent the water from rising to a runup height equal to the wave height at the shoreline (i.e., drawdown will start at the shoreline, reversing the direction of flow). As previously noted, the currents associated with the rundown might have much higher velocities than the currents associated with the runup. No estimates are available for the rundown currents.

Surge runup on a dry bed will have a much higher velocity than the values given by Houston and Garcia (1974) for a tsunami which acts like a rapidly rising tide. Keulegan (1950) gives

$$u = 2(gh)^{1/2} \tag{318}$$

where h is the surge height at any point and u the water velocity at the same point. Fukui, et al. (1963) give a lower value of velocity as

$$u = 1.83(gh)^{1/2} \tag{319}$$

The higher value would be conservative.

2. Interaction with Shore Protection Structures.

Breakwaters and seawalls may provide coastal areas protection from tsunamis. When a tsunami occurs, breakwaters may decrease the volume of water flowing into a harbor and onto the coastline. Proper placement of breakwaters may also decrease wave heights by changing the natural period of an inlet discussed in Section VI, 7. However, breakwaters may also affect the resonant period of a harbor so that wave heights are increased, and seawalls may reflect waves within a harbor. A high seawall along a coastline may prevent flooding of the backshore areas.

A tsunami may damage shore protection structures; therefore, care must be exercised in the design of the structures. Numerous instances of tsunamis damaging or destroying protective structures have been recorded. The 1946 tsunami in Hawaii overtopped and breached the breakwater at Hilo, removing 7.25-metric ton (8 tons) stones to a depth 0.9 meter (3 feet) below the water surface along nine sections of the breakwater crest with a total length of over 1,800 meters (6,000 feet) (U.S. Army Engineer District, Honolulu, 1960). Matuo (1934) refers to the case of an earthern embankment at Yosihama on the northeast coast of Honshu, Japan, which had been constructed to protect a section of coastline. The 1933 Sanriku tsunami overtopped the embankment, and it was swept away, flush with the original ground level.

Iwasaki and Horikawa (1960) investigated areas along the northeast coast of Honshu after the 1960 tsunami. They indicated that a sea dike at Kesennuma Bay failed during the 1960 tsunami because the water from the incident waves, which had overtopped the dike, caused extensive erosion receding at a gap in the dike. The receding water gradually widened the gap. They also noted that a quay wall at Ofunato failed because of scouring of the backfilling, and that a quay wall constructed of reinforced concrete sheet piles at Hachinohe collapsed due to a lack of interlocking strength after backfilling was washed away.

Iwasaki and Horikawa also indicated that receding water may seriously scour the seaward base of a revetment or seawall. The combination of this

scouring and the increased hydrostatic pressure from initial overtopping may cause failure. The concrete seawall along a highway between Hadenya and Mitobe on Shizukawa Bay (Fig. 54) collapsed seaward. Similar failures occurred along a highway on Onagawa Bay and along a quay wall at Kamaishi, Japan. Magoon (1962) noted that approximately 2 meters of sand was scoured at the seaward toe of a steel sheet-pile retaining wall at Crescent City, California, in 1960 which contributed to its partial failure. Also, a woodpile-mooring dolphin was destroyed as a result of the loss of sand at its base. Matuo (1934) mentions a concrete retaining wall which was overturned seaward by the 1933 Sanriku tsunami.

The damage from the 1960 tsunami in Hawaii is evidence of the erosive force of a tsunami. Concrete seawalls 0.9 meter high were washed out and a gully about 3 meters deep and 27 meters wide was washed into a highway along the shoreline at Hilo, extending inland about 18 meters. Large stones from a seawall, weighing up to 20 metric tons (22 tons), were carried inland (Eaton, Richter, and Ault, 1961). Shepard, MacDonald, and Cox (1950) mention a case where water overtopping sand dunes cut a channel about 30 meters wide and about 5 meters (15 feet) deep.

Tsunamis will not always produce the maximum forces on a structure. A concrete seawall protected the buildings at the Puu Maile Hospital at Hilo during the 1946 tsunami. The seawall was undamaged by the tsunami, but a few months later storm waves destroyed parts of the wall and damaged the lower floor of the hospital (Shepard, MacDonald, and Cox, 1950).

Matuo (1934) reports on a dynamometer located on a breakwater at Hatinohe harbor, Japan, during the 1933 Sanriku tsunami. The dynamometer was located 0.76 meter (2.5 feet) below the level of the water surface at the time of arrival of the tsunami. The recorded maximum pressure was 38,300 newtons per square meter (800 pounds per square foot) for a wave with a height of 3.2 meters (10.5 feet) and a period of 6 minutes.

Nasu (1948) developed some empirical criteria for the stability of breakwaters based on the geometric shape of the breakwater. For a breakwater with a seaward slope of 1:2.5 and a landward slope of 1:2, he gives

$$u^2 < \frac{h_v + 0.89b}{0.0358} \tag{320}$$

for the condition of geometric stability, where u is the current velocity in meters per second, h_v the height in meters of the vertical segment of the face of the breakwater against which the current acts, and b the top width of the breakwater in meters.

Kaplan (1955) gives an empirical equation for the volume of overtopping of a seawall at the shoreline. This equation can be rewritten as

$$V = \frac{21.65(Kh_s - h_w)^3}{K^2 h_s} \tag{321}$$

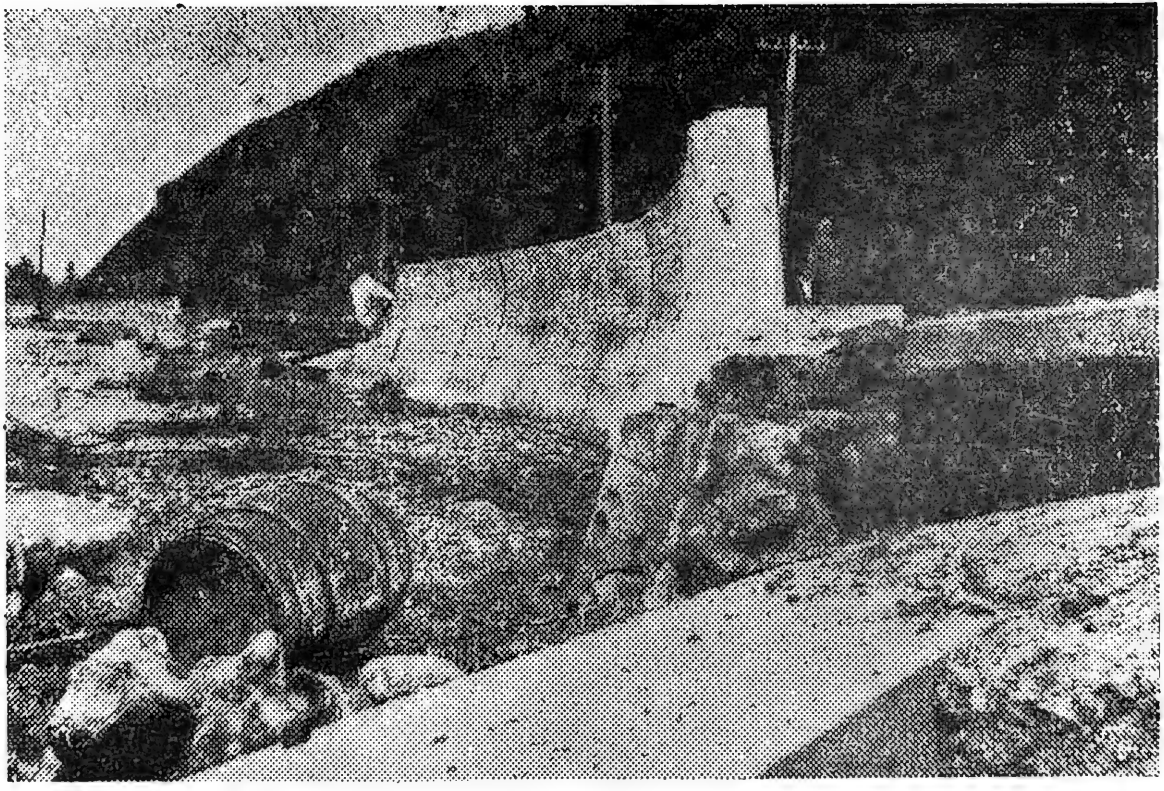

Figure 54. Concrete seawall destroyed by 1960 tsunami, Shizukawa Bay, Japan (from Iwasaki and Horikawa, 1960).

where V is the quantity of water overtopping the wall in cubic meters per meter or cubic feet per foot length of wall, h_s the wave height at the shoreline in meters or feet, h_w the wall height in meters or feet, and

$$K = \frac{R}{h_s} \tag{322}$$

where R would be the vertical height of wave runup on a similar wall high enough to prevent overtopping.

Wiegel (1970) gives the following empirical equation for overtopping volume in cubic meters per meter length of wall

$$V = 0.287 \int_{t_1}^{t_2} \left(\frac{1}{2} h_s \cos \frac{2\pi t}{T} - h_w\right)^{3/2} dt \tag{323}$$

where h_s is the total wave height in meters (crest-to-trough) of the wave at the shoreline, T the wave period, t_1 the point in time where overtopping begins, and t_2 the time when overtopping ends. As the wall height, h_w, is measured in meters from the sea level at the time the tsunami occurs, it varies but its lowest value (i.e., the greatest overtopping) would occur when the sea level is at the highest tidal stage. Values for overtopping are shown in Figure 55.

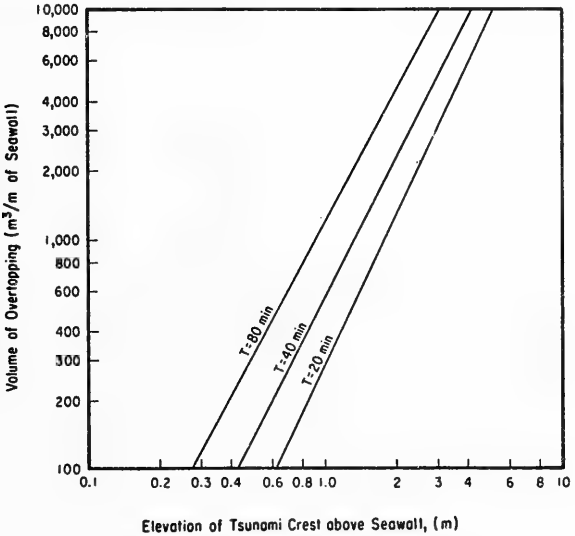

Figure 55. Overtopping volumes (after Wiegel, 1970).

Based on stability tests carried out in a hydraulic model, Kamel (1967) developed suggested breakwater sections for Hilo, Hawaii (Figs. 56 and 57). Allowable overtopping heights are given in Table 5.

Table 5. Allowable overtopping heights (after Kamel, 1967).

	Allowable height of overtopping (m)	
Slope of harborside of barrier	9.1-metric ton Armor stones	18.2-metric ton Armor stones
1:2	0.3	1.0
1:2.5	0.8	1.2
1:3	1.3	1.5
1:3.5	1.6	
1:4	2.0	
1:4.5	2.3	
1:5	2.4	
1:6	2.7	
1:7	2.9	

Iwasaki and Horikawa (1960) show typical cross sections of seawalls at locations on the northeast coast of Honshu (see Fig. 58). In some instances, such as in fishing ports or harbor areas, it is undesirable to have high seawalls directly on the waterfront. The seawall at Yamada (Fig. 59) is in two stages. A low seawall along the waterfront allows access to the water; a higher seawall, set back from the shoreline, protects the town from higher waves. Figures 58 and 59 show that the seaward toe of a wall is protected by rubble to deter scouring. Also, the area behind the top of the shoreline wall, such as at Yamada, is paved to prevent saturation and erosion of the backfill material.

The protection provided by a breakwater depends on its location and the width of the navigation channel through the breakwater. Iwasaki, Miura, and Terada (1961) ran model tests for breakwaters in Kesennuma Bay. They discovered that a breakwater at the mouth of the bay would substantially reduce wave heights in the bay for all wave periods tested. As expected, the greatest reduction in wave height occurred when the area of the breakwater opening was the least. When the ratio of the breakwater opening area to the cross-sectional area of the bay was equal to about 0.1, the wave height was reduced to about 0.25 times the height which would occur without the breakwater. Surprisingly, when the breakwater was moved to the mouth of Kesennuma harbor in the model, at the inner end of the bay, the breakwater had almost no effect in reducing wave heights. The location of the breakwater would be expected to affect the resonant periods of the bay and the harbor. Therefore, care should be exercised in placing a breakwater in any bay or harbor.

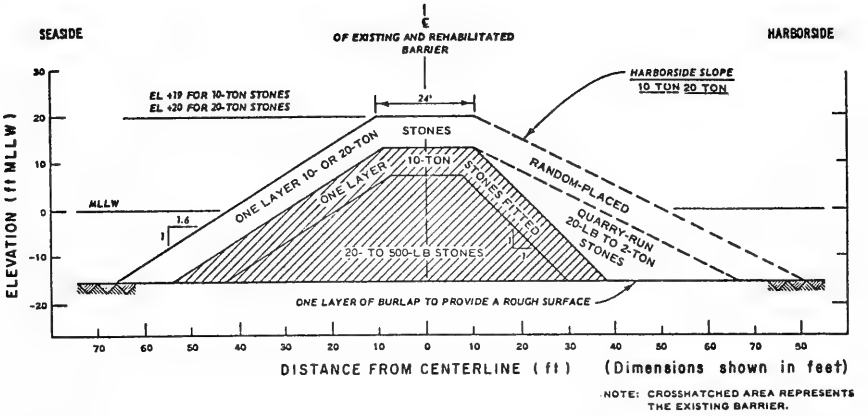

Figure 56. Suggested design for rehabilitated breakwater, Hilo, Hawaii (from Kamel, 1967).

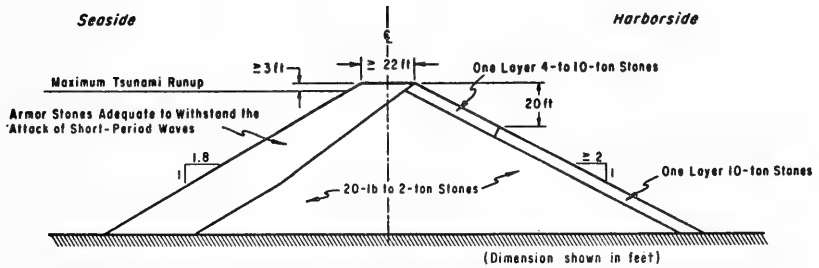

Figure 57. Suggested design, typical nonovertopping barrier section, Hilo, Hawaii (from Kamel, 1967).

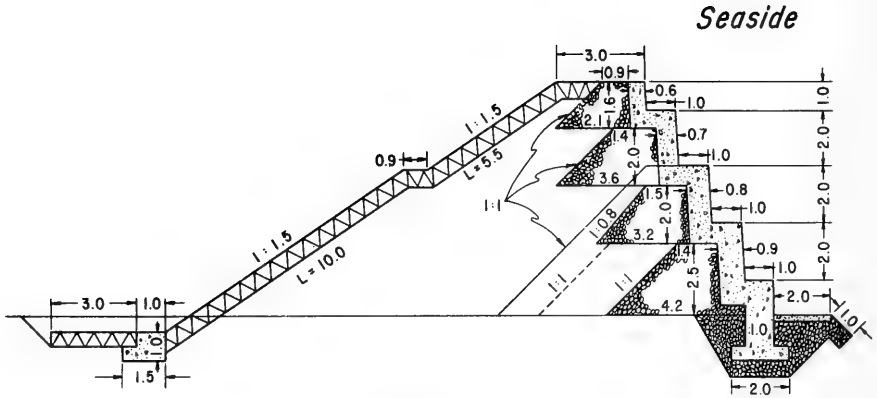

a. Seawall at Taro

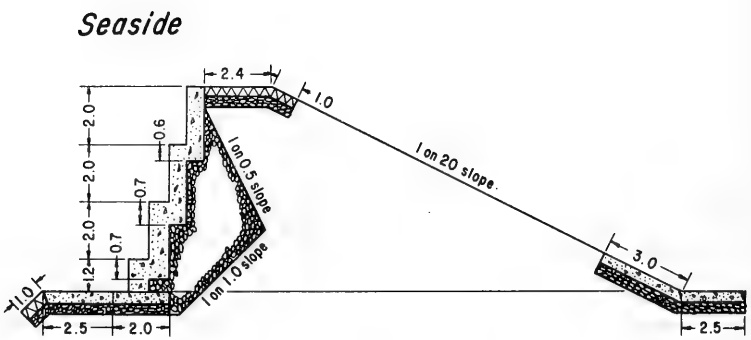

b. Seawall at Yoshihama

Figure 58. Seawall cross sections (from Iwasaki and Horikawa, 1960). Dimensions in meters.

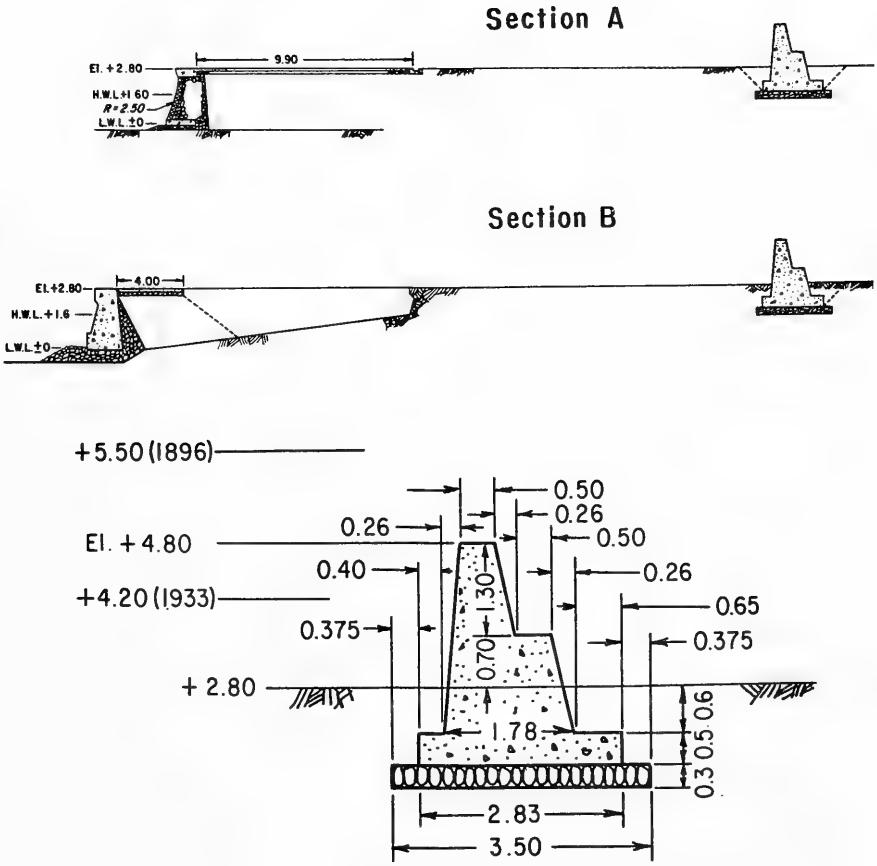

Figure 59. Cross sections of seawall, Yamada, Japan (from Iwasaki and Horikawa, 1960). Dimensions in meters.

Caution is also necessary when placing seawalls in a harbor area. A seawall may cause waves to reflect into the harbor. It was determined at Hilo, Hawaii, that a seawall might aggravate surge conditions within the harbor (U.S. Army Engineer District, Honolulu, 1960).

In some instances, trees may offer some protection against a tsunami surge. Groves of trees alone or as supplements to shore protection structures may dissipate tsunami energy and reduce surge heights. Groves of coconut palms (Fig. 60) may withstand a tsunami surge but may be sheared off by debris carried forward by the tsunami. Other types of trees may be easily uprooted and flattened. Figure 61 shows a grove of pandanus

Figure 60. Coconut palms near shoreline, Hilo, Hawaii (from Matlock, Reese, and Matlock, 1962).

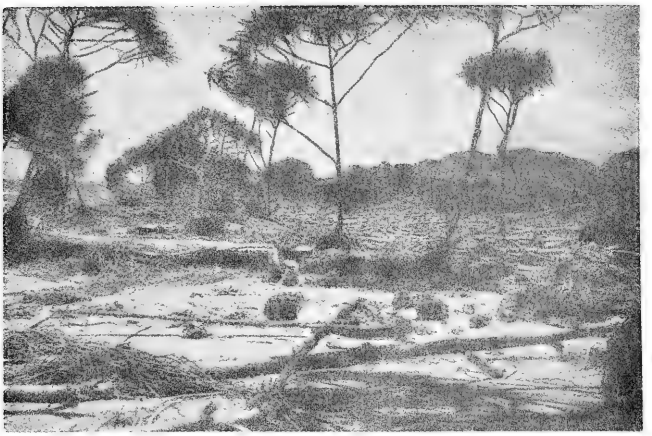

Figure 61. Grove of pandanus trees knocked down by 1946 tsunami on the Island of Kauai, Hawaii (from Shepard, MacDonald, and Cox, 1950).

trees which were knocked over in parallel rows by the 1946 tsunami in Hawaii (Shephard, MacDonald, and Cox, 1950). Reid and Taber (1919) noted that palm trees were uprooted by the 1918 Puerto Rico tsunami. Shepard, MacDonald, and Cox (1950) indicated that dense thickets of hau trees provided effective shields in many places during the 1946 tsunami in Hawaii.

Matuo (1934) calculated that trees could be broken by water velocities of 2 meters per second or greater, but did not analyze specific types of trees. He indicated that trees broken off by higher velocities may add debris to the surge and increase the damages resulting from the surge. Magoon (1965) indicates that a buildup of debris in front of a structure may increase its effective area. This would result in an increased drag force, and may cause the entire structure to be swept away by the tsunami.

3. Other Shoreline Structures.

Damage from a tsunami may occur to structures located at the shoreline or along river channels near the shoreline. In 1964, a dock at Crescent City, California (Fig. 62), was damaged when the water elevation increased to 2 meters above the deck elevation, uplifting a large lumber barge moored to the dock (Wilson and Tørum, 1968). The tsunami surge at Seaside, Oregon, destroyed a bridge over the Necanicum River and a railroad trestle over Neawanna Creek. Shepard, MacDonald, and Cox (1950)

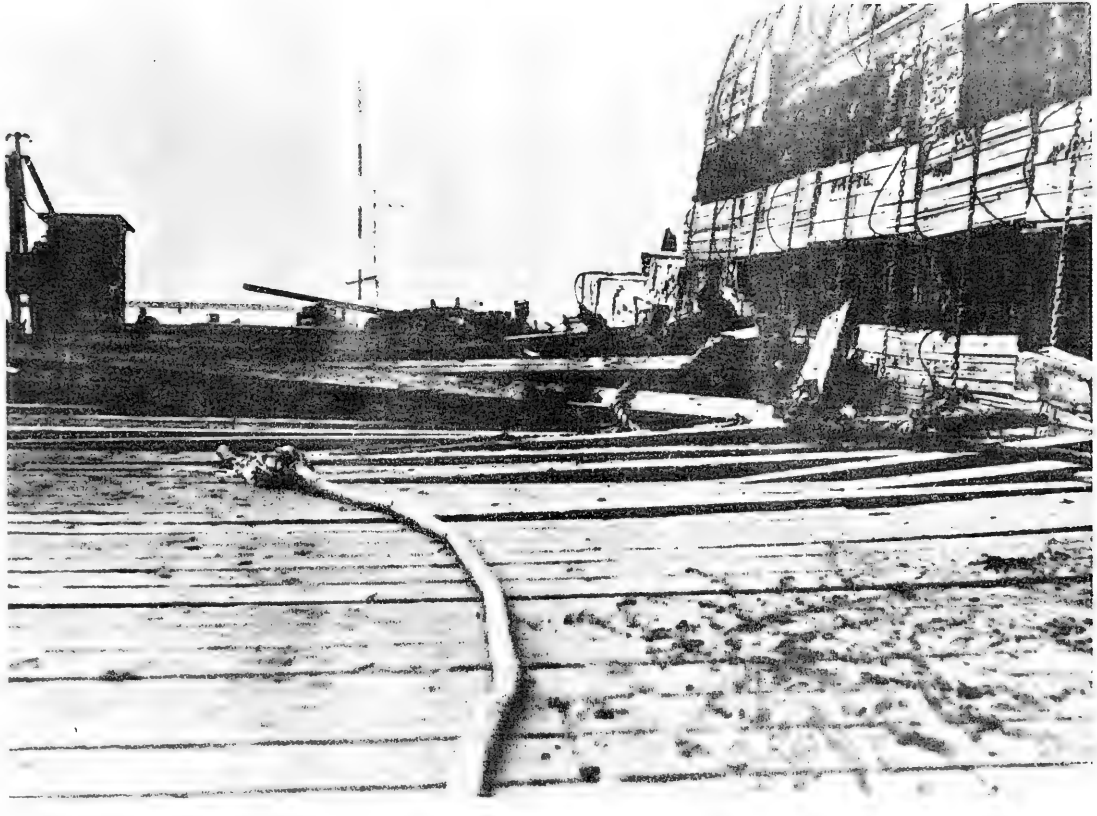

Figure 62. Dock damaged by 1964 tsunami at Crescent City, California (photo by U.S. Coast Guard).

illustrate the damage to the railroad bridge on the Wailuku River (Fig. 63) and the railroad trestle on Kilekole Stream (Fig. 64) caused by the 1946 tsunami in Hawaii. Iwasaki and Horikawa (1960) show a case of Mangoku, Japan, where a bridge support (Fig. 65) slumped almost 1 meter due to the heavy scouring of the channel bottom.

4. Tsunami Surge on the Shoreline.

The determination of the runup height of a tsunami is discussed in Section VII, 1. After the runup height of a tsunami has been established, the effects of this runup on structures and other objects located near the shoreline must be determined. When the tsunami acts as a rapidly rising tide, the resulting incident current velocities are relatively low, and most initial damage will result from buoyant and hydrostatic forces and the effects of flooding. Shepard, MacDonald, and Cox (1950) noted that in many instances the withdrawal of the water occurred much more rapidly than the runup and flooding. In some instances, damage may result from the higher current velocities associated with the withdrawal. These velocities would be on the order of those normally associated with an incident surge. More concern is therefore given to a tsunami which approaches the shoreline as a bore.

When the tsunami forms a borelike wave, the runup on the shoreline has the form of a surge on dry ground. *This surge should not be confused with the bore approaching the shoreline, as different equations govern the motion and profile of the surge.* Miller (1968) noted from laboratory observations that a bore approaching a shoreline exhibits a relative steepening of the bore face just before reaching the shoreline, and that this is followed by a flattening of the face of the surge on the dry slope. The current velocities associated with the surge are proportional to the square root of the surge height, and approximations of the current velocities can be obtained from equations (318) and (319), with equation (318) providing the more conservative result. For a surge height approaching 5 meters, the estimated current velocity would be about 14 meters (46 feet) per second. When the tsunami runup acts as a high velocity surge

Figure 63. Tsunami damage to railroad bridge on Wailuku River, Hilo, Hawaii (photo by Shigeru Ushijima; from Shepard, MacDonald, and Cox, 1950).

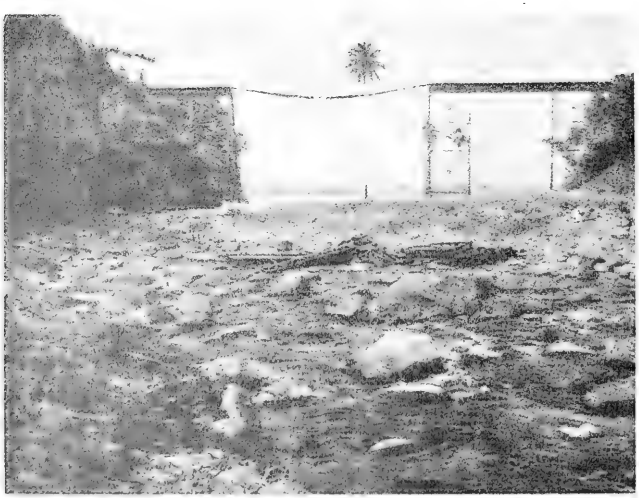

Figure 64. Tsunami damage to railroad trestle on Kolekole Stream, Island of Hawaii (from Shepard, MacDonald, and Cox, 1950).

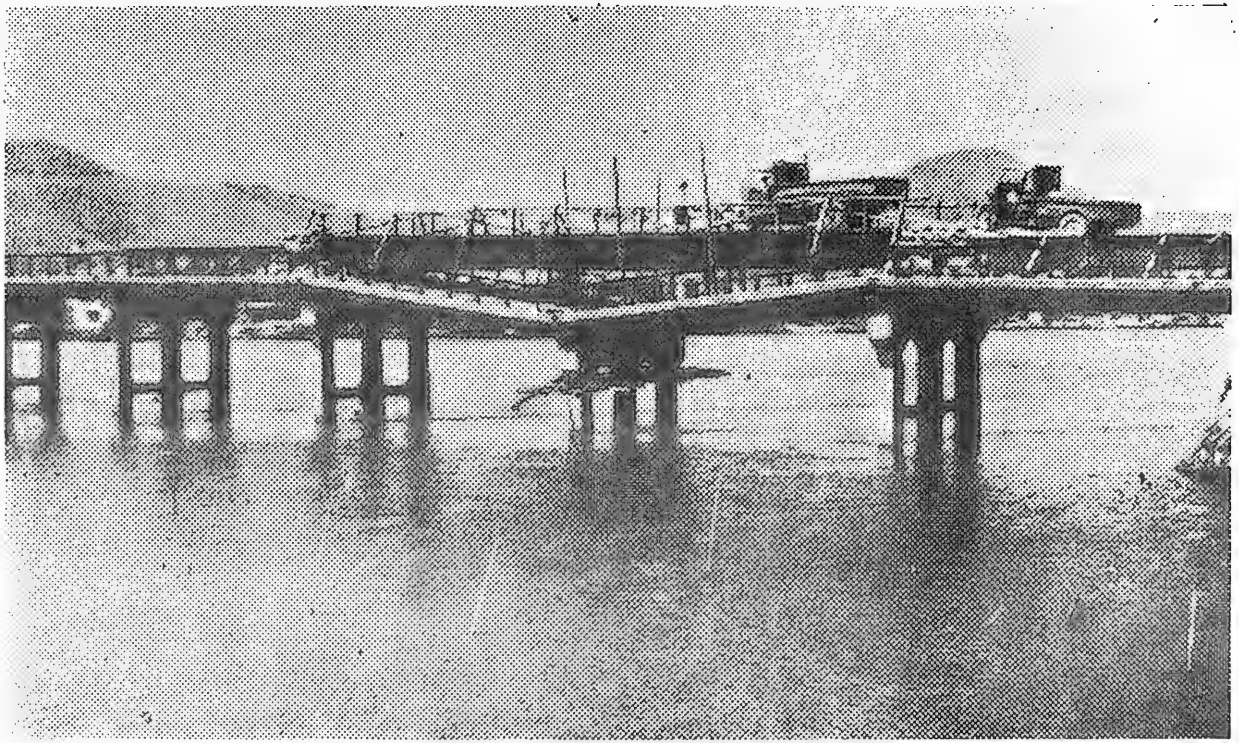

Figure 65. Bridge damaged by 1960 tsunami at Mangoku, Japan (from Iwasaki and Horikawa, 1960).

of water across the ground, five types of forces may result from the surging water:

(a) Buoyant forces caused by partial or total submergence in the surging water. When water or water pressure intrudes under a structure, the buoyant force tends to lift the structure from its foundations. Vehicles and other large items may also be lifted up into the surging water.

(b) Surge forces caused by the leading edge of the surge impinging on a structure. This leading edge has the appearance of an elongated wedge, and the force of the surge on a structure gradually increases as a function of the increase in surge height. The buoyant force also increases as a function of surge height, so that a structure may be carried forward by the leading edge of the surge, or may be destroyed in place if the surge force is high enough and the buoyant force is not sufficient to lift the structure from its foundations.

(c) Drag forces caused by the high velocity of the surging water, where the water level is relatively constant. These forces will displace buildings or other items in the direction of the current, and the high velocity flow may cause severe erosion of the ground and damage waterfront structures by scouring material at the base of the structure.

(d) Impact forces caused by buildings, boats, or other material carried forward by the surging water. These forces may either destroy other structures on impact or create momentum which, when added to other forces, will move a structure in the direction of the current.

(e) Hydrostatic forces caused by partial or total submergence of structures by the tsunami. This can result in cracking or collapse of a structure or wall.

a. Buoyant Forces. Buoyant forces are defined by the weight of the displaced water when objects are partially or totally submerged. For saltwater, taking the density ρ = 1.026 grams per cubic centimeter (1.99 pound-seconds squared per foot^4), the buoyant force is

$$F_B = \rho g \, V \qquad (324)$$

where V is the displaced volume of water. This assumes water intrudes under the structure.

* * * * * * * * * * * * * * EXAMPLE PROBLEM 21 * * * * * * * * * * * * * * *

GIVEN: A house occupies a floor area of 225 square meters (2,422 square feet). Calculations to predict tsunami runup have indicated a probable surge depth of 2 meters at that location. It is assumed that the flow of water will be at a constant depth around the house.

FIND: The buoyant force on the house.

SOLUTION: The buoyant force is given by

$$F_B = \rho g V$$

F_B = 1,026 kilograms per cubic meter (9.81 meters per second squared) (225 square meters) (2 meters)

$$F_B = 4.53 \times 10^6 \text{ kilogram-meters per second squared}$$

$$F_B = 4.53 \times 10^6 \text{ newtons } (1.02 \times 10^6 \text{ pounds})$$

* *

* * * * * * * * * * * * * * EXAMPLE PROBLEM 22 * * * * * * * * * * * * * *

GIVEN: An empty oil storage tank is 3 meters high and 6.1 meters in diameter. Assume that the tank has a mass of 3,180 kilograms (7,000 pound-mass), and that it is filled to a depth of 2.5 meters (8.2 feet) with oil having a specific gravity of 0.88 (density ρ = 880 kilograms per cubic meter). The tsunami water depth is 1.8 meters.

FIND:

(a) The buoyant force on the tank, and

(b) the force holding the tank in place.

SOLUTION:

(a) The buoyant force is given by

$$F_B = \rho g V$$

$$F_B = 1{,}026(9.81)\left(\frac{\pi}{4}\right)(6.1)^2(1.8)$$

$$= 5.29 \times 10^5 \text{ kilogram-meters per second squared}$$

$$F_B = 5.29 \times 10^5 \text{ newtons } (1.19 \times 10^5 \text{ pounds})$$

(b) The force holding the tank in place is the mass, M, of the empty tank multiplied by g plus the volume of oil multiplied by its density and g, so that

$$F = 3{,}180(9.81) + 880(9.81)\left(\frac{\pi}{4}\right)(6.1)^2(2.5)$$

$$F = 6.62 \times 10^5 \text{ newtons } (1.49 \times 10^5 \text{ pounds})$$

It can be seen that very little reserve force remains to resist drag forces from the surge. With a lower level of oil in the tank, the buoyant force could overcome the mass of the tank and the oil plus the strength of any structural anchorages.

* *

In Shepard, MacDonald, and Cox's (1950) discussion of the 1946 tsunami in Hawaii, a house at Kawela Bay on Oahu was floated off its foundation and deposited in a canefield 61 meters inland, leaving breakfast cooking on the stove and dishes intact on shelves. Many other houses were also gently floated from their foundations, and some houses could be moved back to their original foundations with very little repair work required. Damage caused by buoyant forces was the result of buildings being deposited on uneven ground, the fact that some buildings had weak structures and broke apart when lifted from their foundations, and minor damage from the breaking of water pipes and electric lines.

In many instances, where tsunamis act like rapidly rising tides, the current velocity associated with the waves is very low, so that the major damages are similar to those discussed above. Shepard, MacDonald, and Cox (1950) mentioned instances of people wading through chest-high water to escape from the tsunami.

b. Surge Forces. Cross (1967) showed that the force per unit length of vertical wall, from the leading edge of a surge impinging normally to the wall could be given as

$$F = \frac{\rho g h^2}{2} + C_F \rho u^2 h \tag{325}$$

where F is the force in newtons per meter of width, h the surge height in meters, u the surge velocity in meters per second, and C_F a force coefficient defined by

$$C_F = (\tan \theta)^{1.2} + 1 \tag{326}$$

where θ is the inclination of the water surface of the surge shown in Figure 66; $\tan \theta$ is given by the equation

$$\tan \theta = \frac{dh}{dz} = \frac{u^2}{C_h^2 h} + b \tag{327}$$

where C_h is the Chezy roughness coefficient, Z the distance from the leading edge, and b given by

$$b = \frac{1}{g} \frac{du}{dt} - S \tag{328}$$

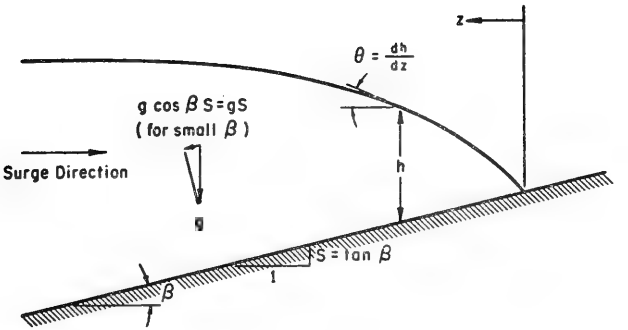

Figure 66. Definition sketch of surge on a dry bed (slope exaggerated).

where S is the bottom slope (negative upward), and du/dt the acceleration term for flow under the tip of the surge.

Substituting equations (326), (327), and (328) into equation (325)

$$F = \frac{1}{2}\rho g h^2 + \left[\left(\frac{u^2}{C_h^2 h} + \frac{1}{g}\frac{du}{dt} - S\right)^{1.2} + 1\right]\rho u^2 h \qquad (329)$$

If it is assumed that

$$\frac{du}{dt} = gS \qquad (330)$$

i.e., the acceleration is equal to the influence of gravity acting along the slope (see Fig. 66), then b = 0 and

$$\frac{dh}{dz} = \frac{u^2}{C_h^2 h} \qquad (331)$$

or, defining u from equation (318) and assuming that the value is relatively constant under the surge

$$\frac{u^2}{C_h^2 h} = \frac{dh}{dz} = \frac{4g}{C_h^2} \qquad (332)$$

where C_h varies with depth and is given by

$$C_h = \frac{1.49}{n} h^{1/6} \qquad (333)$$

in the foot-pound-second system of units, or

$$C_h = \frac{h^{1/6}}{n} \tag{334}$$

in the meter-kilogram-second system of units, and n is Manning's roughness coefficient.

Substituting equations (330), (332), and (334) into equation (329) for metric units and collecting terms

$$F = \frac{1}{2}\rho g h^2 + \left[\left(\frac{4gn^2}{h^{1/3}}\right)^{1.2} + 1\right]\rho u^2 h \tag{335}$$

It must be remembered that many approximations have been used in this solution.

The coefficient C_F accounts for both inertial forces and drag forces. It may be noted that when $\theta = 0$, and the velocity remains constant, the force F is simply the hydrostatic force plus a drag force (per meter width) where $C_D = 2$.

* * * * * * * * * * * * * EXAMPLE PROBLEM 23 * * * * * * * * * * * * *

GIVEN: A surge with a maximum height of 2.5 meters impacts normally against the vertical side of a building. The Manning roughness coefficient n = 0.1, and it is assumed that the surge velocity, $u = 2\sqrt{gh}$, remains relatively constant and that the surge profile remains constant.

FIND: The surge force per meter of building width as a function of surge height.

SOLUTION: The surge velocity is determined from the maximum surge height, so that

$$u = 2\sqrt{gh} = 2\sqrt{9.81(2.5)} = 9.9 \text{ meters per second}$$

The surge force is given by equation (335) as

$$F = \frac{1}{2}\rho g h^2 + \left[\left(\frac{4gn^2}{h^{1/3}}\right)^{1.2} + 1\right]\rho u^2 h$$

$$F = \frac{1}{2}(1{,}026)(9.81)h^2 + \left[\left(\frac{4(9.81)(0.1)^2}{h^{1/3}}\right)^{1.2} + 1\right] 1{,}026(9.9)^2\, h$$

$$F = 5{,}033\, h^2 + \left[\left(\frac{0.392}{h^{1/3}}\right)^{1/2} + 1\right] 100{,}560\, h$$

For various values of h, the force, F, is tabulated below:

h, meters	0.5	1.0	1.5	2.0	2.5
F, newtons per meter	73,100	138,300	203,900	270,800	339,500

NOTE:--Calculations will show that $C_F > 1$ at the maximum surge height (where the rate of change of surge height $\rightarrow 0$). This indicates that the calculated value is conservative for design purposes. It can be seen that the hydrostatic pressure component of the force is a relatively small part of the total force.

* *

As indicated by example problem 23 and shown in Figure 66, there is a gradual rise in water level at the front of the surge, although this change in water level appears to occur rapidly with respect to time because of the forward velocity of the surge. A surge on a dry bed has a much flatter front than a bore approaching a shoreline. This is seen in laboratory tests. The buoyant force of the leading edge of the surge tends to lift objects into the surging water, and the force of the surge will then carry these objects forward.

Wilson and Tørum (1968) report on the case at Seward, Alaska, of a tsunami surge overtaking a pickup truck being driven from the shoreline. The truck was swept up by the surge and carried forward like a surfboard into nearby woods.

The water velocity near the leading edge of a surge is relatively high, and the height of the leading edge is relatively low (i.e., the buoyant force is low). Therefore, it is possible that the surge force may destroy a structure before the buoyant force lifts it into the flow.

c. Drag Forces. The velocity of the water in the surge produced by the tsunami runup creates a drag force which tends to move a structure in the direction of the surge. If the velocity is assumed to remain relatively constant under the surge, i.e., acceleration is negligible and its effects can be ignored, then it can be assumed that the inertia or mass coefficient, C_M, approaches zero so that the drag force in newtons is

$$F_D = \rho \cdot C_D \, A \, \frac{u^2}{2} \qquad (336)$$

where

ρ = the density of seawater = 1.026 grams per cubic centimeter = 1,026 kilograms per cubic meter

C_D = a coefficient of drag, depending on the body (Table 6)

A = the projected area of the body normal to the direction of flow in square meters

u = the velocity of the water in meters per second

Table 6. Drag coefficients.

Object	L/d	Reynolds number	C_D
Circular cylinder 	1	10^5	0.63
	5	10^5	0.74
	∞	10^5	1.20
	∞	$>5 \times 10^5$	0.33
Square cylinder 	∞	3.5×10^4	2.0
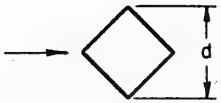	∞	10^4 to 10^5	1.6
Rectangular flat plate (totally submerged) 	1	$>10^3$	1.1
	5	$>10^3$	1.2
	20	$>10^3$	1.5
	∞	$>10^3$	2.0

NOTE.--L = The height of a submerged cylinder, or the length of the flat plate.

d = The projected dimension shown, or the width of the flat plate.

To determine the drag force in pounds, ρ is in units of pound-seconds per foot^4, the area in square feet, and the velocity in feet per second. The coefficient of drag, C_D, is dimensionless and retains the same value as in the kilogram-meter-second system.

Tabulated values of drag coefficients are generally not available for free-surface flow at high Reynolds numbers. Therefore, existing tables of drag coefficients must be used to establish maximum coefficients to ensure safe design. Table 6 gives examples of drag coefficients.

Hallermeier (1976) discusses the importance of the parameter, $u^2/(gd)$, where d is the projected horizontal dimension of the structure transverse to the direction of flow. Where this parameter approaches unity there are strong unidirectional free-surface flow effects. In that case, the coefficients of drag, C_D, given in Table 6 may be too low. Individual model tests would be required to determine a more exact interaction between the tsunami and the structure.

For cases where flow does not overtop a structure, and where there is no underflow, the flow may be treated as flow around an "infinitely long" structure where the ground and the free surface define the boundaries of a layer of fluid. For example, flow around a vertical cylindrical storage tank would be treated as flow around an infinitely long cylinder in order to obtain a drag coefficient.

In cases where there are overtopping and underflow, the ratio of length-to-width for the structure should be determined. This ratio should then be used for determining the coefficient of drag.

For a situation in which there is either *overflow or underflow*, the coefficient of drag can be determined by using an approximation. Assume that the depth of flow around the structure is twice the actual depth, and that the height of the structure is equal to twice the wetted height. Then obtain a coefficient of drag as if there were both underflow and overflow (see Fig. 67). An example of this type of calculation follows:

* * * * * * * * * * * * * EXAMPLE PROBLEM 24 * * * * * * * * * * * * * *

GIVEN: A flat-sided structure is 14 meters wide and normal to the direction of flow. The structure is 3.5 meters (11.5 feet) high and supported on columns so there is a 1.5-meter-high (4.9 feet) open space under the base of the structure. The tsunami surge has a depth of 2.5 meters, giving a wetted height on the structure equal to 1.0 meter (3.3 feet).

FIND:

(a) The coefficient of drag of the structure, and

(b) the coefficient of drag of a similar structure located at ground level with no underflow.

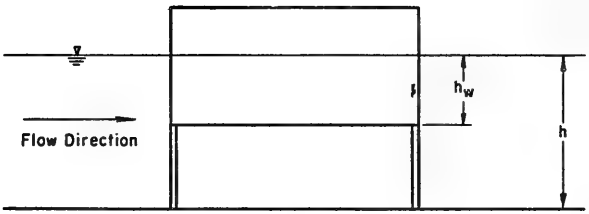

Tsunami surge flowing past elevated structure

h = surge height

h_w = wetted height on structure

L = length measured perpendicular to the sections shown above and below

L/d = L/(2h_w)

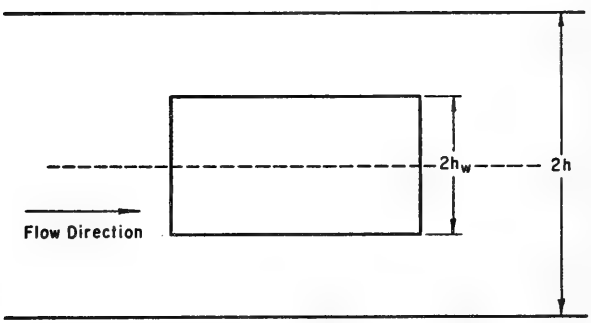

Equivalent body used for determining coefficient of Drag C_D
Flow is assumed symmetrical about the dashline

Figure 67. Determination of C_D when flow passes under a structure.

SOLUTION:

(a) It can be assumed, for purposes of determining the coefficient of drag, that the structure is equivalent to a structure 14 meters wide and 2.0 meters high with both underflow and overflow (Fig. 67). From Table 6, for a flat plate normal to the flow direction where L/d = 7, the coefficient of drag $C_D \simeq 1.25$.

(b) The structure is higher than the depth of flow so there would be neither underflow or overflow. This corresponds to an infinitely high structure where L/d = ∞. From Table 6, $C_D = 2.0$.

* *

* * * * * * * * * * * * * EXAMPLE PROBLEM 25 * * * * * * * * * * * * *

(This example is taken from an actual situation which occurred at Seward, Alaska, in 1964; see Wilson and Tørum, 1968.)

GIVEN: A 104.5-metric ton (230,000 pounds) railroad locomotive was overturned by a tsunami surge. The surge was assumed to have a depth of 1.83 meters. The clear space under the locomotive was approximately 0.91 meter (3 feet) and the length of the locomotive body was 12.5 meters (41 feet). The width between the rails was 1.52 meters (5 feet) and the width of the locomotive body was 3.05 meters (10 feet). The surge was assumed to act normal to the side of the locomotive.

FIND: The overturning force on the locomotive.

SOLUTION: The buoyant force is given by equation (324) as

$$F_B = \rho g V = 1{,}026(9.81)(1.83 - 0.91)(3.05)(12.5)$$

$$F_B = 3.53 \times 10^5 \text{ newtons } (78{,}700 \text{ pounds})$$

As indicated previously, the coefficient of drag can be determined by doubling the wetted height and assuming both underflow and overflow for a flat surface 1.83 meters high and 12.5 meters long. Interpolating in Table 6 for a flat plate for L/d = 6.8 gives

$$C_D = 1.24$$

The velocity can be obtained from equation (318), so for h = 1.83 meters

$$u = 2\sqrt{gh} = 2\sqrt{9.81(1.83)} = 8.47 \text{ meters per second}$$

From equation (336), the drag force is

$$F_D = \rho\, C_D\, A\, \frac{u^2}{2}$$

$$F_D = 1{,}026(1.24)(1.83 - 0.91)(12.5)\, \frac{(8.47)^2}{2}$$

$$F_D = 5.24 \times 10^5 \text{ newtons } (1.17 \times 10^5 \text{ pounds})$$

which will act against the side of the locomotive at a distance, Z, above the ground, given as

$$Z = 0.91 + \frac{(1.83 - 0.91)}{2}$$

$$Z = 1.37 \text{ meters } (4.5 \text{ feet})$$

The downward force from the mass of the locomotive is the mass, m, times gravitational acceleration, g, or

$$F = mg = 104{,}500 \text{ kilograms } (9.81 \text{ meters per second squared})$$

$$F = 1.025 \times 10^6 \text{ newtons } (2.3 \times 10^5 \text{ pounds})$$

Taking overturning moments about a rail, the center of mass of the locomotive is equidistant from the two rails, or 0.76 meter (2.5 feet) from the rail. The buoyancy and drag forces produce overturning moments (+) and the mass of the locomotive a restraining force (-). Summing moments

$$M = F_B(0.76) + F_D Z - F(0.76)$$

$$M = 3.53 \times 10^5(0.76) + 5.24 \times 10^5(1.37) - 1.025 \times 10^6(0.76)$$

$$M = 2.07 \times 10^5 \text{ newton-meters } (1.48 \times 10^5 \text{ foot-pounds})$$

indicating that the overturning moments are greater than the restraining moment. Therefore, the locomotive will be overturned.

* *

* * * * * * * * * * * * * * EXAMPLE PROBLEM 26 * * * * * * * * * * * * * *

GIVEN: A platform, 3 meters above ground level, is supported by square columns with 14- by 14-centimeter (5.5 by 5.5 inches) cross sections. A tsunami creates a surge with a depth of 2.44 meters (8 feet) under the platform. The surge acts normal to the sides of the columns, which are rigidly fixed at ground level.

FIND: The moment of the surge force about the base of a column.

SOLUTION: To determine the coefficient of drag, the columns may be considered as infinitely long columns, and from Table 6, $C_D = 2.0$. From equation (318)

$$u = 2\sqrt{gh} = 2\sqrt{9.81(2.44)} = 9.79 \text{ meters } (32.1 \text{ feet}) \text{ per second}$$

The drag force on a column is given by equation (336) as

$$F_D = \rho\, C_D\, A\, \frac{u^2}{2} = 1{,}026(2)(2.44)(0.14)\, \frac{(9.79)^2}{2}$$

$$F_D = 3.36 \times 10^4 \text{ newtons}$$

The velocity is assumed to be equal over the 2.44-meter depth so that the resultant drag force acts 1.22 meters (4 feet) above ground level. The moment is then

$$M = 3.36 \times 10^4(1.22)$$

$$= 4.1 \times 10^4 \text{ newton-meters } (2.93 \times 10^4 \text{ foot-pounds})$$

on each of the columns.

* *

As indicated in example problem 25 drag forces and surge forces can act in conjunction with buoyant forces. The buoyant forces can lift buildings from their foundations, and the surge or drag forces can slam them into such things as trees or other structures. Buildings that are firmly attached to their foundations to resist the buoyant forces must also have sufficient structural strength to withstand the drag forces acting against them. The drag forces can be lessened by constructing a building on an elevated platform some distance above the ground. In some instances, the first floor of a building may be designed to be carried away by the tsunami, thereby reducing the forces on the building and protecting the higher floors. However, this may be an expensive solution and has the undesirable feature of adding debris to the water.

The high velocity of a tsunami surge can also damage structures by scouring material near the structures' foundations. Shepard, MacDonald, and Cox (1950) noted numerous instances of severe erosion caused by the 1946 tsunami in Hawaii. At Haena Bay, a sand beach eroded and sand was deposited 1.2 meters deep across a highway. A section of shoreline at Moloaa, was cut back about 21 meters (70 feet). At Kalaupapa, the backwash from the tsunami undermined a road. Other instances of erosion were also noted. Erosion and deposition of surface material are quite common when severe tsunamis occur. Imamura (1942) gives an example from 1707, when a tsunami washed away layered sediments which had covered an old ricefield. Conversely, the Earthquake Research Institute (1934) reported instances of ricefields being covered with sand by the 1933 Sanriku tsunami. Instances of deposition of sand are also indicated by Shepard, MacDonald, and Cox (1950) in Hawaii, and by Reid and Taber (1919) in Puerto Rico. Shepard, MacDonald, and Cox noted that dense stands of grass prevented or greatly diminished ground erosion during the 1946 tsunami in Hawaii.

d. Impact Forces. The high velocity of a tsunami surge will sweep large quantities of material forward with the surge. This material may include automobiles, trees, petroleum tanks, buildings, debris from buildings, or other materials in the path of the surge. A large boulder moved by the 1960 tsunami at Hawaii is shown in Figure 68. In higher latitudes, when tsunamis occur during the winter, the material may include large quantities of broken ice.

Figure 68. Large boulder moved by 1960 tsunami, Hilo, Hawaii (from Matlock, Reese, and Matlock, 1962).

Impact forces from material carried forward by the current are not as easily analyzed as other forces. The drag force will initially accelerate material which is swept up into the current. The velocity of forward motion of such material depends on the distance the material has moved, the ratio of the drag force to the actual mass of the object in motion, and the resistance created by the object dragging against the ground or impacting and grinding against other objects.

Analyzing the effects of a structure impacting with another structure also requires knowledge of the rigidity of the structures and the angle of impact. If the flat side of one structure impacts with the flat side of a second structure, the impact force is spread over a wide area. However, if a corner of the first structure impacts with the flat side of the second structure, the force is concentrated and there will be a greater tendency to crush the impacting structures. It should be remembered that if a structure is partially flooded, the water within the structure becomes a part of the mass of the structure.

Considering an object being swept forward from a stationary position by a moving fluid such as a tsunami surge, the velocity of the fluid, u, with respect to the ground is assumed to be constant, and the velocity of the object, u_b, with respect to the ground varies as the object is accelerated. The velocity, u_b, of the object approaches the velocity, u, of the fluid after the object has moved some distance (i.e., the velocity of the object approaches some terminal velocity). The force accelerating the body is a combination of drag forces and inertia forces, and is given by the equation

$$F = C_D \rho A \frac{(u - u_b)^2}{2} + C_M \rho V \frac{d(u - u_b)}{dt} \qquad (337)$$

where

C_D = the coefficient of drag

ρ = the density of water

A = the cross-sectional area of the object transverse to the direction of motion

$(u - u_b)$ = the velocity of the water with respect to the object at any instant in time

C_M = the inertia or mass coefficient

V = the volume of water displaced by the object

t = time

For a structure or any other large object floating in the water, the mass, m, of the object is equal to the displaced mass, ρV, of the water. This mass may vary as water gradually floods the interior of a structure, but for the analysis presented here the mass will be assumed constant. From Newton's second law

$$F = m \frac{du_b}{dt} = \rho V \frac{du_b}{dt} \tag{338}$$

At any instant in time the magnitude of the deceleration of the fluid with respect to the object is equal to the magnitude of the acceleration of the ground with respect to the object (which is equal to the acceleration of the object with respect to the ground), i.e., where u is assumed constant,

$$\frac{d(u - u_b)}{dt} = - \frac{du_b}{dt} \tag{339}$$

so equation (337) becomes

$$F = \rho V \frac{du_b}{dt} = C_D \rho A \frac{(u - u_b)^2}{2} - C_M \rho V \frac{du_b}{dt} \tag{340}$$

or, rearranging terms,

$$\frac{du_b}{dt} = \frac{C_D A}{2V(1 + C_M)} (u - u_b)^2 \tag{341}$$

For an object moving a short distance, the coefficients C_D and C_M will be assumed constant. This is not entirely correct (e.g., the value of C_D will vary as a function of velocity), but will be assumed as approximately correct for a short distance. A constant, α, can then be defined by

$$\alpha = \frac{C_D A}{2V(1 + C_M)} \tag{342}$$

Substituting equation (342) into equation (341) and rearranging terms give

$$\alpha \, dt = \frac{du_b}{(u - u_b)^2} \tag{343}$$

Integrating equation (343),

$$\alpha t = \int_0^{u_b} \frac{du_b}{(u - u_b)^2} = \frac{1}{u - u_b} - \frac{1}{u} \tag{344}$$

which reduces to

$$u_b = u - \frac{u}{\alpha u t + 1} \tag{345}$$

defining the velocity of the object at any time t.

The distance, x, traveled by the object as a function of time can be determined by noting

$$\frac{dx}{dt} = u_b \tag{346}$$

Substituting equation (345) into equation (346) and integrating give

$$x = \int_0^t \left(u - \frac{u}{\alpha u t + 1}\right) dt = \int_0^t u\, dt - \int_0^t \frac{u\, dt}{\alpha u t + 1} \tag{347}$$

which gives

$$x = ut - \frac{1}{\alpha} \ell n\, (\alpha u t + 1) \tag{348}$$

Typical drag coefficients are given in Table 6. The coefficient of added mass, C_M, can be estimated for a rectangular structure by using the results of Riabouchinski (1920) as given by Brater, McNown, and Stair (1958) (Fig. 69). The values in Figure 69 are for irrotational flow without separation, and the formation of a wake behind the structure would be expected to modify these values. Individual model tests would be required to obtain exact values. Example solutions of equation (348) are shown in Figure 70.

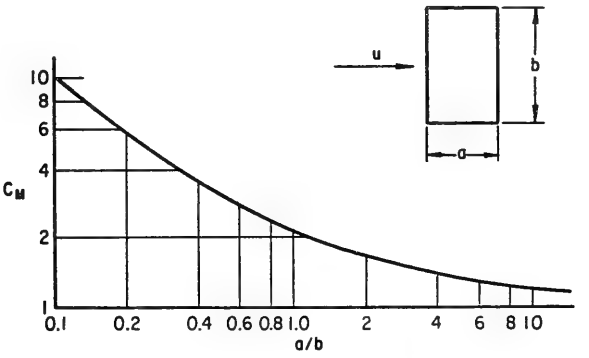

Figure 69. C_M for two-dimensional flow past rectangular bodies (irrotational flow with no separation) (from Riabouchinski, 1920).

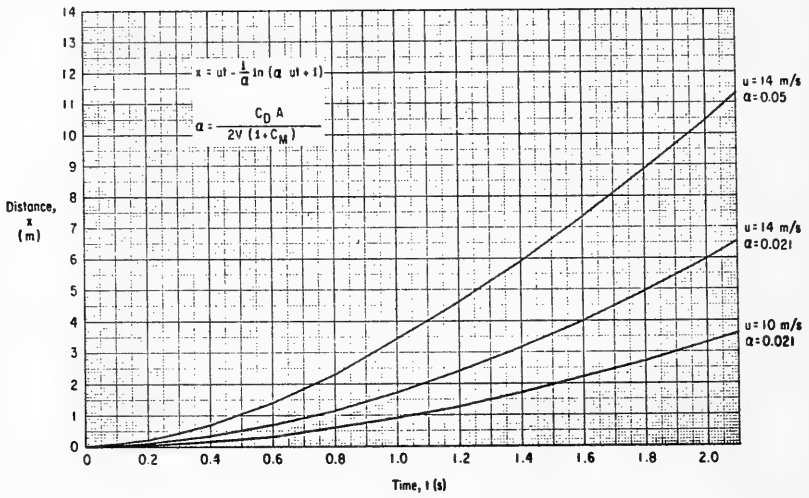

Figure 70. Example plots of x versus t for objects moved by tsunami surge.

* * * * * * * * * * * * * EXAMPLE PROBLEM 27 * * * * * * * * * * * * * * *

GIVEN: A tsunami surge is 5 meters high at the shoreline. A building located at the shoreline is swept forward a distance of 6.1 meters and impacts with another building. The building is rectangular, 12 meters (39.4 feet) wide and 6 meters (19.7 feet) deep in the direction of flow, and is submerged to a 3-meter depth as it is carried forward (see Fig. 71). The velocity of the surge is approximated as u = 14 meters per second.

FIND:

(a) The time required for the building to impact with the other building,

(b) the force accelerating the building at the moment of impact, and

(c) the momentum of the building at the moment of impact.

SOLUTION:

(a) The submerged cross-sectional area of the building, transverse to the direction of the surge, is given as

A = width × submerged depth = 12.0 × 3.0 = 36 square meters

and the submerged volume (the displaced water) is

V = width × length × depth = 12.0 × 6.0 × 3.0 = 216 cubic meters

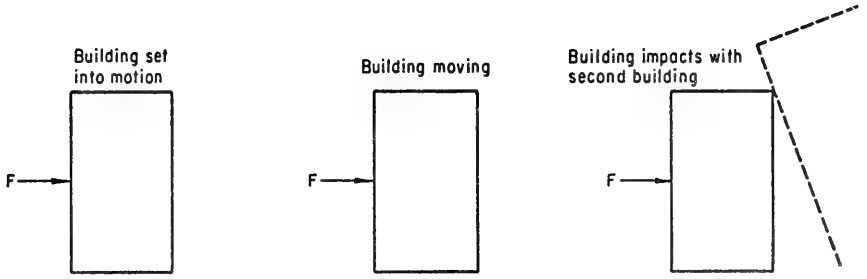

t = 0
x = 0
F = 9.12×10^5 newtons
M_b = 0

t = 1.0 second
x = 1.7 meters
F = 5.45×10^5 newtons
M_b = 7.05×10^5 newton-seconds

t = 2.02 seconds
x = 6.1 meters
F = 3.59×10^5 newtons
M_b = 1.16×10^6 newton-seconds

u = 14 meters/second
C_D = 1.13
C_M = 3.5
A = 36 meters^2
V = 216 meters^3

Figure 71. Building moved by tsunami surge.

The coefficient of drag can be approximated by assuming the side of the building is a flat plate. To determine an equivalent flat plate using Table 6, assume that the submerged depth for underflow and overflow (a totally submerged plate) is twice the depth of the building, or

$$\frac{L}{d} = \frac{12.0}{2 \times 3.0} = 2.0$$

and from Table 6

$$C_D \simeq 1.13$$

From Figure 69, where

$$\frac{a}{b} = \frac{6.0}{12.0} = 0.5$$

then

$$C_M = 3.5$$

and equation (342) gives

$$\alpha = \frac{C_D A}{2V(1 + C_M)} = \frac{1.13 \times 36}{2 \times 216(1 + 3.5)} = 0.021$$

The relationship between distance and time is shown in Figure 70, which gives, for x = 6.1 meters,

$$t = 2.02 \text{ seconds}$$

(b) From equation (345),

$$u_b = u - \frac{u}{\alpha u t + 1} = 14 - \frac{14}{(0.021 \times 14 \times 2.02) + 1}$$

$$u_b = 5.22 \text{ meters (17.1 feet) per second}$$

Substituting equations (342) and (341) into equation (338),

$$F = \rho V \alpha (u - u_b)^2$$

$$F = 1{,}026 \times 216 \times 0.021(14 - 5.22)^2$$

$$= 3.59 \times 10^5 \text{ kilogram-meters per second squared}$$

$$F = 3.59 \times 10^5 \text{ newtons } (8.1 \times 10^4 \text{ pounds})$$

(c) Momentum, M_o, at impact is

$$M_o = u_b \times \text{mass}$$

taking the mass of the building equal to the mass of the displaced water for a partially submerged building which is floating (the mass includes water within the building),

$$\text{mass} = \rho V = 1{,}026 \text{ kilograms per cubic meter} \times 216 \text{ cubic meters}$$

and the momentum is

$$M_o = u_b \times \text{mass} = 5.22 \times 1{,}026 \times 216$$

$$= 1.16 \times 10^6 \text{ kilogram-meters per second}$$

$$(2.56 \times 10^5 \text{ pound-seconds})$$

* *

Magoon (1965) indicates that substantial damage occurred at Crescent City during the 1964 tsunami as a result of debris impacting on structures. This debris included logs, automobiles, and baled lumber. The impact forces either destroyed the load-carrying capacity of walls, or caused bending or breaking of light columns.

Wilson and Tørum (1968) discussed some instances of impact damage resulting from the 1964 Alaskan tsunami. Figure 72 illustrates the damage at the Union Oil Company tank farm at Whittier. Buildings and larger tanks were able to withstand the force of the tsunami; however, smaller

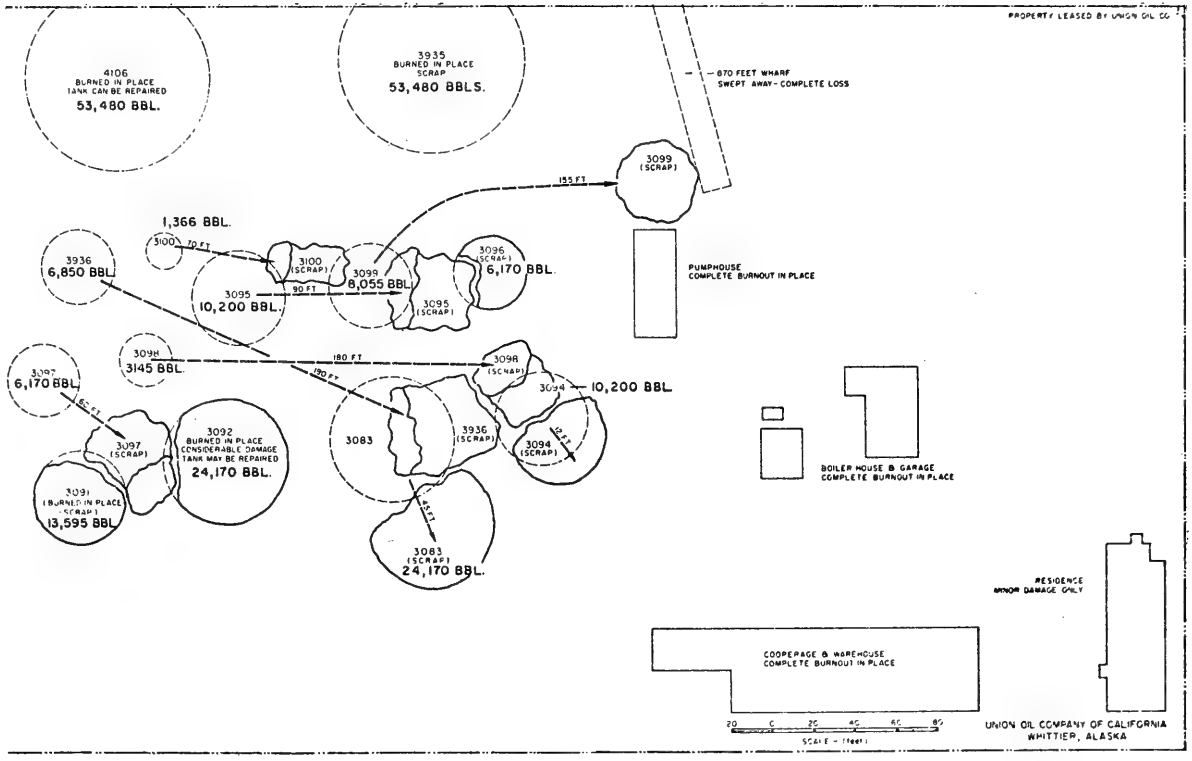

Figure 72. Damage to oil tank farm at Whittier, Alaska (from Wilson and Tørum, 1968; data from Union Oil Company of California).

tanks were carried forward by the surge and impacted with other tanks. Some of the larger tanks were apparently set into motion by the impact, and most of the tanks were ruptured. A resulting fire destroyed the tank farm.

Wilson and Tørum also mentioned the problem of a small-craft harbor located immediately in front of a developed shoreline at Kodiak City. The boat harbor contained a large number of fishing boats and yachts which were carried into the adjacent waterfront business area by the tsunami, adding substantially to the damage. Van Dorn (1965) notes that harbor regulations could be instituted requiring ships large enough to damage harbor structures to stand clear of a harbor in the event of a tsunami warning. In the case at Kodiak City there was only about 30 minutes between the tsunami warning and the arrival of the first large wave crest of the tsunami (Spaeth and Berkman, 1972). However, when tsunamis are generated from distant sources there may be enough time to clear the harbors.

An interesting example of impact forces is reported by Wilson and Tørum (1968). During the 1964 tsunami a house was washed out to sea near Point Whiteshed. The house was swept more than 12 miles along the shoreline, carried into the harbor at Cordova, and rammed the dock, destroying the end of the dock.

e. Hydrostatic Forces. Hydrostatic forces are normally relatively small compared to surge and drag forces. The hydrostatic force on a wall, per foot width of wall, for a water depth h is

$$F = \frac{1}{2} \rho g h^2 \tag{349}$$

As seen in example problem 4, the hydrostatic force would probably not exceed 10 to 20 percent of the drag force at higher water levels, and would appear to be relatively insignificant at lower water levels.

Once the initial surge has passed a structure, assuming that water levels are equal on all sides of the structure, the hydrostatic force will not contribute to the motion or potential motion of the structure. However, this force can cause cracking of exterior walls and interior flooding of the structure.

Magoon (1962) indicated that the flooding caused by a tsunami can saturate the fill behind a retaining wall. Combined with the large drawdown of the water level which may occur at the seaward toe of a wall during the withdrawal of a tsunami wave, large hydrostatic forces on the wall may result. It is believed that this contributed to the partial failure of a retaining wall at Crescent City, California.

There was an unusual occurrence at the abandoned Kahuku Airfield on Oahu during the 1946 tsunami (Shepard, MacDonald, and Cox, 1950). Blocks

of pavement were tilted in circular areas 1 to 1.5 meters (3 to 5 feet) across, apparently as a result of hydraulic pressure from water penetrating into the sand under the pavement when the tsunami flooded the area. The higher pressure under the pavement has not been explained, but could have resulted from water trapped in the sand during a rapid withdrawal of the tsunami.

f. Other Hazards. When considering the total effects of a tsunami surge, additional hazards should be considered in addition to the actual forces of the surge. Some of these are listed below:

(a) Contamination from debris carried in the surging water;

(b) effects of flooding, including spoilage of goods and materials, shorting of electrical lines and transformers, and contamination of water supplies with saltwater;

(c) fire and explosion from the impact and rupturing of petroleum tanks or containers of chemicals (see Fig. 72); and

(d) release of poisonous gas or toxic materials from ruptured containers.

VIII. TSUNAMI WARNING SYSTEM AND INSTRUMENTATION

Cox (1964) discusses the development of the tsunami warning system in Japan. Local, informal warning systems operated sporadically for centuries, and a formal tsunami warning system was recommended as early as the late 19th century. The Japan Meteorological Agency organized the present Japanese system in 1941.

Spaeth and Berkman (1972) discuss the early history of the seismic sea wave (tsunami) warning system in the United States. The need for a warning system in the United States was recognized following the 1 April 1946 tsunami generated in the Aleutian Islands. That tsunami caused heavy damage and resulted in the loss of many lives in Hawaii, particularly at Hilo.

The present tsunami warning system was organized by the former U.S. Coast and Geodetic Survey (now the National Ocean Survey, National Oceanic and Atmospheric Administration - NOAA). Tsunami detectors were designed and installed at tide stations to alert personnel of forthcoming tsunamis. The first detector was installed at Honolulu in 1947. Meetings to discuss implementation of the warning system throughout the Pacific coastal areas were held in 1948. The tentative communication plan for the warning system was approved in 1948. Initially, the warning system supplied information to civil authorities in Hawaii and to military bases throughout the Pacific. In 1953, Civil Defense Agencies of California, Oregon, and Washington were added to the agencies receiving tsunami warning information, and the system has expanded since that time.

Weigel (1974) notes that management of the tsunami warning system was transferred to the Environmental Research Laboratories, NOAA, in 1971, then to the National Weather Service in 1973.

1. The Tsunami Warning System.

The Intergovernmental Oceanographic Commission (IOC) maintains an International Coordination Group for the Tsunami Warning System in the Pacific. Member countries are Canada, Chile, China, Ecuador, France, Guatemala, Japan, Korea, New Zealand, Peru, Philippines, Thailand, U.S.S.R., and the United States. The warning system is based on 51 tide stations and 32 seismograph stations (1976 IOC data). The tsunami warning system in the United States is based at the Honolulu Observatory and receives data from 18 seismograph stations and 16 tide states in the United States (including Alaska and Hawaii, but excluding Pacific Ocean territories), as well as the remaining 14 seismograph and 35 tide stations of the Tsunami Warning System in the Pacific (including Pacific Ocean territories). Tsunami warnings for the United States are based primarily on the stations in the United States and on those stations located in both North and South America. Stations in the Pacific Ocean territories of the United States and those in the remainder of the Pacific provide additional information on the tsunamis; but generally, tsunamis that would create a hazard on the coastlines of the United States do not arrive from those directions.

The tsunami warning system functions best for distantly generated tsunamis, i.e., tsunamis where the arrival time is several hours after the initial wave generation. However, the warning system can also alert the population to the possibility of tsunami generation from nearby seismic activity. As the period of the tsunami varies from several minutes to approximately 30 to 40 minutes, continuously recording tide gages are required. Modern, digital tide gages which provide a tide height every several minutes will not provide sufficient data for recording tsunamis.

An alarm attached to the seismograph at Honolulu Observatory is triggered by the arrival of seismic waves, initiating activity in the Tsunami Warning System. The 1964 Alaska earthquake began at 0336 G.m.t. (Spaeth and Berkman, 1972), and the alarm sounded at Honolulu Observatory at 0344 G.m.t. (G.m.t. times are used to provide a uniform time at all points in the system.) After the alarm, inquiries are sent to various seismic observatories in the system to obtain seismic readings. After receiving and evaluating initial data, a decision is made as to whether or not an advisory bulletin should be issued. If there is a possibility of tsunami generation, an advisory bulletin is sent to dissemination agencies in the warning system.

Charts showing tsunami traveltimes between various coastal points and tsunami-generating areas have been prepared. These charts are used to predict the arrival time of a potential tsunami at the various coastal points after the epicenter of the earthquake has been determined.

Inquiries are sent to tide stations near the earthquake epicenter to determine if tsunami waves have been generated. If there is reasonable cause to assume that a tsunami may have been generated (based on seismic records or observations at tide stations), an advisory bulletin is issued giving estimated times of arrival (ETA's) of the tsunami at various coastal points.

The Honolulu Observatory continues to receive reports and issue bulletins to Civil Defense agencies as information becomes available. Various agencies are kept advised of the status of the tsunami until an all-clear bulletin is issued. If a tsunami was generated, various reporting stations continue to report water levels to the Honolulu Observatory until all information has been obtained from the tide stations of the Tsunami Warning System in the Pacific.

Cox (1964) indicates that tsunami warnings, as distinct from advisory bulletins, are issued only under the following circumstances:

(a) Unusual sea level disturbances having tsunami characteristics are recorded at one or more of the warning system tide stations scattered about the Pacific.

(b) No reply is received from a tide station in a critical recording position in response to a query from the Honolulu Observatory after the occurrence of an earthquake large enough to trigger the seismograph alarm.

(c) An earthquake occurs whose epicenter is in or on the borders of the Pacific Ocean in such a location that a tsunami generated there would not arrive at any tide stations sufficiently in advance of its arrival at a particular shoreline to allow warning that shoreline.

It is the responsibility of agencies receiving tsunami warnings to disseminate information to the civilian population. This may be done through broadcasting news media (radio and television), by police and civil defense personnel, or by sounding signals on sirens. Schank (1978) discusses the public warning system in the State of Hawaii. Broadcasters in the State are linked together in a system called "Civ-Alert." If it is considered probable that a tsunami will cause property damage and loss of life, a tsunami alert is given. The first alert is given 2 hours before the estimated ETA by sounding an alert on all of the sirens in the State. Civ-Alert broadcasts information and instructions. The alert is repeated at 1 hour and then a half hour before the estimated ETA. The alert is extended by police, fire, forestry, and Civil Air Patrol personnel. Maps of potential tsunami hazard areas are included in the county telephone directories in Hawaii to define areas which should be evacuated.

Cox (1978) considered the cost of false alarms, i.e., tsunami alerts when no significant tsunami occurs, giving the cost of false alarms at $264,000 per year (1977) in Hawaii alone. The cost of false alarms must

be balanced against the high cost of casualties to the local population if a tsunami occurs without sufficient warning.

Cox and Stewart (1972) discuss the particular problems of providing tsunami warnings to areas near a tsunami source. Tsunami warnings must be timely to be effective. To reduce the hazards on particular coastlines, a policy of regional evaluation was adopted in 1966. Adams (1978) discusses the local tsunami warning system used in Hawaii. Seismic detection instruments have been placed in police and fire stations and similar locations. Seismic activity with a magnitude which may generate a tsunami triggers an alarm. A decision is then made at the local level as to whether or not the local population should be alerted and evacuated.

Various investigators have called attention to phenomena occurring just before a tsunami. These include the unusual feeding habits of fish before a tsunami due to the presence of large quantities of bottom-adherent diatoms in the upper layer of the sea (Suyehiro, 1934) and increases in the Earth's magnetic field preceding an earthquake (Moore, 1972). The study of such phenomena has not been developed enough to be included in a formal tsunami warning system.

2. Human Response.

Spaeth and Berkman (1972) note that the response of a local population to a tsunami warning may be slow unless the population is well trained to respond. Approximately 30 minutes after the Alaska earthquake of 1964, the U.S. Fleet Weather Central at Kodiak Naval Station received word of a large tsunami at Cape Chiniak, Alaska, and had the Armed Forces Radio Station broadcast a tsunami warning. Military and government personnel promptly evacuated the endangered areas. Although reasonably prompt, the evacuation of the city of Kodiak was not as well carried out (there were eight deaths at Kodiak). The first large tsunami wave crest arrived at Kodiak about 30 minutes after the warning, so a prompt response to the warning was essential.

Haas (1978) separates tsunamis into the following four types (summarized in Table 7):

(a) Type I. Shoreline slumping, earthslides, and large rock and ice falls coincident with the earthquake. Large waves generated onto the shoreline almost immediately.

(b) Type II. Very heavy Earth temblors can be felt by the local population for a period up to several minutes. The tsunami arrives within 10 minutes.

(c) Type III. Noticeable Earth shocks felt by the local population for a period up to several minutes. Severe Earth temblors not present. Tsunami arrives within 30 minutes.

(d) Type IV. No local Earth shocks. The tsunami is generated at a distant source.

Table 7. Typology of tsunami events (after Haas, 1978).

Tsunami type	Physical clues	Approximate time for evacuation	Maximum credible preventive action
I	Visible slumping or sliding	Less than 1 minute	Almost none
II	Severe Earth temblors	5 to 10 minutes	Ambulatory persons can be evacuated
III	Noticeable Earth shocks	15 to 30 minutes	Some persons can be evacuated
IV	None	45 minutes to 12 hours	Most persons can be evacuated and up to 75 percent of all movable property

Haas notes that while no effective warning can be given for a type I tsunami, the possibility of warnings for types II, III, and IV will depend on the education of the public and the effectiveness of warning systems. Evacuation for a type II tsunami requires prompt response by the population based on their individual sensing of strong earthquake shocks, and little time is available for an organized warning system to operate. Therefore, there is almost total reliance on prior education.

For a type III tsunami, public education alone is insufficient because the physical evidence of a possible tsunami is not as strong. A reliable local warning system is needed to alert the public, and the population must be educated to respond to the alert. For a type IV tsunami, a large warning system, such as the Tsunami Warning System in the Pacific, is required.

Weller (1972) cites a number of instances of human response during the 1964 earthquake and tsunami in Alaska. At Seward, the initial slumping of the waterfront gave warning to the residents of the town, and most people evacuated the low areas; but 11 people were killed by a wave 9 to 12 meters (30 to 40 feet) in height. At the village of Kaguyak on Kodiak Island, residents moved to high ground when they observed the initial signs of a tsunami; but three people were killed when they returned to low areas before the arrival of the largest wave. At Ouzinkie, on Spruce Island, the residents evacuated the town when they observed the initial development of wave action offshore, and there was no loss of life.

Many lives are lost either because some residents do not respond to visible signs of a possible tsunami, such as at Seward, or residents

return too soon to low areas, such as at Kaguyak. Spaeth and Berkman (1972) note that several people were killed at Crescent City, California, because they returned to a low area before the arrival of the largest wave. A large amount of damage at Crescent City resulted from the failure to remove vehicles, including a gasoline tank truck, from the endangered area.

3. Ionospheric Waves.

To evaluate the possibility of a tsunami being generated by an earthquake, it is desirable to have information about the source mechanism of the earthquake, i.e., whether the earthquake is a dip-slip type or a strike-slip type. If the earthquake is a strike-slip type, it may be assumed that a large transoceanic tsunami will not be generated, and tsunami alerts can be canceled at all locations except those near the epicenter. If the earthquake is a dip-slip type, there is a high probability that a tsunami may have been generated, and additional information must be obtained from tide stations.

Van Dorn (1965) indicated that a dipolar barometric wave in the atmosphere was associated with the dipolar ground motion of the 1964 Alaska earthquake, and that this raised a possibility for early tsunami prediction. Row (1972) discusses the atmospheric waves associated with the Alaska earthquake in greater detail. Row indicates that there is both an early-arriving pressure disturbance, associated with seismic waves in the Earth, and the late-arriving disturbance (propagating at about 300 meters per second) previously mentioned by Van Dorn. The late-arriving disturbance is associated with the tectonic deformation and, at distances far from the source, would arrive well in advance of gravity waves traveling through the ocean. For example, at a distance of 5,000 kilometers (3,100 miles) from the source, a tsunami traveling across the ocean at a speed of 200 meters per second (447 miles per hour) will arrive approximately 2 hours 20 minutes after the atmospheric wave.

Pressure disturbances also propagate through the ionosphere. Row (1972) discussed the possible association between ground motion and ionospheric waves. Furumoto (1970) reports on the use of a 10-megahertz Doppler recording of Rayleigh waves to estimate the initial phase of the source of the 11 August 1969 Kuril Islands earthquake. He notes that this provides a rapid approach to source mechanism estimation. The Doppler shift associated with the ionospheric waves can be monitored at relatively low cost (Furumoto, 1970). Murty (1977) provides further discussion on ionospheric effects.

The use of atmospheric waves to estimate the ground motion of a tsunami source requires further investigation. However, this method may be useful for the Tsunami Warning System.

4. Deep-Ocean Tsunami Gages.

In addition to supplying information for the Tsunami Warning System, the tide stations provide records of tsunami heights and periods. Unfortunately, the local topography distorts the tsunami recorded on tide gages near the coastline, and these records do not provide information on the

deep-ocean form of the tsunami. Therefore, a means of recording tsunamis in the open ocean is needed.

Vitousek (1961) proposed placing permanent instrument packages in the ocean, connected to abandoned transpacific telegraph cables. A system of this type would provide deep-ocean data, and would also provide additional useful information for the Tsunami Warning System because of the direct connection with the gage. However, Vitousek and Miller (1970) indicate that cable-connected systems would be expensive, and that the cost of laying special cables would be unrealistic.

Vitousek and Miller discuss four possible methods of measuring a tsunami in the open ocean: (a) Free-drop recoverable instrument package, (b) an undership instrument, (c) an underbuoy instrument, and (d) the cable-connected instrument previously discussed by Vitousek. Shinmoto and Vitousek (1978) give details of an air-deployable free-drop tsunami gage which can be emplaced quickly after a tsunami occurs.

While some deployment of open-ocean gages has been carried out, experience in operating such gages is limited. Future use of such gages is required to determine their practicality and reliability as part of the Tsunami Warning System, and to obtain open-ocean tsunami data.

IX. SUMMARY AND CONCLUSIONS

The potentially high value of property in the coastal zone and the intensive development of such land for both private and public use require that careful consideration be given to the possibility of catastrophic flooding of areas of the coastal zone, in or near seismologically active regions, by tsunamis. Small variations in predicted flood levels may affect property worth millions of dollars, and may have substantial effects on flood insurance premiums and permits for utilization of property, so it is necessary to have as high a degree of accuracy as possible in defining flood zones, e.g., the 100-year flood level. Also, large powerplants are typically located at low elevations because of pumping requirements for cooling water, and port facilities are necessarily located near the shoreline, so that well-designed protection is required for high-cost facilities.

Available data on tsunami inundation come from visual observations (including posttsunami surveys) and from tide gage records. Data are generally only available for a few occurrences, and only at specific coastal areas. Some data can be obtained from historical accounts, but such data are dependent on incomplete personal observations, usually by untrained observers. Open-ocean data on tsunamis, needed for verification of numerical investigations, are almost nonexistent.

Numerical data are used to supplement the available field data on tsunami flood levels. Numerical procedures have been developed that allow the simulation of a tsunami source, the generation and propagation of the tsunami waves across the ocean, and the interaction of the tsunami and coastal topography. Procedures have also been developed to simulate tsunami flooding shoreward of the coastline. The numerical results, which are compared to the more limited field measurements for verification,

provide the additional data needed to construct tsunami flood level maps for various probabilities of recurrence.

Numerical procedures can also be verified by comparing with theoretical results for idealized cases. Theoretical solutions exist for wave refraction at coastlines with uniform topography, waves passing over mathematically defined transitions from deep water to shallow water, etc. Deviations between the numerical results and the theoretical solutions indicate the degree of accuracy where the numerical procedures are applied to more complex topography.

A continuing program of gathering field data on tsunamis in the open ocean and coastal inundation by tsunamis is needed. Because of the long periods of time between the occurrence of tsunamis, the accumulation of data for particular coastal points is very slow. It is necessary to maintain tide gages with the capability of recording tsunamis, and also to have standby plans with designated personnel to obtain field observations immediately after tsunamis occur. It is also desirable to maintain a standby capability for dropping instrument packages into the open ocean immediately after a tsunami occurs. This latter capability requires the maintenance of gages and associated instrument packages in operating condition over long periods of time, and the maintenance of a system for placing the instrument packages quickly and on short notice, including the periodic testing of the system by placing and recovering the instruments. An air-dropped system is probably the most practical for this purpose.

Also, continuing improvements are needed in the numerical procedures for simulating tsunamis. A particular area of possible improvement is the treatment of boundaries of the computational grid. Errors in the wave reflection from solid boundaries, and errors at open-ocean boundaries where the waves must pass completely through the boundary, propagate through the computational grid at each succeeding time step. These errors grow with increasing time so that the solution is not accurate for long periods of real time. It becomes necessary to use large time steps to reduce computational errors, and consequently to use a course grid, i.e., to use long real distances between grid points. This smooths out the topographical variations so that wave scattering caused by small topographical features is not properly accounted for. Because of the limited field data available, the numerical solutions cannot always be verified and adjusted to match field data.

Improvements in the numerical simulation of tsunami generation are also desirable. However, this requires both accurate data on real tsunami-generating mechanisms, and open-ocean tsunami data so that errors in simulating tsunami generation can be separated from errors in the simulation of nearshore propagation.

Continued research should be carried out in areas such as shelf resonance. In particular, theoretical solutions are needed for simple topography to provide verification for numerical procedures where field data do not exist. At the present time, the various effects on tsunami propagation cannot be adequately separated in the computational procedure as the available data are mainly from tide gages and visual observations of maximum inundation levels.

LITERATURE CITED

ABE, K., "Reliable Estimation of the Seismic Moment of Large Earthquakes," *Journal of Physics of the Earth*, Vol. 23, 1975, pp. 381-390.

ABE, K., "Size of Great Earthquakes of 1837-1974 Inferred from Tsunami Data," *Journal of Geophysical Research*, Vol. 84, No. B4, Apr. 1979, pp. 1561-1568.

ADAMS, W.M., "Relationship of Instruments and Policy in the Hawaii Warning System," *Proceedings of the Symposium on Tsunamis*, Department of Fisheries and the Environment, Ottawa, Canada, 1978, pp. 205-217.

AMBRASEYS, N.N., "The Seismic Sea Wave of July 9, 1956, in the Greek Archipelago," *Journal of Geophysical Research*, Vol. 65, No. 4, Apr. 1960, pp. 1257-1265.

AMBRASEYS, N.N., "Data for the Investigation of Seismic Sea-Waves in Europe," Monograph No. 29, European Seismological Commission, International Union of Geodesy and Geophysics, Paris, France, Nov. 1965.

BEARD, L.R., "Statistical Methods in Hydrology," U.S. Army Engineer District, Sacramento, Sacramento, Calif., Jan. 1962.

BENJAMIN, T.B., BONA, J.L., and MAHONY, J.J., "On Model Equations for Long Waves in Nonlinear Dispersive Systems," *Philosophical Transactions of the Royal Society*, Series A, Vol. 272, 1972, pp. 47-78.

BENJAMIN, T.B., and FEIR, J.E., "The Disintegration of Wave Trains on Deep Water," *Journal of Fluid Mechanics*, Vol. 27, Part 3, 1967, pp. 417-430.

BEN-MENAHEM, A., "Radiation of Seismic Surface-Waves from Finite Moving Sources," *Bulletin of the Seismological Society of America*, Vol. 51, No. 3, July 1961, pp. 401-435.

BERG, E., "The Alaska Earthquake; Its Location and Seismic Setting," *Proceedings of the 15th Alaska Science Conference*, American Association for the Advancement of Science, 1964, pp. 218-232.

BERG, E., et al., "Field Survey of the Tsunamis of 28 March 1964 in Alaska, and Conclusions as to the Origin of the Major Tsunami," Report No. HIG-70-2, Hawaii Institute of Geophysics, Honolulu, Hawaii, Jan, 1970.

BLANCH, G., "Mathieu Functions," *Handbook of Mathematical Functions*, Ch. 20, National Bureau of Standards, U.S. Government Printing Office, Washington, D.C., 1964.

BOURODIMOS, E.L., and IPPEN, A.T., "Wave Reflection and Transmission in Channels of Variable Section," *Proceedings of the 11th Conference on Coastal Engineering*, American Society of Civil Engineers, Ch. 13, 1968, pp. 195-212.

BOWEN, A.J., and INMAN, D.L., "Edge Waves and Crescentic Bars," *Journal of Geophysical Research*, Vol. 76, No. 36, Dec. 1971, pp. 8662-8671.

BRANDSMA, M., DIVOKY, D., and HWANG, L-S., "Seawave - A Revised Model for Tsunami Applications," Final Report, National Science Foundation, Washington, D.C., Apr. 1975.

BRANDSMA, M., DIVOKY, D., and HWANG, L-S., "Tsunami Atlas for the Coasts of the United States," Report No. TC-486, U.S. Nuclear Regulatory Commission, Washington, D.C., Nov. 1979.

BRATER, E.F., McNOWN, J.S., and STAIR, L.D., "Wave Forces on Submerged Structures," *Journal of the Hydraulics Division*, Vol. 84, No. HY6, Nov. 1958.

BRETSCHNEIDER, C.L., and WYBRO, P.G., "Tsunami Inundation Prediction," *Proceedings of the 15th Conference on Coastal Engineering*, American Society of Civil Engineers, Ch. 60, 1976, pp. 1006-1024.

BUTLER, H.L., and DURHAM, D.L., "Applications of Numerical Modeling to Coastal Engineering Problems," *Proceedings of the 1976 Army Numerical Analysis and Computers Conference*, Sept. 1976, pp. 471-508.

BYRNE, R.J., "Field Occurrences of Induced Multiple Gravity Waves," *Journal of Geophysical Research*, Vol. 74, No. 10, May 1969, pp. 2590-2596 (copyrighted by American Geophysical Union).

CAMFIELD, F.E., "Wave Trapping of a Coastline Approximated by a Circular Arc," *Proceedings of the Symposium on Long Waves in the Ocean*, Department of Fisheries and the Environment, Ottawa, Canada, 1979, pp. 183-187.

CAMFIELD, F.E., and STREET, R.L., Stanford University, Department of Civil Engineering, Palo Alto, Calif., unpublished data, 1967.

CAMFIELD, F.E., and STREET, R.L., "The Effects of Bottom Configuration of the Deformation, Breaking and Runup of Solitary Waves," *Proceedings of the 11th Conference on Coastal Engineering*, American Society of Civil Engineers, Ch. 11, Sept. 1968, pp. 173-189.

CAMFIELD, T.W., "The 'Great Flood' of 1866," *Port Townsend Leader*, Summer Supplement, Port Townsend, Wash., 1975.

CARRIER, G.F., SHAW, R.P., and MIYATA, M., "Channel Effects in Harbor Resonance," *Journal of the Engineering Mechanics Division*, Vol. 97, No. EM6, Dec. 1971, pp. 1703-1716.

CHAN, R.K.C., and STREET, R.L., "A Computer Study of Finite-Amplitude Water Waves," *Journal of Computational Physics*, Vol. 6, Aug. 1970a, pp. 68-94.

CHAN, R.K.C., and STREET, R.L., "Shoaling of Finite-Amplitude Waves on Plane Beaches," *Proceedings of the 12th Coastal Engineering Conference*, American Society of Civil Engineers, 1970b.

CHAN, R.K.C., STREET, R.L., and FROMM, J.E., "The Digital Simulation of Water Waves--An Evaluation of SUMMAC," *Proceedings of the Second International Conference on Numerical Methods in Fluid Dynamics*, Department of Civil Engineering, Stanford University, Palo Alto, Calif., 1970.

CHAN, R.K.C., STREET, R.L., and STRELKOFF, T., "Computer Studies of Finite-Amplitude Water Waves," Technical Report No. 104, Department of Civil Engineering, Stanford University, Palo Alto, Calif., June 1969.

CHAO, Y-Y., "The Theory of Wave Refraction in Shoaling Water, Including the Effects of Caustics and the Spherical Earth," Report No. TR-70-7, New York University, Geophysical Sciences Laboratory, New York, N.Y., June 1970.

CHAO, Y-Y., and PIERSON, W.J., "An Experimental Study of Gravity Wave Behavior Near a Straight Caustic," Report No. TR-70-17, New York University, Geophysical Sciences Laboratory, New York, N.Y., Dec. 1970.

CHEN, H.S., and MEI, C.C., "Oscillations and Wave Forces in an Offshore Harbor (Applications of the Hybrid Finite Element Method to Water-Wave Scattering)," Report No. 190, Massachusetts Institute of Technology, Cambridge, Mass., 1974.

CHEN, M., DIVOKY, D., and HWANG, L-S., "Nearfield Tsunami Behavior," Final Report, National Science Foundation, Washington, D.C., Apr. 1975.

CHEN, T.C., "Experimental Study on the Solitary Wave Reflection Along a Straight Sloped Wall at Oblique Angle of Incidence," TM 124, U.S. Army, Corps of Engineers, Beach Erosion Board, Washington, D.C., Mar. 1961.

COCHRANE, J.D., and ARTHUR, R.S., "Reflection of Tsunami," *Journal of Marine Research*, Vol. 7, No. 3, 1948, pp. 239-251.

COX, C., and STEWART, H.B., "Technical Evaluation of the Seismic Sea Wave Warning System," *The Great Alaska Earthquake of 1964, Oceanography and Coastal Engineering*, National Academy of Sciences, National Research Council, Washington, D.C., 1972, pp. 229-245.

COX, D.C., "Tsunami Forecasting," Report HIG-64-15, Hawaii Institute of Geophysics, Honolulu, Hawaii, Aug. 1964.

COX, D.C., PARARAS-CARAYANNIS, G., and CALEBAUGH, J.P., "Catalog of Tsunamis in Alaska," Report SE-1, World Data Center A, Solid Earth Geophysics, National Oceanic and Atmospheric Administration, Rockville, Md., Mar. 1976.

CROSS, R.H., "Tsunami Surge Forces," *Journal of the Waterways, Harbors, and Coastal Engineering Division*, Vol. 93, No. WW4, Nov. 1967, pp. 201-231.

DAVIS, T.N., and ECHOLS, C., "A Table of Alaska Earthquakes, 1788-1961," Report No. 8 (UAG-R131), University of Alaska Geophysical Institute, Fairbanks, Alaska, 1962.

DAVISON, C., *Great Earthquakes*, Thomas Murby & Co., London, 1936.

DEAN, R.G., "Long Wave Modification by Linear Transitions," *Journal of the Waterways and Harbors Division*, Vol. 90, No. WW1, Feb. 1964, pp. 1-29.

EARTHQUAKE RESEARCH INSTITUTE, "Reports on the Tsunami of 1933 on the Sanriku Coast, Japan," *Bulletin of the Earthquake Research Institute*, Tokyo Imperial University, Tokyo, Japan, Vol. 1, Part II (7), 1934.

EATON, J.P., RICHTER, D.H., and AULT, W.U., "The Tsunami of May 23, 1960, on the Island of Hawaii," *Bulletin of the Seismological Society of America*, Vol. 51, No. 2, Apr. 1961, pp. 135-157.

FREEMAN, J.C., and LE MEHAUTE, B., "Wave Breakers on a Beach and Surges on a Dry Bed," *Journal of the Hydraulics Division*, Vol. 90, No. HY2, Mar. 1964, pp. 187-216.

FROMM, J.E., IBM Research Report RJ531, IBM Research Laboratory, San Jose, Calif., 1968.

FUKUI, Y., et al., "Hydraulic Study on Tsunami," *Coastal Engineering in Japan*, Vol. 6, 1963, pp. 67-82.

FUKUUCHI, H., and ITO, Y., "On the Effect of Breakwaters Against Tsunami," *Proceedings of the 10th Conference on Coastal Engineering*, American Society of Civil Engineers, Ch. 47, 1966, pp. 821-839.

FURUMOTO, A.S., "Ionospheric Recordings of Rayleigh Waves for Estimating Source Mechanisms," *Tsunamis in the Pacific Ocean*, Ch. 9, East-West Center Press, Honolulu, Hawaii, 1970, pp. 119-134.

GAGNON, M.L., and BOCCO, M.V., "The Effect of a Gradual Change of Depth on a Train of Surface Waves," S.M. Thesis, Department of Civil Engineering, Massachusetts Institute of Technology, Cambridge, Mass., 1962.

GALLAGHER, B., "Generation of Surf Beat by Non-Linear Wave Interactions," *Journal of Fluid Mechanics*, Vol. 49, Part 1, 1971, pp. 1-20.

GALVIN, C.J., "Resonant Edge Waves on Laboratory Beaches," *Transactions of the American Geophysical Union*, Vol. 46, 1965, p. 112.

GALVIN, C.J., "Finite-Amplitude, Shallow Water-Waves of Periodically Recurring Form," *Proceedings of the Symposium on Long Waves*, University of Delaware, Newark, Del., 1970, pp. 1-32 (also Reprint 5-72, U.S. Army, Corps of Engineers, Coastal Engineering Research Center, Fort Belvoir, Va., NTIS AD 754 868).

GELLER, R.J., "Scaling Relations for Earthquake Source Parameters and Magnitudes," *Bulletin of the Seismological Society of America*, Vol. 66, No. 5, Oct. 1976, pp. 1501-1523.

GELLER, R.J., and KANAMORI, H., "Magnitudes of Great Shallow Earthquakes from 1904 to 1952," *Bulletin of the Seismological Society of America*, Vol. 67, No. 3, June 1977, pp. 587-598.

GORING, D.G., "Tsunamis - The Propagation of Long Waves Onto a Shelf," W.M. Keck Laboratory Report No. KH-R-38, California Institute of Technology, Pasadena, Calif., Nov. 1978.

GUTENBERG, B., and RICHTER, C.F., *Seismicity of the Earth and Associated Phenomena*, 2d ed., Princeton University Press, Princeton, New Jersey, 1954.

GUTENBERG, B., and RICHTER, C.F., *Seismicity of the Earth and Associated Phenomena*, Hafner, New York, 1965.

GUZA, R.T., and BOWEN, A.J., "The Resonant Instabilities of Long Waves Obliquely Incident on a Beach," *Journal of Geophysical Research*, Vol. 80, No. 33, Nov. 1975, pp. 4529-4534.

GUZA, R.T., and BOWEN, A.J., "Finite-Amplitude Edge Waves," *Journal of Marine Research*, Vol. 34, No. 1, 1976, pp. 269-293.

GUZA, R.T., and DAVIS, R.E., "Excitation of Edge Waves by Waves Incident on a Beach," *Journal of Geophysical Research*, Vol. 79, No. 9, Mar. 1974, pp. 1285-1291.

GUZA, R.T., and INMAN, D.L., "Edge Waves and Beach Cusps," *Journal of Geophysical Research*, Vol. 80, No. 21, July 1975, pp. 2997-3012 (copyrighted by American Geophysical Union).

HAAS, J.E., "Human Response to the Tsunami Warning System," *Proceedings of the Symposium on Tsunamis*, Department of Fisheries and the Environment, Ottawa, Canada, 1978, pp. 224-235.

HALLERMEIER, R.J., "Nonlinear Flow of Wave Crests Past a Thin Pile," *Journal of the Waterways, Harbors and Coastal Engineering Division*, Vol. 102, No. WW4, Nov. 1976, pp. 365-377.

HAMMACK, J.L., "A Note on Tsunamis: Their Generation and Propagation in an Ocean of Uniform Depth," *Journal of Fluid Mechanics*, Vol. 60, Part 4, 1973, pp. 769-799.

HAMMACK, J.L., and SEGUR, H., "The Korteweg-deVries Equation and Water Waves, Part 2, Comparison with Experiments," *Journal of Fluid Mechanics*, Vol. 65, Part 2, 1974, pp. 289-314.

HARRIS, D.L., "Tides and Tidal Datums," U.S. Army, Corps of Engineers, Coastal Engineering Research Center, Fort Belvoir, Va. (in preparation, 1980).

HASKELL, N.A., "Elastic Displacements in the Near-Field of a Propagating Fault," *Bulletin of the Seismological Society of America*, Vol. 59, 1969, pp. 865-908.

HECK, N.H., *Earthquake*, Princeton University Press, Princeton, N.J., 1936.

HECK, N.H., "List of Seismic Sea Waves," *Bulletin of the Seismological Society of America*, Vol. 37, No. 4, Oct. 1947.

HEITNER, K.L., "A Mathematical Model for Calculation of the Runup of Tsunamis," Dissertation, Earthquake Engineering Research Laboratory, California Institute of Technology, Pasadena, Calif., 1969.

HIDAKA, K., "A Theory of Shelf Seiches," *The Memoirs of the Imperial Marine Observatory*, Kobe, Japan, Vol. 6, No. 1, Dec. 1935a, pp. 9-11.

HIDAKA, K., "Seiches Due to a Submarine Bank," *The Memoirs of the Imperial Marine Observatory*, Kobe, Japan, Vol. 6, No. 1, Dec. 1935b, pp. 1-8.

HIRONO, T., "The Chilean Earthquake of 1960," *Journal of Geography*, Tokyo Geographical Society, Tokyo, Japan, Vol. 70, No. 3, 1961, pp. 20-31 (in Japanese with English abstract).

HODGSON, E.A., and DOXSEE, W.W., "The Grand Banks Earthquake, November 18, 1929," *Earthquake Notes*, Vol. 2, Nos. 1 and 2, 1930, pp. 72-81.

HOLDEN, E.S., "A Catalogue of Earthquakes on the Pacific Coast, 1769 to 1897," Smithsonian Miscellaneous Collections 1087, Smithsonian Institution, Washington, D.C., 1898.

HORIKAWA, K., and WIEGEL, R.L., "Secondary Wave Crest Formation," Series 89, Issue 4, Wave Research Laboratory, Institute of Engineering Research, University of California, Berkeley, Calif., Feb. 1959.

HOUSNER, G.S., "Engineering Estimates of Ground Shaking and Maximum Earthquake Magnitude," *Proceedings of the Fourth World Conference on Earthquake Engineering*, 1969.

HOUSTON, J.R., "Long Beach Harbor Numerical Analysis of Harbor Oscillations, Report 1, Existing Conditions and Proposed Improvements," Miscellaneous Paper H-76-20, U.S. Army Engineer Waterways Experiment Station, Vicksburg, Miss., Sept. 1976.

HOUSTON, J.R., "Los Angeles Harbor Numerical Analysis of Harbor Oscillations," Miscellaneous Paper H-77-2, U.S. Army Engineer Waterways Experiment Station, Vicksburg, Miss., Feb. 1977.

HOUSTON, J.R., CARVER, R.D., and MARKLE, D.G., "Tsunami-Wave Elevation Frequency of Occurrence for the Hawaiian Islands," Technical Report H-77-16, U.S. Army Engineer Waterways Experiment Station, Vicksburg, Miss., Aug. 1977.

HOUSTON, J.R., and GARCIA, A.W., "Type 16 Flood Insurance Study: Tsunami Predictions for Pacific Coastal Communities," Technical Report H-74-3, U.S. Army Engineer Waterways Experiment Station, Vicksburg, Miss., May 1974.

HOUSTON, J.R., and GARCIA, A.W., "Type 16 Flood Insurance Study: Tsunami Predictions for the West Coast of the Continental United States," Technical Report H-78-26, U.S. Army Engineer Waterways Experiment Station, Vicksburg, Miss., Dec. 1978.

HOUSTON, J.R., et al., "Probable Maximum Tsunami Runup for Distant Seismic Events," Appendix 2.4B, Amendment 23, NORCO-NP-1 PSAR, Puerto Rico Water Resources Authority, Puerto Rico, May 1975a.

HOUSTON, J.R., et al., "Effect of Source Orientation and Location in the Aleutian Trench on Tsunami Amplitude Along the Pacific Coast of the Continental United States," Research Report H-75-4, U.S. Army Engineer Waterways Experiment Station, Vicksburg, Miss., July 1975b.

HWANG, L-S., and DIVOKY, D., "Tsunami Generation," *Journal of Geophysical Research*, Vol. 75, No. 33, Nov. 1970, pp. 6802-6817.

HWANG, L-S., and DIVOKY, D., "A Numerical Model of the Major Tsunami," *The Great Alaska Earthquake of 1964, Oceanography and Coastal Engineering*, National Academy of Sciences, National Research Council, Washington, D.C., 1972, pp. 191-210.

HWANG, L-S., and DIVOKY, D., "Numerical Investigations of Tsunami Behaviour," Final Report, National Science Foundation, Washington, D.C., Mar. 1975.

IIDA, K., "Magnitude, Energy, and Generation Mechanisms of Tsunamis and a Catalogue of Earthquakes Associated with Tsunamis," *Proceedings of the 10th Pacific Science Congress Symposium*, International Union of Geodesy and Geophysics, Monograph No. 24, 1961, pp. 7-18.

IIDA, K., "The Generation of Tsunamis and the Focal Mechanism of Earthquakes," *Tsunamis in the Pacific Ocean*, Ch. 1, East-West Center Press, Honolulu, Hawaii, 1970, pp. 3-18.

IMAMURA, A., "An Interpretation of the Reexposure of an Old Rice Field Buried in the Ground," *Zisin*, Vol. 14, No. 6, 1942, pp. 149-153 (in Japanese).

IPPEN, A.T., and GODA, Y., "Wave Induced Oscillations in Harbors: The Solution for a Rectangular Harbor Connected to the Open-Sea," Report No. 59, Massachusetts Institute of Technology, Hydrodynamics Laboratory, Cambridge, Mass., July 1963.

IPPEN, A.T., RAICHLEN, F., and SULLIVAN, R.K., Jr., "Wave Induced Oscillations in Harbors: Effect of Energy Dissipators in Coupled Basin Systems," Report No. 52, Massachusetts Institute of Technology, Hydrodynamics Laboratory, Cambridge, Mass., July 1962.

ISHIMOTO, M., and HAGIWARA, T., "The Phenomenon of Sea Water Overflowing the Land," *Bulletin of the Earthquake Research Institute*, Tokyo Imperial University, Tokyo, Japan, Supplementary Vol. 1, 1934, pp. 17-23.

IWASAKI, T., and HORIKAWA, K., "Tsunami Caused by Chile Earthquake in May, 1960 and Outline of Disasters in Northeastern Coasts of Japan," *Coastal Engineering in Japan*, Vol. III, 1960, pp. 33-48.

IWASAKI, T., MIURA, A., and TERADA, S., "On the Effect of the Breakwater in Case of Tsunami, Part 1 (The Model Experiment of Tsunami in Kesennuma Bay)," *The Technology Reports of the Tohoku University*, Sendai, Japan, Vol. 25, No. 2, 1961, pp. 123-135.

JAGGAR, T.A., "A Big Atlantic Earthquake," *The Volcano Letter*, Dec. 1929.

JORSTAD, F.A., "Fjellskredet ved Tjelle; et 200-ars minne," *Naturen*, Vol. 80, No. 6, 1956, pp. 323-333.

KAJIURA, K., "On the Partial Reflection of Water Waves Passing Over a Bottom of Variable Depth," *Proceedings of the 10th Pacific Science Congress on Tsunami Hydrodynamics*, International Union of Geodesy and Geophysics, Monograph No. 24, 1963, pp. 206-230.

KAMEL, A., "Stability of Rubble-Mound Tsunami Barrier Hilo Harbor, Hawaii," Technical Report No. 2-792, U.S. Army Engineer Waterways Experiment Station, Vicksburg, Miss., Aug. 1967.

KANAMORI, H., "Mechanism of Tsunami Earthquakes," *Physics of the Earth and Planetary Interiors*, Vol. 6, 1972, pp. 346-359.

KANAMORI, H., and CIPAR, J.J., "Focal Processes of the Great Chilean Earthquake, May 22, 1960," *Physics of the Earth and Planetary Interiors*, Vol. 9, 1974, pp. 128-136.

KAPLAN, K., "Generalized Laboratory Study of Tsunami Run-up," TM-60, U.S. Army, Corps of Engineers, Beach Erosion Board, Washington, D.C., Jan. 1955.

KELLER, J.B., "The Solitary Wave and Periodic Waves in Shallow Water," *Communications in Pure and Applied Mathematics*, Vol. 1, 1948, pp. 323-339.

KEULEGAN, G.H., "Wave Motion," *Engineering Hydraulics*, Ch. 11, John Wiley and Sons, Inc., New York, 1950, pp. 711-768.

KISHI, T., and SAEKI, H., "The Shoaling, Breaking and Runup of the Solitary Wave on Impermeable Rough Slopes," *Proceedings of the 10th Conference on Coastal Engineering*, American Society of Civil Engineers, Ch. 21, 1966, pp. 322-348.

KONONKOVA, G.E., and REIHRUDEL, A.E., "Experimental Study of Solitary Tsunami Waves," *Proceedings of the Tsunami Research Symposium*, Bulletin 15, Royal Society of New Zealand, 1976.

LAMB. H., *Hydrodynamics*, 6th ed., Dover Publications, Inc., New York, 1932.

LEBLOND, P.H., and MYSAK, L.A., "Trapped Coastal Waves and Their Role in Shelf Dynamics," *Marine Modeling, The Sea,* Ch. 10, Vol. 6, 1977, pp. 459-495.

LEE, J.J., "Wave Induced Oscillations in Harbors of Arbitrary Shape," Report No. KH-R-20, W.N. Keck Laboratory of Hydraulics and Water Resources, California Institute of Technology, Pasadena, Calif., Dec. 1969.

LEE, J.J., "Wave Induced Oscillations in Harbors of Arbitrary Geometry," *Journal of Fluid Mechanics,* Vol. 45, 1971, pp. 375-393.

LEENDERTSE, J.J., "Aspects of a Computational Model for Long-Period Water-Wave Propagation," Memorandum RM-5294-PR, Rand Corporation, Santa Monica, Calif., May 1967.

LEVY, D.M., and KELLER, J.B., "Water Wave Production by Point Sources and Extended Sources," *Proceedings of the 10th Pacific Science Congress on Tsunami Hydrodynamics,* International Union of Geodesy and Geophysics, Monograph No. 24, 1961, pp. 162-166.

LINSLEY, R.K., Jr., KOHLER, M.A., and PAULHUS, J.L.H., *Hydrology for Engineers,* McGraw-Hill Book Company, New York, 1958.

LOZANO, C., and MEYER, R.E., "Leakage and Response of Waves Trapped by Round Islands," *The Physics of Fluids,* Vol. 19, No. 8, Aug. 1976, pp. 1075-1088.

MADSEN, O.S., and MEI, C.C., "The Transformation of a Solitary Wave Over an Uneven Bottom," *Journal of Fluid Mechanics,* Vol. 39, Part 4, 1969, pp. 781-791.

MAGOON, O.T., "The Tsunami of May 1960 as it Affected Northern California," American Society of Civil Engineers, presented at the Hydraulics Division Conference, Aug. 1962 (unpublished).

MAGOON, O.T., "Structural Damage by Tsunamis," *Proceedings of the Coastal Engineering Specialty Conference,* American Society of Civil Engineers, Ch. 4, 1965, pp. 35-68.

MALLOY, R.J., "Crustal Uplift Southwest of Montague Island, Alaska," *Science,* Vol. 146, 1964, pp. 1048-1049.

MASON, M.A., and KEULEGAN, G.H., "A Wave Method for Determining Depths Over Bottom Discontinuities," TM-5, U.S. Army, Corps of Engineers, Beach Erosion Board, Washington, D.C., May 1944.

MATLOCK, H., REESE, L.C., and MATLOCK, R.B., "Analysis of Structural Damage from the 1960 Tsunami at Hilo, Hawaii," Report DASA-1268, Structural Mechanics Research Laboratory, University of Texas, Austin, Tex., Mar. 1962.

MATUO, H., "Estimation of Energy of Tsunami and Protection of Coasts," *Bulletin of the Earthquake Research Institute*, Tokyo Imperial University, Tokyo, Japan, Mar. 1934, pp. 55-64.

MEI, C.C., and LE MEHAUTE, B., "Note on the Equations of Long Waves Over an Uneven Bottom," *Journal of Geophysical Research*, Vol. 71, No. 2, Jan. 1966, pp. 393-400.

MICHE, R., "Movement Ondulatores de Mers en Profondour Cons," *Ann. Ponts Chaussees*, Vol. 114, 1944.

MILES, J.W., "Coupling of a Cylindrical Tube to a Half Space," *Journal of the Acoustical Society of America*, Vol. 20, No. 5, 1948, pp. 652-664.

MILES, J.W., "Resonant Response of Harbors: An Equivalent-Circuit Analysis," *Journal of Fluid Mechanics*, Vol. 46, Part 2, 1971, pp. 241-265.

MILES, J.W., "Wave Propagation Across the Continental Shelf," *Journal of Fluid Mechanics*, Vol. 54, Part 1, 1972, pp. 63-80.

MILLER, D.J., "Giant Waves in Lituya Bay, Alaska," Professional Paper 354-c, U.S. Geological Survey, Washington, D.C., 1960.

MILLER, R.L., "Experimental Determination of Runup of Undular and Fully Developed Bores and an Examination of Transition Modes and Internal Structure," Technical Report No. 8, Department of Geophysical Sciences, University of Chicago, Chicago, Ill., June 1968.

MILNE, W.E., *Numerical Solution of Differential Equations*, John Wiley & Sons, Inc., New York, 1953.

MOORE, G.W., "Magnetic Disturbances Preceding the Earthquake," *The Great Alaska Earthquake of 1964, Seismology and Geodesy*, National Academy of Sciences, National Research Council, Washington, D.C., 1972, pp. 518-525.

MUNK, W., SNODGRASS, F., and GILBERT, F., "Long Waves on the Continental Shelf: An Experiment to Separate Trapped and Leaky Modes," *Journal of Fluid Mechanics*, Vol. 20, Part 4, 1964, pp. 529-554.

MURTY, T.S., "Seismic Sea Waves - Tsunamis," Bulletin 198, Department of Fisheries and the Environment, Fisheries and Marine Service, Ottawa, Canada, 1977.

MURTY, T.S., and WIGEN, S.O., "Tsunami Behavior on the Atlantic Coast of Canada and Some Similarities to the Peru Coast," *Proceedings of the Tsunami Research Symposium*, Royal Society of New Zealand, Bulletin 15, 1976, pp. 51-60.

MURTY, T.S., WIGEN, S.O., and CHAWLA, R., "Some Features of Tsunamis on the Pacific Coast of South and North America," Series No. 36, Marine Sciences Directorate, Department of the Environment, Ottawa, Canada, 1975.

NAGAOKA, H., "On Destructive Sea Waves (Tsunami)," *Proceedings of the Tokyo Mathematico-Physical Society*, Vol. 2, No. 2, 1901, pp. 126-136.

NAKANO, M., "Preliminary Note on the Accumulation and Dissipation of Energy of the Secondary Undulations in a Bay," *Proceedings of the Physico-Mathematical Society of Japan*, Vol. 14, 1932, pp. 44-56.

NASU, N., "Heights of Tsunamis and Damage to Structures," *Bulletin of the Earthquake Research Institute*, Tokyo Imperial University, Tokyo, Japan, Vol. 1, Mar. 1934, pp. 218-226.

NASU, N., "Local Phenomena of Tsunami, Part 2," *Bulletin of the Earthquake Research Institute*, Tokyo Imperial University, Tokyo, Japan, Vol. 26, Nos. 1-4, 1948, pp. 27-35.

NISHIMURA, H., HORIKAWA, K., and SHUTO, N., "On the Function of Tsunami Breakwaters," *Coastal Engineering in Japan*, Tokyo, Japan, Vol. 14, 1971, pp. 63-72.

O'BRIEN, M.P., Discussion of "Similitude in Coastal Engineering" by B. Le Mehaute, *Journal of the Waterway, Port, Coastal, and Ocean Division*, Vol. 103, No. WW3, Aug. 1977, pp. 393-400.

PALMER, R.Q., MULVIHILL, M.E., and FUNASAKI, G.T., "Hilo Harbor Tsunami Model - Reflected Waves Superimposed," *Proceedings of the Coastal Engineering Santa Barbara Specialty Conference*, American Society of Civil Engineers, Ch. 2, 1965, pp. 21-31.

PARARAS-CARAYANNIS, G., "Catalog of Tsunamis in the Hawaiian Islands," Report WDCA-T 69-2, ESSA - Coast and Geodetic Survey, Boulder, Colo., May 1969.

PEREGRINE, D.H., "Long Waves on a Beach," *Journal of Fluid Mechanics*, Vol. 27, No. 4, 1967, pp. 815-827.

PEREGRINE, D.H., "Long Waves in Two and Three Dimensions," *Proceedings of the Symposium on Long Waves*, University of Delaware, 1970, pp. 63-90.

PERROUD, P.H., "The Solitary Wave Reflection Along a Straight Vertical Wall at Oblique Incidence," University of California, Institute of Engineering Research, Berkeley, Calif., Series 99, Issue 3, Sept. 1957.

PETRAUSKAS, C., and BORGMAN, L.E., "Frequencies of Crest Heights for Random Combinations of Astronomical Tides and Tsunamis Recorded at Crescent City, California," Technical Report HEL 16-8, Hydraulic Engineering Laboratory, University of California, Berkeley, Calif., Mar. 1971.

PIERSON, W.J., "Wave Behavior Near Caustics in Models and in Nature," *Waves on Beaches*, Academic Press, New York, 1972, pp. 163-180.

PLAFKER, G., "Tectonic Deformation Associated with the 1964 Alaska Earthquake," *Science*, Vol. 148, June 1965, pp. 1675-1687.

PUGET SOUND WEEKLY, Seattle, Wash., 31 Dec. 1866 (newspaper).

RAYLEIGH, LORD, *The Theory of Sound*, Vol. II, Ch. XVI, Reprint of 1896 ed., Dover Publications, Inc., New York, 1945.

REID, H.F., "The Lisbon Earthquake of November 1, 1755," *Bulletin of the Seismological Society of America*, Vol. 4, No. 2, June 1914, pp. 53-80.

REID, H.F., and TABER, S., "The Puerto Rico Earthquake of 1918, Report of the Earthquake Investigation Commission," H.D. 269, 66th Cong., 1st Sess., U.S. Government Printing Office, Washington, D.C., 1919.

RIABOUCHINSKI, D., "Sur la Resistance des Fluides," International Congress of Mathematics, Strasbourg, France, 1920, pp. 568-585.

RICHTER, C.F., *Elementary Seismology*, W.H. Freeman & Sons, San Francisco, Calif., 1958.

ROW, R.V., "Atmospheric Waves," *The Great Alaska Earthquake of 1964, Seismology and Geodesy*, National Academy of Sciences, Washington, D.C., pp. 494-507.

SCHANK, R.E., "Hazard Reduction and the Mitigation of Tsunami Effects Through Effective Public Warning in Hawaii," *Proceedings of the Symposium on Tsunamis*, Department of Fisheries and the Environment, Series No. 48, 1978, pp. 252-254.

SEELIG, W.N., HARRIS, D.L., and HERCHENRODER, B.E., "A Spatially Integrated Numerical Model of Inlet Hydraulics," GITI Report 14, U.S. Army Coastal Engineering Research Center, Fort Belvoir, Va., and U.S. Army Engineer Waterways Experiment Station, Vicksburg, Miss., Nov. 1977.

SHAW, R.P., "The Outer Boundary Integral Equation Method Applied to Wave Scattering in an Infinite, Locally Inhomogeneous Medium," Report No. HIG-74-6 (NOAA-JTRE-126), Hawaii Institute of Geophysics and Joint Tsunami Research Effort, University of Hawaii, Honolulu, Hawaii, Sept. 1974.

SHAW, R.P., "An Outer Boundary Integral Equation Applied to Transient Wave Scattering in an Inhomogeneous Medium," *Journal of Applied Mechanics*, Vol. 42, No. 1, Mar. 1975, pp. 147-152.

SHEN, M.C., "Wave Resonance Near Shores," *Waves on Beaches*, Academic Press, New York, 1972, pp. 123-161.

SHEN, M.C., and MEYER, R.E., "Surface Wave Resonance on Continental and Island Slopes," Technical Summary Report No. 781, Army Mathematics Research Center, University of Wisconsin, Madison, Wisc., Sept. 1967.

SHEPARD, F.P., MacDONALD, G.A., and COX, D.C., "The Tsunami of April 1, 1946," *Bulletin of the Scripps Institution of Oceanography*, Vol. 5, No. 6, 1950, pp. 391-528.

SHINMOTO, D.Y., and VITOUSEK, M.J., "An Inexpensive Air-Deployable Midocean Tsunami Gauge," *Proceedings of the Symposium on Tsunamis*, Department of Fisheries and the Environment, Series No. 48, 1978, pp. 242-244.

SMITH, R.A., "Annotated Bibliography on Water Waves Caused by Explosions--1946 to 1966," DASIAC Special Report 58, DASA Information and Analysis Center, Apr. 1967.

SOLOVIEV, S.L., "Recurrence of Tsunamis in the Pacific," *Tsunamis in the Pacific Ocean*, Ch. 11, East-West Center Press, Honolulu, Hawaii, 1970, pp. 149-164.

SOLOVIEV, S.L., and FERCHEV, M.D., "Summary of Data on Tsunamis in the USSR," *Bulletin of the Council for Seismology*, Academy of Sciences of the U.S.S.R., No. 9, 1961, pp. 23-55 (translated by W.G. Van Campen, Hawaii Institute of Geophysics).

SOLOVIEV, S.L., et al., "Materials for Preliminary Tsunami Zonation of Kurile-Kamchatka Coast Based on Hydrodynamical Calculations," *Proceedings of the Tsunami Research Symposium*, Royal Society of New Zealand, Bulletin 15, 1976, pp. 29-38.

SPAETH, M.G., *Annotated Bibliography on Tsunamis*, Monograph No. 27, International Union of Geodesy and Geophysics, Paris, France, July 1964.

SPAETH, M.G., and BERKMAN, S.C., "The Tsunamis as Recorded at Tide Stations and the Seismic Sea Wave Warning System," *The Great Alaska Earthquake of 1964, Oceanography and Coastal Engineering*, National Academy of Sciences, Washington, D.C., 1972, pp. 38-110.

SPIELVOGEL, L.Q., "Single-Wave Runup on Sloping Beaches," *Journal of Fluid Mechanics*, Vol. 74, Part 4, 1975, pp. 685-694.

STEIN, S., et al., "Earthquakes Along the Passive Margin of Canada Induced by Deglaciation," *Geophysical Research Letters* (in preparation, 1980).

STOKES, G.G., "On the Theory of Oscillatory Waves," *Transactions of the Cambridge Philosophical Society*, Vol. 8, 1847, pp. 441-455.

STREET, R.L., BURGESS, S.J., and WHITFORD, P.W., "The Behavior of Solitary Waves on a Stepped Slope," Technical Report No. 93, Department of Civil Engineering, Stanford University, Palo Alto, Calif., Aug. 1968.

STREET, R.L., and CAMFIELD, F.E., "Observations and Experiments on Solitary Wave Deformation," *Proceedings of the 10th Conference on Coastal Engineering*, American Society of Civil Engineers, Ch. 19, 1966, pp. 284-301.

STREET, R.L., CHAN, R.K.C., and FROMM, J.E., "The Numerical Simulation of Long Water Waves: Progress on Two Fronts," *Tsunamis in the Pacific Ocean*, Ch. 30, W.M. Adams, ed., East-West Center Press, University of Hawaii, Honolulu, Hawaii, 1970, pp. 453-473.

STRIEM, H.L., and MILOH, T., "Tsunamis Induced by Submarine Slumpings off the Coast of Israel," Report IA-LD-1-102, Israel Atomic Energy Commission, Israel, July 1975.

SUYEHIRO, Y., "Some Observations on the Unusual Behaviour of Fishes Prior to an Earthquake," *Bulletin of the Earthquake Research Institute*, Tokyo Imperial University, Tokyo, Japan, Vol. 1, 1934.

TABER, S., "Seismic Activity in the Atlantic Coastal Plain Near Charleston, South Carolina," *Bulletin of the Seismological Society of America*, Vol. 4, No. 3, Sept. 1914, pp. 108-160.

TOWNLEY, S.D., and ALLEN, M.W., "Descriptive Catalog of Earthquakes of the Pacific Coast of the United States 1769 to 1928," *Bulletin of the Seismological Society of America*, Vol. 29, No. 1, Jan. 1939, pp. 1-297.

U.S. ARMY ENGINEER DISTRICT, HONOLULU, "Hilo Harbor, Hawaii, Report on Survey for Tidal Wave Protection and Navigation," Nov. 1960.

U.S. ARMY ENGINEER DISTRICT, HONOLULU, "The Tsunami of 23 May 1960 in Hawaii - Final Post Flood Report," 1960.

VAN DORN, W.G., "Source Mechanism of the Tsunami of March 28, 1964 in Alaska," *Proceedings of the Ninth Conference on Coastal Engineering*, American Society of Civil Engineers, Ch. 10, 1964, pp. 166-190.

VAN DORN, W.G., "Tsunamis," *Advances in Hydroscience*, Vol. 2, Academic Press, New York, 1965 (also published as Scripps Institution of Oceanography Report, Federal Clearinghouse No. AD457729, Jan. 1965).

VAN DORN, W.G., LE MEHAUTE, B., and HWANG, L-S., "Handbook of Explosion-Generated Water Waves, Volume I - State-of-the-Art," Report No. TC-130, Tetra Tech, Inc., Pasadena, Calif., Oct. 1968.

VITOUSEK, M.J., "Proposed Mid-Ocean Tsunami Gage and Oceanography Instrument System," *Proceedings of the Tsunami Meetings Associated With the 10th Pacific Science Conference*, International Union of Geodesy and Geophysics, 1961, pp. 131-133.

VITOUSEK, M.J., and MILLER, G., "An Instrumentation System for Measuring Tsunamis in the the Deep Ocean," *Tsunamis in the Pacific Ocean*, Ch. 16, East-West Center Press, Honolulu, Hawaii, 1970, pp. 239-252.

WEIGEL, E.P., *Tsunami!* National Oceanic and Atmospheric Administration, Vol. 4, No. 1, Jan. 1974.

WELLER, J.M., "Human Response to Tsunami Warnings," *The Great Alaska Earthquake of 1964, Oceanography and Coastal Engineering*, National Academy of Sciences, National Research Council, Washington, D.C., 1972, pp. 222-228.

WHITMAN, G.B., "Non-Linear Dispersion of Water Waves," *Journal of Fluid Mechanics*, Vol. 27, Part 2, 1967, pp. 339-412.

WIEGEL, R.L., *Oceanographical Engineering*, Prentice-Hall, Englewood Cliffs, N.J., 1964.

WIEGEL, R.L., "Protection of Crescent City, California from Tsunami Waves," Report for the Redevelopment Agency of the City of Crescent City, Crescent City, Calif., Mar. 1965.

WIEGEL, R.L., "Tsunamis," *Earthquake Engineering*, Ch. 11, R.L. Wiegel, ed., Prentice-Hall, Englewood Cliffs, N.J., 1970, pp. 253-306.

WILSON, B.W., "Long Waves Generated by Nuclear Explosions," Appendix I, Investigation of Long Waves and Their Effects on the Coastal and Harbor Environment of the Lower Chesapeake Bay, Vol. II, National Engineering Science Co., Report No. DASA-1355, Apr. 1963.

WILSON, B.W., "Earthquake Occurrence and Effects in Ocean Areas," Technical Report CR. 69.027, U.S. Naval Civil Engineering Laboratory, Port Hueneme, Calif., Feb. 1969.

WILSON, B.W., "Estimate of Tsunami Effect at San Onofre Nuclear Generating Station Units 2 and 3, California," Southern California Edison Co., Los Angeles, Calif., Dec. 1972.

WILSON, B.W., and TØRUM, A., "The Tsunami of the Alaskan Earthquake, 1964; Engineering Evaluation," TM-25, U.S. Army Coastal Engineering Research Center, Washington, D.C., May 1968.

WILSON, B.W., WEBB, L.M., and HENDRICKSON, J.A., "The Nature of Tsunamis; Their Generation and Dispersion in Water of Finite Depth," Technical Report No. SN 57-2, National Engineering Science Co., Aug. 1962.

ZABUSKY, N.J., and GALVIN, C.J., "Shallow-Water Waves, the Korteweg-deVries Equation and Solitons," *Journal of Fluid Mechanics*, Vol. 47, Part 4, 1971, pp. 811-824.

APPENDIX

TSUNAMIS OCCURRING BETWEEN 1891 AND 1961

Date	Source	Remarks
30 July 1891	Lerdo, Mexico	Tidal wave of considerable height at head of the Gulf of California.
29 Nov. 1891	Seattle, Washington	Water in Lake Washington surged on to the beach 2 feet above the mark of the highest water and 8 feet above the lake stage on that date.
16 May 1892	Marianas Islands	Minor tsunami at Guam.
1893	Greece	----------
1894	------	Wave 4 feet high at Bizerte, Tunisia; some damage.
22 Mar. 1894	Nemuro, Japan	Tsunamis associated with these earthquakes were generally small.
Apr. 1894	Lokris, Greece	----------
10 June 1894	Turkey	Large tsunamis induced by earthquakes at Constantinople (Istanbul).
9 Jan. 1896	Kashima Sea	Slight tsunami in Japan.
15 June 1896	Sanriku, Japan	Much damage and loss of life, devastated ports along the northeast coast of Japan. Runup 80 feet high at Shirahama. Variation in terrestrial magnetism observed at Sendai preceding the tsunami. Maximum height of 30 feet at Napoopoo, Hawaii.
5 Aug. 1897	Tohoku District, Japan	Tsunami.
21 Sept. 1897	Sulu Sea	Severe damage at Tacloban, Philippines (western shores of Basilan Island).
29 Nov. 1897	West Indies	Large tsunami at Montserrat.
1898	Greece	----------
22 Jan. 1899	Southwest Peloponessus, Greece	Tsunami reported at Marathos.
Sept. 1899	Yakutat Bay, Alaska	Waves generated did little damage.
30 Sept. 1899	Banda Sea	Large tsunami on south coast of Ceram, Indonesia.
7 Oct. 1899	Kyushu	Tsunami in Tagonoura, Japan.
9 Aug. 1901	Rikuchu, Japan	Tsunami at Hilo, Kailua, and Keauhou, Hawaii; minor damage.
26 Feb. 1902	El Salvador	Tsunami in El Salvador and Guatemala.
5 July 1902	Thessaloniki, Greece	Saloniki Harbor flooded by waves.
25 June 1904	Kamchatka	Wave at Avachinskaya Bay.
1905	------	Tsunami at Bizerte, Tunisia; believed minor.
8 Sept. 1905	Calabria, Italy	Possible tsunami.
31 Jan. 1906	Ecuador - Columbia	Waves observed in Hawaii; maximum height 3.6 meters observed at Hilo; no damage.

TSUNAMIS OCCURRING BETWEEN 1891 AND 1961--Continued

Date	Source	Remarks
19 Aug. 1906	Valparaiso, Chile	Recorded in Hawaii and Japan; negligible along Chilean coast; some damage in Hawaii.
15 Sept. 1906	Dampier Strait	Tsunami in New Guinea.
14 Jan. 1907	Jamaica	Tsunami generated, main damage at Kingston.
14 Apr. 1907	Mexico	Thirty-foot wave at Acapulco, Mexico.
23 Oct. 1907	Calabria, Italy	Tsunami recorded at Messina and Catania.
20 Sept. 1908	Puna, Hawaii	Weak tsunami.
28 Dec. 1908	Messina, Italy	Heavy damage along shoreline; breakwater destroyed at Messina.
30 Jan. 1911	Philippine Islands	Seismic waves in Lake Bombon washed away several villages; some loss of life; waves 2.5 to 3 meters high on shoreline.
26 Feb. 1913	South Island, New Zealand	Small tsunami.
14 Mar. 1913	Sangi, East Indies	Tsunami generated.
11 Oct. 1913	Near east end of New Guinea	Weak tsunami.
12 Jan. 1914	Sakurajima, Japan	Wave with 10-foot amplitude caused serious damage to small boats in Kagoshima Harbor.
26 May 1914	North coast of New Guinea	Probable tsunami.
7 Aug. 1915	Ionian Sea	Wave height about 5 feet on Greek coast.
1 Jan. 1916	New Britain	Water level in Rabaul Harbor fell 15 feet and rose again rapidly; causeway washed out.
1 May. 1917	Kermadec Islands	Weak tsunami in Hawaii.
26 June 1917	Tonga Islands	Forty-foot wave in Samoa; wave recorded at Honolulu.
15 Aug. 1918	Southern Mindanao, Philippine Islands	Wave swept coast from Lebak to Glan; height estimated at 24 feet at some points.
7 Sept. 1918	Kuril Islands	Tsunami at Uruppu Island, 24 men killed on Simusirijimi; minor damage at Hilo, Hawaii.
11 Oct. 1918	Puerto Rico	Tsunami caused fatalities and damage at Point Borinquen and Aguadilla; also damage at Mayaguez.
8 Nov. 1918	------	Tsunami observed at Futami Harbor, Bonin Islands.
4 Dec. 1918	Copiapo, Chile	Tsunami height 5 meters at Port of Caldera where it caused damage.
30 Apr. 1919	North of Vava'u, Tonga	Observed in Hawaii.
5 May 1919	New Britain	Wave similar to 1 January 1916.
20 Sept. 1920	New Hebrides Islands	Slight tsunami at Samoa.

TSUNAMIS OCCURRING BETWEEN 1891 AND 1961--Continued

Date	Source	Remarks
18 Dec. 1920	Strait of Otranto	Wave height 10 feet on Albanian coast.
11 Nov. 1922	Atacuma, Chile	Tsunami destructive in many places along the coast of Chile; minor damage in Hawaii.
3 Feb. 1923	East Kamchatka	Tsunami in Hawaii; maximum amplitude 15 feet at Hilo; one person killed, much damage; tsunami on coast of Kamchatka.
13 Apr. 1923	Kamchatka	Tsunami observed in Hawaii.
1 Sept. 1923	Kwanto, Japan	Tsunami hit towns on shore of Sagami Bay; maximum height of 26 feet at Atami.
9 Jan. 1924	------	Tsunami on French coast (Atlantic coast); possibly a storm surge.
14 Apr. 1924	South China Sea	Small tsunami at Agno, Pangasman, caused minor damage.
16 Mar. 1926	Tonga Island	Wave swept Palmerston Island, 300 miles northwest of Raratonga; one person killed; all buildings swept away except the church.
16 Sept. 1926	Solomon Islands	Tsunami at Guadalcanal.
18 Nov. 1926	Saint Pierre and Miquelon	Possible minor tsunami.
7 Mar. 1927	Tango, Japan	Height of tsunami about 5 feet on Sea of Japan coastline.
26 June 1927	Black Sea	Small tsunami recorded in Crimea.
11 and 12 Sept. 1927	Black Sea	Small tsunami recorded in Crimea.
4 Nov. 1927	California	Six-foot wave at Surf; 0.24 inch high at LaJolla.
28 Dec. 1927	Kamchatka, U.S.S.R.	Minor tsunami recorded at Hilo.
25 Apr. 1928	Near Piraeus, Greece	Waves 7 feet high on north coast of Crete.
17 June 1928	Mexico	Waterfront damaged at Puerto Angel, Mexico.
17 Jan. 1929	Cumana, Venezuela	Many boats wrecked.
6 Mar. 1929	Aleutian Islands	Tsunami measured in Hawaii (maximum amplitude 1 foot at Hilo).
26 May 1929	Queen Charlotte Islands, Canada	Four-foot wave at Queen Charlotte City.
18 Nov. 1929	Grand Banks	Tsunami hit Newfoundland; damage and loss of life on Burin Peninsula.
3 Oct. 1931	Solomon Islands	Eighteen native villages destroyed on San Christobal Island; approximately 50 persons killed.
3 June 1932	Jalisco, Mexico	Railroad track swept away between Cayutlan and Manzanillo, Mexico.
18 June 1932	Jalisco, Mexico	Small tsunami.

TSUNAMIS OCCURRING BETWEEN 1819 AND 1961--Continued

Date	Source	Remarks
22 June 1932	Jalisco, Mexico	Small tsunami, some damage.
26 Sept. 1932	Hierissos, Greece	Small tsunami noted in Gulf of Orphano.
3 Mar. 1933	Sanriku coast, Japan	Immense damage; 3,022 people killed; 8,831 houses destroyed; 8,180 vessels wrecked.
14 Feb. 1934	China Sea	Tsunami at San Esteban, Philippine Islands.
27 Oct. 1936	Lituya Bay, Alaska	Maximum runup of 400 feet.
3 Nov. 1936	Off Kinkazan, Japan	Minor tsunami on Japan coast.
28 and 29 May 1937	Blanche Bay, New Britain	Volcanic eruption. Highest waves 14 to 16 feet from crest to trough.
6 Mar. 1938	Solomon Islands	Minor tsunami.
22 Mar. 1938	Queen Charlotte Islands, Canada	Minor tsunami.
19 May 1938	Macassar Strait	Minor tsunami.
23 May 1938	Ibaraki, Japan	Small tsunami.
5 Nov. 1938	Off Iwaki, Japan	Tsunami observed in northern Japan.
10 Nov. 1938	Off south coast of Alaska	Minor tsunami.
1 May 1939	Near Ogasima, Japan	Tsunami observed along coast of Sea of Japan; some damage.
2 Aug. 1940	Northern part of Sea of Japan	Tsunami on coast of Hokkaido.
5 Dec. 1941	Panama - Costa Rica	Slight tsunami at Punta Arenas, Costa Rica; height of 0.75 foot.
24 Aug. 1942	Near Lima, Peru	Slight tsunami recorded in Peru.
6 Apr. 1943	Chile	Small tsunami at Valparaiso; amplitudes more than 3 feet.
7 Dec. 1944	Japan (Kumanonoda)	Amplitude less than 2 feet in Aleutians; waves along Pacific coast of Japan 2.5 to 5 meters high near the Kii Peninsula.
27 Nov. 1945	Arabian Sea	Heavy damage on coast of Pakistan and India; tsunami at Karachi and Bombay where there was damage and loss of life; two new islands appeared in the Arabian Sea.
1 Apr. 1946	Aleutian Islands, Alaska	Damage and loss of life in Alaska; heavy damage and many lives lost in Hawaii.
23 June 1946	British Columbia, Canada	Bottom of Deep Bay sank from 9 to 84 feet; waves generated in Georgia Strait flooded fields and highways.
Aug. 1946	Dominican Republic	Town of Matanzas badly damaged and abandoned; more than 100 persons killed; minor damage on coast of Haiti.
12 and 13 Nov. 1946	Matua Island, Kurile Islands	Volcanic explosion. Tsunami generated.

TSUNAMIS OCCURRING BETWEEN 1891 AND 1961--Continued

Date	Source	Remarks
21 Dec. 1946	Honshu, Japan (Nankai Earthquake)	Damage on south coast of Japan (Wakayama Prefecture); 1,500 people killed on Shikoku Island.
6 Oct. 1947	Kononi, Messenia, Greece	Large wave on coast of Methoni, believed caused by a submarine landslide.
9 Feb. 1948	Sea of Crete	Eight-foot wave.
8 Sept. 1948	Tonga Island	Minor tsunami in Hawaii.
22 Aug. 1949	Queen Charlotte Islands, Canada	Two-foot wave at Ketchikan, Alaska.
20 Oct. 1949	Solomon Sea	Minor (very slight) tsunami in Hawaii.
29 Dec. 1949	Philippine Islands	Tsunami killed one person near Mercedes.
5 Oct. 1950	Costa Rica	Very slight tsunami in Hawaii.
23 Oct. 1950	Guatemala	Very slight tsunami in Hawaii.
14 Dec. 1950	Guerrero, Mexico	Very slight tsunami in Hawaii.
21 Aug. 1951	Kona, Hawaii	Cliff collapsed near Napoopoo creating a 12-foot wave which destroyed a boat dock.
4 Mar. 1952	Tokachi-Oki Earthquake, Japan	Tsunami on Pacific coast of Hokkaido from Nemuro to Hidaka (main damage in Kirittapu and Tokotan); mass of ice accompanied the tsunami.
17 Mar. 1952	South of Hawaii	Slight tsunami at Kalapana.
19 Mar. 1952	East of Mindanao, Philippines	Small tsunami.
13 July 1952	Near New Hebrides	Small tsunami.
Sept. 1952	Myojin Reef	Submarine volcano eruption at Myojin Reef (400 kilometers south of Tokyo, Japan). Tsunami generated; largest wave 24 September, presumed to have destroyed hydrographic research vessel.
4 Nov. 1952	Paramushir Island, Kurile Islands	East Kamchatka Earthquake. Large tsunami; maximum height of 12 feet at Hilo, Hawaii.
31 May 1953	Near Dominican Republic	Very slight tsunami; amplitude of 0.2 foot at Puerto Plata.
11 Aug. 1953	Ionian Islands	Tsunami.
10 Sept. 1953	Cyprus	Series of Waves at Paphus, Cyprus (no major damage).
14 Sept. 1953	Suva Earthquake	Tsunami in Fiji Islands; amplitude of 0.7 foot.
26 Nov. 1953	Boso-Oki, Japan	Tsunami had maximum height of 3 meters at Choshi.
12 Dec. 1953	Peruvian Earthquake	Wave amplitude of 3.2 feet at Talara, Peru.
18 Jan. 1955	------	Tsunami caused damage at LaVela, Venezuela.
19 Apr. 1955	Central Chile	Slight Tsunami in Hawaii.
5 Mar. 1956	North coast of Hokkaido, Japan	----------

TSUNAMIS OCCURRING BETWEEN 1891 AND 1961--Continued

Date	Source	Remarks
30 Mar. 1956	Near Kamchatka	----------
9 July 1956	Greek Archipelago	Wave believed to be caused by submarine landslides; wave 100 feet high near source.
2 Nov. 1956	Volos, Greece	Four-foot wave.
9 Mar. 1957	Aleutian Islands	Tsunami waves in Hawaii; heavy damage.
28 July 1957	Mexico	Tsunami recorded at Acapulco and Salina Cruz.
19 Jan. 1958	Ecuador	Tsunami damaged Esmeraldas and Quayaquil; some deaths.
9 July 1958	Lituya Bay, Alaska	Giant wave from rockfall; wave runup estimated at 1,740 feet at one point.
6 Nov. 1958	Iturup Earthquake, Pacific coast, U.S.S.R.	Waves 3 to 5 meters high in South Kurile Islands (referred to as Etorofu-Oki Earthquake by Japanese).
22 Jan. 1959	East coast of Honshu	Very faint tsunami at Miyako.
7 Feb. 1959	Northern Peru	Tsunami recorded at Talara.
4 May 1959	Near Kamchatka	Slight tsunami in Hawaii and the Aleutian Islands.
18 Aug. 1959	Hebgen Lake, Montana	Waves in lake from earthquake.
13 Jan. 1960	Southern Peru	Small tsunami struck Ancon.
29 Feb. 1960	Morocco	Tsunami at Agadir, Morocco.
20 Mar. 1960	Coast of Japan	Five-foot wave locally.
22 May 1960	Chile	Ofunato, Shizukawa, and Kiritappu heavily damaged in Japan; damage at Hilo, Hawaii.
20 Nov. 1960	Coast of Peru	Damage and deaths along Peruvian coast.
16 Jan. 1961	Ibaraki-Oki Earthquake	Small tsunami.
27 Feb. 1961	Hiuga-Nada, Japan	Tsunami on coast of Miyazaki prefecture occurred at low tide; height small.

☆U.S. GOVERNMENT PRINTING OFFICE: 1980-622-607

Camfield, Frederick E.

Tsunami engineering / by Frederick E. Camfield. – Fort Belvoir, Va. : U.S. Coastal Engineering Research Center, 1980.
222 p. : ill ; 27 cm. – (Special report – U.S. Coastal Engineering Research Center ; no. 6)
Cover title.
Bibliography : p. 201.

This report provides a source of state-of-the-art information on tsunami engineering. The report summarizes available information, identifies gaps in existing knowledge, and discusses methods of predicting tsunami flooding. The generating mechanisms of tsunamis and the method of determining the probability of occurrence are given.
1. Coastal engineering. 2. Offshore structures. 3. Edge waves. 4. Mathematical models. Tsunamis. 5. Water waves. I. Title. II. Series: U.S. Coastal Engineering Research Center. Special report no. 6.
TC203 .U581sr no. 6 627

Camfield, Frederick E.

Tsunami engineering / by Frederick E. Camfield. – Fort Belvoir, Va. : U.S. Coastal Engineering Research Center, 1980.
222 p. : ill ; 27 cm. – (Special report – U.S. Coastal Engineering Research Center ; no. 6)
Cover title.
Bibliography : p. 201.

This report provides a source of state-of-the-art information on tsunami engineering. The report summarizes available information, identifies gaps in existing knowledge, and discusses methods of predicting tsunami flooding. The generating mechanisms of tsunamis and the method of determining the probability of occurrence are given.
1. Coastal engineering. 2. Offshore structures. 3. Edge waves. 4. Mathematical models. Tsunamis. 5. Water waves. I. Title. II. Series: U.S. Coastal Engineering Research Center. Special report no. 6.
TC203 .U581sr no. 6 627

Camfield, Frederick E.

Tsunami engineering / by Frederick E. Camfield. – Fort Belvoir, Va. : U.S. Coastal Engineering Research Center, 1980.
222 p. : ill ; 27 cm. – (Special report – U.S. Coastal Engineering Research Center ; no. 6)
Cover title.
Bibliography : p. 201.

This report provides a source of state-of-the-art information on tsunami engineering. The report summarizes available information, identifies gaps in existing knowledge, and discusses methods of predicting tsunami flooding. The generating mechanisms of tsunamis and the method of determining the probability of occurrence are given.
1. Coastal engineering. 2. Offshore structures. 3. Edge waves. 4. Mathematical models. Tsunamis. 5. Water waves. I. Title. II. Series: U.S. Coastal Engineering Research Center. Special report no. 6.
TC203 .U581sr no. 6 627

Camfield, Frederick E.

Tsunami engineering / by Frederick E. Camfield. – Fort Belvoir, Va. : U.S. Coastal Engineering Research Center, 1980.
222 p. : ill ; 27 cm. – (Special report – U.S. Coastal Engineering Research Center ; no. 6)
Cover title.
Bibliography : p. 201.

This report provides a source of state-of-the-art information on tsunami engineering. The report summarizes available information, identifies gaps in existing knowledge, and discusses methods of predicting tsunami flooding. The generating mechanisms of tsunamis and the method of determining the probability of occurrence are given.
1. Coastal engineering. 2. Offshore structures. 3. Edge waves. 4. Mathematical models. Tsunamis. 5. Water waves. I. Title. II. Series: U.S. Coastal Engineering Research Center. Special report no. 6.
TC203 .U581sr no. 6 627

Camfield, Frederick E.

Tsunami engineering / by Frederick E. Camfield. – Fort Belvoir, Va. : U.S. Coastal Engineering Research Center, 1980.
222 p. : ill ; 27 cm. – (Special report – U.S. Coastal Engineering Research Center ; no. 6)
Cover title.
Bibliography : p. 201.

This report provides a source of state-of-the-art information on tsunami engineering. The report summarizes available information, identifies gaps in existing knowledge, and discusses methods of predicting tsunami flooding. The generating mechanisms of tsunamis and the method of determining the probability of occurrence are given.
1. Coastal engineering. 2. Offshore structures. 3. Edge waves. 4. Mathematical models. Tsunamis. 5. Water waves. I. Title. II. Series: U.S. Coastal Engineering Research Center. Special report no. 6.
TC203 .U581sr no. 6 627

Camfield, Frederick E.

Tsunami engineering / by Frederick E. Camfield. – Fort Belvoir, Va. : U.S. Coastal Engineering Research Center, 1980.
222 p. : ill ; 27 cm. – (Special report – U.S. Coastal Engineering Research Center ; no. 6)
Cover title.
Bibliography : p. 201.

This report provides a source of state-of-the-art information on tsunami engineering. The report summarizes available information, identifies gaps in existing knowledge, and discusses methods of predicting tsunami flooding. The generating mechanisms of tsunamis and the method of determining the probability of occurrence are given.
1. Coastal engineering. 2. Offshore structures. 3. Edge waves. 4. Mathematical models. Tsunamis. 5. Water waves. I. Title. II. Series: U.S. Coastal Engineering Research Center. Special report no. 6.
TC203 .U581sr no. 6 627

Camfield, Frederick E.

Tsunami engineering / by Frederick E. Camfield. – Fort Belvoir, Va. : U.S. Coastal Engineering Research Center, 1980.
222 p. : ill ; 27 cm. – (Special report – U.S. Coastal Engineering Research Center ; no. 6)
Cover title.
Bibliography : p. 201.

This report provides a source of state-of-the-art information on tsunami engineering. The report summarizes available information, identifies gaps in existing knowledge, and discusses methods of predicting tsunami flooding. The generating mechanisms of tsunamis and the method of determining the probability of occurrence are given.
1. Coastal engineering. 2. Offshore structures. 3. Edge waves. 4. Mathematical models. Tsunamis. 5. Water waves. I. Title. II. Series: U.S. Coastal Engineering Research Center. Special report no. 6.
TC203 .U581sr no. 6 627